Development of cost-effective and sustainable microbial fuel cells for water quality monitoring

Chouler, Jon

Award date:
2018

Awarding institution:
University of Bath

Development of cost-effective and sustainable microbial fuel cells for water quality monitoring

Chouler, Jon

Award date:
2018

Awarding institution:
University of Bath

Development of cost-effective and sustainable microbial fuel cells for water quality monitoring

Jon Chouler

A thesis submitted for the degree of Doctor of Philosophy

University of Bath

Department of Chemical Engineering, Centre for Sustainable Chemical Technologies

September 2017

Acknowledgements

I've had an incredible four years in Bath (nine if you count the undergraduate studies!), and I owe a lot of thanks to countless people, who without their help and friendship this work would not have been possible.

I would like to thank my supervisor Dr. Mirella Di Lorenzo for inspiring me to be my best and to work towards the greater good. My thanks also go to my second supervisor, Dr. Petra Cameron, whose help and guidance I am extremely grateful for (and for making electrochemistry bearable!).

I also give thanks to the Centre for Sustainable Chemical Technologies. Without the countless opportunities that you have given me over the years, I would not be half the professional I am today. It's also been a pleasure going through this PhD with my cohort DTC '13, who have provided countless laughs and good times along the way.

I would like to thank those in the Department of Chemical Engineering; first of all, the Biofuel Cell & Biosensors group, its various members have made the laboratory a great place to work. I also thank the staff and postgraduate students of the department who make the place an invigorating and exciting place to work; and my thanks also to its excellent technical team who always have time for sharing ideas and fixing problems. My thanks also extend to the technical teams in Mechanical and Electrical Engineering, who have also helped me solve many a problem. I give thanks also to the Chemical Engineering Masters students who have conducted research with me throughout the last few years, teaching and supervising you has been a treat, and without your help, this work would not have been possible.

I would like to thank my wonderful and soon to be wife, Nicola Ansell, for joining me, sticking by me, and for all your love and support during this PhD. You've made the tough times far easier, and the good times even better. To our cats, Calcaneus and Olecranon, thanks for walking over my keyboard frequently, and being a welcome distraction whilst writing up. I owe much to Giovanni L'Immigrato, who I've loved playing music for, you all have kept me sane (through your insanity) throughout the years!

I would like to thank my family. To my parents, Fiona and Peter, I am thankful for your support, upbringing, and belief in me over these years. To my siblings Ed, Abbie

and Terri, and nieces and nephew Courtney, Ella and Vinnie, I'd like to thank you for always being there, and making the time to see me on my infrequent journeys home.

I'm sure I may have forgotten to thank someone at this point, but I extend my thanks to everyone who I've had the pleasure of meeting, working, drinking and laughing with throughout this work.

Thank you.

Abstract

The sustainable provision of clean and secure water is one of the biggest challenges the global population is currently faced with. To ensure access to clean water, the control and monitoring of contaminants released into water systems is critical, and thus effective water quality monitoring methods that are low cost, rapid, simple to use and have onsite capability are needed. Recently, the microbial fuel cell (MFC) technology has shown great promise as a real time sensing tool. The aim of this thesis is to design and develop cost-effective and sustainable MFC biosensors for the straightforward and rapid assessment of water quality.

First, a single chamber miniature (128 μL) MFC was developed. The effect of electrode length and spacing on its power performance was assessed. Moreover, the improvement of current generation by electrically stacking the MFCs was demonstrated. The use of various low cost materials for MFC production was then investigated. Natural and synthetic membrane materials (eggshell membrane and polydimethylsiloxane) were used to replace the commonly used and expensive Nafion membrane. Then the use of biomass derived oxygen reduction reaction catalysts at the cathode to improve baseline current was studied. The ability of this miniature MFC device to detect the labile organic carbon content, and the presence of formaldehyde (as a model toxicant) and atrazine was then demonstrated.

Next, an innovative and extremely cheap (£0.43 per unit), portable, screen-printed, paper-based MFC was created for the purpose of water quality monitoring in developing countries. Additionally, the use of microalgae as an alternative biorecognition element at the miniature MFC anode was investigated, with the purpose to enhance the sensitivity towards trace organic compound pollutants. To this end, a miniature photosynthetic MFC biosensor was developed. The ability of both these innovative devices to detect formaldehyde in water, thus providing a proof of concept for their use as water quality monitoring biosensors, was then studied.

To conclude, this thesis demonstrates the development of a miniature single chamber MFC that uses sustainable and cost-effective materials and provides investigations for its potential as a powerful water quality monitoring tool. Also, for the first time, the biosensing capability of an innovative paper-based MFC and photosynthetic MFC are demonstrated.

Dissemination

Journal articles

Published

J. Chouler, M. Di Lorenzo, Water Quality Monitoring in Developing Countries; Can Microbial Fuel Cells be the Answer?, Biosensors. 5 (2015) 450–470. doi:10.3390/bios5030450.

J. Chouler, G.A. Padgett, P.J. Cameron, K. Preuss, M.-M. Titirici, I. Ieropoulos, M. Di Lorenzo, Towards effective small scale microbial fuel cells for energy generation from urine, Electrochim. Acta. 192 (2016) 89–98. doi:10.1016/j.electacta.2016.01.112.

J. Chouler, I. Bentley, F. Vaz, A. O'Fee, P.J. Cameron, M. Di Lorenzo, Exploring the use of cost-effective membrane materials for Microbial Fuel Cell based sensors, Electrochim. Acta. 231 (2017) 319–326. doi:10.1016/j.electacta.2017.01.195.

J. Chouler, Á. Cruz-Izquierdo, S.Rengaraj, J. L. Scott, M. Di Lorenzo, A screen-printed paper microbial fuel cell biosensor for detection of toxic compounds in water, Biosens. Bioelec. 102 (2018) 49-56. doi: 10.1016/j.bios.2017.11.018.

Manuscripts in preparation

J. Chouler, M. Di Lorenzo, Influence of operational factors on the performance of a miniature microbial fuel cell as a toxicity sensor.

J. Chouler, M.Monti, W. Morgan, P. J. Cameron, M. Di Lorenzo, A miniature photosynthetic microbial fuel cell biosensor for the detection of bioactive compounds in water.

Co-authored articles

A. M. R. Hall, J. Chouler, A. Codina, P. T. Gierth, J. P. Lowe, U. Hintermair, Practical aspects of real-time reaction monitoring using multi-nuclear high resolution FlowNMR spectroscopy. Cat. Sci. Tech. 6 (2016) 8406-8417. doi: 10.1039/C6CY01754A

Conferences

Water and Health Advanced Materials Research Sandpit, Brotas, Brazil, 28-30 August 2017, Facilitator.

International Water Association Young Water Professionals, Bath, UK, 10-12 April 2017, Oral presentation, organiser and roundtable discussion chair.

U4C Colloquium, Campinas, Brazil, 16-19 November 2016, Oral presentation.

EU-International Society for Microbial Electrochemistry and Technology, Rome, 26-28 September 2016, Oral presentation.

Science in Public, Canterbury, UK, 13-15 July 2016, Oral presentation.

International Water Association Young Water Professionals, Norwich, UK, 29-30 March 2016, Poster presentation.

European Fuel Cell, Naples, Italy, 15-18 December 2015, Oral presentation.

British Interactive Group BIG Event 2015, Norwich, UK, 22-24 July 2015, Participant.

IChemE ChemEng Day UK, Sheffield, UK, 8-10 April 2015, Poster presentation.

Prizes

Royal Academy of Engineering: Ingenious Award, May 2016, Buskineers Engineering Communication Project, Project leader.

Engineering Young Entrepreneur Scheme, Best environmental project winner, June 2016.

The Worshipful Company of Engineers, Water Engineering Prize, July 2016

International Water Association Young Water Professionals, Norwich, UK, 29-30 March 2016, Poster prize.

Vice Chancellors Public Engagement Prize for Postgraduate Research, April 2015.

IChemE ChemEng Day UK, Sheffield, UK, 8-10 April 2015, Poster prize.

Table of contents

List of figures xii

List of tables xviii

1 Introduction 1

1.1 The global water crisis 1

1.2 Microbial fuel cells for water quality monitoring 2

1.3 Aims and objectives 4

1.4 Outline of the thesis 5

1.5 References 7

2 Literature review 11

2.1 Abstract 13

2.2 Freshwater security 14

2.3 Current approaches to water quality monitoring in the developing world 14

2.3.1 Detection of chemicals 14

2.3.2 Bioassays 17

2.4 Biosensors and the potential of microbial fuel cell based sensors 17

2.4.1 Biosensors for water quality monitoring 17

2.4.2 Principles of MFC technology 19

2.4.3 MFCs as biosensors: operating principles and concepts 22

2.4.4 MFCs as sensors for the labile organic carbon content in water 25

2.4.5 MFCs as toxicity sensors 27

2.5 Challenges of implementing MFC biosensor technology for developing countries 33

2.5.1 Simplicity of use 33

2.5.2 Use of inexpensive materials 34

2.5.3 Onsite capability 35

2.6 Conclusions 37

2.7 Associated content 38

2.8 References 39
3 Theory 49
3.1 Electrochemical fundamentals for microbial fuel cells 49
3.2 Electrochemical methods for microbial fuel cells 52
3.2.1 Potentiostat 52
3.2.2 Polarisation curves 53
3.2.3 Cyclic voltammetry 55
3.2.4 Electrochemical impedance spectroscopy 56
3.2.5 Fuel cell efficiency 59
3.3 Associated content 60
3.4 References 63
4 Towards effective small scale microbial fuel cells for energy generation from urine 67
4.1 Abstract 69
4.2 Introduction 70
4.3 Experimental 72
4.3.1 Materials 72
4.3.2 Microbial fuel cells 72
4.3.3 Use of a biomass derived oxygen reduction reaction catalyst 73
4.3.4 Operation of the MFCs 74
4.3.5 Stacking 75
4.3.6 Calculations 75
4.4 Results and discussion 76
4.4.1 Effect of electrode length on performance 76
4.4.2 Stacking the miniature MFCs 80
4.4.3 Use of biomass derived ORR catalysts 81
4.5 Conclusions 84
4.6 Associated content 85
4.7 References 87

5 Exploring the use of cost-effective membrane materials for microbial fuel cell based sensors 93
5.1 Abstract 95
5.2 Introduction 96
5.3 Experimental 98
5.3.1 Materials 98
5.3.2 Microbial fuel cells and membrane assembly 98
5.3.3 Operation of the MFCs 99
5.3.4 Testing the MFCs as sensors for labile organic carbon content 100
5.3.5 Calculations 101
5.4 Results and discussion 101
5.4.1 Electrochemical performance of the MFCs 101
5.4.2 Detecting labile organic carbon content in wastewater 104
5.5 Conclusions 108
5.6 Associated content 109
5.7 Supporting information 111
5.8 References 119
6 Influence of operational factors on the performance of a miniature microbial fuel cell as a toxicity sensor 127
6.1 Abstract 129
6.2 Introduction 130
6.3 Experimental 132
6.3.1 Materials 132
6.3.2 Microbial fuel cells 132
6.3.3 Operation of the MFCs 132
6.3.4 Testing the MFCs as biosensors 133
6.3.5 Calculations 134
6.4 Results and discussion 135
6.4.1 Effect of temperature, pH and ionic strength 135

6.4.2 Testing the use of the miniature MFC as a sensor 139
6.5 Conclusions 144
6.6 Associated content 144
6.7 Supporting information 147
6.8 References 149
7 A screen-printed paper microbial fuel cell biosensor for detection of toxic compounds in water 157
7.1 Abstract 159
7.2 Introduction 160
7.3 Experimental 162
7.3.1 Device fabrication 162
7.3.2 Device material characterisation 163
7.3.3 Biofilm analysis 164
7.3.4 Operation of the paper-based MFCs 164
7.3.5 Electrochemical analysis 165
7.3.6 Toxicant analysis 165
7.4 Results and discussion 166
7.4.1 Device fabrication 166
7.4.2 Microbial fuel cell operation 168
7.4.3 Biosensing capability: detection of formaldehyde 172
7.5 Conclusions 174
7.6 Associated content 175
7.7 Supporting information 178
7.8 References 185
8 A miniature photosynthetic microbial fuel cell biosensor for the detection of bioactive compounds in water 191
8.1 Abstract 193
8.2 Introduction 194
8.3 Experimental 196

8.3.1 Materials 196
8.3.2 Photosynthetic MFC construction 197
8.3.3 Operation of the photosynthetic MFC 198
8.3.4 Electrochemical methods 199
8.3.5 Toxicant analysis 199
8.3.6 Residence time distribution analysis 201
8.3.7 Scanning electron microscopy 202
8.4 Results and discussion 202
8.4.1 Enrichment of the photosynthetic MFC 202
8.4.2 Electrochemical characterisation 204
8.4.3 Formaldehyde detection 206
8.5 Conclusions 209
8.6 Associated content 211
8.7 Supporting information 213
8.8 References 215
9 Conclusions and future work 221
9.1 Comparison: MFCs as biosensors 221
9.1.1 Detection of labile organic load 221
9.1.2 Formaldehyde 223
9.1.3 Challenges ahead 224
9.2 Monitoring real water quality 225
9.3 Novel designs 230
9.4 Photosynthetic MFC biosensors 232
9.5 References 233

List of figures

Figure 2.1. Schematic of a biosensor..... 18

Figure 2.2. Operating principles of a two chamber MFC (not to scale). The electroactive biofilm at the anode break down an organic substrate to produce electrons, protons and CO_2. The electrons pass through an external load to be reduced at the cathode 20

Figure 2.3. A schematic of three electron transfer mechanisms of microbes at the anode surface: [**A**] direct transfer by contact, [**B**] indirect electron transfer by redox shuttles (S_{RE} = reduced electron shuttle, S_{OX} = oxidized electron shuttle), [**C**] electron transfer by conductive nanowire matrix…… 21

Figure 2.4. Basic principle of an MFC as a biosensor……... 23

Figure 3.1. Simplified circuit diagram for a potentiostat, with potential source, e_i…….... 53

Figure 3.2. An example polarisation and power curve for a microbial fuel cell, with activation losses **1**, ohmic losses **2**, and concentration losses **3** highlighted……..…….... 55

Figure 3.3. Voltage sweep waveform used for cyclic voltammetry, where voltage is swept from the first potential vertex, E_1, up to the second potential vertex, E_2, and back again.. 55

Figure 3.4. Typical cyclic voltammagram curve for a single redox reaction between vertices E_1 and E_2, showing oxidation and reduction peaks, and peak separation..... 56

Figure 3.5. Typical impedance response for a single electrode MFC system, showing identification of R_Ω and R_{ct}. [**A**] Complex plane plot [**B**] Bode plot 58

Figure 3.6. Example equivalent circuit typically used as an equivalent circuit model to simulate impedance data: **A:** Randles circuit commonly used for a 3 electrode set up (left); **B:** equivalent circuit used for two electrode set up 58

Figure 4.1. MFCs used in this study; [**A**]: Photograph of MFC_S; [**B**]: Photograph of MFC_L; [**C**]: Schematic layout of the device 73

Figure 4.2. Schematic for electrical stacking MFC units in series [**A**] and in parallel [**B**]: R1 = external load, VM = voltmeter 75

Figure 4.3. Power and polarisation curves. [**A**]: MFC_S; [**B**]: MFC_L. Current density refers to the anode surface area: MFC_S = 16 mm^2; MFC_L = 32 mm^2. Volumetric power density refers to the MFC chamber volume: MFC_S = 64 µL; MFC_L = 128 µL. For each geometry, data is the average of 3 devices, with up to 22% error 77

Figure 4.4. Effect of length of MFC channel on mass transfer coefficient and diffusion-layer thickness moving from 0.5 to 25 mm. Values plotted are for a flow rate of 0.36 mL min^{-1} 79

Figure 4.5. Power and polarisation curves. [**A**] Refers to MFC_S, operated alone, in series and in a parallel stack. Current density refers to the anode surface area, 16 mm^2 for a single unit, 48 mm^2 for the stack. [**B**] Refers to MFC_L, operated alone and in a parallel stack. Current density refers to the anode surface area, 32 mm^2 for a single unit, 96 mm^2 for the stack 81

Figure 4.6. Power and polarisation curves. [**A**] Refers to MFC_BC1; [**B**] refers to MFC_BC2; Current density refers to the anode surface area: MFC_BC1, MFC_BC2 = 32 mm^2. Volumetric power density refers to the MFC chamber volume: MFC_BC1, MFC_BC2 = 128 µL. MFC_BC1 is data from one device, and MFC_BC2 is an average of two units with 17% error 82

Figure 4.7. SEM images of the two biomass derived ORR catalyst doped cathode surfaces. [**A**] and [**B**] refer to the cathode used for MFC_BC1; [**C**] and [**D**] to the case of MFC_BC2 83

Figure 5.1. Polarisation curves for the MFCs after 2 weeks of enrichment for: [**A**] MFC_N; [**B**] MFC_E; [**C**] MFC_P; [**D**] MFC_M. Current density refers to the anode surface area, 0.32 cm^2. Data is the average of 2 devices with up to 19.5% error 103

Figure 5.2. Maximum power densities obtained for each membrane material used and relative electrode spacing. The power density refers to the MFC chamber volume, (electrode spacing 4 mm = 128 µL, electrode spacing 6 mm = 192 µL, electrode spacing 8 mm = 256 µL). Electrode spacing for each device (in mm) is denoted by the corresponding number on the x-axis. Data is the average of 2 devices with up to 19.5% error 104

Figure 5.3. Amperometric response of the MFC sensors to increasing values of COD in the feeding solution. Semi-log plot. [**A**] MFC_N, [**B**] MFC_E, [**C**] MFC_P, **[D]** MFC_M. Numbers within each figure denote the electrode spacing of each device (mm). Error bars refer to two replicates 105

Figure 5.4: Summary of the sensitivities towards BOD for each MFC device. The values refer to an anode surface area of 0.32 cm^{-2}. Electrode spacing for each device (in mm) is denoted by the corresponding number on the x-axis. Error bars refer to two replicates 106

Figure 5.5. SEM images of the membranes/cathode facing the anode chamber after 12 weeks of operation. [**A**] MFC_E; [**B**] MFC_M; [**C**] MFC_N; [**D**] MFC_P 108

Figure S5.1. Extraction of eggshell membrane from a fresh egg 114

Figure S5.2. Preparation of PDMS membrane onto carbon cloth 114

Figure S5.3. Experimental set up for the MFC biosensors testing 114

Figure S5.4. Power curves for the MFCs after 2 week of enrichment. [**A**]: MFC_N devices, with MFC_N8 expanded for clarity. [**B**]: MFC_E devices. [**C**]: MFC_P devices. [**D**]: Power MFC_M devices. Current density refers to the anode surface area, 0.32 cm^2. Power density refers to the MFC chamber volume, (electrode spacing 4 mm = 128 µL, electrode spacing 6 mm = 192 µL, electrode spacing 8 mm = 256 µL). Data is the average of 2 devices with up 19.5% error 115

Figure S5.5. Linear range of the amperometric response of the MFC sensors to increasing values of COD in the feeding solution. [**A**]**:** MFC_N, [**B**] MFC_E, [**C**] MFC_P, [**D**] MFC_M. Numbers within each figure denote the electrode spacing of each device (mm). Error bars refer to two replicates 116

Figure S5.6. SEM images of unused membranes, treated with the same assay for cell fixation. [**A**] MFC_E; [**B**] cathode facing the anode chamber in the membrane-less device MFC_M; [**C**] MFC_N; [**D**] MFC_P 117

Figure 6.1. Power and polarisation curves for the MFC biosensor after one week of enrichment. Current density refers to the anode surface area, 0.32 cm^2. Power density refers to the MFC chamber volume, 128 µL. Data is the average of 3 devices with up to 6.2% error 136

Figure 6.2. [**A**] Average steady state current from MFC biosensors as a function of temperature. Data is an average of 3 MFCs with up to 6% error. [**B**] Average steady state current from MFC biosensors as a function of pH. Data is an average of 3 MFCs with up to 12% error. [**C**] Average steady state current from MFC biosensors as a function of conductivity. Data is an average of 3 MFCs with up to 11% error. 138

Figure 6.3. MFC response to AW containing varying potassium acetate concentrations indicated (in mM) with numbers in the figure. [**A**] Current output change with time. [**B**] Average steady state current from MFC biosensors as a function of potassium acetate concentration. Data is an average of 3 MFCs with 8.4% error..... 141

Figure 6.4. MFC biosensor response to formaldehyde. [**A**] Current output versus time. Formaldehyde in AW was injected into the MFCs for 10 min; subsequently the MFCs were fed with AW with no formaldehyde. The number adjacent to each line indicate the concentration of formaldehyde (ppm). [**B**] Change in current after formaldehyde injection

versus formaldehyde concentration. For all data response is an average of 3 MFCs with up to a 12.5% error..... 142

Figure 6.5. MFC biosensor response to atrazine. [**A**] Current output versus time. Atrazine in AW was injected into the MFCs for 30 min; subsequently the MFCs were fed with AW with no atrazine. Number adjacent to each line indicate the concentration of atrazine (ppm). [**B**] Change in current after atrazine injection versus atrazine concentration. For all data response is an average of 3 MFCs with up to 24% error..... 145

Figure S6.1. Experimental set up for testing the MFC biosensors. Disturbances (e.g. change in temperature, pH, ionic strength, labile organic content or a toxic compound) are introduced *via* a 3 way valve prior to the MFC using an alternative feed tanks (1 & 2). Feed tank temperature is controlled by a water bath..... 149

Figure S6.2. MFC current response with respect to time for AW with variations in environmental factors (as indicated with numbers in the figure of °C and mS cm^{-1} for temperature and conductivity respectively). [A] Temperature, data is an average of 3 MFCs with up to 6% error; [B] pH, data is an average of 3 MFCs with up to 12% error; [C] conductivity. Data is an average of 3 MFCs with up to 11% error..... 150

Figure 7.1. [**A**] Schematic of the pMFC and electrical connection; [**B**] Photograph of the actual pMFC, showing size; [**C**] Principle of operation of the pMFC; and [**D**] Assembly of the fpMFC by folding two pMFCs back-to-back (**1),** with parallel electrical connection (**2**). 170

Figure 7.2. SEM images of: [**A**] paper surface after cross-linking, [**B**] non-cross-linked paper, [**C**] electrode cross section after cross-linking, [**D**] non-cross-linked electrode cross section. 172

Figure 7.3. Enrichment of pMFC. Arrows indicate replacement of 10% of the feed with fresh AW containing 10 mM potassium acetate and no anaerobic sludge. At almost 6 days (indicated with a *) electrochemical analysis (linear sweep voltammetry and electrochemical impedance spectroscopy) was performed. Error bars (referring to experiments conducted in duplicate) are indicated by grey shaded region..... 173

Figure 7.4. [**A**] Power and [**B**] polarisation curves for the pMFC and fpMFC. Power and current densities refer to the geometric anodic electrode area: 2 cm^2. [**C**] Comparison of electrochemical impedance spectroscopy curves for the pMFC and fpMFC. 174

Figure 7.5. SEM images of the anode surface after 24 h inoculation in AW, containing 10% *v/v* anaerobic sludge for: [**A**] cpMFC; [**B**] pMFC. In both cases the anodes were connected to the cathode through a 1 kΩ external resistor and the cell voltage was monitored..... 176

Figure 7.6. Amperometric response of the pMFC and fpMFC to an injection of 1000 ppm formaldehyde. The grey shaded region refers to the error between duplicate measurements 177

Figure S7.1. Calibration curve for HPLC peak area against glycolic acid concentration..185

Figure S7.2. Schematic of the operation mode of the pMFC and fpMFC..... 186

Figure S7.3. Effect of the degree of cross-linking on the tensile strength of the wetted paper. The concentrations of glyoxal in the final treated paper were achieved by exposure of paper to 0, 3, 6, 12, and 24 *w/v*% aqueous solutions of glyoxal..... 186

Figure S7.4. Cyclic voltammetry tests of the pMFC before and after cross-linking, performed with the anode immersed in 5 mM ferricyanide solution and the cathode exposed to air. The anode was operated as the working electrode and the cathode as the counter electrode. Five cycles were performed at a scan rate of 5 mV s^{-1}. 187

Figure S7.5. SEM image of the biofilm on the anode of the pMFC after 10 days of operation. 187

Figure S7.6. Relative growth of the biofilm on the anode of a pMFC when doped with and without chitosan..... 188

Figure S7.7. Cyclic voltammetry tests of the cpMFC after cross linking, performed with the anode immersed in 5 mM ferricyanide solution and the cathode exposed to air. The anode was operated as the working electrode and the cathode as the counter electrode. Scan rate: 5 mV s^{-1}. 188

Figure 8.1. Schematic of the operation of light dependent bioelectrochemical systems: [**A**] complex photosynthetic microbial fuel cells; [**B**] biophotovoltaic systems. 199

Figure 8.2. [**A**] Schematic of the photoMFC construction (to scale); [**B**] schematic of the experimental set up for operation of the photoMFC. 201

Figure 8.3. Characterisation of a typical amperometric toxicant response curve from the photoMFC device. 205

Figure 8.4. Enrichment of the electrochemically active microbial culture within the miniature photoMFC. 207

Figure 8.5. Average day time and night time currents of the photosynthetic MFCs: [**A**] over their one month operation period, * indicates period of static enrichment; [**B**] to the end of their lifetime from days 21 to 34. Data is an average of three devices..... 208

Figure 8.6. [**A**] Polarisation and power curve for the photoMFC. Power and current density refer to anodic geometric surface area, 0.32 cm^2. Data is the average of three devices. [**B**] Complex plane (Nyquist) plot for the photoMFC, with the asymmetric plot overlaid. 209

Figure 8.7. PhotoMFC amperometric response to formaldehyde. [**A**] Current output *versus* time when dosed with AW containing formaldehyde at 10 – 2000 ppm. A 30 min long formaldehyde injection was applied to the system, followed by feeding with AW containing no formaldehyde. Legend refers to the specific formaldehyde concentration (ppm) applied. Data is the average of 3 devices with 14% accuracy. [**B**] Normalised change in current during the toxic event *versus* the formaldehyde concentration dosed. Error bars refer to triplicate experiments. 212

Figure 8.8. SEM images of the anodic biofilm within the photoMFC with: [**A**]: analysis subsequent to formaldehyde dosing; [**B**]: analysis of devices never subjected to formaldehyde. 213

Figure S8.1. Equivalent circuit model used to model EIS data. Where R_Ω is the ohmic resistance, R_{ct} is the charge transfer resistance, W_d is the diffusion-related resistance (using a Warburg diffusion element), and CPE is a constant phase shift element. Constant phase shift elements have been used to account for the depressed nature of the semicircles, and to account for surface roughness and inhomogeneity at the electrode surface. 218

Figure S8.2. Initial slope of the current response towards the injection of formaldehyde at concentrations between 10 – 2000 ppm. Error bars refer to triplicate experiments. 218

Figure S8.3. Step tracer experiment data for residence time distribution analysis of the photoMFC. F(t) represents the step response curve of the normalised concentration of tracer compound, fluorescein, and E(t) represents the residence time distribution function as previously described 219

Figure 9.1. Example factors in water systems that may affect the biosensing capability of an MFC for water quality monitoring described 224

Figure 9.2. Concept for MFC biosensing in field. The MFC may be installed at the effluent of the process, and used to monitor its quality in real time. Filtration of the MFC outlet may be required to prevent microbial contamination of the effluent. 226

Figure 9.3. MFCs as shock biosensors. During normal operation the MFC produces a current between an upper and lower current limit, I_U and I_L respectively, which will account for natural variation of the influent. A toxic event causes the current to fall outside the safety range, and an alarm is given for further testing and/or a call for containment of the toxic event. 228

Figure 9.4. Concept for the use of paper-based MFC biosensors. **1**) Pre-enrichment of an electroactive biofilm on the MFC; **2**) Storage of the MFC; **3**) Deployment of the MFC in a water source for detecting toxicants and signal sent to user (for instance to a mobile phone); **4**) Safe disposal of device by biodegradation. 229

List of tables

Table 2.1. Commercially used field based test methods for common toxicants..... 16

Table 2.2. Summary of analytical performance, construction and functional characteristics of MFCs used as BOD sensors 26

Table 2.3. Summary of the analytical performance, construction, and functional characteristics of MFCs used as toxicant sensors..... 31

Table 4.1. Summary of performance of the several MFCs tested in this study.....82

Table 5.1. A summary of MFC based BOD biosensors..... 107

Table S5.1. Summary of biosensors used for BOD measurement. For comparison the standard BOD_5 test is also shown..... 111

Table S5.2. Steady state current output of the MFCs after 2 weeks of enrichment, data is an average of 2 devices 112

Table S5.3 Summary of the performance of the MFCs used in this study. 113

Table 6.1. Summary of other MFC based biosensors for formaldehyde detection..... 143

Table S6.1. Summary of the sensing performance of the MFC towards labile organic content and environmental parameters. Sensitivity is normalised by the anodic surface area (0.32 cm^2). 148

Table S6.2. Summary of the sensing performance of the MFC towards formaldehyde and atrazine. Sensitivity is normalised by the anodic surface area (0.32 cm^2)..... 149

Table S7.1. Summary of paper-based microbial fuel cells described in the scientific literature..... 182

Table S7.2. Degree of cross-linking of paper by use of glyoxal and corresponding tensile strength of the paper samples 184

Table S7.3. Summary of performance of the pMFC and fpMFC. Power and current densities refer to an anodic electrode area of 2 cm^2. 184

Table S7.4. Summary of the sensing capability of the pMFC and fpMFC towards a 1000 ppm injection of formaldehyde. 184

Table S7.5. Summary of other MFC based biosensors for formaldehyde detection 185

Table S8.1. Summary of the power performance of the photoMFC. Power and current density refer to anodic geometric surface area, 0.32 cm^2. 217

Table S8.2. Summary of other MFC based biosensors for formaldehyde detection 217

Table 9.1. Summary of MFC biosensors developed in this thesis for detecting organic load 222

Table 9.2. Summary of MFC biosensors developed in this thesis for formaldehyde toxicity detection 223

Table 9.3. Number of experimental runs required to fulfil factorial DOE methods 226

1 Introduction

1.1 The global water crisis

The sustainable and secure provision of water is currently one of the biggest challenges faced by the global population. Due to a rapid growth in population, continued economic development and growing demands on global agriculture, the scarce supply of freshwater has become a major threat to sustainable socio-economic development, and the livelihood of humans and ecosystems [1]. This is especially evident in developing countries [2]. As such, in 2015, the World Economic Forum defined the water supply crisis as the top high-impact risk factor for our current times [3]. Moreover, the United Nations has defined the reduction of the number of people suffering from water scarcity as one of their Sustainable Development Goals [4]. Currently, it is estimated that 844 million people do not have access to clean water, and 2.3 billion don't have access to adequate sanitation [5]. Therefore, the provision of freshwater to all is essential to combat the water crisis we currently face. However, this is no simple task.

Water is extensively used in industrial, agricultural and domestic applications [2,6,7]. The continued use and improper management of water sources has led to the contamination of vital water sources with a plethora of contaminants [7,8]. These include: macro-contaminants, such as nitrogen, phosphorous, natural organic constituents, salts; micro-contaminants, such as heavy metals, metalloids, pesticides, pharmaceuticals and biocides [6,8], all of which pose a serious risk to sustainable drinking water supply and the maintenance of human health and the aquatic ecosystem [2]. Therefore, to ensure the provision of safe and secure water, effective water quality monitoring programmes are required [7,9]. These can dramatically improve the understanding of health risks of water sources and aid in the effective management of water sources, such as aquifers, riverine environments, rainwater harvesting systems, and treated wastewater [10].

Effective water quality monitoring programmes, however, heavily rely on the deployment of methods that are rapid, reliable, cost-effective, and preferably onsite and continuous in operation [1,7,10]. Classically, chemical methods for water analysis

are used, such as chromatographic and spectroscopic methods. Despite their accuracy however, they represent a high cost and heavy time requirement which make them unsuitable for large scale water quality monitoring programmes [9,11]. Biological methods, namely bioassays (which use microorganisms such as daphnia, algae or fish), can provide a means to test for the overall toxicity of water sources containing bioactive compounds. The methods can unfortunately be complex in use, and due to the time required for analysis, are not suitable for online and continuous analysis [12]. In recent years, the development of biosensors has shown great promise for straightforward, rapid and cost-effective monitoring of water quality. In particular, microbial fuel cell (MFC) technology has emerged as a promising means for the detection of pollutants in water sources. Henceforth, the focus of this thesis is on the development of MFC technology for water quality monitoring.

1.2 Microbial fuel cells for water quality monitoring

MFCs are devices capable of converting chemical energy into electrical energy *via* the metabolic processes of microorganisms (most commonly bacteria) [13]. The principles of operation of an MFC are described in detail in Chapter 2. MFCs have the distinct ability to utilise complex and waste biomass as a fuel source, and are able to sustain long term operation at ambient temperatures [14] and neutral pH [15,16]. Therefore, research surrounding MFC technology has focussed on applications such as wastewater treatment [17], energy harvesting and utilisation [18], the powering of remote sensors [19] and the generation of energy for remote location applications [20].

Additionally, MFCs have also recently received much interest for use as sensors. Microbes respond with good sensitivity, specificity and accuracy to their own environment [21]; and since an MFC can capture the microbial response *via* the electricity it generates, MFCs have an excellent inherent capability to act as sensors for their environment. Therefore, the development of MFCs as biosensors for biological oxygen demand (BOD) [22,23] and toxic compounds [24,25] has been demonstrated. Indeed, MFC biosensors have been shown to be sensitive to bioactive compounds such as Cu^{2+} [26], Ni [27] and formaldehyde [28], with dynamic ranges and detection limits lower than 1 ppm. However, for the commercial realisation of

MFC biosensors, certain challenges must be overcome. These are summarised below, but a further discussion of these can be found in Chapter 2.

Firstly, the simplicity of MFC sensing systems must be improved. For this, the design and mode of operation of MFCs should be simplified to allow straightforward use. For instance, many MFC biosensors rely on a two chamber configurations, which inflicts additional pumping and material costs. Therefore, the investigation towards the use of single chamber devices, which utilise an air breathing cathode design, should be sought.

The miniaturisation of MFCs also has the potential to enable their practical deployment. Miniaturisation allows the cost of the device to fall, whilst enabling the potential to assemble MFCs into stacks for multiple readings and detection of a range of pollutants onsite. Miniaturisation also enhances the power density achievable by the device, by increasing the surface-area-to-volume ratio of the MFC. This improves mass transfer processes within the MFC chamber [29], thus enhancing the detection of pollutants in the bulk solution of the device and improves detection response times [25,30].

Secondly, an effort to reduce the cost of MFC biosensors must be conducted. This may be realised through a combination of miniaturisation, but also through the use of alternative and inexpensive membrane materials and cathode catalyst materials- which heavily influence the cost of MFC devices [31]. Currently, studies for alternative membrane materials [32] and cathode catalysts [33–36] have been conducted for MFC energy generation devices, but their application and effect for MFC biosensors is seldom reported.

Last of all, the MFC biosensing capability in real water samples should be understood, since the device may be susceptible to a range of toxic compounds as well as changes in the environmental conditions of the analyte solution. In this instance, the MFC should be able to identify the presence of toxic compounds and still provide a simple means to analyse the resultant data. Moreover, the development of MFC systems that are capable of detecting emerging contaminants in water systems, such as pesticides, herbicides and pharmaceuticals, should be sought.

1.3 Aims and objectives

This thesis is aimed at the development of a simple, cost-effective and real time method to test water quality. In this context, the aim of this research is to design and develop cost-effective MFCs and to demonstrate the use of this technology as a water quality monitoring tool that is cheap, simple to use, rapid, and sustainable.

The objectives to address this aim are described within broad themes as follows:

1) Miniaturisation for improved MFC biosensors:
    a. Design a miniaturised MFC device.
    b. Assess the MFC capability to generate energy.
    c. Determine the effect of stacking MFCs for increasing power output.
2) Development of cost-effective devices:
    a. Investigate the use of alternative cost-effective membrane materials for the miniature MFC.
    b. Assess the applicability of said membrane materials for MFC biosensors (in the context of detecting labile organic carbon content).
    c. Determine the effect of biomass derived catalysts for enhancing the power performance of the miniature MFC.
    d. Design, develop and test a small scale cost-effective paper-based MFC biosensor.
    e. Assess the capability of said paper-based MFC for water quality monitoring.
3) Development of MFC biosensors for water quality monitoring:
    a. Determine the effect of environmental factors (temperature, pH, ionic strength) on MFC performance.
    b. Determine the capability for the miniature MFC to detect contaminants in water, in this case formaldehyde (model compound) and atrazine (trace organic compound).
    c. Investigate the use of photosynthetic MFCs (using microalgae) for development of water quality biosensors.

1.4 Outline of the thesis

This thesis opens with a literature review describing the current freshwater scarcity problem the world currently faces, and the importance of water quality monitoring in addressing this. Since those in the poorest regions, including many in developing countries, are the most susceptible to this problem, Chapter 2 has a particular focus on water quality monitoring in developing countries. Current chemical and biological methods of monitoring water quality are discussed, and a review of current MFC technology for this application is presented. The chapter closes with a discussion of the current barriers for the practical implementation of MFC biosensors in this context.

Chapter 3 provides the necessary theory for the thesis, more specifically the electrochemical fundamentals of MFCs is given. Moreover, essential electrochemical methods such as polarisation experiments, cyclic voltammetry, and electrochemical impedance spectroscopy are explained, and criteria for assessing MFC power performance are provided.

In Chapter 4, the design and development of miniature single chamber MFCs is pursued. This case looks at the devices capability to generate energy from a waste feedstock, urine. The concept here is to develop an MFC that generates appreciable amounts of energy, which will render it more suitable for biosensing applications (since an appreciable baseline current is required). Therefore the effect of device geometry, specifically the anodic chamber length, on power performance is investigated, and the effects of this on mass transfer processes within the cell are discussed. To further enhance the energy generation from the MFC whilst pursuing a low cost design, two biomass derived catalysts for oxygen reduction reactions at the air cathode are investigated. Finally, with the aim of increasing power generation from the system further, the effect of stacking miniature MFCs electrically is studied.

Since the cost of MFC devices currently limits their commercial realisation, Chapter 5 investigates the potential of alternative low cost membrane materials for use in MFCs, and assesses the subsequent devices ability to detect the labile organic content in wastewater. A natural polymer (eggshell membrane) and synthetic polymer (polydimethylsiloxane, PDMS) are used, as well as a membrane-less design and an MFC with the commonly used Nafion membrane. Moreover, the effect of device geometry is once again investigated to further guide the design of miniature MFC

biosensors, with the focus this time on electrode spacing and its effect on power performance and sensing capability.

The capability of the developed MFC biosensor as a water quality monitoring tool is then further investigated, by assessing the ability to detect toxic compounds in wastewater in Chapter 6. As a proof of concept toxicant, formaldehyde is used to initiate a toxic event to the MFC system, and the corresponding current responses are investigated. The applicability of the MFC biosensor towards detection of trace organic compounds is also studied, by investigating the effect of atrazine on the current generation of the MFC. Since real water samples will experience changes in organic load and environmental factors such as pH, temperature and conductivity, the effect of these on the current generation from the MFC are also investigated. The chapter also provides a perspective into enabling the MFC technology for water quality monitoring through use of factorial design of experiment methodology.

Chapter 7 presents a study focused on the development of extremely low cost and easy to dispose MFC biosensors, through the development of screen-printed, biodegradable and portable paper-based MFCs. The design of a single component paper-based MFC is presented, with a focus on enhancing its structural properties to render it suitable for water monitoring applications. Then its potential to detect contaminants in water is investigated. The proof of concept for toxicant detection is demonstrated with formaldehyde, and a simple method (by stacking the MFC devices) to improve the current baseline and sensor sensitivity is also shown.

Finally, with an effort to enhance the sensitivity of MFC based biosensors towards emerging contaminants such as herbicides, pesticides and pharmaceuticals, the use of microalgae as a novel sensing element in a miniature photosynthetic MFC is demonstrated in Chapter 8. This work portrays the development of a light dependent photosynthetic MFC and its power generation properties are investigated, before a proof of concept towards water quality monitoring is shown through the detection of formaldehyde in water, thus paving the way for future research with these systems.

1.5 References

[1] J. Liu, H. Yang, S.N. Gosling, M. Kummu, M. Flörke, S. Pfister, N. Hanasaki, Y. Wada, X. Zhang, C. Zheng, J. Alcamo, T. Oki, Water scarcity assessments in the past, present, and future, Earth's Future. 5 (2017) 545–559. doi:10.1002/2016EF000518.

[2] W.A. Jury, H.J. Vaux, The Emerging Global Water Crisis: Managing Scarcity and Conflict Between Water Users, Adv. Agron. 95 (2007) 1–76. doi:10.1016/S0065-2113(07)95001-4.

[3] World Economic Forum, Global Risks 2015, Geneva, 2015. http://www3.weforum.org/docs/WEF_Global_Risks_2015_Report15.pdf (accessed September 7, 2017).

[4] United Nations, Sustainable development goals - United Nations, (2017). http://www.un.org/sustainabledevelopment/sustainable-development-goals/ (accessed September 7, 2017).

[5] World Health Organisation (WHO), United Nations Children's Fund (UNICEF), Progress on Drinking Water, Sanitation and Hygiene: 2017 Update and SDG Baselines., Geneva, 2017. http://www.wipo.int/amc/en/ (accessed September 7, 2017).

[6] R.P. Schwarzenbach, T. Egli, T.B. Hofstetter, U. von Gunten, B. Wehrli, Global Water Pollution and Human Health, Annu. Rev. Environ. Resour. 35 (2010) 109–136. doi:10.1146/annurev-environ-100809-125342.

[7] F. Lagarde, N. Jaffrezic-Renault, Cell-based electrochemical biosensors for water quality assessment., Anal. Bioanal. Chem. 400 (2011) 947–964. doi:10.1007/s00216-011-4816-7.

[8] E.A. Murphy, G.B. Post, B.T. Buckley, R.L. Lippincott, M.G. Robson, Future Challenges to Protecting Public Health from Drinking-Water Contaminants, Annu. Rev. Public Health. 33 (2012) 209–224. doi:10.1146/annurev-publhealth-031811-124506.

[9] M. Woutersen, S. Belkin, B. Brouwer, A.P. van Wezel, M.B. Heringa, Are luminescent bacteria suitable for online detection and monitoring of toxic compounds

in drinking water and its sources?, Anal. Bioanal. Chem. 400 (2011) 915–929. doi:10.1007/s00216-010-4372-6.

[10] S.B. Velasquez-Orta, D. Werner, J.C. Varia, S. Mgana, Microbial fuel cells for inexpensive continuous in-situ monitoring of groundwater quality, Water Res. 117 (2017) 9–17. doi:10.1016/j.watres.2017.03.040.

[11] E. Awuah, K.B. Nyarko, P.A. Owusu, K. Osei-Bonsu, Small town water quality, Desalination. 248 (2009) 453–459. doi:10.1016/j.desal.2008.05.087.

[12] R.E. Dewhurst, J.R. Wheeler, K.S. Chummun, J.D. Mather, A. Callaghan, M. Crane, The comparison of rapid bioassays for the assessment of urban groundwater quality, Chemosphere. 47 (2002) 547–554. doi:10.1016/S0045-6535(02)00060-7.

[13] M.C. Potter, Electrical Effects Accompanying the Decomposition of Organic Compounds, Proc. R. Soc. B Biol. Sci. 84 (1911) 260–276. doi:10.1098/rspb.1911.0073.

[14] L.H. Li, Y.M. Sun, Z.H. Yuan, X.Y. Kong, Y. Li, Effect of temperature change on power generation of microbial fuel cell, Environ. Technol. 34 (2013) 1929–1934. doi:10.1080/09593330.2013.828101.

[15] Z. He, Y. Huang, A.K. Manohar, F. Mansfeld, Effect of electrolyte pH on the rate of the anodic and cathodic reactions in an air-cathode microbial fuel cell, Bioelectrochemistry. 74 (2008) 78–82. doi:10.1016/j.bioelechem.2008.07.007.

[16] M. Kim, S.M. Youn, S.H. Shin, J.G. Jang, S.H. Han, M.S. Hyun, G.M. Gadd, H.J. Kim, Practical field application of a novel BOD monitoring system, J. Environ. Monit. 5 (2003) 640–643. doi:10.1039/b304583h.

[17] D. Jiang, M. Curtis, E. Troop, K. Scheible, J. Mcgrath, B. Hu, S. Suib, D. Raymond, B. Li, A pilot-scale study on utilizing multi-anode/cathode microbial fuel cells (MAC MFCs) to enhance the power production in wastewater treatment, 36 (2011) 876–884. doi:10.1016/j.ijhydene.2010.08.074.

[18] I. Ieropoulos, J. Greenman, C. Melhuish, I. Horsfield, EcoBot-III: a robot with guts, in: Artif. Life XII, 2010: pp. 733–740.

[19] C. Donovan, A. Dewan, H. Peng, D. Heo, H. Beyenal, Power management system for a 2.5W remote sensor powered by a sediment microbial fuel cell, J. Power Sources. 196 (2011) 1171–1177. doi:10.1016/j.jpowsour.2010.08.099.

[20] I.A. Ieropoulos, A. Stinchcombe, I. Gajda, S. Forbes, I. Merino-Jimenez, G. Pasternak, D. Sanchez-Herranz, J. Greenman, J. De France, L. Fewtrell, Pee power urinal – microbial fuel cell technology field trials in the context of sanitation, Environ. Sci. Water Res. Technol. 2 (2016) 336–343. doi:10.1039/C5EW00270B.

[21] C. Santoro, C. Arbizzani, B. Erable, I. Ieropoulos, Microbial fuel cells: From fundamentals to applications. A review, J. Power Sources. 356 (2017) 225–244. doi:10.1016/j.jpowsour.2017.03.109.

[22] B.H. Kim, I.S. Chang, G.C. Gil, H.S. Park, H.J. Kim, Novel BOD (biological oxygen demand) sensor using mediator-less microbial fuel cell, Biotechnol. Lett. 25 (2003) 541–545. doi:10.1023/A:1022891231369.

[23] X.C. Abrevaya, N.J. Sacco, M.C. Bonetto, A. Hilding-Ohlsson, E. Cortón, Analytical applications of microbial fuel cells. Part I: Biochemical oxygen demand., Biosens. Bioelectron. 63 (2015) 580–590. doi:10.1016/j.bios.2014.04.034.

[24] B.H. Kim, I.S. Chang, G.M. Gadd, Challenges in microbial fuel cell development and operation., Appl. Microbiol. Biotechnol. 76 (2007) 485–494. doi:10.1007/s00253-007-1027-4.

[25] M. Di Lorenzo, A.R. Thomson, K. Schneider, P.J. Cameron, I. Ieropoulos, A small-scale air-cathode microbial fuel cell for on-line monitoring of water quality., Biosens. Bioelectron. 62 (2014) 182–188. doi:10.1016/j.bios.2014.06.050.

[26] Y. Shen, M. Wang, I.S. Chang, H.Y. Ng, Effect of shear rate on the response of microbial fuel cell toxicity sensor to Cu(II)., Bioresour. Technol. 136 (2013) 707–710. doi:10.1016/j.biortech.2013.02.069.

[27] N.E. Stein, H.V. Hamelers, C.N. Buisman, Influence of membrane type, current and potential on the response to chemical toxicants of a microbial fuel cell based biosensor, Sensors Actuators B Chem. 163 (2012) 1–7. doi:10.1016/j.snb.2011.10.060.

[28] D. Dávila, J.P. Esquivel, N. Sabaté, J. Mas, Silicon-based microfabricated microbial fuel cell toxicity sensor., Biosens. Bioelectron. 26 (2011) 2426–2430. doi:10.1016/j.bios.2010.10.025.

[29] F. Qian, D.E. Morse, Miniaturizing microbial fuel cells., Trends Biotechnol. 29 (2011) 62–69. doi:10.1016/j.tibtech.2010.10.003.

[30] N.E. Stein, H.M. Hamelers, G. van Straten, K.J. Keesman, On-line detection of toxic components using a microbial fuel cell-based biosensor, J. Process Control. 22 (2012) 1755–1761. doi:10.1016/j.jprocont.2012.07.009.

[31] M. Behera, P.S. Jana, M.M. Ghangrekar, Performance evaluation of low cost microbial fuel cell fabricated using earthen pot with biotic and abiotic cathode., Bioresour. Technol. 101 (2010) 1183–9. doi:10.1016/j.biortech.2009.07.089.

[32] S.M. Daud, B.H. Kim, M. Ghasemi, W.R.W. Daud, Separators used in microbial electrochemical technologies: Current status and future prospects, Bioresour. Technol. 195 (2015) 170–179. doi:10.1016/j.biortech.2015.06.105.

[33] L. Zhang, C. Liu, L. Zhuang, W. Li, S. Zhou, J. Zhang, Manganese dioxide as an alternative cathodic catalyst to platinum in microbial fuel cells., Biosens. Bioelectron. 24 (2009) 2825–2829. doi:10.1016/j.bios.2009.02.010.

[34] H. Yuan, L. Deng, Y. Qi, N. Kobayashi, J. Tang, Nonactivated and Activated Biochar Derived from Bananas as Alternative Cathode Catalyst in Microbial Fuel Cells, Sci. World J. 2014 (2014).

[35] Y. Yuan, T. Yuan, D. Wang, J. Tang, S. Zhou, Sewage sludge biochar as an efficient catalyst for oxygen reduction reaction in an microbial fuel cell, Bioresour. Technol. 144 (2013) 115–120. doi:10.1016/j.biortech.2013.06.075.

[36] L. Deng, M. Zhou, C. Liu, L. Liu, C. Liu, S. Dong, Development of high performance of Co/Fe/N/CNT nanocatalyst for oxygen reduction in microbial fuel cells., Talanta. 81 (2010) 444–8. doi:10.1016/j.talanta.2009.12.022.

2 Literature review

This thesis aims to demonstrate the development of cost-effective and sustainable microbial fuel cells (MFCs) for water quality monitoring. As such, this chapter provides a review of current water quality monitoring techniques. The principles of operation of an MFC are described, and their use as biosensors is explained. A review of the current state-of-the-art for MFC biosensors is given, and finally the challenges to progress this technology towards water quality monitoring are discussed. This chapter has been published as detailed on the following page, with minor amendments made to account for style consistency throughout the report (which are done for all following published chapters). Additions for the most up to date literature are also made here.

Statement of authorship

This declaration concerns the article entitled:	Water Quality Monitoring in Developing Countries; can Microbial Fuel Cells be the Answer?
Publication status:	Published
Publication details:	J. Chouler, M. Di Lorenzo, Water Quality Monitoring in Developing Countries; Can Microbial Fuel Cells be the Answer?, Biosensors. 5 (2015) 450–470. doi:10.3390/bios5030450.
Authorship contributions:	Formulation of ideas and manuscript prepared by JC with supervision from MDL.
Statement from candidate:	This paper reports on original research I conducted during the period of my Higher Degree by Research candidature.

Signed: Date:

Water quality monitoring in developing countries, can microbial fuel cells be the answer?

Jon Chouler [a,b], Mirella Di Lorenzo [b]

[a] Centre for Sustainable Chemical Technologies, University of Bath, Bath, BA2 7AY, UK

[b] Department of Chemical Engineering, University of Bath, Bath, BA2 7AY, UK

2.1 Abstract

The provision of safe water and adequate sanitation to developing countries is a must. A range of chemical and biological methods are currently used to ensure the safety of water for consumption. These methods however suffer from high costs, complexity of use and inability to function onsite and in real time. The microbial fuel cell (MFC) technology has great potential for the rapid and simple testing of the quality of water sources. MFCs have the advantages of high simplicity and possibility for onsite and real time monitoring. Depending on the choice of the manufacturing materials, this technology can also be highly cost effective. This review covers the state-of-the-art research on MFC sensors for water quality monitoring, and explores enabling factors for their use in developing countries.

2.2 Freshwater security

The provision of safe and secure water and adequate sanitation is critical to improve livelihood security, economic growth, and to reduce health risks and vulnerability in communities. It has therefore been described as a key target within the Millennium Goals [1–3]. Currently more than 700 million people lack access to safe water, and 2.5 billion do not have access to adequate sanitation. Unsafe water and poor sanitation systems lead to dehydration, malnutrition, and easily preventable diarrheal diseases, which cause over 1.6 million deaths per year. More than 99% of these water-related deaths are concentrated in developing nations, where 84% of those with no access to drinking water live in remote areas [4,5].

Providing freshwater is no simple task. The quality of water systems is affected by changes in nutrients, sedimentation, temperature, pH, and by a multitude of trace compounds, such as heavy metals, non-metallic toxicants, persistent organics and pesticides and biological factors [6,7]. More than one third of the Earth's accessible renewable freshwater is used for agricultural, industrial and domestic purposes, which in turn leads to water contamination *via* a diverse range of synthetic and natural chemicals. In particular, in regions such as South-East Asia and Africa, fluoride and arsenic are compounds of major concern [8]. In India alone, it is estimated that 66 million are at risk due to high fluoride content in groundwater and over 10 million due to excess arsenic [9].

2.3 Current approaches to water quality monitoring in the developing world

2.3.1 Detection of chemicals

As well as sourcing freshwater in developing nations, it is imperative to guarantee the safety of the water for consumption. Water quality monitoring is therefore an important part of providing safe water and improving subsequent water management [10]. Currently, a range of methods are used to test water quality, which may either be laboratory-based assessments or field test kits. Laboratory-based assessments are

required when accurate detection of specific compounds must be completed. These analyses require expensive equipment at central laboratories. For example, arsenic in water systems is commonly detected by atomic absorption spectroscopy [11], while fluoride is typically detected using a potentiometric ion-selective electrode method or ion chromatography [12]. These analyses are off-line and require sample collection which can be a problem in developing countries if the sampling location is in a remote area. This distance between sampling site and testing location adds undue time delays and costs to the water quality monitoring process [13].

Field kit tests offer a useful alternative that provides onsite water monitoring. These kits are generally used for basic analysis such as water temperature, transparency and pH. The detection of specific contaminants by onsite tests is however more difficult. The assessment *via* field based methods for some common contaminants is shown in Table 2.1. Although the detection limits are good, ranging from 2-1000 ppb for arsenic for instance, the analytical quality control of these tests may be questionable and their reproducibility is often limited too [14]. The costs of field based tests may vary widely too, from as low as ~$0.5 up to ~$11.3. Considering the large amount of samples that need testing before a water source can be safely consumed, and the relatively large amount of samples needed for frequent monitoring, these tests can also become costly and unpractical [15]. The requirement of a power source for some field-tests kits, such as for colorimeters, can also be a problem in remote and rural areas.

Table 2.1. Commercially used field based test methods for common toxicants

Toxicant	Threshold value* ($\mu g\ L^{-1}$)	Method	Detection limit ($\mu g\ L^{-1}$)	Approx. cost ($ per test)	Test time (min)	Reference/ Company
Arsenic	10	Merckoquant test strip	20-500	0.5	40	Merck Millipore
		Wagtech Arsenator	0-1000	2.5	40	Wagtech Projects
		Hach EZ test kit	10-500	0.6	20	[16]
		ITS EconoQuick	10-1000	0.6	15	[16]
		Apryon Tech Arsenic test kit	5-800	1.50	30	Apryon Tech
Cadmium	3	Wagtech Metalyser HM 1000	5-1000	11.3	10	Wagtech Projects
		Merckoquant test strip	2-500	1.4	15	Merck Millipore
Fluoride	1500	Wagtech Potakit(r)	0-1500	6.6	40	Wagtech Projects
		Merckoquant test strip	150-800	2	15	Merck Millipore
		HANNA Instruments colorimetric	0-20000	1.4	15	HANNA Instruments
Lead	10	Wagtech Metalyser HM 1000	5-1000	11.3	10	Wagtech Projects
		Merckoquant test strip	20000-500000	1.4	15	Merck Millipore
Nitrate (ion)	50	Wagtech Potakit(r)	0-20000	6.6	40	Wagtech Projects
		Merckoquant test strip	0-20000	1.4	15	Merck Millipore
		HANNA Instruments test kit	0-50000	0.5	10	HANNA Instruments
Nitrite (ion)	3	Wagtech Potakit(r)	0-20000	6.6	40	Wagtech Projects
		Merckoquant test strip	0-20000	1.4	15	Merck Millipore
		HANNA Instruments test kit	0-1000	0.5	10	HANNA Instruments

* as recommended by [17]

2.3.2 Bioassays

Traditional chemical and physical tests for contaminants in water must often be coupled with biological methods (bioassays) to assess their biological availability and bio-toxicity and, consequently, to evaluate their potential effects on human health and the aquatic biota. These assays involve the surveying and measurement of responses from biological organisms to water sources [18]. Biological testing can also determine the effect of bioaccumulation of contaminants over long periods of time, thus giving important indications on the effects of prolonged exposures.

Traditional bioassays involve the use of bacteria as well as complex organisms, such as fish, daphnia, and algae. The responses of these organisms to chemical and physical disturbances and environmental strains is observed during a defined period of time and used as a direct indicator of the safety of the water source [19]. Bioassays are particularly useful in differentiating between biologically active and inactive isomeric molecules. They can also be used to detect very small amounts of compounds in a water body, which proves useful for understanding dose effects of a compound [20]. Moreover, bioassays can give an understanding of the combined effects of multiple contaminants in water (co-contamination). Nonetheless these assays present critical limitations. Firstly, the response of the organism may be affected by their natural cycles (e.g. life stage, reproduction cycle), with the consequence of generating data difficult to interpret and to reproduce. Most bioassays also require long incubation times (in the order of days to weeks) and hence are not viable for onsite monitoring [21].

2.4 Biosensors and the potential of microbial fuel cell based sensors

2.4.1 Biosensors for water quality monitoring

The development of biosensors in recent years has opened great perspectives to the onsite, simplified and cost-effective monitoring of water quality. In a biosensor, a biological recognition element is combined with a physical transducer to convert the biological response to a signal that depends on the analyte concentration [22].

Within a biosensor, the biological recognition element (bioreceptor) responds to a target analyte and the transducer converts the biological response to a detectable signal, often with an amplification and processing step before data is displayed, Figure 2.1. The bioreceptor used can vary widely, from enzymes, antibodies, microorganisms, tissues, cells to higher organisms [23]. Biosensors can be compact, relatively inexpensive and potentially disposable. They can also allow onsite monitoring, thus eliminating the costs associated with collecting, isolating, packaging and transporting the sample to be analysed, as well as providing timely readings [24].

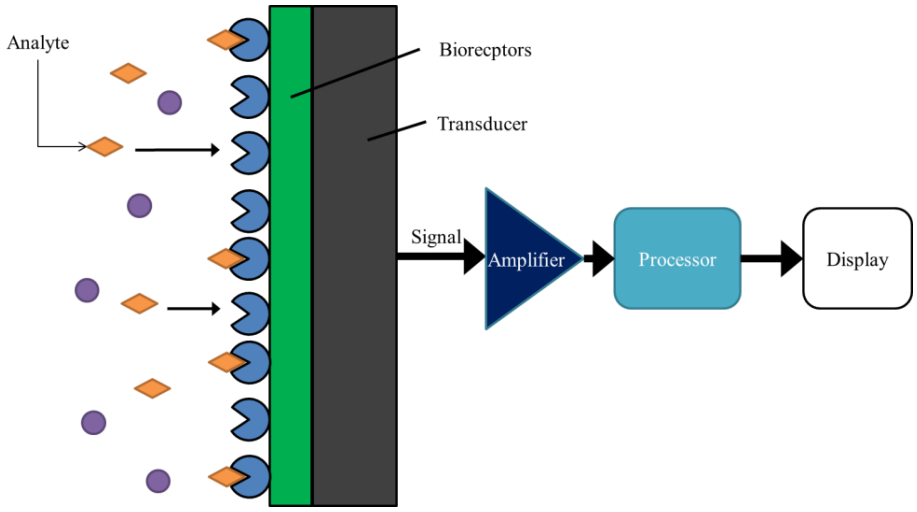

Figure 2.1. Schematic of a biosensor

Large proportions of biosensors are enzymatic and operate *via* electrochemical means. Enzymatic biosensors have the advantage of high selectivity towards the target analyte [24]. They suffer, however, from time consuming and costly enzyme purification and immobilisation protocols, and short life time and poor stability, due to enzyme deactivation or leaching [25]. The use of bacteria offers instead the advantage of great simplicity associated with biocatalyst preparation, especially when large quantities are required. Microbial biosensors are also more versatile and sensitive to a large variety of analytes, thanks to the mixture of enzymes that they contain in their cells [25]. Electrochemical approaches, e.g. amperometry, potentiometry, and conductometry, are usually implemented for microbial sensors [26]. Optical microbial biosensors are, however, also common [23].

Microbial biosensors have been investigated mainly as water quality monitoring devices and currently, few prototypes used as water toxicity sensors have been commercialised [25,26]. The use of microbes that survive under highly alkaline, acidic, high temperature, and saline conditions opens attractive perspectives on water monitoring for industrial process waste monitoring [27]. The full deployment of microbial biosensors is however faced with various challenges. These include low selectivity, low detection limits, risk of contamination with other microorganisms, and mass transfer limitations caused by the necessary permeation of substrates and products through the cells [20,27].

2.4.2 Principles of MFC technology

Microbial fuel cells are devices that directly convert the chemical energy in organic matter into electricity *via* metabolic processes of microorganisms [28]. An MFC comprises of two electrodes, an anode and a cathode, in the presence of an electrolyte. The two electrodes are usually divided by a proton exchange membrane (PEM), and are connected by an external circuit that includes an external load, Figure 2.2. Electroactive bacteria (anodophiles) reside at the anode of the device in the form of a biofilm. The anodophiles oxidize the biodegradable organic molecules present in the feed solution and generate electrons, protons and carbon dioxide. In the absence of oxygen and other soluble oxygen acceptors, the electrons are extracellularly transferred to the anode and flow through the external circuit towards the cathode thus producing electricity. Protons migrate through the PEM to the cathode and react with electrons and an electron accepter (usually oxygen) to form water.

Usually, carbon based materials are implemented as electrodes. These are typically in the form of carbon cloth, carbon paper, graphite rods, plates, granules, and reticulated vitreous carbon [29]. The anode material must be porous and have a large surface area to accommodate biofilm growth. The cathode is usually doped with catalysts, such as platinum, in order to increase the rate of oxygen reduction reactions at the electrode surface. The most typically used PEM are made from Nafion or Ultrex. Figure 2.2 shows the two chamber configuration, which is the simplest form of MFC. Single chamber devices with the cathode, directly exposed to air as an oxygen source and a membrane bound to the cathode, are also very common. The air-cathode configuration,

can lead to a more compact and simpler device. The costs of operation are also reduced due to the catholyte pumping and air/oxygen purging not being required.

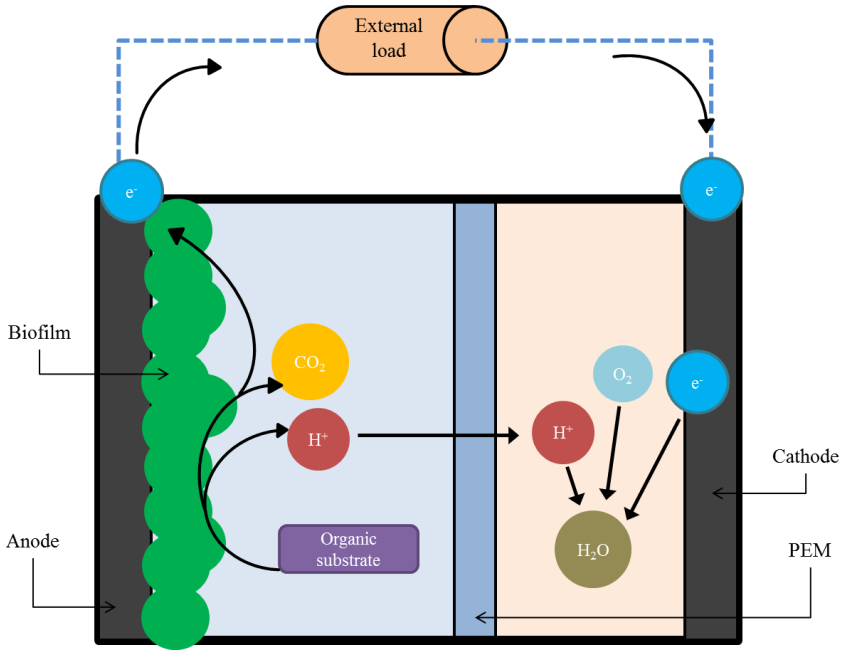

Figure 2.2. Operating principles of a two chamber MFC (not to scale). The electroactive biofilm at the anode break down an organic substrate to produce electrons, protons and CO_2. The electrons pass through an external load to be reduced at the cathode.

Electron transfer from the biofilm to the anode surface may occur by direct electron transfer (DET), *via* either direct contact or nanowires, or by mediated electron transfer (MED), which involves the use of exogenous and/or endogenous mobile electron shuttles, Figure 2.3 [30,31]. Bacteria, such as *Shewanella* species can use either of these mechanisms and are therefore defined as 'true anodophiles'. *Pseudomonas* species instead can only transfer electrons *via* a MED process involving endogenous compounds such as phenazines [32]. Examples of exogenous chemical mediators are neutral red or athraquinone-2,6-disulfonate. These are added to the anodic side to enable electron relay by bacteria that would usually be unable to transfer electrons to the electrode. The use of exogenous mediators is however not suitable for practical applications of MFCs since the cost of operation increases and possible toxicological problems of mediator release or treatment arise [20].

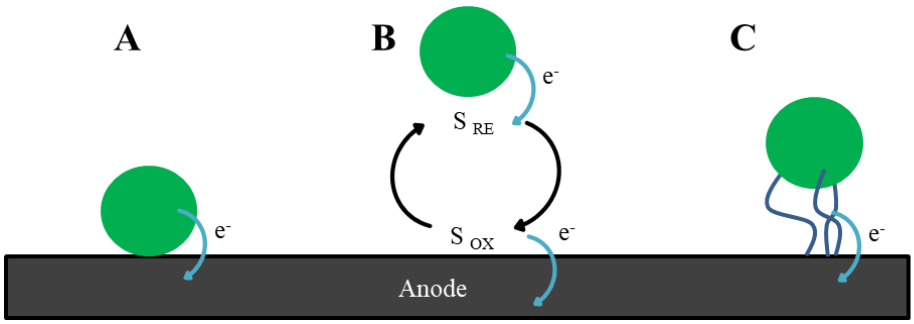

Figure 2.3. A schematic of three electron transfer mechanisms of microbes at the anode surface: [**A**] direct transfer by contact, [**B**] indirect electron transfer by redox shuttles (S_{RE} = reduced electron shuttle, S_{OX} = oxidized electron shuttle), [**C**] electron transfer by conductive nanowire matrix.

The anodophiles in MFCs can degrade a multitude of organic molecules in wastewater, such as acetate, propionate, butyrate [33], while simultaneously generating electricity [34,35]. The most intuitive use of the MFC technology regards therefore the development of devices that treat wastewater whilst generating electricity [36]. MFCs are in particular considered as an energy conversion technology complementary to anaerobic digesters [34,37]. Against conventional anaerobic digestion, MFC technology has the distinct advantage of treating waste with low concentrations of organics (e.g. low chemical oxygen demand, COD) and at low operational temperatures (below 20°C) [37].

Niche applications of MFCs have also been considered. The most promising regards its use as a sensor for water quality [26,38]. Given its simplicity and potential cost-effectiveness, MFC based sensors can be the answer to effective water sensing in developing countries. So far, the use of MFCs for the measurement of the biological oxygen demand (BOD) of water has been proved [39–41]. There are also some preliminary encouraging applications as toxicity sensors [42–44].

2.4.3 MFCs as biosensors: operating principles and concepts

MFC biosensors are an avenue towards simple and sustainable monitoring for target analytes in water [45] that can be operated *in situ* and online. The current generated by an MFC directly relates to the metabolic activity of the electroactive biofilm at the anode surface [46]. Any disturbances of their metabolic pathways are translated into a change on the production of electricity. If operational parameters such as pH, temperature and conductivity of the feeding solution are kept constant, this current change can be correlated to the specific disturbance applied [26,33]. This is the basic principle behind the use of MFCs as electrochemical microbial biosensors.

The anodic biofilm of the MFC acts as the recognition component (bioreceptor). Its response to the specific disturbance affects the rate of flow of electrons to the anode (the transducer) and it is transduced into a measurable current change, Figure 2.4. While in other types of amperometric biosensors for a substrate/analyte oxidation an external voltage has to be applied for proper biosensor function, in MFCs the driving potential is secured by a coupled oxidation of fuel on the anode surface and reduction of an oxidant on the cathode surface [47].

Providing that the anodic reactions are the limiting step, under non-saturated fuel conditions, an alteration in the concentration of biodegradable organic matter fed to the system will result in a direct change in the amount of electrons transferred to the anode and will thus cause a change in the output current [46].Under these operating conditions, MFCs may be used as biosensors for the monitoring of the labile organic carbon in water [41]. Conversely, when the MFC is operated under saturated fuel conditions, with all other environmental factors such as temperature, pH, salinity and anode potential kept constant, a sudden change in the output current may be attributed to the presence of a bioactive compound in the feed stream [48]. The MFC technology could therefore be used to detect toxicants and biologically active components in water.

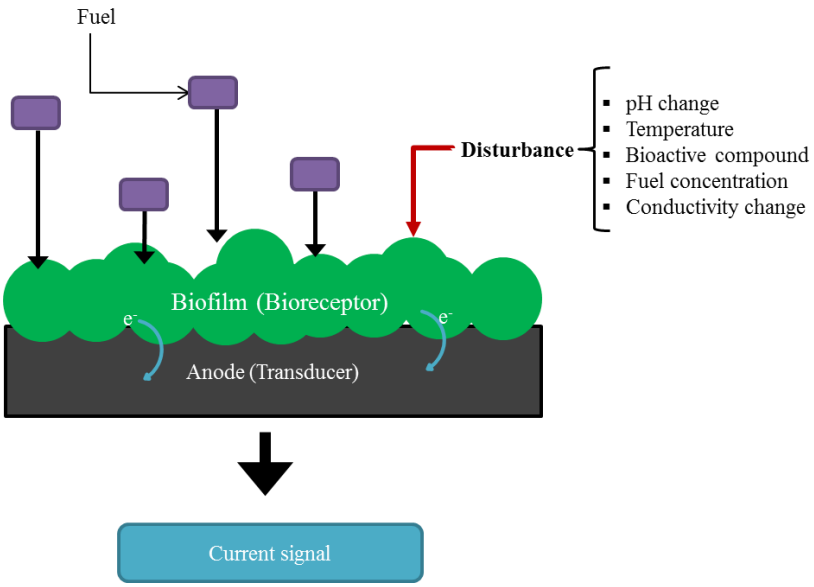

Figure 2.4. Basic principle of an MFC as a biosensor.

In developing the MFC technology for sensing purposes some key requirements must be met, which may differ from those associated with its use for energy harvesting. When the purpose is to generate electricity the focus is on maximising the power output and fuel efficiency. To be used as a biosensor, the MFC must show high sensitivity towards the compound to be detected with minimal risks of false positive or negative alarms. The sensitivity is defined as the electrical signal change per unit change of analyte concentration and is usually referred to the anode surface area, according to Equation 2.1 [46]:

$$sensitivity = \frac{\Delta I}{\Delta C \times A} \qquad \text{Equation 2.1}$$

Where ΔI (μA) is the unit change in the current output; ΔC (mM) is the unit change in the analyte concentration; and A is the electrode surface area (cm^2). High sensitivities are therefore associated with large current changes per unit change in the concentration of the target toxicant.

It is also very important that the sensor generates a constant and stable current output (baseline) [48]. In this regard, Stein *et al.* have suggested, for toxicant monitoring, to carefully control the anodic overpotential and pH of the feed solution to the MFC,

whilst maintaining substrate concentration to a saturated level [48]. In this particular study, anode potentials between -0.4 V and -0.35 V vs. Ag/AgCl provided the most stable output current density.

The MFC biosensor outputs should also be reproducible and independent of operational factors, such as changes in pH, temperature and conductivity of the water samples [20]. The response time, usually defined as the time required to achieve 95% of the steady state current response, should be as short as possible. The recovery time, e.g. the time required to recover from the disturbance applied, should also be fast and the original baseline current should be fully recovered after the toxic event.

To interpret the MFC sensor outputs, the use of artificial neural networks (ANN) was suggested [43]. ANN are a form of flexible mathematical model that are used to identify complex nonlinear relationships between input and output data sets. Acetate, butyrate, glucose and corn starch were able to be correctly identified by ANN in an MFC operated under batch mode [43]. This study therefore provides a good approach for the identification of target compounds from a given MFC signal response. However no relationships between compound concentration and signal response were established for the chemicals studied.

The advantages of MFCs over other biosensors rely on their mechanical and electrical simplicity in both design and operation. No external transducers are required to convert the biological response into a signal, as the presence of a pollutant in the feeding stream is immediately detected by a distinct current change from the system. Although the use of pure cultures has been reported [49], mixed cultures of naturally available microorganisms are usually implemented. The use of mixed cultures guarantees greater stability and it has also shown to lead to MFC-biosensors with better performance [50]. There is no need for time consuming immobilisation procedures of the bioreceptor, as the electroactive biofilm is spontaneously formed onto the biocompatible surface of the anode during the enrichment [51]. MFC based sensors have been shown to be able to operate onsite and continuously to provide real-time monitoring [50]. Furthermore, the electricity generated by the MFC opens the perspective for self-sustaining devices, thereby making them suitable for use in remote area without access to energy [52].

2.4.4 MFCs as sensors for the labile organic carbon content in water

The biochemical oxygen demand (BOD) is a parameter traditionally used to quantify the degree of organic contamination in water systems. The BOD is commonly estimated with the BOD_5 test that requires at least five days of incubation. This test is therefore not suitable for real-time monitoring where rapid feedback is required. In recent years, microbial biosensors have been shown to be a valid alternative to the BOD_5 test for real-time and onsite measurements of the organic carbon content in water. Microbial fuel cells have been widely investigated as BOD sensors [39–41]. The first use of an MFC biosensor for BOD measurement was demonstrated in 1977 [53]. It was shown that the measured current from the device was proportional to the concentration of glutamic acid in a feed solution, with saturation reached at 400 mg L^{-1} (100 µA). The first in field use of the MFC sensor was, however, reported only in 2003 [39]. The sensor showed stable performance for a period up to five years without particular maintenance, with good stability and a correlation between the sensor measurements and the BOD_5. Table 2.2 gives an overview on the MFC based BOD sensors in the literature, and a recent review on the use of MFCs for BOD monitoring can be found in [20]. As reported in Table 2.2, within a certain range, the electrical signal from the MFC biosensor is a direct indicator of the substrate concentration in the feed [54]. It can also be noted that the response time varies with the device design and it reaches its minimum (2.8 min) with a miniature single chamber device (anodic volume: 2 cm^3). As shown in Table 2.2, MFC devices with either a platinum-doped cathode or a catalyst-free cathode have been reported, with no marked difference in performance. It can also be observed that usually the anode is inoculated with mixed bacteria for high substrate versatility and long term stability.

Table 2.2. Summary of analytical performance, construction and functional characteristics of MFCs used as BOD sensors

Microbe assayed (origin)	Anode	Cathode	Membrane used	Configuration	Detection range (BOD_5, mg L^{-1})	Saturation signal	Response time	Reference
Clostridium butyricum	Pt	Carbon	Anion exchange membrane	Two chamber	10-300	120 µA	70 min	[53]
Enriched consortium (wastewater)	Graphite felt	Graphite felt	Cation exchange membrane	Two chamber	2.58-206 (based on charge)	1.1 mA	0.5-10 h	[39]
Consortium (activated sludge)	Graphite felt	Graphite felt	Cation exchange membrane	Two chamber	23-100	6 mA	1 h	[40]
Consortium (activated sludge)	Graphite felt	Graphite felt with Pt	Cation exchange membrane	Two chamber	20-200	5.5 mA	5-36 min	[55]
Consortium (wastewater)	Carbon paper	Carbon cloth with Pt	Cation exchange membrane	Single chamber (air breathing cathode)	38-324	286 mW m^{-2}	0.6 h	[56]
Consortium (anaerobic sludge)	Graphite granules	Carbon paper with Pt	Cation exchange membrane	Single chamber (air breathing cathode)	50-500	0.6 mA	40 min – 2 h	[41]
Consortium (primary clarifier)	Carbon paper	Carbon paper with Pt	Cation exchange membrane	Two chamber	10-250	233 mA m^{-2}	40 min	[57]
Consortium (from an active MFC)	Carbon cloth	Carbon cloth	Cation exchange membrane	Single chamber (air breathing cathode)	3-164	35 µA	2.8-8.7 min	[46]

2.4.5 MFCs as toxicity sensors

Recently, the MFC technology has also been investigated as a sensor for the detection of toxicants in water systems, which are summarised in Table 2.3. The use of MFCs as toxicity sensors was demonstrated for the first time in 2007 by Kim *et al.* who reported an MFC response to contaminants such as Pb^{2+}, Hg, Diazinon (an organophosphorus pesticide) and polychlorinated biphenyls (PCBs) [45]. The lower detection limit was as low as 1 mg L^{-1}; while the upper detection limits were not fully identified given the short concentration ranges studied. Moreover, limited quantitative measurements were provided. The adaptation of the microbial community to toxic substances under continuous operation was highlighted as a concern, which suggests that an MFC biosensor could be used as a shock sensor for toxicants as opposed to a continuous operation mode sensor. The risk of microbial resistance to toxic substances has been raised by [42], who identified the use of immobilized or entrapped cells as a potential solution to this problem. Moreover the continuous regeneration of the anode biofilm with pre-cultured electrochemically-active bacteria could provide another solution [45].

To model the effect of the toxic compound on the MFC performance, Stein *et al.* proposed the use of a modified version of the Butler Volmer Monod (BVM) equation [58]. In particular, the BVM model was modified to include four types of toxic responses related to the four inhibition kinetics of the enzyme involved in the biochemical and electrochemical reaction at the anode. These are the non-competitive, uncompetitive, mixed and competitive inhibition kinetic, characterized by the kinetic parameter, K_i. The resulting model was used to predict the optimum anode overpotential that leads to the highest sensitivity towards a specific toxicant. To verify its validity, the authors used this model to describe the polarisation curves under non-toxic and toxic conditions for three concentrations of Ni (10, 20 and 30 mg L^{-1}) [58]. By identifying the kinetic inhibition type from the relative polarisation curves, this model was suggested as a means to address the specificity of the MFC sensor to given toxicants. More work is however needed to support this proposition.

Another method to model the effect of a toxic compound on the MFC current generation was conducted by relating the concentration of a toxicant injection, in this case formaldehyde between 0.01 – 0.10%, to the current output response of an MFC [59] with an exponential decay equation. Good correlation was found between the

concentration of formaldehyde and the exponent within the model, providing a route for methods to analyse the current response for other toxicant events.

A number of works have investigated characteristics of the MFC design and operation that may affect their performance as a toxicity sensor. Certain characteristics include membrane type, anodic flow regimes, external resistance control methods, shear rate, single chamber devices, and miniaturisation.

The membrane in an MFC isolates the anode and cathode whilst facilitating the necessary proton transport for the redox reaction that generates the cell potential, it also helps preventing oxygen diffusion to the anode. Charged toxicant species may pass through, or be absorbed into, the membrane [60] and hence the selection of the membrane material may affect its performance as a sensor. The effect of the membrane implemented on the MFC biosensor response was investigated [60]. In particular four ion selective membranes were tested: cation exchange, anion exchange, monovalent cation exchange and bipolar membranes. It was shown that the selection of the membrane type appeared to not significantly affect the sensitivity of the device.

To enhance the sensitivity of the MFC biosensor for the detection of Cu^{2+}, the use of a flow through anode was investigated [61]. Moreover, the sensing performance when controlled by a constant external load or a fixed anode potential was studied. By using a flow through anode configuration, the sensitivity of Cu^{2+} detection was enhanced between 15-41 times compared to a parallel flow-by anode due to an improvement of proton mass transfer in the anodic biofilm and improved supply of substrate and toxicant to the biofilm. Controlling the anode potential (to -0.15 V vs. a saturated calomel electrode) gave an almost 60% increase in current change on toxicant exposure when compared to a fixed external load operation.

The effect of the external resistance applied to the MFC on recovery time and sensitivity was investigated [62]. It was found that a low resistance increased sensitivity, and a high resistance resulted in a shorter recovery time. Moreover, the use of external resistance to control the response of the MFC to toxicants was concluded to be preferable over the method of controlling anode potential or current, due to faster recovery times experienced when only external resistance was controlled.

By applying a transient external resistance mode of operation to an MFC (i.e. alternating a connection to and off of an external load at a rate of 1 Hz), the sensitivity towards detection of Cu^{2+} in wastewater was improved by a factor of 2.5 when

compared to running the MFC with a continuous and fixed external resistance [63]. When using the transient state control, it was found that the sensitivity of the voltage response towards organic load changes was increased during the 'on' cycle (i.e. external resistance connected), and sensitivity to a toxic compound exposure was increased with the 'off' cycle (i.e. external load disconnected). This study therefore demonstrated a potential way to monitor for both organic load and a toxic compound in the same water sample through the electrical mode of operation.

The shear rate influences the biofilm formation and structure, and the production of extracellular polymeric substances (EPS) by the bacteria; factors which will affect the diffusivity of toxicants and their interaction with the biofilm [61,62]. Therefore these effects can have an impact on the MFC sensor performance. To investigate this effect the flow rate of the feed, containing Cu^{2+} as a model toxicant, was altered and intermittent nitrogen during enrichment was sparged [66]. In particular, the authors analysed the relationships between biofilm density, porosity and EPS content of the biofilm on the sensitivity, where EPS content is an important component of the biofilm since it impacts the structural integrity of the biofilm matrix [65]. It resulted that low flow rates, leading to biofilms with low density and high porosity, as well as low EPS content improved the sensitivity of the MFC towards Cu^{2+}. Moreover, the use of intermittent sparging during enrichment was beneficial for the sensor sensitivity as it reduced the EPS content, where a reduced EPS content of the biofilm was beneficial as it allows improved mass transport of ions towards the bacteria at the electrode surface.

The performance of a single chamber MFC devices for toxicity sensing has been compared with a two chamber device [67]. In this study, the toxicant events were simulated by altering the pH (by addition of HCl) of the inlet solution. The study demonstrated higher sensitivities for the case of the single chamber device. Moreover, by decreasing the hydraulic retention time the sensitivity improved. Liu *et al.* reported the use of a simple single chamber batch MFC developed as a shock sensor for detection of Cr^{6+}, Fe^{3+}, and NO_3^- in wastewater influents [68].The MFC sensor was able to distinguish between toxic and non-toxic events based on voltage changes produced from the device. Notably Cr^{6+} ions produced a far greater response than Fe^{3+} ions. The NO_3^- ions produced however little effect to the output voltage of the device. Finally, the open circuit potential of the anode was found to be related to the voltage

change response of the device, indicating that the sensitivity of the sensor is dependent on the activity of the biofilm at the anode.

The use of a micro scale MFC toxicant biosensor has been demonstrated [69]. A silicon based device was designed, comprising two 144 µL chambers divided by a proton exchange membrane, with two silicon plates sputter coated with a 150 nm Ti/Ni/Au tri-layer (active area 80 × 80 μm^2) as current collectors. A solution containing potassium ferricyanide was used to assist the oxygen reduction reactions at the cathode. To operate the micro scale MFC as a toxicity sensor, the cell was set at a fixed current (1 µA- equivalent to a current density of 4 µA cm^{-2}) to ensure a stable baseline signal, and observing the changes in output voltage in order to detect the presence of a toxic compound. The effect of formaldehyde was tested in the MFC sensor, and concentrations between 0.1% and 4% *v/v* resulted in a complete drop in output voltage and hence an irreversible inactivation of the biofilm in the cell.

The first single chamber miniature device reported consisted of a small scale and simple single chamber air-cathode MFC fabricated by layer by layer 3D printing [46]. When the fuel cell was operated under saturated conditions, the presence of cadmium ions in the feeding solution was instantaneously detected by a measurable drop in the output current. This change was proportional to the concentration of cadmium within the whole range of concentration considered 1 – 100 µg L^{-1}. The dose-response relationship of the device was established, with a dynamic range of detection between 1 – 25 µg L^{-1} and a sensitivity of 0.2 µA μg^{-1} L^{-1} cm^{-2}. Within the linear range, the changes to the electroactive biofilm were reversible, and recovery after the shock event was possible within 12 minutes. Variance of the data provided showed good repeatability, with a variability of MFC responses within 1.5%. This study highlighted the importance of micro-scaling an MFC sensor, where the use of microfabrication allowed enhanced sensitivity of the sensor and faster response times.

Table 2.3. Summary of the analytical performance, construction, and functional characteristics of MFCs used as toxicant sensors.

Microbe/s assayed (origin)	Anode	Cathode	Membrane	Toxicant detection range	Baseline signal	Response time	Reference
Consortium (activated sludge)	Graphite felt	Graphite felt	Cation exchange membrane	Diazinon 1-10 mg L^{-1} Pb^{2+} 1-10 mg L^{-1} Hg^{2+} 1-10 mg L^{-1} PCBs 1-10 mg L^{-1}	0.04 mA	20 min - 2 h	[45]
Consortium (from an active MFC)	Graphite plate	Graphite plate	Cation exchange membrane	Cu^{2+} 85 mg L^{-1}	1.37 A m^{-2}	50-100 min	[48]
Consortium (primary wastewater)	Graphite rod	Graphite rod	Cation exchange membrane	sulfamethoxazole 0.05–1000 µg L^{-1} sulfadiazine 0.01–1000 µg L^{-1} chloramine B 0.16–3.96 mg L^{-1} $Cu2^{+}$ 0.01–6.0 mg L^{-1} Ag^{+} 0.02–1.0 mg L^{-1} Pb^{2+} 0.41–12.48 mg L^{-1} Hg^{2+} 0.83–8.33 mg L-1	No Data	No Data	[42]
Geobacter sulfurr-educens DSM 12127	Ti/Ni/Au tri-layer	Ti/Ni/Au tri-layer	Cation exchange membrane	Formaldehyde 0.1-4%	4 µA cm^{-2}	< 5 min	[69]
Consortium (from an active MFC)	Graphite plate	Graphite plate	Cation exchange membrane	Ni 10 mg L^{-1}	2.25 mA	30 min	[56,63]
Consortium (real domestic wastewater)	Carbon cloth	Carbon cloth coated with Pt	Cation exchange membrane	Cu^{2+} 5-7 µg L^{-1}	No Data	4 h	[66]
Consortium (wastewater)	Carbon cloth	PTFE treated carbon cloth with Pt	None	Cr^{6+} 1-8 mg L^{-1} Fe^{3+} 1,8,48 mg L^{-1} NO_3^- 1,8,48 mg L^{-1}	0.10 - 0.12 V	5 min	[68]

Table 2.3. (continued) Summary of the analytical performance, construction, and functional characteristics of MFCs used as toxicant sensors.

Microbe/s assayed (origin)	Anode	Cathode	Membrane	Toxicant detection range	Baseline signal	Response time	Reference
Consortium (from an active MFC)	Carbon cloth	Carbon cloth	Cation exchange membrane	Cd^{2+} 0.1-100 µg L^{-1}	32.2 µA	12 min	[46]
Consortium (from an active MFC)	Graphite felt	Carbon fibre brush	Cation exchange membrane	Cu^{2+} 2 mg L^{-1}	0.09 – 1.69 mA	2 h	[61]
Shewanella oneidensis MR-1	Graphite rod	Pt	None	Formaldehyde 0.01 – 0.10%	0.1 mA	> 9.7 h	[59]
Consortium (activated sludge)	Graphite felt	Graphite felt	Cation exchange membrane	Cu^{2+} 1-4 mg L^{-1} Hg^{2+} 2 mg L^{-1} Zn^{2+} 2 mg L^{-1} Cd^{2+} 2 mg L^{-1} Pb^{2+} 2 mg L^{-1} Cr^{3+} 2 mg L^{-1}	~500 mV	~4-20 h	[71]
Consortium (from an active MFC)	Graphite felt	Carbon fibre brush	Cation exchange membrane	Cu^{2+} 2-8 mg L^{-1}	~120 – 400 mV	~ 1 h	[63]
Wild type *pseudo-monas aeruginosa* PA01	Carbon cloth	PTFE treated carbon cloth with Pt	Cation exchange membrane	Formaldehyde 0.003 – 0.075%	15 µA	90 min	[72]
Ochrobactrum anthropi	Carbon paper	Carbon paper	Cation exchange membrane	Cr^{6+} 0.0125 – 5 mg L^{-1}	268 mV	45 min	[73]

2.5 Challenges of implementing MFC biosensor technology for developing countries

Microbial fuel cells hold great potential as simple-to-use, rapid and cost-effective sensing devices for water quality monitoring, as an alternative to traditional analytical methods that are limited by high cost, long test times, and being offline. As a consequence, MFCs could provide great benefits to organisations operating in developing countries [74]. So far, it has been demonstrated that MFC sensors can be sensitive to target compounds with identifiable dynamic ranges and detection limits lower than 1 ppm, and are potentially stable over long term operations. A number of key challenges must, however, be addressed for the practical deployment of this technology. These challenges are discussed below.

2.5.1 Simplicity of use

MFC biosensors have the potential to provide a much simpler detection of bioactive toxicants in water than traditional chemical and biological methods. In the presence of a toxicant in the feeding solution, the MFC sends in fact an instantaneous warning that is easily detected as a change in the output current and does not require complex and expensive transducers. Although conceptually simple, the MFC response to a given toxicant can however be difficult to interpret. Little work has so far been performed on MFC data processing to transform the sensor readings into simple outputs easy to understand by non-experts. Artificial neural networks may provide an avenue towards simplified data outputs from the MFC [43].

The MFC assembly and the testing system must be straightforward and simple, thus allowing straightforward start-up and maintenance of the technology. The MFC design must therefore be simplified and single chamber air breathing cathode MFCs should be better explored for this [46].The majority of the MFC biosensors mentioned in this review rely on a two chamber configurations where either sparged oxygen or ferricyanide are fed to the cathode as an electron acceptor. The benefits of using an air breathing, single chamber device over a two chamber design include reduced operating costs associated with controlling a second feed solution, reduced capital costs of design [75], and a sustainable, passively-fed source of oxygen [76]. This in turn allows the

assembly of the MFC device with fewer parts, and therefore simplify the system set-up and operation. Single chamber devices are also easier to miniaturise [77]. Miniaturisation of MFC devices paves the way for ready-made 3D printed devices that could also be easily assembled into stacks for multiple readings and/or for simultaneous detection of a range of toxicants. Although a couple of small scale single chamber air breathing cathode MFCs have been developed as MFC biosensors [46,65], the development of micro scale MFC biosensors as simple-to-manufacture and effective toxicant sensors still needs to be pursued. As well as reducing costs, miniaturisation also improves mass transport within the fuel cell, and hence any differences in concentration of analyte at the input and at the biofilm on the electrode are reduced- thus leading to a more reliable sensor [70]. Shorter distances within the MFC also allow a faster sensor response time [69]. Response times as short as 3 minutes [46] have been reported for miniature MFC sensors with clear advantages over current time consuming biological methods. However, the process of miniaturisation of MFC biosensors is still in its infancy with further scope for miniaturisation available in order to enhance MFC biosensor performance [46].

2.5.2 Use of inexpensive materials

MFC devices may be cheap to manufacture, as they are commonly made out of plastics (such as acrylic) and carbon materials materials used as electrodes [29]. The manufacturing costs can be further decreased by miniaturisation and by using 3D printing techniques [46]. Despite this, there must be an enhanced effort on MFC cost reduction for applications of MFC based biosensors in developing countries. Both the membrane and the cathode catalyst heavily impact on the device cost. Usually MFCs employ expensive proton exchange membrane, typically made from Nafion or Ultrex, which are also difficult to source in developing regions. Some inexpensive alternative materials have been tested as membranes, such as latex condom [78], pre-fabricated latex gloves [79] and cast ceramics [80], with very promising results. Membrane-less design have also been proposed, where a biofilm develops on both the anode and the cathode surfaces, and provided promising output powers [75,76]. All these studies on alternative membranes are focused on MFCs applications such as energy generation but the use of such materials for sensing purposes has not been demonstrated yet.

The cathode electrode in MFCs is often doped with expensive and precious metals (e.g. Pt), although prototypes with catalyst-free cathodes have been reported [46]. Recently, the use of bio-based catalysts which are recovered from waste and applicable for use as catalysts has been suggested as means to obtain the optimal performance achieved with a Pt cathode, whilst reducing device cost and its carbon footprint. In particular, biochars derived from wood [83], sewage sludge [84], and bananas [85], have been shown to function as effective catalysts in MFC devices for the purpose of energy generation. The full potential of these biomass derived catalysts has not been fully exploited yet and their possible benefit in enhancing sensing performance of MFCs has not been investigated.

2.5.3 Onsite capability

Although many studies have considered the use of real wastewater [45,63,65], the possibility to operate the MFC technology in the field has still to be fully proven. Kim *et al.* have installed an MFC biosensor into a wastewater treatment plant effluent line, which contained a mixture of substances such as aluminium, zinc, mercury and arsenic [45]. Even in this case however, the shock event was mimicked by manually introducing into the feed solution a cadmium and lead mixture. The results show great promise for MFC deployment onsite; however it is necessary to better investigate the sensor behaviour in real contexts.

The effect of a mixture of toxicants in real water supplies on MFC sensing performance must be identified. MFC biosensors must be able to identify toxicants within a mixed contaminant environment and still present a simple and easy to understand output signal. For instance, a recent study by Yu *et al.* studied the ability of an MFC biosensor to detect various heavy metals in water (Cu^{2+}, Hg^{2+}, Zn^{2+}, Cd^{2+}, Pb^{2+} and Cr^{3+}), and observed that the current change of the MFC when exposed to all the toxic compounds together was less than the sum of the individual current changes when exposed to each toxicant separately [71]. Thus the co-contaminant effects of toxicants in MFC biosensors should be investigated further and accounted for. Indeed, Stein *et al.* have suggested to alter the anode overpotential as a way to tune the sensitivity of an MFC biosensor towards specific bioactive compounds [60]. In this way the simultaneous detection of toxicants could be performed by using an array of MFCs operated at

various anode potentials [46]. The principle behind this is that the MFC sensitivity and robustness is controlled not only by the mode action of the toxic component, the affinity of the toxic component and its concentration, but also by the anode overpotential at which the MFC operates [86].

In order to offset the effect of environmental conditions on the MFC signal response, Yang *et al.*have suggested the use of a reference MFC running in parallel with the MFC biosensor [72]. It was demonstrated that current changes due to the effects of temperature and flow rate could be offset from the MFC biosensor signal when detecting formaldehyde in water, thus providing a means to detect the presence of toxicants despite changing environmental conditions. However, the effect of further environmental factors and co-contamination events should be the focus of future study.

In fact, when presented with a wider range of environmental factors (pH, temperature, salinity and nutrient load) it was found that an MFC using a pure strain chromium reducing bacteria, *Ochrobactrum anthropi*, demonstrated reliable detection of Cr^{6+} in water whilst being adaptable to changes in environmental conditions [73]. The use of pure strains in this case may also highlight the opportunity for use of specific microbes to tune the sensitivity of the MFC towards certain toxicants in water.

For onsite capability MFC biosensors must be compact and readily portable. MFC water sensors will need to be operated as stacks for effective water monitoring, and the miniaturisation of devices can lead to a kit easy to transport. Onsite sensors should also be able to wirelessly transmit their outputs to a mobile device, such as a computer or a smart phone. The wireless device would comprise of three elements: a sensing unit (i.e. the MFC itself), a processing unit for processing raw data to store the results (a device capable of analysing the output current response from the MFC) and a transceiver unit for sharing data with the end user [87]. The energy generated by an MFC could be used to power some of these components, thus leading to a self-sustainable device. This is especially attractive for applications in remote areas without easy access to electricity. Renewable energy supplies, such as solar batteries, could be also considered instead, and their combination with MFCs would help ensure constant operational capability [88-89]. These renewable energy conversion techniques would be an attractive alternative to conventional batteries, which are not renewable and need periodic replacements.

There is little work on conventional MFC devices being used as power sources for sensor nodes, except for a 340 mL device used to power a piezo resistive pressure sensor node [90]. Most research in this area focusses on the use of sediment based MFCs fed with terrestrial wastewater [57,82,85,86], freshwater [93] and benthic MFCs fed with seawater [94] have been used to power a wireless sensor node within a network. The power generated by these MFCs is however susceptible to the environmental conditions in which it resides. Power generation performance of a wireless MFC device can in fact be affected by the environmental temperature [93] and the pH [91]. Moreover, the power generated by MFCs is still too low (order of W m^{-3}) to be able to power alone principle components within the sensor node, such as the transceivers and controllers [89]. In order to reliably provide the correct amount of electricity and voltage elevation to the device, an intelligent power management system must be utilized [57,87] A power management system stores energy from the MFC device and converts it into power that is high enough to operate the wireless sensor node [92], and may include such components as capacitors, charge pumps, and DC-AC converters [95].

2.6 Conclusions

The developing world is challenged with providing safe water and adequate sanitation for its population. Effective water quality monitoring methods are required in these areas that are low cost, simple to use, rapid and have onsite capability. Microbial fuel cell technology is a very promising technology with the potential to satisfy this need, especially given their recent development as sensitive and small scale devices. Research is however, still in its infancy. In order for MFCs to be fully realized for water quality monitoring in developing countries research must focus on: 1) producing low cost and easy to manufacture devices by using inexpensive electrode and membrane materials- ideally the cost should be less than $0.5 per test to contend with existing testing methods; 2) MFCs must be tested as sensors in realistic environments, where the system would be exposed to a complex mix of toxicants and environmental factors, whilst still providing a simple output response; 3) Response times of devices and device portability should be further optimized by miniaturisation; 4) A self-sustaining and wireless MFC biosensor needs to be developed to ensure fully functional onsite water quality monitoring for remote regions or areas with poor

infrastructure. Addressing these challenges is not an easy task and requires clear research focus and effort. The outcome will be a powerful device that can drastically improve wellbeing and livelihoods of people living in developing countries and remote areas.

2.7 Associated content

Author Contributions

Formulation of ideas and manuscript prepared by JC with supervision from MDL.

Conflicts of Interest

The authors declare no conflict of interest.

Acknowledgments

Funding from the Engineering and Physical Sciences Research Council (EPSRC) and the EPSRC Centre for Doctoral Training in Sustainable Chemical Technologies (EP/G03768X/1) is acknowledged.

Abbreviations

ANN: Artificial neural network,

BOD: Biological oxygen demand,

BVM: Butler Volmer Monod,

COD: Chemical oxygen demand,

DET: Direct electron transfer,

EPS: extracellular polymeric substance,

MED: Mediated electron transfer,

MFC: Microbial fuel cell,

PCB: Polychlorinated biphenyl,

PEM: Proton exchange membrane.

Nomenclature

A: Electrode surface area,

ΔC: Unit change in the analyte concentration,

ΔI: Unit change in the current output.

2.8 References

[1] Poverty-Environment, Partnership, Linking Poverty Reduction and Water Management., 2006.

[2] World Bank, World Development Report 2008: Agriculture for Development, 2007.

[3] United Nations Educational, Scientific and Cultural Organization (UNESCO), The United Nations World Water Development Report 3: Water in a Changing World, 2009.

[4] World Health Organisation (WHO), United Nations Children's Fund (UNICEF), Progress on Drinking Water and Sanitation : 2014 Update, 2014.

[5] World Health Organisation (WHO), United Nations Children's Fund (UNICEF), Progress on Drinking Water and Sanitation, Geneva Switzerland/New York, 2008.

[6] G.M. Carr, J.P. Neary, Water Quality for Ecosystem and Human Health, 2008.

[7] R.P. Schwarzenbach, T. Egli, T.B. Hofstetter, U. von Gunten, B. Wehrli, Global Water Pollution and Human Health, Annu. Rev. Environ. Resour. 35 (2010) 109–136. doi:10.1146/annurev-environ-100809-125342.

[8] WaterAid, Water quality standards and testing policy, 2011.

[9] I. Khurana, R. Sen, Drinking water quality in rural India : Issues and approaches, 2008.

[10] W. Dixon, B. Chiswell, Review of aquatic monitoring program design, Water Res. 30 (1996) 1935–1948. doi:10.1016/0043-1354(96)00087-5.

[11] A. van Geen, Z. Cheng, A.A. Seddique, M.A. Hoque, A. Gelman, J.H. Graziano, H. Ahsan, F. Parvez, K.M. Ahmed, Reliability of a Commercial Kit To Test Groundwater for Arsenic in Bangladesh, Environ. Sci. Technol. 39 (2005) 299–303. doi:10.1021/es0491073.

[12] K. Brindha, R. Rajesh, R. Murugan, L. Elango, Fluoride contamination in groundwater in parts of Nalgonda District, Andhra Pradesh, India, Environ. Monit. Assess. 172 (2011) 481–492. doi:10.1007/s10661-010-1348-0.

[13] A. Safarzadeh-Amiri, P. Fowlie, A.I. Kazi, S. Siraj, S. Ahmed, A. Akbor, Validation of analysis of arsenic in water samples using Wagtech Digital Arsenator., Sci. Total Environ. 409 (2011) 2662–2667. doi:10.1016/j.scitotenv.2011.03.016.

[14] M.M. Rahman, D. Mukherjee, M.K. Sengupta, U.K. Chowdhury, D. Lodh, C.R. Chanda, S. Roy, M. Selim, Q. Quamruzzaman, A.H. Milton, S.M. Shahidullah, M.T. Rahman, D. Chakraborti, Effectiveness and Reliability of Arsenic Field Testing Kits: Are the Million Dollar Screening Projects Effective or Not?, Environ. Sci. Technol. 36 (2002) 5385–5394. doi:10.1021/es020591o.

[15] E. Awuah, K.B. Nyarko, P.A. Owusu, K. Osei-Bonsu, Small town water quality, Desalination. 248 (2009) 453–459. doi:10.1016/j.desal.2008.05.087.

[16] C.M. George, Y. Zheng, J.H. Graziano, S. Bin Rasul, Z. Hossain, J.L. Mey, A. van Geen, Evaluation of an arsenic test kit for rapid well screening in Bangladesh., Environ. Sci. Technol. 46 (2012) 11213–11219. doi:10.1021/es300253p.

[17] WHO, Guidelines for Drinking-water Quality, 2011. doi:10.1016/S1462-0758(00)00006-6.

[18] EPA, Monitoring and Assessing Water Quality, (2015).

[19] IUPAC, Compendium of Chemical Terminology, 2nd ed. (the “Gold Book”), 2nd editio, Blackwell Scientific Publications, Oxford, 1997. doi:doi:10.1351/goldbook.

[20] X.C. Abrevaya, N.J. Sacco, M.C. Bonetto, A. Hilding-Ohlsson, E. Cortón, Analytical applications of microbial fuel cells. Part I: Biochemical oxygen demand., Biosens. Bioelectron. 63 (2015) 580–590. doi:10.1016/j.bios.2014.04.034.

[21] R.E. Dewhurst, J.R. Wheeler, K.S. Chummun, J.D. Mather, A. Callaghan, M. Crane, The comparison of rapid bioassays for the assessment of urban groundwater quality, Chemosphere. 47 (2002) 547–554. doi:10.1016/S0045-6535(02)00060-7.

[22] A. Chaubey, B.D. Malhotra, Mediated biosensors, Biosens. Bioelectron. 17 (2002) 441–456. doi:10.1016/S0956-5663(01)00313-X.

[23] L. Su, W. Jia, C. Hou, Y. Lei, Microbial biosensors: a review., Biosens. Bioelectron. 26 (2011) 1788–1799. doi:10.1016/j.bios.2010.09.005.

[24] B. Eggins, Biosensors: An Introduction, Wiley, 1997.

[25] F. Lagarde, N. Jaffrezic-Renault, Cell-based electrochemical biosensors for water quality assessment., Anal. Bioanal. Chem. 400 (2011) 947–964. doi:10.1007/s00216-011-4816-7.

[26] Y. Lei, W. Chen, A. Mulchandani, Microbial biosensors., Anal. Chim. Acta. 568 (2006) 200–210. doi:10.1016/j.aca.2005.11.065.

[27] S.F. D'Souza, Microbial biosensors, Biosens. Bioelectron. 16 (2001) 337–353. doi:10.1016/S0956-5663(01)00125-7.

[28] H. Liu, B.E. Logan, Electricity generation using an air-cathode single chamber microbial fuel cell in the presence and absence of a proton exchange membrane., Environ. Sci. Technol. 38 (2004) 4040–4046. http://www.ncbi.nlm.nih.gov/pubmed/15298217.

[29] B. Logan, J. Regan, Microbial challenges and applications, Environ. Sci. Technol. 40 (2006) 5172–5180. doi:10.1021/es0627592.

[30] B. Logan, B. Hamelers, R. Rozendal, U. Schroder, J. Keller, S. Freguia, P. Aelterman, W. Verstraete, K. Rabaey, Critical Review Microbial Fuel Cells : Methodology and Technology, Environ. Sci. Technol. 40 (2006) 5181–5192. doi:10.1021/es0605016.

[31] H. Ren, H.-S. Lee, J. Chae, Miniaturizing microbial fuel cells for potential portable power sources: promises and challenges, Microfluid. Nanofluidics. 13 (2012) 353–381. doi:10.1007/s10404-012-0986-7.

[32] Y. Yang, M. Xu, J. Guo, G. Sun, Bacterial extracellular electron transfer in bioelectrochemical systems, Process Biochem. 47 (2012) 1707–1714. doi:10.1016/j.procbio.2012.07.032.

[33] Z. Du, H. Li, T. Gu, A state of the art review on microbial fuel cells: A promising technology for wastewater treatment and bioenergy., Biotechnol. Adv. 25 (2007) 464–482. doi:10.1016/j.biotechadv.2007.05.004.

[34] D.C. Holzman, Microbe power!, Environ. Health Perspect. 113 (2005) A754-757.

[35] H. Liu, R. Ramnarayanan, B.E. Logan, Production of Electricity during Wastewater Treatment Using a Single Chamber Microbial Fuel Cell, Environ. Sci. Technol. 38 (2004) 2281–2285. doi:10.1021/es034923g.

[36] W. Habermann, E.H. Pommer, Biological fuel cells with sulphide storage capacity, Appl. Microbiol. Biotechnol. 35 (1991) 128-133. doi:10.1007/BF00180650.

[37] T.H. Pham, K. Rabaey, P. Aelterman, P. Clauwaert, L. De Schamphelaire, N. Boon, W. Verstraete, Microbial Fuel Cells in Relation to Conventional Anaerobic Digestion Technology, Eng. Life Sci. 6 (2006) 285–292. doi:10.1002/elsc.200620121.

[38] S. Das, N. Mangwani, Recent developments in microbial fuel cells: a review, J. Sci. Ind. Res. 69 (2010) 727–731. http://nopr.niscair.res.in/bitstream/123456789/10294/1/JSIR 69%2810%29 727-731.pdf (accessed April 16, 2015).

[39] B.H. Kim, I.S. Chang, G.C. Gil, H.S. Park, H.J. Kim, Novel BOD (biological oxygen demand) sensor using mediator-less microbial fuel cell, Biotechnol. Lett. 25 (2003) 541–545. doi:10.1023/A:1022891231369.

[40] I.S. Chang, J.K. Jang, G.C. Gil, M. Kim, H.J. Kim, B.W. Cho, B.H. Kim, Continuous determination of biochemical oxygen demand using microbial fuel cell type biosensor, Biosens. Bioelectron. 19 (2004) 607–613. doi:10.1016/S0956-5663(03)00272-0.

[41] M. Di Lorenzo, K. Scott, T.P. Curtis, K.P. Katuri, I.M. Head, Continuous Feed Microbial Fuel Cell Using An Air Cathode and A Disc Anode Stack for Wastewater Treatment, Energy & Fuels. 23 (2009) 5707–5716. doi:10.1021/ef9005934.

[42] S. Patil, F. Harnisch, U. Schröder, Toxicity response of electroactive microbial biofilms--a decisive feature for potential biosensor and power source applications., Chemphyschem. 11 (2010) 2834–2837. doi:10.1002/cphc.201000218.

[43] Y. Feng, W. Barr, W.F. Harper, Neural network processing of microbial fuel cell signals for the identification of chemicals present in water., J. Environ. Manage. 120 (2013) 84–92. doi:10.1016/j.jenvman.2013.01.018.

[44] B.H. Kim, I.S. Chang, G.M. Gadd, Challenges in microbial fuel cell development and operation., Appl. Microbiol. Biotechnol. 76 (2007) 485–494. doi:10.1007/s00253-007-1027-4.

[45] M. Kim, M.S. Hyun, G.M. Gaddb, H.J. Kim, A novel biomonitoring system using microbial fuel cells, J. Environ. Monit. 9 (2007) 1323–1328. doi:10.1039/b713114c.

[46] M. Di Lorenzo, A.R. Thomson, K. Schneider, P.J. Cameron, I. Ieropoulos, A small-scale air-cathode microbial fuel cell for on-line monitoring of water quality., Biosens. Bioelectron. 62 (2014) 182–188. doi:10.1016/j.bios.2014.06.050.

[47] D.R. Lovley, The microbe electric: conversion of organic matter to electricity., Curr. Opin. Biotechnol. 19 (2008) 564–571. doi:10.1016/j.copbio.2008.10.005.

[48] N.E. Stein, H.V.M. Hamelers, C.N.J. Buisman, Stabilizing the baseline current of a microbial fuel cell-based biosensor through overpotential control under non-toxic conditions., Bioelectrochemistry. 78 (2010) 87–91. doi:10.1016/j.bioelechem.2009.09.009.

[49] H. Kim, M. Hyun, I. Chang, B. Kim, A microbial fuel cell type lactate biosensor using a metal-reducing bacterium, Shewanella putrefaciens, J. Microbiol. Biotechnol. 9 (1999) 365–367. http://apps.webofknowledge.com/full_record.do?product=UA&search_mode=GeneralSearch&qid=5&SID=X2FUTw7xQIACPyG88CD&page=1&doc=1 (accessed May 29, 2015).

[50] M. Kim, S.M. Youn, S.H. Shin, J.G. Jang, S.H. Han, M.S. Hyun, G.M. Gadd, H.J. Kim, Practical field application of a novel BOD monitoring system, J. Environ. Monit. 5 (2003) 640–643. doi:10.1039/b304583h.

[51] M. Di Lorenzo, T.P. Curtis, I.M. Head, K. Scott, A single-chamber microbial fuel cell as a biosensor for wastewaters., Water Res. 43 (2009) 3145–3154. doi:10.1016/j.watres.2009.01.005.

[52] C. Melhuish, I. Ieropoulos, J. Greenman, I. Horsfield, Energetically autonomous robots: Food for thought, Auton. Robots. 21 (2006) 187–198. doi:10.1007/s10514-006-6574-5.

[53] I. Karube, T. Matsunaga, S. Mitsuda, S. Suzuki, Microbial electrode BOD sensors., Biotechnol. Bioeng. 19 (1977) 1535–1547. doi:10.1002/bit.260191010.

[54] I.S. Chang, H. Moon, O. Bretschger, J.K. Jang, H. Il Park, K.H. Nealson, B.H. Kim, Electrochemically active bacteria (EAB) and mediator-less microbial fuel cells, J. Microbiol. Biotechnol. 16 (2006) 163–177.

[55] H. Moon, I.S. Chang, K.H. Kang, J.K. Jang, B.H. Kim, Improving the dynamic response of a mediator-less microbial fuel cell as a biochemical oxygen demand (BOD) sensor., Biotechnol. Lett. 26 (2004) 1717–1721. doi:10.1007/s10529-004-3743-5.

[56] B. Min, B.E. Logan, Continuous Electricity Generation from Domestic Wastewater and Organic Substrates in a Flat Plate Microbial Fuel Cell, Environ. Sci. Technol. 38 (2004) 5809–5814. doi:10.1021/es0491026.

[57] Y. Zhang, I. Angelidaki, Submersible microbial fuel cell sensor for monitoring microbial activity and BOD in groundwater: focusing on impact of anodic biofilm on sensor applicability., Biotechnol. Bioeng. 108 (2011) 2339–2347. doi:10.1002/bit.23204.

[58] N.E. Stein, H.V.M. Hamelers, G. van Straten, K.J. Keesman, Effect of toxic components on microbial fuel cell-polarization curves and estimation of the type of toxic inhibition., Biosensors. 2 (2012) 255–268. doi:10.3390/bios2030255.

[59] X. Wang, N. Gao, Q. Zhou, Concentration responses of toxicity sensor with Shewanella oneidensis MR-1 growing in bioelectrochemical systems., Biosens. Bioelectron. 43 (2013) 264–267. doi:10.1016/j.bios.2012.12.029.

[60] N.E. Stein, H.V. Hamelers, C.N. Buisman, Influence of membrane type, current and potential on the response to chemical toxicants of a microbial fuel cell based biosensor, Sensors Actuators B Chem. 163 (2012) 1–7. doi:10.1016/j.snb.2011.10.060.

[61] Y. Jiang, P. Liang, C. Zhang, Y. Bian, X. Yang, X. Huang, P.R. Girguis, Enhancing the response of microbial fuel cell based toxicity sensors to Cu(II) with the applying of flow-through electrodes and controlled anode potentials., Bioresour. Technol. 190 (2015) 367–372. doi:10.1016/j.biortech.2015.04.127.

[62] N.E. Stein, H.V. Hamelers, C.N. Buisman, The effect of different control mechanisms on the sensitivity and recovery time of a microbial fuel cell based biosensor, Sensors Actuators B Chem. 171–172 (2012) 816–821. doi:10.1016/j.snb.2012.05.076.

[63] Y. Jiang, P. Liang, P. Liu, B. Miao, Y. Bian, H. Zhang, X. Huang, Enhancement of the sensitivity of a microbial fuel cell sensor by transient-state operation, Environ. Sci. Water Res. Technol. 3 (2017) 472–479. doi:10.1039/C6EW00346J.

[64] A.P. Borole, G. Reguera, B. Ringeisen, Z.-W. Wang, Y. Feng, B.H. Kim, Electroactive biofilms: Current status and future research needs, Energy Environ. Sci. 4 (2011) 4813-4819. doi:10.1039/c1ee02511b.

[65] D. Celmer, J.A. Oleszkiewicz, N. Cicek, Impact of shear force on the biofilm structure and performance of a membrane biofilm reactor for tertiary hydrogen-driven denitrification of municipal wastewater., Water Res. 42 (2008) 3057–3065. doi:10.1016/j.watres.2008.02.031.

[66] Y. Shen, M. Wang, I.S. Chang, H.Y. Ng, Effect of shear rate on the response of microbial fuel cell toxicity sensor to Cu(II)., Bioresour. Technol. 136 (2013) 707–710. doi:10.1016/j.biortech.2013.02.069.

[67] Y.J. Shen, O. Lefebvre, Z. Tan, H.Y. Ng, Microbial fuel-cell-based toxicity sensor for fast monitoring of acidic toxicity, Water Sci. Technol. 6 (2012) 1223–1228. doi:10.2166/wst.2012.957.

[68] B. Liu, Y. Lei, B. Li, A batch-mode cube microbial fuel cell based “shock” biosensor for wastewater quality monitoring., Biosens. Bioelectron. 62 (2014) 308–314. doi:10.1016/j.bios.2014.06.051.

[69] D. Dávila, J.P. Esquivel, N. Sabaté, J. Mas, Silicon-based microfabricated microbial fuel cell toxicity sensor., Biosens. Bioelectron. 26 (2011) 2426–2430. doi:10.1016/j.bios.2010.10.025.

[70] N.E. Stein, H.M. Hamelers, G. van Straten, K.J. Keesman, On-line detection of toxic components using a microbial fuel cell-based biosensor, J. Process Control. 22 (2012) 1755–1761. doi:10.1016/j.jprocont.2012.07.009.

[71] D. Yu, L. Bai, J. Zhai, Y. Wang, S. Dong, Toxicity detection in water containing heavy metal ions with a self-powered microbial fuel cell-based biosensor, Talanta. 168 (2017) 210–216. doi:10.1016/j.talanta.2017.03.048.

[72] W. Yang, X. Wei, S. Choi, A Dual-Channel, Interference-Free, Bacteria-Based Biosensor for Highly Sensitive Water Quality Monitoring, IEEE Sens. J. 16 (2016) 8672–8677. doi:10.1109/JSEN.2016.2570423.

[73] G.-H. Wang, C.-Y. Cheng, M.-H. Liu, T.-Y. Chen, M.-C. Hsieh, Y.-C. Chung, Utility of Ochrobactrum anthropi YC152 in a Microbial Fuel Cell as an Early Warning Device for Hexavalent Chromium Determination, Sensors. 16 (2016) 1272-1285. doi:10.3390/s16081272.

[74] M. Palaniappan, P.H. Gleick, L. Allen, M.J. Cohen, J. Christian-Smith, C. Smith, Clearing the Waters: A focus on water quality solutions, Oakland, CA, USA, 2010.

[75] A. Elmekawy, H.M. Hegab, X. Dominguez-Benetton, D. Pant, Internal resistance of microfluidic microbial fuel cell: challenges and potential opportunities., Bioresour. Technol. 142 (2013) 672–682. doi:10.1016/j.biortech.2013.05.061.

[76] Y.-P. Chen, Y. Zhao, K.-Q. Qiu, J. Chu, R. Lu, M. Sun, X.-W. Liu, G.-P. Sheng, H.-Q. Yu, J. Chen, W.-J. Li, G. Liu, Y.-C. Tian, Y. Xiong, An innovative miniature microbial fuel cell fabricated using photolithography., Biosens. Bioelectron. 26 (2011) 2841–2846. doi:10.1016/j.bios.2010.11.016.

[77] G.-X. Yang, Y.-M. Sun, X.-Y. Kong, F. Zhen, Y. Li, L.-H. Li, T.-Z. Lei, Z.-H. Yuan, G.-Y. Chen, Factors affecting the performance of a single-chamber microbial fuel cell-type biological oxygen demand sensor., Water Sci. Technol. 68 (2013) 1914–1919. doi:10.2166/wst.2013.415.

[78] J. Winfield, I. Ieropoulos, J. Rossiter, J. Greenman, D. Patton, Biodegradation and proton exchange using natural rubber in microbial fuel cells., Biodegradation. 24 (2013) 733–739. doi:10.1007/s10532-013-9621-x.

[79] J. Winfield, L.D. Chambers, A. Stinchcombe, J. Rossiter, I. Ieropoulos, The power of glove: Soft microbial fuel cell for low-power electronics, J. Power Sources. 249 (2014) 327–332. doi:10.1016/j.jpowsour.2013.10.096.

[80] M. Behera, P.S. Jana, M.M. Ghangrekar, Performance evaluation of low cost microbial fuel cell fabricated using earthen pot with biotic and abiotic cathode., Bioresour. Technol. 101 (2010) 1183–1189. doi:10.1016/j.biortech.2009.07.089.

[81] C. Santoro, I. Ieropoulos, J. Greenman, P. Cristiani, T. Vadas, A. Mackay, B. Li, Current generation in membrane-less single chamber microbial fuel cells (MFCs) treating urine, J. Power Sources. 238 (2013) 190–196. doi:10.1016/j.jpowsour.2013.03.095.

[82] P. Cristiani, M.L. Carvalho, E. Guerrini, M. Daghio, C. Santoro, B. Li, Cathodic and anodic biofilms in Single Chamber Microbial Fuel Cells., Bioelectrochemistry. 92 (2013) 6–13. doi:10.1016/j.bioelechem.2013.01.005.

[83] T. Huggins, H. Wang, J. Kearns, P. Jenkins, Z.J. Ren, Biochar as a sustainable electrode material for electricity production in microbial fuel cells, Bioresour. Technol. 157 (2014) 114–119. doi:10.1016/j.biortech.2014.01.058.

[84] Y. Yuan, T. Yuan, D. Wang, J. Tang, S. Zhou, Sewage sludge biochar as an efficient catalyst for oxygen reduction reaction in an microbial fuel cell, Bioresour. Technol. 144 (2013) 115–120. doi:10.1016/j.biortech.2013.06.075.

[85] H. Yuan, L. Deng, Y. Qi, N. Kobayashi, J. Tang, Nonactivated and Activated Biochar Derived from Bananas as Alternative Cathode Catalyst in Microbial Fuel Cells, Sci. World J. 2014 (2014) 1-8. doi:10.1155/2014/832850.

[86] N.E. Stein, K.J. Keesman, H.V.M. Hamelers, G. van Straten, Kinetic models for detection of toxicity in a microbial fuel cell based biosensor., Biosens. Bioelectron. 26 (2011) 3115–3120. doi:10.1016/j.bios.2010.11.049.

[87] F. Akhtar, M.H. Rehmani, Energy replenishment using renewable and traditional energy resources for sustainable wireless sensor networks: A review, Renew. Sustain. Energy Rev. 45 (2015) 769–784. doi:10.1016/j.rser.2015.02.021.

[88] Y.R.J. Thomas, M. Picot, A. Carer, O. Berder, O. Sentieys, F. Barrière, A single sediment-microbial fuel cell powering a wireless telecommunication system, J. Power Sources. 241 (2013) 703–708. doi:10.1016/j.jpowsour.2013.05.016.

[89] F. Yang, K.-C. Wang, Y. Huang, Energy-Neutral Communication Protocol for Very Low Power Microbial Fuel Cell Based Wireless Sensor Network, Sensors Journal, IEEE. 15 (2105) 2306–2315. http://ieeexplore.ieee.org/xpls/icp.jsp?arnumber=6975034#sec6 (accessed April 29, 2015).

[90] T. Tommasi, A. Chiolerio, M. Crepaldi, D. Demarchi, A microbial fuel cell powering an all-digital piezoresistive wireless sensor system, Microsyst. Technol. 20 (2014) 1023–1033. doi:10.1007/s00542-014-2104-0.

[91] A. Pietrelli, A. Micangeli, V. Ferrara, A. Raffi, Wireless Sensor Network Powered by a Terrestrial Microbial Fuel Cell as a Sustainable Land Monitoring Energy System, Sustainability. 6 (2014) 7263–7275. doi:10.3390/su6107263.

[92] C. Donovan, A. Dewan, H. Peng, D. Heo, H. Beyenal, Power management system for a 2.5W remote sensor powered by a sediment microbial fuel cell, J. Power Sources. 196 (2011) 1171–1177. doi:10.1016/j.jpowsour.2010.08.099.

[93] A. Shantaram, H. Beyenal, R.R.A. Veluchamy, Z. Lewandowski, Wireless Sensors Powered by Microbial Fuel Cells, Environ. Sci. Technol. 39 (2005) 5037–5042. doi:10.1021/es0480668.

[94] J.J. Guzman, K.G. Cooke, M.O. Gay, S.E. Radachowsky, P.R. Girguis, M.A. Chiu, Benthic microbial fuel cells: long-term power sources for wireless marine sensor networks, in: E.M. Carapezza (Ed.), SPIE 7666, Sensors. doi:10.1117/12.854896.

[95] F. Zhang, L. Tian, Z. He, Powering a wireless temperature sensor using sediment microbial fuel cells with vertical arrangement of electrodes, J. Power Sources. 196 (2011) 9568–9573. doi:10.1016/j.jpowsour.2011.07.037.

3 Theory

This chapter covers the basic principles and electrochemical fundamentals for microbial fuel cell systems. It also provides an overview of commonly used electrochemical techniques used to analyse the performance of microbial fuel cells (polarisation, cyclic voltammetry and electrochemical impedance spectroscopy).

3.1 Electrochemical fundamentals for microbial fuel cells

Electricity is generated within an MFC only if the overall reaction is thermodynamically favourable. The maximum work performed from the reactions within a system can be determined by using the Gibbs free energy [1]:

$$\Delta G_r = \Delta G_r^0 + RTln(\Pi) \qquad \text{Equation 3.1}$$

Where ΔG_r (J) is the Gibbs free energy for the specific conditions, ΔG_r^0 (J) is the Gibbs free energy under standard conditions, R is the universal gas constant (8.314 J mol^{-1} K^{-1}), T is absolute temperature (K), and Π is the reaction quotient calculated as the ratio of the activities of the products and the activities of the reactants. For the purpose of MFC analysis however, it is convenient to determine the overall electromotive force (emf), E_{emf} (V), for the cell, which is given as [2]:

$$E_{emf} = E_{cell} = E_{cat} - E_{an} \qquad \text{Equation 3.2}$$

Where E_{cell} is the cell potential (V) (which can be considered equivalent to the electromotive force) E_{cat} is the cathode potential (V), E_{an} is the anode potential (V), and the minus sign is due to the definition of the anode potential as a reduction reaction. This subsequently can be related to the work done by the system, W (J) [1,3]:

$$W = E_{emf}Q = -\Delta G_r \qquad \text{Equation 3.3}$$

Where Q is the charge transferred in the reaction (Coulombs), F is Faraday's constant (9.649×10^4 C mol^{-1}). And using $Q = nF$ where n is the number of electrons per reaction mol [4], E_{emf} can be expressed as:

$$E_{emf} = -\frac{\Delta G_r}{nF} \qquad \text{Equation 3.4}$$

Then if evaluated at standard conditions (i.e. Π = 1):

$$E^0_{emf} = -\frac{\Delta G^0_r}{nF} \qquad \text{Equation 3.5}$$

Where E^0_{emf} is the standard cell electromotive force (V). Equation 3.1, Equation 3.4 and Equation 3.5 can be combined to express the overall reaction scheme in terms of potentials, *via* the Nernst equation [1,4]:

$$E_{emf} = E^0_{emf} - \frac{RT}{nF}\ln(\Pi) \qquad \text{Equation 3.6}$$

The value of E_{emf} can give a value for the maximum theoretically achievable potential for the MFC system, and as such can be determined if reaction schemes in the fuel cell are known [2]. For instance, when acetate is oxidised at the anode of an MFC, and oxygen is reduced at the cathode, we observe the following reaction scheme, with corresponding equations for cell potentials [5]:

Anode $CH_3COO^- + 4H_2O \rightarrow 2HCO_3^- + 9H^+ + 8e^-$ $E_{an} = E^0_{an} - \frac{RT}{nF}\ln\left(\frac{[CH_3COO^-]}{[HCO_3^-]^2[H^+]^9}\right)$ Equation 3.7

Cathode $O_2 + 4H^+ + 4e^- \rightarrow 2H_2O$ $E_{cat} = E^0_{cat} - \frac{RT}{nF}\ln\left(\frac{1}{[pO_2][H^+]^4}\right)$ Equation 3.8

Using the standard potentials available for these two half reactions in water (as specified in [5]), with E^0_{an} = 0.187, E^0_{cat} = 1.229 (relative to normal hydrogen electrode) , [CH_3COO^-] = 5 mM, [HCO_3^-] = 5 mM, pO_2 = 0.2, n = 8 for CH_3COO^- and n = 4 for O_2, and pH = 7 [5], the theoretical electromotive force for the MFC can be calculated by combining Equation 3.2, Equation 3.7 and Equation 3.8:

$$E_{emf} = E_{cat} - E_{an}$$

$$E_{emf} = E^0_{cat} - \frac{RT}{nF}\ln\left(\frac{1}{[pO_2][H^+]^4}\right) - E^0_{an} - \frac{RT}{nF}\ln\left(\frac{[CH_3COO^-]}{[HCO_3^-]^2[H^+]^9}\right)$$

$$E_{emf} = (0.805) - (-0.296) = 1.1V$$

The open circuit voltage (OCV) is the cell potential that can be measured in the absence of a current, and should approach the theoretical E_{emf}. In reality, however the OCV is much lower, due to various potential losses. These losses can be considered as the sum of the overpotentials of the anode and the cathode along with the ohmic loss of the system [2]:

$$E_{cell} = E_{emf} - (\eta_{an} + |\eta_{cat}| + IR_\Omega) \qquad \text{Equation 3.9}$$

Where η_{an} and η_{cat} are the overpotentials of the anode and cathode respectively (i.e. the difference between electrode potential and equilibrium potential), and R_Ω is the ohmic losses in the system. Considering that overpotentials of the electrodes in the absence of current can be summarised in an OCV term, and the current dependent electrode overpotentials and ohmic losses can be captured by use of the internal resistance, R_{int}, then Equation 3.9 can be simplified to [2]:

$$E_{cell} = OCV - IR_{\text{int}} \qquad \text{Equation 3.10}$$

The overpotentials of the electrodes can be categorised as follows [6,7]: 1) *Activation losses*- which arise from the activation energy needed for a given oxidation or

reduction reaction at the electrode; 2) *Bacterial metabolic losses*- which are due to the metabolic energy required for bacteria to transport electrons through the electron transport chain to the anode; 3) M*ass transport/concentration losses*- which occurs when the rate of mass transfer of a substrate to the electrodes limits the electrochemical process, which may occur in systems when diffusion is limited or with fast reaction kinetics at the electrode.

For systems where the reaction kinetics are limiting the system, i.e. when the system is well stirred and concentration of species are equivalent in the bulk solution and electrode surface, the Butler-Volmer equation can be used to define the electron transfer reaction at an electrode [4]:

$$i = i_0 \left[e\left(\frac{\alpha_{an} nF\eta}{RT}\right) - e\left(-\frac{\alpha_{cat} nF\eta}{RT}\right) \right] \quad \text{Equation 3.11}$$

Where i is the electrode current density (A m^{-2}), i_0 is the exchange current density (A m^{-2}), and α_{an} and α_{cat} are the charge transfer coefficients for anode and cathode respectively. On the other hand, when the electrode processes are mass transfer limited, the diffusion limited current at the electrode can be expressed as [8]:

$$i = nFD\frac{\Delta C}{\lambda} \quad \text{Equation 3.12}$$

Where D is the normalised diffusivity of the limiting substrate (m^2 s^{-1}), ΔC is the concentration gradient of the limiting substrate (mol dm^{-3}), and λ is the diffusion layer thickness (m).

3.2 Electrochemical methods for microbial fuel cells

3.2.1 Potentiostat

A potentiostat is an extremely useful device in the field of electrochemistry, used to control the potential difference between two electrodes, whilst measuring the resultant

current [9]. This may either be done using a two electrode set up (with a working electrode (WE) and counter electrode (CE)) to analyse the whole electrochemical system, or with a three electrode set up (using a reference electrode (RE)) to observe a single electrode. The RE is connected to a high-input impedance circuit so that no current flows through it. Commonly, a three-electrode set up is used.

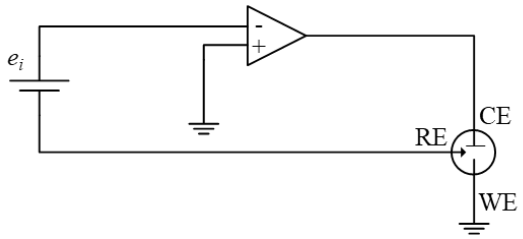

Figure 3.1. Simplified circuit diagram for a potentiostat, with potential source, e_i [4].

A simplified schematic is shown in Figure 3.1. A complex system of resistors, capacitors and amplifiers is used to measure and control the potential between the WE and RE, based on the amplified signal from a potential source. Meanwhile, current is measured between the WE and CE [4]. For microbial fuel cells, a potentiostat is commonly used to conduct a range of analytical electrochemical methods to provide a quantitative understanding of anode and cathode kinetics, biofilm development, mass transport and internal resistances in MFCs [10]. Typical methods include and linear sweep voltammetry (LSV) [11], cyclic voltammetry (CV) [12–14] and electrochemical impedance spectroscopy (EIS) [10,15].

3.2.2 Polarisation curves

Polarisation curves are a valuable means for the understanding and assessment of fuel cell processes [6]. A polarisation experiment may either be conducted by linear sweep voltammetry (LSV) (using a potentiostat) or by varying the electrical load between the electrode. With LSV, the potential between the WE and CE or RE (depending on whether two or three electrode set up is used) is varied from the open circuit voltage, at a given scan rate (in V s^{-1}), and the resultant current is measured [11,16]. Alternatively, when varying the electrical load between the electrodes, an incremental

and periodic change in resistance, R, is applied to the system, the resultant voltage, V, measured, and the corresponding current, I, or current density, I_d (normalised to the electrode surface area, A), is calculated, as per Ohm's law:

$$I = \frac{V}{R} \quad \text{Equation 3.13}$$

$$I_d = \frac{V}{RA} \quad \text{Equation 3.14}$$

Since the voltage and current are now known, power, P, and power density, P_d (normalised to the electrode surface area), can be determined by Joule's law:

$$P = VI \quad \text{Equation 3.15}$$

$$P_d = \frac{VI}{A} \quad \text{Equation 3.16}$$

Commonly, current and power are normalised to the anodic surface area in order to allow comparison of performance of MFCs and other energy generation techniques [17]. Alternatively the current and power may be divided by the MFC chamber volume to yield the volumetric power density, which is particularly useful for engineering and design calculations, i.e. the sizing and costing of MFC systems for a given energy generation application [18].

A plot of voltage against the current will yield a polarisation curve, and a plot of power against current will give a power curve. Such data can be used to assess the MFC performance and quantify sources of polarisation losses in the system, Figure 3.2. Polarisation losses can be characterised as: 1) close to the OCV, *activation losses* are dominant; 2) as the voltage falls linearly with the current, *ohmic losses* dominate (due to solution, electronic and contact resistances in the system); 3) *concentration losses* occur at higher currents due to mass transfer limitations [6,19]. The power curve can also be used to determine the optimal external load to attach to the cell to maximise the power output, and at this point the external resistance is theoretically equivalent to the internal resistance of the MFC [20]. Finally, the gradient of the linear region of the polarisation curve can be used to determine the internal resistance ($R_{int} = -\Delta V/\Delta I$) [7].

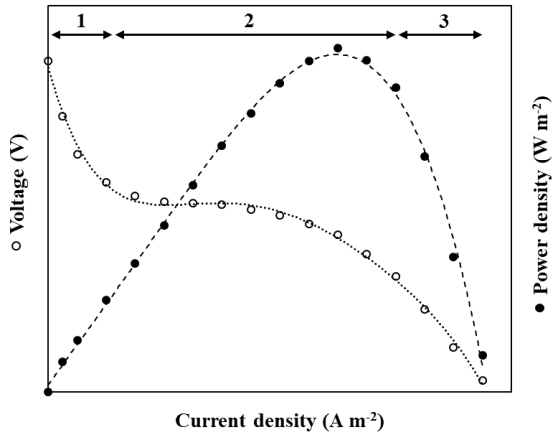

Figure 3.2. An example polarisation and power curve for a microbial fuel cell, with activation losses **1**, ohmic losses **2**, and concentration losses **3** highlighted [6].

3.2.3 Cyclic voltammetry

Cyclic voltammetry (CV) is a widely used potentiodynamic electrochemical method in which the potential difference between the WE and RE is cycled at a constant scan rate between a given voltage range, and the resultant current is measured between the WE and CE [4]. A CV will typically cycle between the vertices of a voltage range, E_1 and E_2, which will allow all essential redox reactions to occur, and a typical voltage sweep is shown in Figure 3.3 [21]:

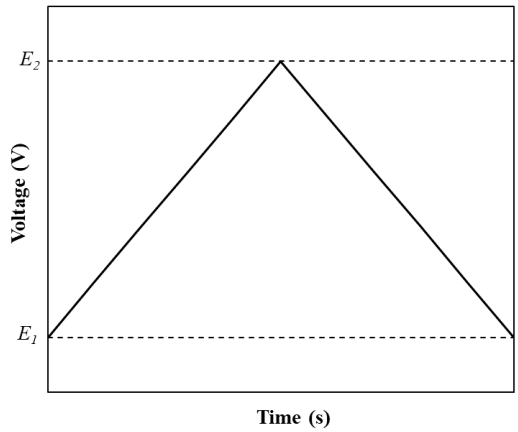

Figure 3.3. Voltage sweep waveform used for cyclic voltammetry, where voltage is swept from the first potential vertex, E_1, up to the second potential vertex, E_2, and back again [21].

The measured current is plotted *versus* the potential applied to give a cyclic voltammagram, with the reduction current appearing negative and the oxidation current positive, Figure 3.4, which shows a single redox reaction with oxidation and reduction peaks at given potentials, E_{ox} and E_{red} respectively. Information, such as the peak separation, ΔE_p, and peak current for oxidation and reduction reactions, I_{ox} and I_{red} respectively, can be determined [14]. Peak separation can give information on the reversibility of the redox reactions, where a constant peak separation with a change in scan rate indicates fast electron transfer kinetics. For systems with slow electron transfer kinetics, the peak currents will vary linearly with the square root of the scan rate, and as such can be used to estimate the active surface area of the electrode *via* the Randles-Sevcik equation [5]. For MFC systems, CV has been used to show that some microbes are capable of discharging electrons at multiple potentials and *via* different electron transfer methods [12,13,22] (e.g. direct electron transfer, through mediators or through nanowires [7,23]).

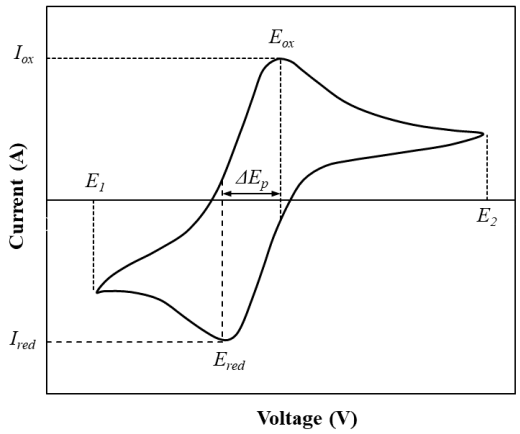

Figure 3.4. Typical cyclic voltammagram curve for a single redox reaction between vertices E_1 and E_2, showing oxidation and reduction peaks, and peak separation.

3.2.4 Electrochemical impedance spectroscopy

In EIS the response of an electrochemical system to a small amplitude AC current or (more usually) voltage stimulus is measured. This test can provide insight into electrochemical processes occurring in the MFC on the (sub) microsecond to second

time scale. EIS can therefore give useful information on electron transfer and ion transfer in devices [15].

EIS measurements are done in two-electrode mode by applying the AC stimulus between the anode and cathode. Alternatively, three electrode measurements are done by placing the RE (typically Ag/AgCl) in either the anode or cathode compartment, depending on which electrode is acting as the working electrode. For MFCs, two electrode mode measurements are typically used to determine the total internal resistance (R_{int}) of the MFC [24]. Typically, the MFC is operated either at open circuit or at a set potential for a period of time until the response has stabilised and EIS spectra are collected by applying a 5-10 mV amplitude AC stimulus at frequencies 100 kHz to 1 mHz. Data are commonly presented in two ways: a complex plane plot (also named a Nyquist plot), and a Bode plot. Figure 3.5 shows a complex plane plot and a Bode plot showing a typically shaped response for an electrode in a fuel cell. The high frequency intercept with the real axis gives the value of the series resistance, which is commonly referred to as ohmic resistance, R_{Ω}, and made up of contributions from the electronic resistance of the electrode material, contact resistances and the electrolyte resistance (solution resistance to charge carriers). Charge transfer at an electrode is described by the charge transfer resistance, R_{ct}. The total internal resistance (R_{int}) of an MFC is usually reported as being the resistance at which the lowest frequency intercept with the real axis occurs. To exemplify – in the case where only one semi-circular response is seen in the Nyquist plot, Figure 3.5A; R_{int} would be given by $R_{\Omega} + R_{ct}$ [25]. Where multiple semi-circles are observed R_{int} is reported as the sum of all the resistances measured.

The difference between the internal resistance and the ohmic resistance is often labelled the 'polarisation resistance' (R_p). R_p is a combination of the charge transfer resistances (R_{ct}); the membrane resistance (R_{mem} where present) and resistance due to diffusion of ions through the electrolyte (R_W where W denotes Warburg after the circuit element most frequently used to model diffusion) [26]. The total internal resistance can then be defined as the sum of all the resistive processes measured (the anode and cathode are denoted by a superscript *a* and *c* respectively [10,27]. All of the resistances listed in Equation 3.17 and Equation 3.18 could contribute to the internal resistance, but it is unlikely that they would all be clearly resolvable in the spectrum.

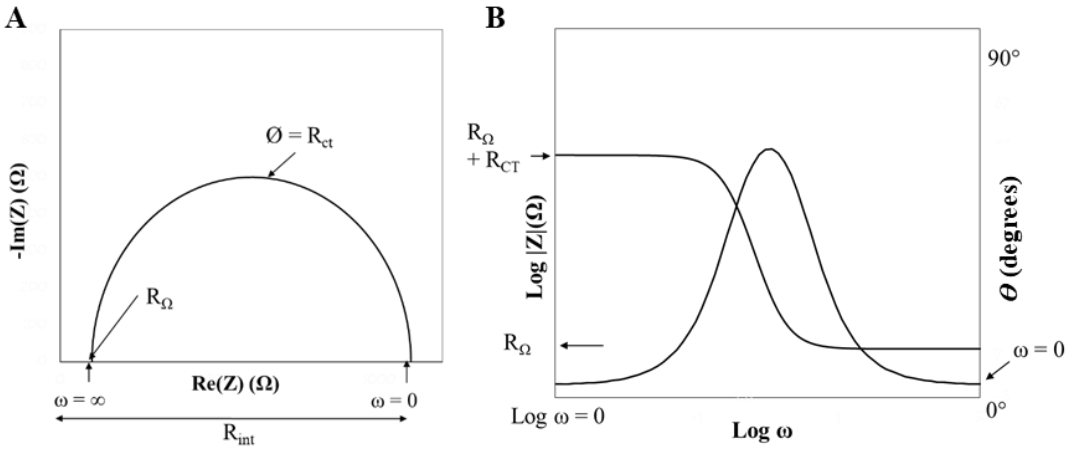

Figure 3.5. Typical impedance response for a single electrode MFC system, showing identification of R_Ω and R_{ct}. [**A**] Complex plane plot [**B**] Bode plot [10,24]. Re(Z) and Im(Z) refer to real and complex elements of the impedance respectively. θ refers to the phase shift. ω refers to frequency. Diffusion processes are not shown on these plots.

$$R_{int} = R_\Omega + R_{ct}^a + R_{ct}^c + R_W^a + R_W^c + R_{mem} \qquad \text{Equation 3.17}$$

$$R_p = R_{ct}^a + R_{ct}^c + R_W^a + R_W^c + R_{mem} \qquad \text{Equation 3.18}$$

For practical and objective comparisons, it may be necessary to normalise the resistances by the projected areas of all the components [28]. Resistance and capacitance values are usually obtained by fitting an equivalent circuit to the EIS data [4]. Two typical circuits for EIS studies of MFCs are shown in Figure 3.6. A simple Randles circuit is often used as the equivalent circuit in 3-electrode MFC measurements, Figure 3.6A. When using a two-electrode set up, an equivalent circuit incorporating another charge transfer resistance and capacitance in parallel is used, Figure 3.6B.

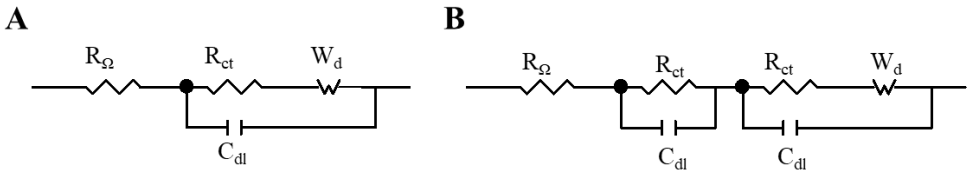

Figure 3.6. Example equivalent circuit typically used as an equivalent circuit model to simulate impedance data: [**A**]: Randles circuit commonly used for a 3 electrode set up (left) [4]; [**B**]: equivalent circuit used for two electrode set up [10].

The double layer capacitance in the fuel cell is represented by the element C_{dl}. A constant phase shift element (CPE) can be used to replace the double layer capacitance element in the equivalent circuit to account for inhomogeneous conditions at the electrode (e.g. electrode roughness, biofilm distribution, electrode and biofilm porosity, coating, distribution of reaction rate) [4,29]. EIS has proved a useful tool to study MFCs, however care must be taken not to over interpret the data. In general, multiple equivalent circuits can fit observed EIS responses and the model chosen needs to be linked to a physical understanding of the system being studied [30].

3.2.5 Fuel cell efficiency

The Coulombic efficiency, ε_c, of a microbial fuel cell gives the efficiency of charge transfer in an electrochemical reaction [19]. In other words, the Coulombic efficiency signifies the ratio between the total amount of charge, in Coulombs, transferred from the substrate to the anode, against the theoretical amount of charge available in the substrate, which for most applications of MFCs will be defined as the chemical oxygen demand (COD) availability. The total charge transferred by a batch system is given by the integral of current up to a batch time, t_b, which can be used to determine the Coulombic efficiency thus [31]:

$$\varepsilon_C = \frac{M_R \int_0^{t_b} I\, dt}{FnV_a \Delta COD} \qquad \text{Equation 3.19}$$

Where M_R = 32 g mol^{-1}, the molecular weight of oxygen, I is current (A), F is Faradays constant (9.649 × 10^4 C mol^{-1}), n = 4 (the number of electrons per mole of oxygen), V_a is anodic chamber volume, and ΔCOD is the difference in Chemical Oxygen Demand (COD) over batch time, t_b. For continuous based systems, Coulombic efficiency is related to the steady state current produced [7]:

$$\varepsilon_C = \frac{M_R\, I}{FnQ_f \Delta COD} \qquad \text{Equation 3.20}$$

Where Q_f is the volumetric flow rate of the feed, and ΔCOD is the difference in the influent and effluent COD. The Coulombic efficiency of an MFC system may be reduced by the presence of alternative electron acceptors or competitive processes occurring at the anode [26].

3.3 Associated content

Abbreviations

CE: Counter electrode,

COD: Chemical oxygen demand,

CPE: Constant phase element,

CV: Cyclic voltammetry,

EIS: Electrochemical impedance spectroscopy,

LSV: Linear sweep voltammetry,

MFC: Microbial fuel cell,

OCV: Open circuit voltage,

RE: Reference electrode,

WE: Working electrode.

Nomenclature

Roman symbols

A: Electrode surface area,

ΔC: Concentration gradient of the limiting substrate,

C_{dl}: Double layer capacitance,

ΔCOD: Difference in chemical oxygen demand,

E_1: First potential vertex,

E_2: Second potential vertex,

E_{an}: Anode potential,

E_{an}^0: Standard anode potential,

E_{cat}: Cathode potential,

E_{cat}^0: Standard cathode potential,

E_{cell}: Cell potential,

E_{emf}: Electromotive force,

E_{emf}^0: Standard cell electromotive force,

ΔE_p: Peak separation,

F: Faraday's constant,

ΔG_r: Gibbs free energy for specific conditions,

ΔG_r^0: Gibbs free energy under standard conditions,

I: Current,

I_d: Current density,

I_{ox}: Oxidation peak current,

I_{red}: Reduction peak current,

i: Electrode current density,

i_0: Exchange current density,

M_R: Molecular weight,

n: Number of electrons per reaction mol

P: Power,

P_d: Power density,

Q: Charge transferred in the reaction,

Q_f: Volumetric flow rate of the feed,

R: Resistance,

R: Universal gas constant,

R_{ct}: Charge transfer resistance,

R_{in}: Internal resistance,

R_{mem}: Membrane resistance,

R_p: Polarisation resistance,

R_W: Warburg resistance,

R_Ω: Ohmic losses,

T: Absolute temperature,

t_b: Batch time,

V: Voltage,

V_a: Anodic chamber volume,

W: Work done.

Greek symbols

α_{an}: Charge transfer coefficients for the anode,

α_{cat}: Charge transfer coefficients the cathode,

ε_c: Coulombic efficiency,

η_{an}: Anode overpotential,

η_{cat}: Cathode overpotential,

λ: Diffusion layer thickness,

Π: Reaction quotient.

3.4 References

[1] F. Scholz, Thermodynamics of Electrochemical Reactions, in: Electroanal. Methods, Springer Berlin Heidelberg, Berlin, Heidelberg, 2010: pp. 11–31. doi:10.1007/978-3-642-02915-8_2.

[2] B.E. Logan, Microbial Fuel Cells, Wiley, 2008.

[3] P.W. (Peter W. Atkins, J. De Paula, Atkins' Physical chemistry, Oxford University Press, 2006.

[4] A.J. Bard, L.R. Faulkner, Electrochemical Methods: Fundamentals and Applications, John Wiley & Sons, Ltd, 1980.

[5] A.J. Bard, R. Parsons, J. Jordan, International Union of Pure and Applied Chemistry., Standard potentials in aqueous solution, M. Dekker, 1985.

[6] G. Hoogers, Fuel Cell Technology Handbook, CRC Press, 2002.

[7] B. Logan, B. Hamelers, R. Rozendal, U. Schroder, J. Keller, S. Freguia, P. Aelterman, W. Verstraete, K. Rabaey, Critical Review Microbial Fuel Cells : Methodology and Technology, Environ. Sci. Technol. 40 (2006) 5181–5192. doi:10.1021/es0605016.

[8] H. Ren, C.I. Torres, P. Parameswaran, B.E. Rittmann, J. Chae, Improved current and power density with a micro-scale microbial fuel cell due to a small characteristic length., Biosens. Bioelectron. 61 (2014) 587–592. doi:10.1016/j.bios.2014.05.037.

[9] J. Larminie, A. Dicks, Fuel cell systems explained, Wiley, 2000.

[10] X. Dominguez-Benetton, S. Sevda, K. Vanbroekhoven, D. Pant, The accurate use of impedance analysis for the study of microbial electrochemical systems., Chem. Soc. Rev. 41 (2012) 7228–7246. doi:10.1039/c2cs35026b.

[11] V.J. Watson, B.E. Logan, Analysis of polarization methods for elimination of power overshoot in microbial fuel cells, Electrochem. Commun. 13 (2011) 54–56. doi:10.1016/j.elecom.2010.11.011.

[12] K. Fricke, F. Harnisch, U. Schröder, On the use of cyclic voltammetry for the study of anodic electron transfer in microbial fuel cells, Energy Environ. Sci. 1 (2008) 144–147. doi:10.1039/b802363h.

[13] S.M. Strycharz, A.P. Malanoski, R.M. Snider, H. Yi, D.R. Lovley, L.M. Tender, Application of cyclic voltammetry to investigate enhanced catalytic current generation by biofilm-modified anodes of Geobacter sulfurreducens strain DL1 vs. variant strain KN400, Energy Environ. Sci. 4 (2011) 896–913. doi:10.1039/c0ee00260g.

[14] F. Harnisch, S. Freguia, A Basic Tutorial on Cyclic Voltammetry for the Investigation of Electroactive Microbial Biofilms, Chem. - An Asian J. 7 (2012) 466–475. doi:10.1002/asia.201100740.

[15] D. Kashyap, P.K. Dwivedi, J.K. Pandey, Y.H. Kim, G.M. Kim, A. Sharma, S. Goel, Application of electrochemical impedance spectroscopy in bio-fuel cell characterization: A review, Int. J. Hydrogen Energy. 39 (2014) 20159–20170. doi:10.1016/j.ijhydene.2014.10.003.

[16] L. Zhang, C. Liu, L. Zhuang, W. Li, S. Zhou, J. Zhang, Manganese dioxide as an alternative cathodic catalyst to platinum in microbial fuel cells., Biosens. Bioelectron. 24 (2009) 2825–2829. doi:10.1016/j.bios.2009.02.010.

[17] J. You, J. Greenman, C. Melhuish, I. Ieropoulos, Small-scale microbial fuel cells utilising uric salts, Sustain. Energy Technol. Assessments. 6 (2014) 60–63. doi:10.1016/j.seta.2014.01.005.

[18] R.A. Bullen, T.C. Arnot, J.B. Lakeman, F.C. Walsh, Biofuel cells and their development., Biosens. Bioelectron. 21 (2006) 2015–2045. doi:10.1016/j.bios.2006.01.030.

[19] F. Barbir, PEM fuel cells theory and practice, Elsevier Academic, 2005.

[20] L. Woodward, M. Perrier, B. Srinivasan, C. Hc, B. Tartakovsky, Maximizing Power Production in a Stack of Microbial Fuel Cells Using Multiunit Optimization Method, Biotechnol. Prog. 25 (2009) 676–682. doi:10.1021/bp.115.

[21] R.G. Compton, C.E. Banks, Understanding voltammetry, World Scientific, 2007.

[22] K. Rabaey, N. Boon, S.D. Siciliano, M. Verhaege, W. Verstraete, Biofuel Cells Select for Microbial Consortia That Self-Mediate Electron Transfer, Appl. Environ. Microbiol. 70 (2004) 5573–5382. doi:10.1128/AEM.70.9.5373.

[23] H. Ren, H.-S. Lee, J. Chae, Miniaturizing microbial fuel cells for potential portable power sources: promises and challenges, Microfluid. Nanofluidics. 13 (2012) 353–381. doi:10.1007/s10404-012-0986-7.

[24] Z. He, F. Mansfeld, Exploring the use of electrochemical impedance spectroscopy (EIS) in microbial fuel cell studies, Energy Environ. Sci. 2 (2009) 215–219. doi:10.1039/b814914c.

[25] F. Mansfeld, M.W. Kendig, Determination of the polarization resistance from impedance measurements, Mater. Corros. Und Korrosion. 34 (1983) 397–401. doi:10.1002/maco.19830340805.

[26] Y. Fan, H. Hu, H. Liu, Enhanced Coulombic efficiency and power density of air-cathode microbial fuel cells with an improved cell configuration, J. Power Sources. 171 (2007) 348–354. doi:10.1016/j.jpowsour.2007.06.220.

[27] A.K. Manohar, F. Mansfeld, The internal resistance of a microbial fuel cell and its dependence on cell design and operating conditions, Electrochim. Acta. 54 (2009) 1664–1670. doi:10.1016/j.electacta.2008.06.047.

[28] Y. Fan, E. Sharbrough, H. Liu, Quantification of the Internal Resistance Distribution of Microbial Fuel Cells, Environ. Sci. Technol. 42 (2008) 8101–8107. doi:10.1021/es801229j.

[29] C. Hsu, F. Mansfeld, Technical note: Concerning the conversion of the constant phase element parameter Y-0 into a capacitance, Corrosion. 57 (2001) 747–748. doi:10.5006/1.3280607.

[30] J.-B. Jorcin, M.E. Orazem, N. Pébère, B. Tribollet, CPE analysis by local electrochemical impedance spectroscopy, Electrochim. Acta. 51 (2006) 1473–1479. doi:10.1016/j.electacta.2005.02.128.

[31] S. Cheng, H. Liu, B.E. Logan, Increased power generation in a continuous flow MFC with advective flow through the porous anode and reduced electrode spacing., Environ. Sci. Technol. 40 (2006) 2426–2432. doi:10.1021/es051652w.

4 Towards effective small scale microbial fuel cells for energy generation from urine

In this chapter, the design and development of a miniature single chamber MFC is pursued, which in this case looks at the devices capability to generate energy from a waste feedstock, urine. The effect of device geometry, specifically the anodic chamber length, on power performance is investigated, and the effects of this on mass transfer processes within the cell are discussed. The use of two biomass derived catalysts for oxygen reduction reactions at the air cathode are investigated. Finally, with the aim of increasing power generation from the system, the effect of stacking miniature MFCs electrically is studied. This chapter has been published as detailed on the following page.

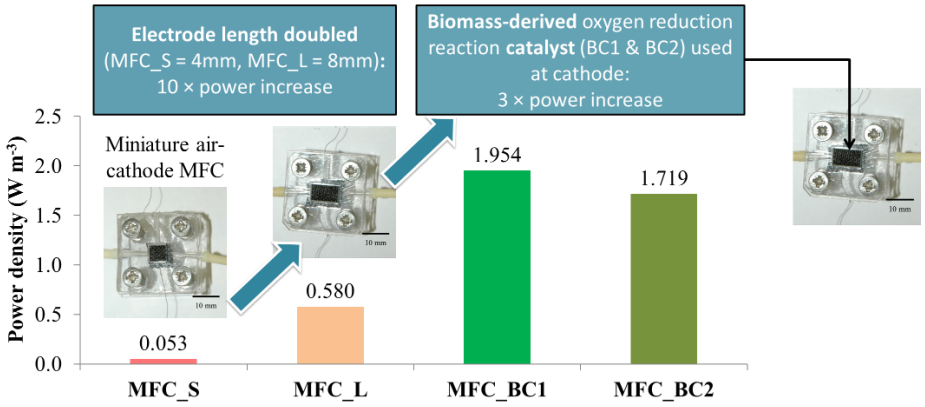

Statement of authorship

This declaration concerns the article entitled:	Towards effective small scale microbial fuel cells for energy generation from urine
Publication status:	Published
Publication details:	J. Chouler, G.A. Padgett, P.J. Cameron, K. Preuss, M.-M. Titirici, I. Ieropoulos, M. Di Lorenzo, Towards effective small scale microbial fuel cells for energy generation from urine, Electrochim. Acta. 192 (2016) 89–98. doi:10.1016/j.electacta.2016.01.112.
Authorship contributions:	Formulation of ideas, design of methodology conducted by JC and MDL. Experiments conducted by JC and GAP, Manuscript preparation by JC. Supervision from MDL, PJC and II.
Statement from candidate:	This paper reports on original research I conducted during the period of my Higher Degree by Research candidature.

Signed: Date:

Towards effective small scale microbial fuel cells for energy generation from urine

Jon Chouler [a,b], George A. Padgett [a], Petra J. Cameron [c], Kathrin Preuss [d,e], Maria-Magdalena Titirici [d,e], Ioannis Ieropoulos [f], Mirella Di Lorenzo [a]

[a] University of Bath, Department of Chemical Engineering, Bath, BA2 7AY, UK

[b] Centre for Sustainable Chemical Technologies, University of Bath, Bath BA2 7AY, UK

[c] University of Bath, Department of Chemistry, Bath, BA2 7AY, UK

[d] Queen Mary University of London, School of Engineering and Materials Science, London, E1 4NS, UK

[e] Queen Mary University of London, Materials Research Institute, London, E1 4NS, UK

[f] Bristol BioEnergy Centre, Bristol Robotics Laboratory, University of the West of England, Bristol, UK

4.1 Abstract

To resolve an increasing global demand in energy, a source of sustainable and environmentally friendly energy is needed. Microbial fuel cells (MFC) hold great potential as a sustainable and green bioenergy conversion technology that uses waste as the feedstock. This work pursues the development of an effective small scale MFC for energy generation from urine. An innovative air-cathode miniature MFC was developed, and the effect of electrode length was investigated. Two different biomass derived catalysts were also studied. Doubling the electrode length resulted in the power density increasing by one order of magnitude (from 0.053 to 0.580 W m^{-3}). When three devices were electrically connected in parallel, the power output was over 10 times higher compared to individual units. The use of biomass derived oxygen reduction reaction catalysts at the cathode increased the power density generated by the MFC up to 1.95 W m^{-3}, thus demonstrating the value of sustainable catalysts for cathodic reactions in MFCs.

4.2 Introduction

In the face of the growing problem of fossil fuel depletion, there is global interest in developing sustainable and environmentally friendly forms of energy. One form of alternative energy that may be viable in addressing this problem is bioenergy [1,2]. In this context, microbial fuel cells (MFC) hold great potential as green and carbon-neutral technology that directly converts biomass into electricity [3].

MFCs are electrochemical devices that take advantage of the metabolic processes of microorganisms to directly convert organic matter into electricity with high theoretical efficiencies (when compared to anaerobic digestion) for long periods of time [4]. Compared to other bioenergy conversion processes (e.g. anaerobic digestion, gasification, fermentation), MFCs have the advantage of reduced amounts of sludge production [5], as well as cost-effective operation, since they operate under ambient environmental conditions (temperature, pressure) [6]. Moreover, MFCs require no energy input for aeration so long as the cathode is passively aerated, for example *via* the use of a single chamber device [7]. Lastly, MFCs have the ability to generate energy remotely by using a range of feed stocks, and can thus be used in areas of poor energy infrastructure. Organic waste used as a feed stock in particular offers attractive prospects from its cost-effectiveness and abundance. Urine has been demonstrated to be an effective feed stock for MFC operation with the additional benefit of nitrogen, phosphate and potassium recovery from the fuel [8]. In particular, according to Ieropoulos *et al.* [9], urea is enzymatically hydrolysed to ammonia and carbon dioxide. Ammonia is then oxidised at the anode of the MFC to generate mainly nitrite and in smaller amounts nitrate [10]. Alternatively, compounds such as peptone, yeast extract, lactate and citrate that are present in urine may act as the electron donor for the biofilm.

Despite the breadth of applications and the growing interest in MFC technology over the past two decades, commercialisation of MFCs for energy generation has not yet been realised. The major limiting factors that hinder the practical implementation of MFCs at large scale, are the cost of materials used, difficulties in the scale-up process and low energy conversion efficiencies when treating real wastewater [11].

Typically the electrodes are made from highly cost-effective materials such as carbon cloth, carbon paper, and graphite based rods, plates and granules. Recently, even some metals, such as copper and silver, have been shown to be effective anode materials

[12]. However, expensive metals, such as platinum, are usually used at the cathode to enhance the oxygen reduction reaction (ORR) [13–15]. Recently, the use of biomass derived catalysts recovered from waste has been proposed as an effective alternative to expensive metal ORR catalysts. In particular, biochar derived from wood [16], sewage sludge [17] and bananas [18] have been shown to function as ORR catalysts to boost MFC performance whilst reducing the device cost and its carbon footprint. Doping these materials with heteroatoms such as nitrogen and sulphur [19], also in combination with iron [20], has been shown to enhance the catalytic activity towards the ORR even further.

Another limitation towards practical implementations of MFCs, is their poor performance due to high internal resistances and ohmic losses experienced upon scale-up [21]. Consequently, the power performance of MFCs is low compared to other renewable energy technologies [8,22]. Considering the thermodynamic limit of an MFC (1.1 V open circuit), the most feasible approach to scale-up the power generated by this technology is to create a collection of multiple MFCs connected together as a stack. By miniaturising individual MFC units, stacks of large numbers of constituent MFCs could be developed, within a compact footprint. This approach has been referred as the 'miniaturisation and multiplication' strategy [9].

MFC miniaturisation offers other advantages as well. The large surface area-to-volume ratio and short electrode distances - typical characteristics of miniature MFCs- provide a pathway to reducing ohmic losses, improving the mass transport processes between bulk liquid, biofilm and electrode and therefore enhancing power performance [23]. The refinement of microfabrication techniques has led to the first prototypes of micro-sized MFCs, which have been discussed in a recent review [11]. Nonetheless, the process of miniaturisation of the MFC technology is still in its infancy. The two chamber configuration is typically adopted for the miniature MFCs reported thus far, and, usually, a ferricyanide solution is used as the catholyte [24]. Given the greater operational simplicity and cost-effectiveness of oxygen diffusion systems, air-cathode MFC designs should be considered instead. Moreover, a more in-depth analysis on how to effectively miniaturise the system for better performance would be beneficial. With the aim of guiding the development of efficient small scale MFCs, this study reports the development of an innovative air-cathode small scale MFC and analyses the effect that the chamber length (and therefore the electrodes length) has on its performance either when operated as a single unit or when assembled in a stack. No

expensive metals have been employed at the cathode, and the use of two types of innovative and highly sustainable biomass derived ORR catalysts are compared with a catalyst-free device.

4.3 Experimental

4.3.1 Materials

All reagents used were of analytical grade and purchased from Sigma-Aldrich and Alfa Aesar. Unless otherwise stated, all aqueous solutions used were prepared with reverse osmosis purified water. Polydimethylsiloxane (PDMS, Dow Corning Sylgard 184) was purchased from Ellsworth Adhesives (UK).

Artificial Urine Medium (AUM) was used as the feedstock and prepared as previously described [25]. Tetrasodium pyrophosphate was added to the AUM as a precipitation inhibitor. The resulting feedstock was then filtered (Grade p8 filter paper, Fisher Scientific, UK) prior to use.

4.3.2 Microbial fuel cells

Two geometries were used in this study, leading to the fuel cells MFC_S (for short length) and MFC_L (for longer length). Both MFCs consisted of a single chamber made of a rectangular piece of PDMS and sandwiched between two Perspex plates, Figure 4.1. The channel mould was made of PA 2200 nylon plastic and purchased from Shapeways, New York, USA. The top plate had a square opening as large as the channel cross sectional area to host the cathode, which was opened to air. The anode was instead placed at the bottom of the channel. The two geometries considered differed from each other according to the length of the anode chamber. In particular, MFC_S was characterised by a total anodic chamber volume of 64 µL (length = 4 mm, width = 4 mm, height = 4 mm), while MFC_L had an anodic volume of 128 µL (MFC_L: length = 8 mm, height = 4mm, width = 4mm).

The anode and cathode (geometric surface area = 16 mm^2 for the case of MFC_S, and 32 mm^2 for MFC_L) were made of carbon cloth (untreated carbon cloth type-B, E-

Tek, USA) and threaded with titanium wire (Advent Research Materials, Oxford, UK) for electrical contact. The proton exchange membrane (Nafion 117, Sigma-Aldrich) was hot pressed to the cathode by applying a pressure of approximately 2.5 bar for 12 minutes at a temperature of 150°C.

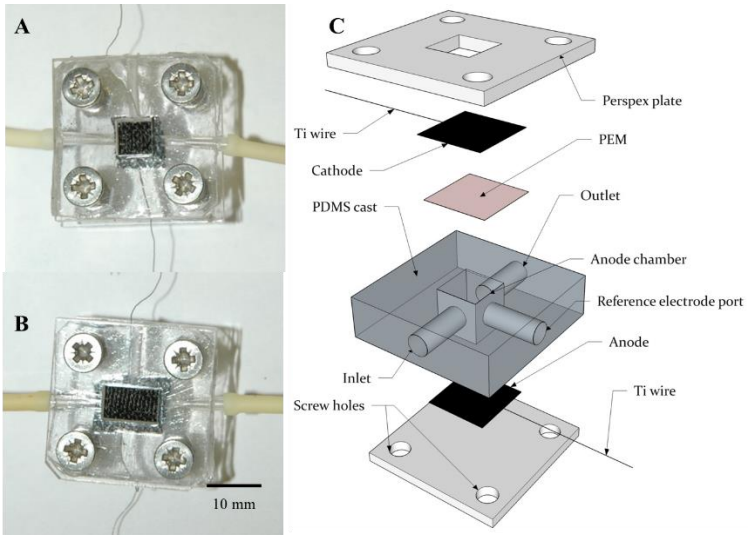

Figure 4.1. MFCs used in this study; [**A**]: Photograph of MFC_S; [**B**]: Photograph of MFC_L; [**C**]: Schematic layout of the device.

4.3.3 Use of a biomass derived oxygen reduction reaction catalyst

Two biomass derived ORR catalysts, provided by Queen Mary University of London, named as BC1 and BC2, produced by hydrothermal carbonisation, were tested at the cathode of MFC_L. Both catalysts were synthesised from glucose and ovalbumin as described in [26] and [19]. BC1 is a nitrogen doped carbon aerogel, while BC2 is a nitrogen and sulphur co-doped aerogel that was prepared with an additional iron source. A loading of 1.5 mg per cm^2 of the cathode area was used for each ORR catalyst. 1.5 mg of catalyst was mixed with 105 μL of Nafion perfluorinated resin solution and sonicated for 3 minutes. The resulting suspension was spread over 1 cm^2 of carbon cloth. Once dried, the doped cathode was bound to the Nafion membrane as shown in Figure 4.1 above. The MFCs with the doped cathodes were named as MFC_BC1 and MFC_BC2, according to the ORR catalyst used. The morphology of the resulting electrodes was characterised using a Hitachi S-4300 scanning electron microscope (SEM).

4.3.4 Operation of the MFCs

All MFCs were fed with AUM at the flow rate of 0.36 mL min^{-1} (hydraulic residence times of 11 seconds and 22 seconds for MFC_S and MFC_L respectively). The cells were connected to a multi-channel peristaltic pump (Ecoline, Ismatech, Germany) *via* Pharmed® BPT tubing, ID 1.6 mm (Cole-Parmer, UK). The anode and cathode were connected to a voltmeter (ADC-24 Pico data logger, Pico Technology, UK) and to an external load to polarise the cell and monitor the cell potential under closed circuit conditions.

Maturing of the electrochemically active bacteria (enrichment) at the anode was performed over a period of five days. It consisted of feeding the MFCs under continuous recirculation conditions with AUM containing 1% *v/v* sewage sludge (anaerobic sludge provided by Wessex Water, Scientific Laboratory in Saltford, UK), which was replaced on a daily basis. The fuel cells were first operated under open circuit conditions for up to 2 hours, and then connected to an external load of 1 kΩ. After the enrichment, the MFCs were fed continuously with AUM and no bacteria.

Polarisation experiments were performed by connecting the MFCs to a series of external loads, varying from 10 Ω to 1000 kΩ, controlled by an external variable resistor (RS-200 Resistance substitute, IET Labs Inc., USA), and by measuring the pseudo steady state output potential after 20 minutes. Before the test, the MFC was left under open circuit for no more than 2 hours to allow a steady state open circuit voltage (OCV) to develop. Ohm's law was used to determine the corresponding current (I) at each external load value ($I = V/R$, where V, and R are voltage and resistance respectively). The power (P) was calculated by using Joule's law ($P = I^2 \times R$). Power density was calculated by dividing the power by the MFC chamber volume, while current density was calculated by dividing the current by the total macro surface area of the anode. The internal resistance (R_{int}) of the MFC was calculated from the linear fit of the ohmic region of each polarisation cell potential curve ($R_{int} = \Delta V/\Delta I$), as previously described [3].

4.3.5 Stacking

To scale-up the power output, MFC units with the same geometry were electrically stacked in series and in parallel, as shown in Figure 4.2. The MFCs were enriched individually and stacked after the five days of enrichment, once a steady current was generated. Once stacked, the MFC units were fed in parallel with AUM and no bacteria. The polarisation experiments on the stack were performed after at least 24 hours of operation. Since the power performance of the stack will change with respect to time, and especially due to repeat polarisation experiments, replicate polarisation experiments were not performed on the MFC stacks.

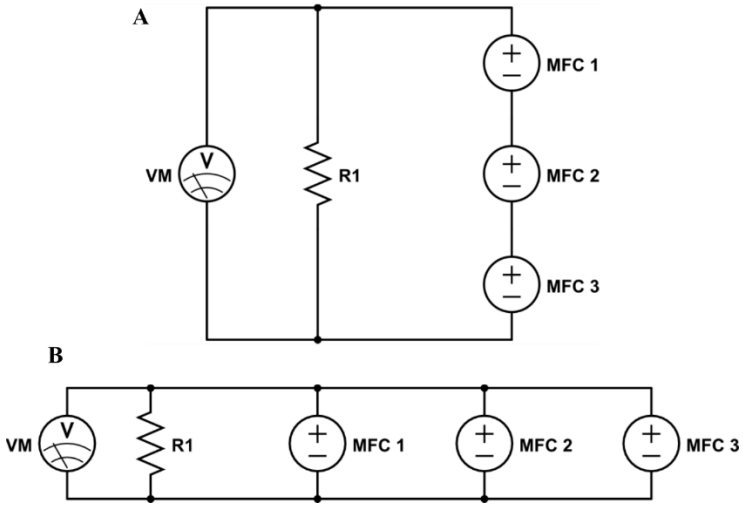

Figure 4.2. Schematic for electrical stacking MFC units in series [**A**] and in parallel [**B**]: R1 = external load, VM = voltmeter.

4.3.6 Calculations

The maximum current density (I_{max}) under mass transport limiting conditions at the electrode, is expressed according to [27] as:

$$I_{max} = nFD\frac{\Delta C}{\lambda} \qquad \text{Equation 4.1}$$

Where n is number of electrons equivalent corresponding to the limiting compound (substrate), F is Faraday's constant (96485 C mol^{-1}), D is the normalised diffusivity of

the limiting compound (substrate) (m^2 s^{-1}), ΔC is the concentration gradient of the limiting compound (mol m^{-3}), and λ is the diffusion layer thickness (m).

The Reynold's number (*Re*) and mass transfer coefficient (k_C, m s^{-1}) for laminar flow in a channel is defined as [28]:

$$Re = \frac{\rho v d_H}{\mu} \quad \text{Equation 4.2}$$

$$k_c = 0.664(Re)^{1/2}\left(\frac{\mu}{\rho D}\right)^{1/3}\left(\frac{D}{H}\right) \quad \text{Equation 4.3}$$

Where ρ is specific density of the fluid (kg m^{-3}), v is the linear velocity of the fluid (m s^{-1}), d_H is the hydraulic diameter of the flow channel (m), H is the channel height (m), and μ is the viscosity of the fluid (kg m^{-1} s^{-1}).

The hydraulic diameter of the channel (d_H) is related to the channel length according to Equation 4.4:

$$d_H = \frac{4(LH)}{2(L+H)} \quad \text{Equation 4.4}$$

Where H is the height (m), and L is the lateral dimension length (m). The diffusion-layer thickness (λ) at the electrode surface was calculated with the following equation:

$$\lambda = \frac{D}{k_c} \quad \text{Equation 4.5}$$

4.4 Results and discussion

4.4.1 Effect of electrode length on performance

The influence of the electrode length on the performance of small scale MFCs, was investigated in this study by operating two different fuel cells geometries, MFC_S and MFC_L, characterised by the same cross sectional area (and therefore the same

electrode spacing, 4 mm) but different channel lengths. In particular, the length of the anodic chamber in MFC_L was two times larger than MFC_S. The resulting performances are compared in terms of the power and cell polarisation curves, produced from the polarisation experiment, as shown in Figure 4.3.

The OCV for MFC_S and MFC_L were 253 ± 86 mV and 312 ± 59 mV respectively. High internal resistances were observed for both devices. In particular, MFC_L showed an internal resistance of 33 kΩ, which is comparable to the values of miniature MFCs reported in the literature [29,30]. The internal resistance of MFC_S was higher at 242 kΩ. From the cell polarisation curves in Figure 4.3, ohmic losses appear to be dominating in both MFC_S and MFC_L, suggesting that the electrical resistances of the electrodes, membrane and electrolyte are mostly responsible for the internal resistance of the MFC. Accordingly, there is little evidence of mass transfer limitations taking place in the MFC, which may be a result of miniaturisation, which, as expected, allows good transfer of substrate from the bulk fluid to the biofilm on the anode [31].

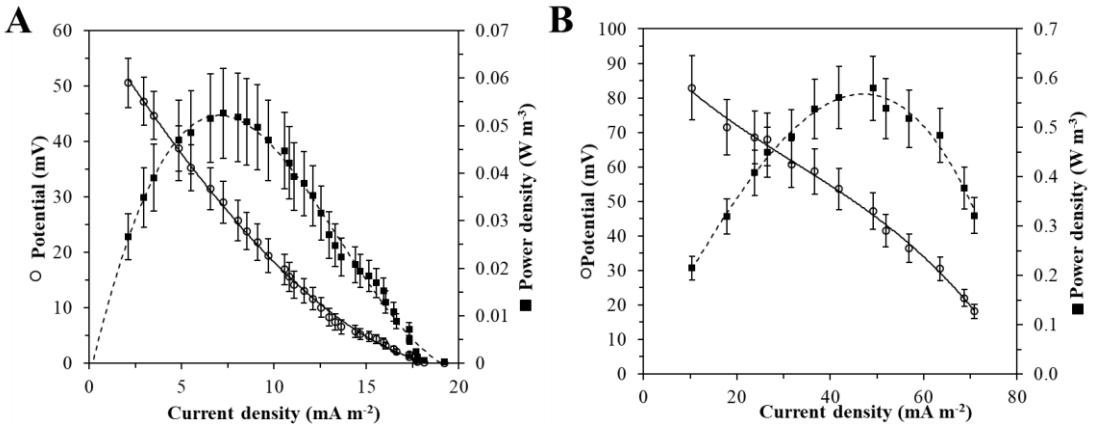

Figure 4.3. Power and polarisation curves. [**A**]: MFC_S; [**B**]: MFC_L. Current density refers to the anode surface area: MFC_S = 16 mm^2; MFC_L = 32 mm^2. Volumetric power density refers to the MFC chamber volume: MFC_S = 64 µL; MFC_L = 128 µL. For each geometry, data is the average of 3 devices, with up to 22% error.

Doubling the length of the anode chamber improved the power density by a factor of 11. The maximum power densities of MFC_S and MFC_L were 0.053 and 0.580 W m^{-3} respectively, and the current densities at the maximum power output were 7.3 and 49.1 mA m^{-2} respectively.

The increase in power and current density is suspected to be due to an increase in the mass transfer between the bulk fluid, biofilm and electrode surface. When observing the cross section of an MFC square electrode chamber, the height, *H*, and the lateral dimension (length), *L*, will affect the performance of the device. On one hand, when the height of the channel is reduced (i.e. the distance between electrodes is reduced) in the MFC, the miniaturised device benefits from a greater rate of mass transfer due to an increase in the surface area to volume ratio of the device [23]. As a result, the power density generated by miniature MFCs is higher than large-scale devices [32]. On the other hand, when the lateral dimension of the channel (length), *L*, of the electrode chamber is increased, the hydraulic diameter of the channel is increased as per Equation 4.4. Consequently, the mass transfer coefficient, k_C, will increase as per Equations 4.2 and 4.3. Therefore, when *L* is increased, whilst maintaining a fixed *H*, the mass transfer coefficient is increased, and hence the diffusion-layer thickness at the electrode surface will decrease (Equation 4.5). By altering the length of the channel, the maximum current density available at the electrode will therefore increase (Equation 4.1), and, consequently, result in high fuel consumption efficiency and an improvement in power performance.

Figure 4.4 demonstrates that increasing the length of the flow channel, for a fixed flow rate, will increase the mass transfer coefficient and decrease the diffusion-layer thickness. Values here have been calculated using Equations 4.1 – 4.5, with the flow rate at 0.36 mL min^{-1}, and a linear velocity of 22.5 mm min^{-1}. For urine, the kinematic viscosity (μ / ρ) is estimated to be 1.07 mm^2 s^{-1} at 20°C [33], and the diffusivity of urea in water is 0.082 mm^2 min^{-1} [34]. Note here, that it is assumed that urea is the key electron donor, but other compounds such as peptone, yeast extract, lactate and citrate, that are present in urine, may also act as substrates for the biofilm.

To ensure that these assumptions are valid, the flow regime in the flow channel must be laminar. This is confirmed by the *Re* values for MFC_S and MFC_L, which are 1.4 and 1.9 respectively, as calculated by considering *L* values of 4 and 8 mm, for MFC_S and MFC_L respectively, and *H* equal to 4 mm.

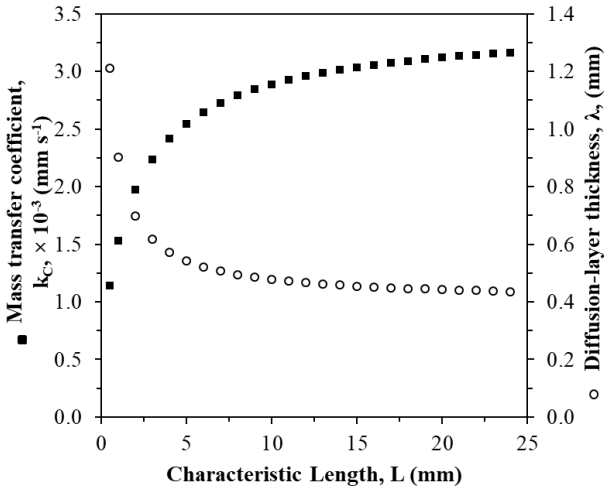

Figure 4.4. Effect of length of MFC channel on mass transfer coefficient and diffusion-layer thickness moving from 0.5 to 25 mm. Values plotted are for a flow rate of 0.36 mL min^{-1}.

By increasing the length of the electrode in the MFC devices, a better fuel efficiency has been achieved, with consequent improvement in performance [35]. This, as well as improving the mass transfer of substrate within the MFC, may be attributed to an increase in the hydraulic residence time in the MFC, thus allowing more time for substrate consumption. This is likely to also be contributing to the improvement in power performance, since a tripling of the mass transfer coefficient alone is unlikely to result in an almost 10 times improvement in power performance. The results in this paper, corroborate with a recent study by [36] whereby increasing the length of a graphite fibre brush anode from 12 mm to 30 mm the power density increased from 1.13 to 1.65 W m^{-2}. The better supply of redox species (*c*) to the anode leads to an increase in the measured current density (*I*), according to Equation 4.6:

$$I = nF\frac{K_c}{\lambda}c \qquad \text{Equation 4.6}$$

Where: n is the moles of electrons involved in the reaction; F (C mol^{-1}) is the Faraday constant; K_c (m s^{-1}) is the mass transfer coefficient; λ (m) is the diffusion layer thickness; c is the concentration of the redox compound (mol m^{-3}).

4.4.2 Stacking the miniature MFCs

To scale-up the power output, MFC_S and MFC_L were arranged in stacks of three units each. The MFC_S units were electrically connected either in parallel or in series to evaluate the best configuration.

Figure 4.5A reports the results from the polarisation experiments. The maximum power output increased almost 4 times when the MFC_S units operated as a series stack compared to individual units, while when stacked in parallel the power output was 14 times higher. This result is in agreement with previous studies that report voltage reversal effects when the MFCs are arranged in series [37]. The reversal in some of the cells in the series stack is caused by the unavoidable increase in the internal resistances of the MFC units operated in series, as previously reported [37,38]. Thereby, power performance is reduced. When operated in parallel however, if the impedances of the MFCs are well matched, then the internal resistance of the MFC stack will tend towards the lowest common denominator and thus be more uniform [39]. This is evident by the reduction in internal resistance of the MFC_S stack from 244 to 76 kΩ. This large reduction in the internal resistance may also explain the increase in the current density of the parallel stack from 7.3 mA m^{-2} to 18.4 mA m^{-2}, as summarised in Table 4.1.

Considering the results obtained for the MFC_S stacks, the MFC_L devices were arranged only in parallel. As shown in Figure 4.5B, in this case the maximum power output of the stack was nearly 6 times higher compared to the MFC_L individual units. The power density increased by a factor of 2, and the internal resistance decreased from 33 kΩ to 1.4 kΩ, Table 4.1. The reason for a more marked increase in power output and density when the MFC_S units were stacked is unknown, and requires further investigation.

The stacking of larger MFCs (mL scale) has been shown to increase the power density of MFCs, albeit not to the extent observed in this report. For example power densities of millilitre scale MFCs (6.25 and 12 mL) were improved by a factor of 1.2-1.4 by stacking multiple units together [9,38]. On the other hand, Aelterman *et al.* demonstrates similar power densities between individual units and MFC stacks when using 60 mL MFCs [40].

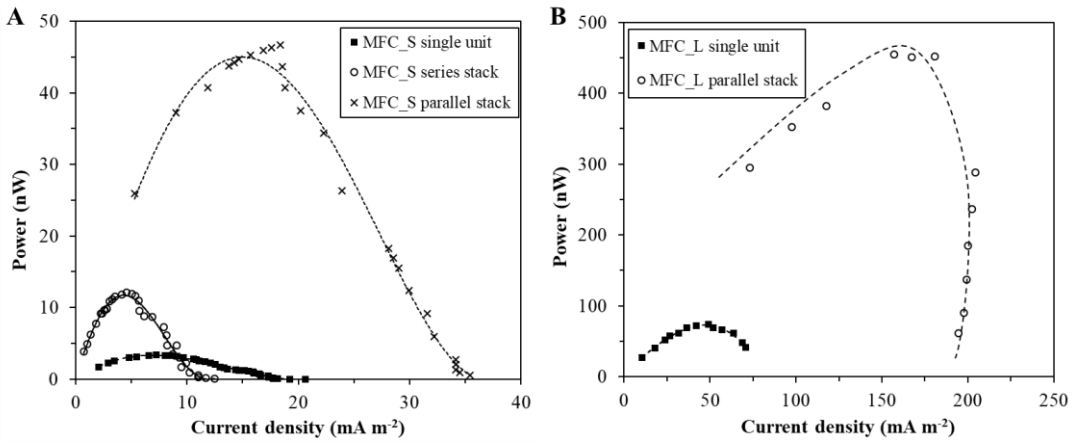

Figure 4.5. Power curves. [**A**] Refers to MFC_S, operated alone, in series and in a parallel stack. Current density refers to the anode surface area, 16 mm^2 for a single unit, 48 mm^2 for the stack. [**B**] Refers to MFC_L, operated alone and in a parallel stack. Current density refers to the anode surface area, 32 mm^2 for a single unit, 96 mm^2 for the stack.

4.4.3 Use of biomass derived ORR catalysts

To enhance power generation, without compromising cost-effectiveness and sustainability, two biomass derived carbon materials, BC1 and BC2, were tested as ORR catalysts at the cathode. Since MFC_L showed better performance, this study was carried out only on this fuel cell design. The resulting fuel cells were named as MFC_BC1 and MFC_BC2 according to the type of catalyst used. Table 4.1 summarises the results obtained and compares them with the catalyst-free fuel cells previously tested. Figure 4.6 shows the polarisation and power curves for both devices. The OCV values for MFC_BC1 and MFC_BC2 were 151 mV and 220 mV respectively, and thus comparable with MFC_L.

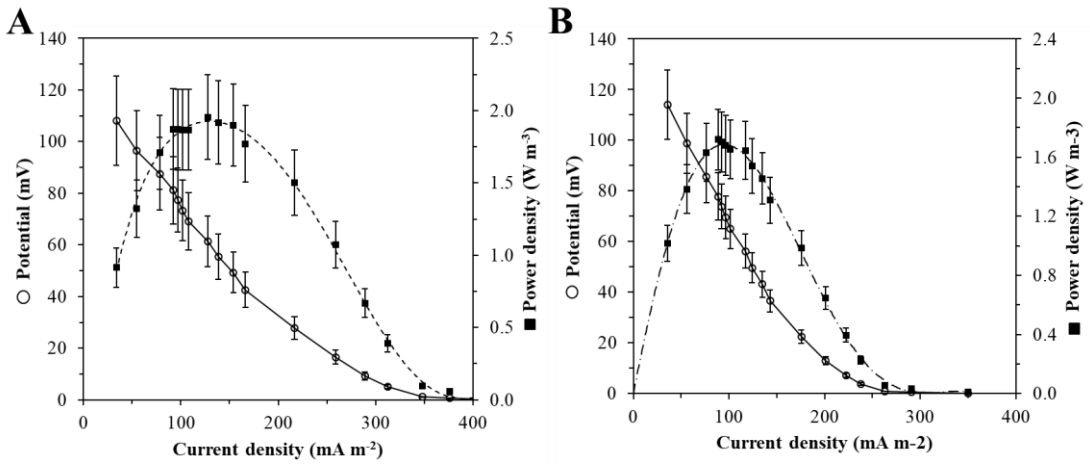

Figure 4.6. Power and polarisation curves. [**A**] Refers to MFC_BC1; [**B**] refers to MFC_BC2; Current density refers to the anode surface area: MFC_BC1, MFC_BC2 = 32 mm^2. Volumetric power density refers to the MFC chamber volume: MFC_BC1, MFC_BC2 = 128 µL. Data is an average of two units with 17% error.

Table 4.1. Summary of performance of the several MFCs tested in this study

MFC configuration	OCV (mV)	Internal resistance (kΩ)	Maximum power output (nW)	Maximum volumetric power density (W m^{-3})	Maximum current density (mA m^{-2})
MFC_S	253	242	3.4	0.053	7.3
MFC_S series stack	151	243	12.1	0.063	4.6
MFC_S parallel stack	206	76	46.7	0.243	18.4
MFC_L	312	33	74.2	0.580	49.1
MFC_L parallel stack	281	1.4	455.1	1.185	157.1
MFC_BC1	151	15	250.1	1.954	127.6
MFC_BC2	220	23	220.1	1.719	88.4

As expected, the ORR catalysts enhanced the power performance of the MFCs, leading to a power output and power density almost 3 times higher than MFC_L. The effectiveness of biomass derived ORR catalysts may be attributed to the large surface area [19] that the materials exhibit on the cathode surface compared to the plain carbon cloth (BC1: 376 m^2 g^{-1} [25]), as well as the capacity of heteroatom doping, such as nitrogen and sulphur, or the incorporation of iron within the catalyst material to

enhance the ORR activity [17,18,41-44]. To validate this, a control involving the use of a biochar without nitrogen, sulphur or iron is needed.

The mechanisms for the catalytic activity for nitrogen and sulphur doped carbons and ORR is, currently, uncertain- with many different conflicting and different interpretations [19]. With nitrogen doped carbons, factors such as enhanced π-bonding, electrical conductivity and Lewis basicity may facilitate reductive O_2 adsorption at the carbon surface [19,25]. Structural defects in the carbon crystal lattice, caused dopant introduction, may result in more catalytically important edge-bound heteroatoms (for example pyridinic nitrogen) [19, 25]. When doping carbons with sulphur, the sulphur may disrupt carbon connection patterns in the material, which induces more strain and defect sites in the carbon material, which facilitates charge localisation and the coupled chemisorption of oxygen. Moreover, sulphur has large polarisation d-orbitals, where the lone pairs of sulphur readily interact with molecules in the surrounding electrolyte [19]. When nitrogen and sulphur are present together in the carbon, it is tentatively proposed that nitrogen activates the oxygen molecule (either directly or indirectly *via* the adjacent carbon atom), while sulfur facilitates the proton transfer during the reduction process [19]. However, the current knowledge in the scientific literature regarding nitrogen and sulphur doped carbons, the functional groups that they produce on the carbon, and ORR is limited, and more fundamental investigations in this field are required.

The internal resistances decreased to values of 15 kΩ and 23 kΩ, for MFC_BC1 and MFC_BC2 respectively, down to half those of MFC_L. Consequently, the current densities were an order of magnitude higher, with a value as high as 127.6 mA m^{-2} for MFC_BC1.

Generally MFC_BC1 performed better, with a 13% higher power density and a 44% increase in current density, compared to MFC_BC2. The structure of the two doped cathodes may be the reason for this difference. From the SEM images of the doped cathodes, Figure 4.7, it can be seen that the two ORR catalysts led to very different surface structures. In particular, it appears that BC1 percolated between the carbon fibres of the carbon cloth. Hence, good contact was formed between the carbon fibre electrode and the biomass derived ORR catalyst, thus allowing a good active surface area for oxygen reduction reactions at the cathode surface. On the other hand, BC2 formed a porous layer on top of the carbon fibres, which have resulted in an added

resistance to the system and may explain the poorer performance of MFC_BC2 with respect to MFC_BC1.

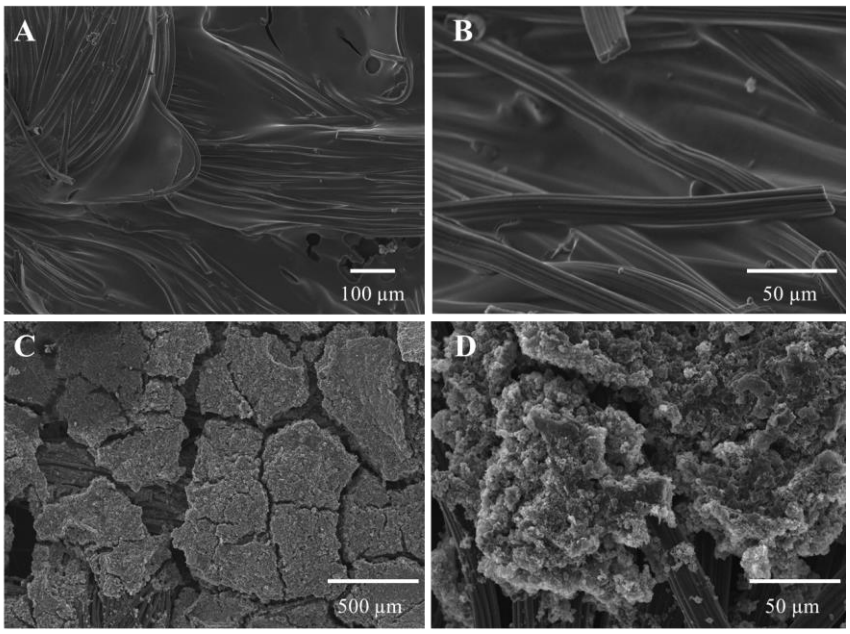

Figure 4.7. SEM images of the two biomass derived ORR catalyst doped cathode surfaces. [**A**] and [**B**] refer to the cathode used for MFC_BC1; [**C**] and [**D**] to the case of MFC_BC2.

4.5 Conclusions

Microbial fuel cells are an extremely attractive technology for the generation of clean electricity from a range of waste streams. The most viable route to boosting power density generated by MFCs is to develop small scale devices and arrange multiple units in stacks.

In this context, our study aims to guide towards the development of effective miniature MFCs. For this purpose we have developed an innovative miniature MFC, which can easily be further miniaturised. We have used an air-cathode configuration since it has the advantage of greater operational simplicity and cost-effectiveness. While fixing the electrodes spacing to 4 mm, we have investigated the effect of the electrodes length, when the system was continuously fed with artificial urine at a fixed flow rate of 0.36 mL min^{-1}.

The doubling of the electrode length of the miniature MFC, and so the hydraulic retention time as well, increased the power density more than tenfold due to enhanced mass transfer properties and substrate consumption at the electrode surface.

By electrically stacking three individual units in parallel, the power output reached the peak value of 1.2 W m^{-3}. Moreover, the use of two different types of biomass derived ORR catalysts at the cathode increased the power density up to threefold. These renewable and cost-effective cathode catalysts are of particular interest for applications in remote or impoverished regions where MFCs could be used for remote and sustainable energy generation from waste. It would be of interest to investigate the effect of stacking the MFC_BC units, to observe if similar enhancements in overall power output can be achieved, as for the the MFC_S and MFC_L devices.

4.6 Associated content

Author Contributions

Formulation of ideas, design of methodology conducted by JC and MDL. Experiments conducted by JC and GAP, Manuscript preparation by JC. Supervision from MDL, PJC and II. Biomass derived catalysts prepared by MMT and KP.

Conflicts of Interest

The authors declare no conflict of interest.

Acknowledgements

The authors thank: Wessex Water for providing anaerobic sludge; the Engineering and Physical Sciences Research Council (EPSRC) and the Doctoral Training Centre for Sustainable Chemical Technologies (CSCT) for funding (EP/G03768X/1); Stephen Bradley for the SEM images of the doped cathodes. Ioannis Ieropoulos is an EPSRC career acceleration fellow (CAF), grant numbers EP/I004653/1 and EP/L002132/1.

Abbreviations

AUM: Artificial urine medium,

MFC: Microbial fuel cell,

MFC_BC1: Microbial fuel cell using ‘biochar 1’,

MFC_BC2: Microbial fuel cell using ‘biochar 2’,

MFC_L: ‘Long’ microbial fuel cell,

MFC_S: ‘Short’ microbial fuel cell,

OCV: Open circuit voltage,

ORR: Oxygen reduction reaction,

PDMS: Polydimethylsiloxane,

SEM: Scanning electron microscope.

Nomenclature

Roman symbols

c: Concentration of redox compound,

ΔC: Concentration gradient of the limiting compound,

D: Normalised substrate diffusivity,

d_H: Hydraulic diameter of the flow channel,

F: Faraday’s constant,

H: Chamber height,

I: Current,

I_{max}: Maximum current density,

k_C: Mass transfer coefficient,

L: Lateral dimension chamber length,

n: Available substrate electrons,

P: Power,

R: Resistance,

Re: Reynold's number

R_{int}: Internal resistance,

V: Voltage,

v: Linear velocity of the fluid.

Greek symbols

λ: Diffusion layer thickness,

μ: Fluid viscosity,

ρ: Specific fluid density.

4.7 References

[1] O. Edenhofer, R. Pichs-Madruga, Y. Sokona, K. Seyboth, P. Matschoss, S. Kadnert, Renewable Energy Sources and Climate Change Mitigation- Special Report of the Intergovernmental Panel on Climate Change, 2011.

[2] A.P.C. Faaij, Bio-energy in Europe: changing technology choices, Energy Policy. 34 (2006) 322–342. doi:10.1016/j.enpol.2004.03.026.

[3] B. Logan, B. Hamelers, R. Rozendal, U. Schroder, J. Keller, S. Freguia, P. Aelterman, W. Verstraete, K. Rabaey, Critical Review Microbial Fuel Cells : Methodology and Technology, Environ. Sci. Technol. 40 (2006) 5181–5192. doi:10.1021/es0605016.

[4] I. Ieropoulos, J. Greenman, C. Melhuish, Urine utilisation by microbial fuel cells; energy fuel for the future., Phys. Chem. Chem. Phys. 14 (2012) 94–98. doi:10.1039/c1cp23213d.

[5] H. Ren, H.-S. Lee, J. Chae, Miniaturizing microbial fuel cells for potential portable power sources: promises and challenges, Microfluid. Nanofluidics. 13 (2012) 353–381. doi:10.1007/s10404-012-0986-7.

[6] K. Rabaey, W. Verstraete, Microbial fuel cells: novel biotechnology for energy generation., Trends Biotechnol. 23 (2005) 291–298. doi:10.1016/j.tibtech.2005.04.008.

[7] H. Liu, B.E. Logan, Electricity generation using an air-cathode single chamber microbial fuel cell in the presence and absence of a proton exchange membrane., Environ. Sci. Technol. 38 (2004) 4040–4046. http://www.ncbi.nlm.nih.gov/pubmed/15298217.

[8] I. Ieropoulos, P. Ledezma, A. Stinchcombe, G. Papaharalabos, C. Melhuish, J. Greenman, Waste to real energy: the first MFC powered mobile phone., Phys. Chem. Chem. Phys. 15 (2013) 15312–15316. doi:10.1039/c3cp52889h.

[9] I. Ieropoulos, J. Greenman, C. Melhuish, Miniature microbial fuel cells and stacks for urine utilisation, Int. J. Hydrogen Energy. 38 (2013) 492–496. doi:10.1016/j.ijhydene.2012.09.062.

[10] Z. He, J. Kan, Y. Wang, Y. Huang, F. Mansfeld, K.H. Nealson, Electricity Production Coupled to Ammonium in a Microbial Fuel Cell, Environ. Sci. Technol. 43 (2009) 3391–3397. doi:10.1021/es803492c.

[11] S. Choi, Microscale microbial fuel cells: Advances and challenges, Biosens. Bioelectron. 69 (2015) 8–25. doi:10.1016/j.bios.2015.02.021.

[12] A. Baudler, I. Schmidt, M. Langner, A. Greiner, U. Schröder, Does it have to be Carbon? Metal Anodes in Microbial Fuel Cells and related Bioelectrochemical Systems, Energy Environ. Sci. 8 (2015) 2048–2055. doi:10.1039/C5EE00866B.

[13] B. Logan, J. Regan, Microbial challenges and applications, Environ. Sci. Technol. 40 (2006) 5172–5180. doi:10.1021/es0627592.

[14] L. Deng, M. Zhou, C. Liu, L. Liu, C. Liu, S. Dong, Development of high performance of Co/Fe/N/CNT nanocatalyst for oxygen reduction in microbial fuel cells., Talanta. 81 (2010) 444–448. doi:10.1016/j.talanta.2009.12.022.

[15] L. Zhang, C. Liu, L. Zhuang, W. Li, S. Zhou, J. Zhang, Manganese dioxide as an alternative cathodic catalyst to platinum in microbial fuel cells., Biosens. Bioelectron. 24 (2009) 2825–2829. doi:10.1016/j.bios.2009.02.010.

[16] T. Huggins, H. Wang, J. Kearns, P. Jenkins, Z.J. Ren, Biochar as a sustainable electrode material for electricity production in microbial fuel cells, Bioresour. Technol. 157 (2014) 114–119. doi:10.1016/j.biortech.2014.01.058.

[17] Y. Yuan, T. Yuan, D. Wang, J. Tang, S. Zhou, Sewage sludge biochar as an efficient catalyst for oxygen reduction reaction in an microbial fuel cell, Bioresour. Technol. 144 (2013) 115–120. doi:10.1016/j.biortech.2013.06.075.

[18] H. Yuan, L. Deng, Y. Qi, N. Kobayashi, J. Tang, Nonactivated and Activated Biochar Derived from Bananas as Alternative Cathode Catalyst in Microbial Fuel Cells, Sci. World J. 2014 (2014) 1–8. doi:10.1155/2014/832850.

[19] S.-A. Wohlgemuth, R.J. White, M.-G. Willinger, M.-M. Titirici, M. Antonietti, A one-pot hydrothermal synthesis of sulfur and nitrogen doped carbon aerogels with enhanced electrocatalytic activity in the oxygen reduction reaction, Green Chem. 14 (2012) 1515-1523. doi:10.1039/c2gc35309a.

[20] M. Li, Y. Xiong, X. Liu, C. Han, Y. Zhang, X. Bo, L. Guo, Iron and nitrogen co-doped carbon nanotube@hollow carbon fibers derived from plant biomass as efficient catalysts for the oxygen reduction reaction, J. Mater. Chem. A. 3 (2015) 9658–9667. doi:10.1039/C5TA00958H.

[21] T.H. Pham, K. Rabaey, P. Aelterman, P. Clauwaert, L. De Schamphelaire, N. Boon, W. Verstraete, Microbial Fuel Cells in Relation to Conventional Anaerobic Digestion Technology, Eng. Life Sci. 6 (2006) 285–292. doi:10.1002/elsc.200620121.

[22] L. Woodward, M. Perrier, B. Srinivasan, C. Hc, B. Tartakovsky, Maximizing Power Production in a Stack of Microbial Fuel Cells Using Multiunit Optimization Method, Biotechnol. Prog. 25 (2009) 676–682. doi:10.1021/bp.115.

[23] F. Qian, D.E. Morse, Miniaturizing microbial fuel cells., Trends Biotechnol. 29 (2011) 62–69. doi:10.1016/j.tibtech.2010.10.003.

[24] F. Qian, Z. He, M.P. Thelen, Y. Li, A microfluidic microbial fuel cell fabricated by soft lithography., Bioresour. Technol. 102 (2011) 5836–40. doi:10.1016/j.biortech.2011.02.095.

[25] T. Brooks, C.W. Keevil, A simple artificial urine for the growth of urinary pathogens., Lett. Appl. Microbiol. 24 (1997) 203–206. http://www.ncbi.nlm.nih.gov/pubmed/9080700.

[26] R.J. White, N. Yoshizawa, M. Antonietti, M.-M. Titirici, A sustainable synthesis of nitrogen-doped carbon aerogels, Green Chem. 13 (2011) 2428-2434. doi:10.1039/c1gc15349h.

[27] H. Ren, C.I. Torres, P. Parameswaran, B.E. Rittmann, J. Chae, Improved current and power density with a micro-scale microbial fuel cell due to a small characteristic length., Biosens. Bioelectron. 61 (2014) 587–592. doi:10.1016/j.bios.2014.05.037.

[28] T.K. Sherwood, R.L. Pigford, C.R. Wilke, Mass Transfer, McGraw-Hill, New York, 1975.

[29] S. Choi, H.-S. Lee, Y. Yang, P. Parameswaran, C.I. Torres, B.E. Rittmann, J. Chae, A μL-scale micromachined microbial fuel cell having high power density., Lab Chip. 11 (2011) 1110–1117. doi:10.1039/c0lc00494d.

[30] F. Qian, M. Baum, Q. Gu, D.E. Morse, A 1.5 μL microbial fuel cell for on-chip bioelectricity generation., Lab Chip. 9 (2009) 3076–3081. doi:10.1039/b910586g.

[31] A. Elmekawy, H.M. Hegab, X. Dominguez-Benetton, D. Pant, Internal resistance of microfluidic microbial fuel cell: challenges and potential opportunities., Bioresour. Technol. 142 (2013) 672–682. doi:10.1016/j.biortech.2013.05.061.

[32] H.-Y. Wang, A. Bernarda, C.-Y. Huang, D.-J. Lee, J.-S. Chang, Micro-sized microbial fuel cell: a mini-review., Bioresour. Technol. 102 (2011) 235–243. doi:10.1016/j.biortech.2010.07.007.

[33] B. Inman, W. Etienne, R. Rubin, R. Owusu, T. Oliveira, D. Rodriques, P. Maccarini, P. Stauffer, A. Mashal, M. Dewhirst, The impact of temperature and urinary constituents on urine viscosity and its relevance to bladder hyperthermia treatment, Int. J. Hyperth. 29 (2013) 206–210. doi:10.3109/02656736.2013.775355.

[34] B.Y. Louis, D. Akeley, A Study of the Diffusion of Urea in Water at 25 C with the Gouy Interference Method, J. Am. Chem. Soc. 74 (1952) 2058–2060. doi:10.1021/ja01128a060.

[35] J. Lee, K.G. Lim, G.T.R. Palmore, A. Tripathi, Optimization of microfluidic fuel cells using transport principles., Anal. Chem. 79 (2007) 7301–7307. doi:10.1021/ac070812e.

[36] C. Liu, J. Li, X. Zhu, L. Zhang, D. Ye, R.K. Brown, Q. Liao, Effects of brush lengths and fiber loadings on the performance of microbial fuel cells using graphite fiber brush anodes, Int. J. Hydrogen Energy. 38 (2013) 15646–15652. doi:10.1016/j.ijhydene.2013.03.144.

[37] I. Ieropoulos, J. Greenman, C. Melhuish, Improved energy output levels from small-scale Microbial Fuel Cells., Bioelectrochemistry. 78 (2010) 44–50. doi:10.1016/j.bioelechem.2009.05.009.

[38] P. Ledezma, J. Greenman, I. Ieropoulos, MFC-cascade stacks maximise COD reduction and avoid voltage reversal under adverse conditions., Bioresour. Technol. 134 (2013) 158–165. doi:10.1016/j.biortech.2013.01.119.

[39] G. Papaharalabos, J. Greenman, C. Melhuish, I. Ieropoulos, A novel small scale Microbial Fuel Cell design for increased electricity generation and waste water treatment, Int. J. Hydrogen Energy. 40 (2015) 4263–4268. doi:10.1016/j.ijhydene.2015.01.117.

[40] P. Aelterman, K. Rabaey, H.T. Pham, N. Boon, W. Verstraete, Continuous Electricity Generation at High Voltages and Currents Using Stacked Microbial Fuel Cells, Environ. Sci. Technol. 40 (2006) 3388–3394. doi:10.1021/es0525511.

[41] J. Liu, P. Song, Z. Ning, W. Xu, Recent Advances in Heteroatom-Doped Metal-Free Electrocatalysts for Highly Efficient Oxygen Reduction Reaction, Electrocatalysis. 6 (2015) 132–147. doi:10.1007/s12678-014-0243-9.

[42] N. Daems, X. Sheng, I.F.J. Vankelecom, P.P. Pescarmona, Metal-free doped carbon materials as electrocatalysts for the oxygen reduction reaction, J. Mater. Chem. A. 2 (2014) 4085–4110. doi:10.1039/C3TA14043A.

[43] F. Charreteur, F. Jaouen, S. Ruggeri, J.-P. Dodelet, Fe/N/C non-precious catalysts for PEM fuel cells: Influence of the structural parameters of pristine commercial carbon blacks on their activity for oxygen reduction, Electrochim. Acta. 53 (2008) 2925–2938. doi:10.1016/j.electacta.2007.11.002.

[44] U.I. Kramm, J. Herranz, N. Larouche, T.M. Arruda, M. Lefèvre, F. Jaouen, P. Bogdanoff, S. Fiechter, I. Abs-Wurmbach, S. Mukerjee, J.-P. Dodelet, Structure of

the catalytic sites in Fe/N/C-catalysts for O2-reduction in PEM fuel cells., Phys. Chem. Chem. Phys. 14 (2012) 11673–11688. doi:10.1039/c2cp41957b.

5 Exploring the use of cost-effective membrane materials for microbial fuel cell based sensors

This chapter investigates the potential for alternative low cost membrane materials in MFCs, and then compares their ability to detect the labile organic content in wastewater. A natural polymer (eggshell membrane) and synthetic polymer (polydimethylsiloxane, PDMS) are used, as well as a membrane-less design and an MFC with the commonly used Nafion membrane. Device geometry is also investigated by studying the effect of electrode spacing on power and sensing performance. This chapter has been published as detailed on the following page.

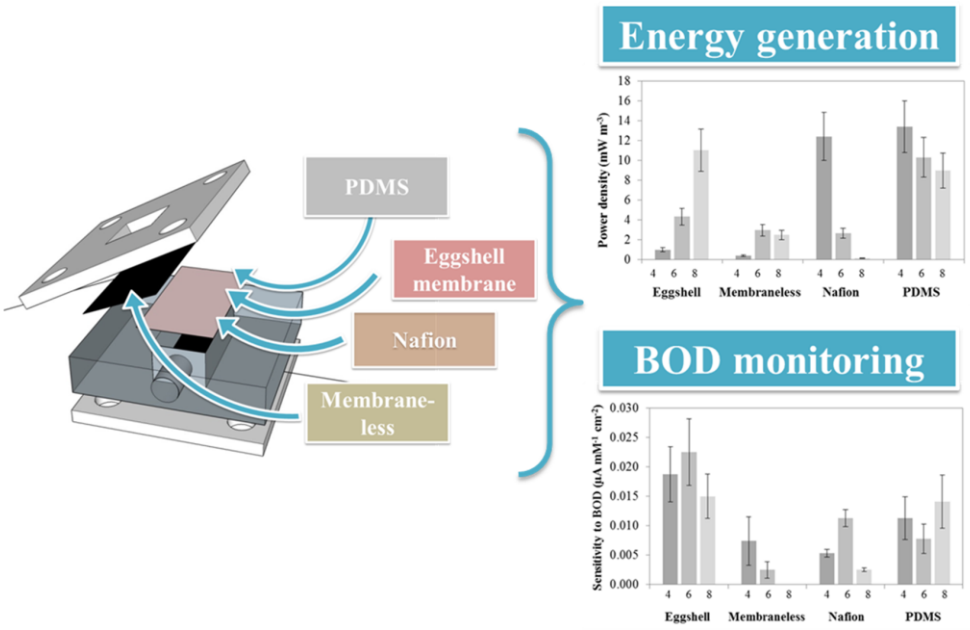

Statement of authorship

This declaration concerns the article entitled:	Exploring the use of cost-effective membrane materials for microbial fuel cell based sensors
Publication status:	Published
Publication details:	J. Chouler, I. Bentley, F. Vaz, A. O'Fee, P.J. Cameron, M. Di Lorenzo, Exploring the use of cost-effective membrane materials for Microbial Fuel Cell based sensors, Electrochim. Acta. 231 (2017) 319–326. doi:10.1016/j.electacta.2017.01.195.
Authorship contributions:	Formulation of ideas, design of methodology conducted by JC and MDL. Experiments conducted by JC, IB, FV, AO. Manuscript preparation by JC. Supervision from MDL and PJC.
Statement from candidate:	This paper reports on original research I conducted during the period of my Higher Degree by Research candidature.

Signed: Date:

Exploring the use of cost-effective membrane materials for microbial fuel cell based sensors

Jon Chouler [a,b], Isobel Bentley [a], Flavia Vaz [a], Annabel O'Fee [a], Petra J. Cameron [c], Mirella Di Lorenzo [a]

[a] University of Bath, Department of Chemical Engineering, Bath, BA2 7AY, UK

[b] Centre for Sustainable Chemical Technologies, University of Bath, Bath BA2 7AY, UK

[c] University of Bath, Department of Chemistry, Bath, BA2 7AY, UK

5.1 Abstract

Microbial fuel cells show great potential as a self-powered, real time and onsite technology for monitoring the labile organic carbon content (e.g. Biochemical Oxygen Demand, BOD) in water systems. By drastically reducing their cost of manufacture, MFCs can become an important tool for water quality monitoring, accessible also in the poorest and most remote areas of the world. To enable this, this study investigates for the first time the use of two low cost membrane materials: a natural polymer (eggshell membrane), and a synthetic polymer (polydimethylsiloxane, PDMS). The energy generation and sensing capability of the resulting devices were compared with a membrane-less device, while the well-known Nafion membrane was used as a control. For each device, the effect of electrode spacing on performance was also investigated. The use of PDMS led to a power density similar to the case of the much more expensive Nafion membrane. The electrode spacing affected the output power, but it had a negligible effect on the BOD sensing capability of the devices. In particular, for the case of the eggshell membrane and the membrane-less devices, the higher the electrode spacing the better the power performance. The opposite trend was observed when a synthetic membrane was used. Finally, although more unstable than the other devices, the eggshell membrane devices were associated with the lowest internal resistances and the highest sensitivity. In conclusion, this study not only demonstrates the use of inexpensive membranes in MFCs, but it also provides

guidelines on design, in terms of electrode spacing and cross-sectional area, according to the material used.

5.2 Introduction

The biological oxygen demand (BOD) is a measure of the labile organic carbon content in water and is used as an index for sizing wastewater treatment plants and measuring the efficacy of wastewater treatments [1]. The standard method to determine BOD, the 5-day BOD test (BOD_5), is, however, time consuming and not compatible with rapid and onsite monitoring needs [2]. As a result, in the past decades, a lot of effort has been dedicated to the search for technologies that are less time consuming and more reliable [3]. Table S5.1 in the Supporting Information, reports a selection of available BOD biosensors in the literature, and highlights their performance and limitations. In principle, all these biosensors show promise for rapid online monitoring of BOD in water with response times ranging from 3 up to 120 minutes. The majority of them, however, present very poor operational stability, low substrate versatility and a small measuring range. Moreover, those that rely on single microbial strains have low accuracy, due to the limited range of biodegradable compounds that they can detect.

Recently, the microbial fuel cell (MFC) has proven to be an attractive technology for BOD monitoring. The striking features of MFC based BOD sensors are their simplicity, short period of analysis, wide measurement range, low maintenance, and the ability to work online and onsite [4-8]. When a microbial consortium is used as the bio-recognition element, rather than a single species, MFCs can detect a diverse range of biodegradable compounds in water. Moreover, the several types of MFC based BOD sensors reported in the literature demonstrate appreciable long term stabilities and good correlation between the BOD content of the water and current output generated by the MFC sensor [5,6]. Most of these devices employ a two chamber configuration [9,10]. Single chamber designs are, however, preferable because of lower operational costs, higher design simplicity and, therefore, better possibilities for industrial scale-up [11-15].

Despite recent design efforts, reducing operational costs remains a key factor in the commercialisation of MFCs. The majority of the MFCs reported in the literature

employ platinum as the catalyst at the cathode and expensive membranes, such as Nafion [5,6,16-18]. To address these issues, catalyst-free devices have been reported, and recently the use of biomass derived carbon materials has been investigated as a sustainable and cost-effective alternative to platinum [19-21] Several studies on exploring the use of alternative membranes and separators have been also reported. These include: cation exchange membranes, such as sulfonated poly-ether ether ketone (SPEEK) [22], sulfonated polystyrene-ethylene-butylene-polystyrene (SPSEBS) [23], CMI-7000 [24], and Hyflon Ion [25]; anion exchange membranes, such as AMI-7000 [24,26]; salt bridges [27]; and porous materials such as J-Cloth [9,28], glass fibre filters and nylon [29], non-woven cloth [30], earthenware pot [31], ceramic and terracotta [32], compostable bags [33] and latex glove and condoms [34,35]. Although cheaper than Nafion, some of these materials, are still relatively expensive, can be difficult to handle and can be associated with low power performance due to high internal resistances [18]. Membrane-less designs, where a biofilm at the cathode acts as the catalyst and as a living separator, have also been suggested [36,37]. In batch mode, however, these MFCs suffer from reduced power outputs over time, due to biofilm overgrowth at the cathode that reduces the efficacy of electron transfer [36]. The focus for the majority of these studies has been on the improvement of power performance. The use of alternative membranes in MFCs has also been explored for sensing applications. Examples are the single chamber MFC based BOD sensors that use a SPEEK membrane [38] or a microporous filter paper membrane [15]. Lastly, an MFC based on flat filter paper, where the paper acted as both the membrane material and the support for the anode and cathode, was tested to detect chromium and nickel [39].

In order to pursue the development of cost-effective MFC based sensors, this work looks towards the use of low cost membranes, which would further reduce the manufacturing costs of miniature MFC devices. It is expected that practical applications require the simultaneous use of more than one MFC unit. This approach would allow either increasing the current baseline, when the units are electrically connected to each other [40], or providing multiple readings for better reliability, when the units are electrically isolated from each other [14,41]. As such, it is important to minimise, as much as possible, the cost of a single MFC device.

With this purpose, the use of a natural polymer, such as eggshell membrane, and of a synthetic polymer, such as polydimethylsiloxane (PDMS) are tested here for the first time. In previous work, eggshell membrane has been used as a template for a 3D

fibrous cathode in solid oxide fuel cells [42], while egg yolk has been tested as a base material for a biodegradable cathode in MFCs [43]. PDMS has been used as a base material for a carbon based cathode constructed around a stainless steel mesh in an MFC, in which the PDMS prevented water leakage from the device and acted as a diffusion layer [44]. This study is, however, the first that investigates the use of these materials as a membrane in an MFC for BOD sensing. The energy generation and sensing capability of the resulting devices are analysed and compared with the case of a membrane-less device, while Nafion is used as a control. Finally, for each membrane material used, the relevance that the spacing between the anode and cathode had on performance was also investigated.

5.3 Experimental

5.3.1 Materials

All reagents used were of analytical grade and purchased from Sigma-Aldrich and Alfa Aesar. All solutions used were prepared with reverse osmosis purified water. Polydimethylsiloxane (PDMS, Dow Corning Sylgard 184) was purchased from Ellsworth Adhesives (UK). Nafion 117 was purchased from Sigma Aldrich.

Artificial Wastewater (AW), adapted from [14], was used as the feedstock containing (per litre): 0.27 g $(NH_4)_2SO_4$, 0.06 g $MgSO_4.7H_2O$, 0.006 g $MnSO_4.H_2O$, 0.13 g $NaHCO_3$, 0.003 g $FeCl_3.6H_2O$, 0.004 $MgCl_2$, 3.1 $NaH_2PO_4.H_2O$ and 10.9 Na_2HPO_4. Potassium acetate was added to the AW (between 0.1 – 200 mM) and used as the carbon source for the bacteria. The resulting medium was autoclaved prior to use.

5.3.2 Microbial fuel cells and membrane assembly

The single chamber miniature MFCs were manufactured as previously described [45]. The length of the devices was 8 mm and the width was 4 mm. The height of the MFCs, corresponding to the electrode spacing, was varied from 4 mm (anodic chamber volume, V_A = 128 µL) to 6 mm (V_A = 192 µL) and 8 mm (V_A = 256 µL). Both the anode and cathode were made of carbon cloth (untreated carbon cloth, type-B, E-Tek, USA),

and the cathode was open to the air. Four MFC configurations were manufactured using different membrane materials, Nafion (MFC_N), eggshell membrane (MFC_E) and PDMS (MFC_P), along with a membrane-less device, where the cathode was directly exposed to the anodic chamber (MFC_M). For each type of MFC, the electrode spacing is denoted by a suffixed number (e.g. MFC_N4 denotes a Nafion membrane with an electrode spacing of 4 mm). In the case of MFC_N, Nafion was hot-pressed to the cathode as previously described [45]. For MFC_E, the eggshell membrane was carefully peeled off from the shell of fresh eggs, Figure S5.1, and thoroughly rinsed with deionised water prior to use. It was then cut into a 15 × 15 mm square and hot pressed to the cathode by applying a pressure of approximately 2.5 bar for 5 minutes at a temperature of 100°C. For MFC_P, 69 mg cm^{-2} of PDMS was spin coated at 1900 rpm (SCK-100 Spin Coater, Instras Scientific) for 1 min onto the cathode surface and then cured for 40 min at 100°C, Figure S5.2. MFC_M used a carbon cloth cathode with no further treatment. All the experiments were conducted using duplicates for each device.

5.3.3 Operation of the MFCs

The MFCs were fed with AW at a flow rate of 0.36 mL min^{-1} (hydraulic retention time of 22 seconds), and their voltage continuously monitored as previously described [45]. An external load was connected to the MFC to polarise the cell, as shown in Figure S5.3. Enrichment and further operation of the MFCs was undertaken as previously described [45], except that AW contained 1% *v/v* of anaerobic sludge (provided by Wessex Water from a wastewater treatment plant in Avonmouth, UK), and 100 mM potassium acetate was used to enrich the MFCs for a period of 14 days. After enrichment, no sludge was added in the feed solution. The feed solution was kept anaerobic; however, depending on the specific system set-up used, we expect oxygen diffusion through the system *via* the cathode, leading to the formation of an aerobic biofilm at the cathode.

Polarisation experiments and calculations of current, power, and internal resistance were performed as previously described [45]. Current and power densities refer to the projected surface area of the anode (0.32 cm^2) and to the anodic chamber volume

respectively. After polarisation, the MFCs were operated at the external resistance that gave the highest power performance.

The morphology of the biofilm onto the membrane surface was characterised using a Jeol JSM-6480LV scanning electron microscope (SEM). Fixation of biofilm samples for SEM were prepared using the standard method with hexamethyldisilazane (HMDS) as the drying agent. All biological samples were coated with Au prior to imaging. The full method is shown in the Supporting Information.

5.3.4 Testing the MFCs as sensors for labile organic carbon content

The MFCs were tested as sensors for the labile organic carbon content in water. With this purpose, the concentration of acetate, in the AW fed to the MFCs, was varied between 0.1 – 200 mM (corresponding to 9.8 – 19600 ppm acetate). A three-way valve was used to change the feed solutions, as shown in Figure S5.3. All experiments were carried out at room temperature, 20 ± 3°C. Dissolved oxygen (DO) of the feed was 0.1 ± 0.03 mg O_2 L^{-1}. The feed solution was buffered at pH 7.5. Due to the very short residence times used, it was observed that this value of the pH did not change between the MFC inlet and outlet ports. Each solution was fed to the MFCs until a steady-state voltage was established, which was defined as the point where the change in potential over time, $^{\delta mV}/_{\delta t}$ is $\leq$ 0.02 mV min^{-1}.

This study refers to chemical oxygen demand (COD), which was varied within the rage 9.8 – 19600 ppm and determined by the standard method using potassium dichromate as the oxidant (all samples filtered using 0.2 µm PTFE filter and analysed with high range COD vials). Since acetate was the only organic compound in the AW feed, in this specific simplified system the COD was considered to be equivalent to the BOD. Nonetheless, we wish to clarify that the two measurements markedly differ from each other, and the COD cannot substitute the BOD technique in complex organic systems.

5.3.5 Calculations

The sensitivity of the MFC towards the change in COD was referred against the anode total surface area (A = 0.32 cm^2) and calculated as follows [14]:

$$sensitivity = \frac{\Delta I}{\Delta C \times A} \qquad \text{Equation 5.1}$$

Where ΔI (µA) is the unit change in the current output, ΔC (mM) is the change in the COD value of the feed solution. The ratio $\Delta I/\Delta C$ was obtained from the linear slope of the current output *versus* COD value curve, within the linearity range. The sensor response time to changes in COD was calculated as the time taken to reach 95% of the new steady state current.

5.4 Results and discussion

5.4.1 Electrochemical performance of the MFCs

The MFCs were enriched for two weeks and the steady-state output current generated is reported in Table S5.2. After enrichment, the MFCs were fed with AW for one week and then polarisation experiments were performed. Table S5.3 reports the performance of each device, while Figure 5.1 shows the polarisation curves results obtained. As shown, ohmic losses appear to be significant for all devices, thus suggesting that the electrical resistances of the electrodes, membrane and electrolyte are the main contributors to the internal resistance. On the other hand, mass transfer limitations are not observed within the device. This may be a consequence of miniaturisation, which allows effective mass transport of substrate from the bulk fluid to the biofilm at the anode surface [46]. Similar trends are observed in the literature for other miniature MFCs [47-49].

The internal resistance was calculated from the polarisation curves as previously described [45]. All of the MFCs had a relatively high internal resistance ranging between 1 and 30 kΩ, Table S5.3, which is in agreement with other miniature MFCs

reported in the literature [47,50,51]. When comparing the internal resistances between devices, MFC_N and MFC_P exhibited overall the greatest internal resistance, which was on average almost 8.5 times greater than the MFC_E and MFC_M devices. This result could be caused by the protons mass transfer resistance introduced by PDMS and Nafion [18]. This hypothesis is supported by the fact that the membrane-less configuration, MFC_M, was associated with the lowest internal resistance. It has been demonstrated already that the removal of a membrane component leads to a reduction in the ohmic resistances inside the MFC [52]. The resistance introduced by the membrane depends on the membrane thickness as well as on intrinsic characteristics like porosity, proton permeability and specific surface area. MFC_E, with a membrane thickness in the order of 50 – 90 μm [53], had an internal resistance 8.6 times lower than MFC_N (183 μm) and 2.3 lower than MFC_P (approximate thickness 40 μm [54]). The internal resistance was also influenced by the electrode spacing. For the case of Nafion, it increased by approximately 30% when the electrode spacing was increased from 4 mm to 8 mm. The opposite trend was observed for the eggshell membrane, where the increase in the electrode spacing caused a 70% reduction in the internal resistance. No evident difference was observed for the case of the MFC_P and MFC_M devices, as any variation was within experimental error.

Figure 5.2 compares the maximum power density obtained with each device, while the relative power curves are reported in Figure S5.4. Despite demonstrating the highest internal resistances, MFC_N and MFC_P were associated to the greatest power densities. On average, MFC_N and MFC_P had almost twice the power density than MFC_E and MFC_M. In particular, MFC_P provided the highest power density (13.4 ± 2.6 mW m^{-3}), followed by MFC_N (12.4 ± 2.4 mW m^{-3}), MFC_E (11.0 ± 2.1 mW m^{-3}) and MFC_M (2.9 ± 0.6 mW m^{-3}). These results might be caused by the inevitable oxygen diffusion in to the anode chamber in the case of MFC_E and MFC_M, which leads to a reduction in power performance [52]. Both MFC_E and MFC_M presented unstable performance over time. When increasing the electrode spacing from 4 to 8 mm, the power density of MFC_E and MFC_M improved by a factor of 11 and 6 respectively. This result is probably due to a reduction in the oxygen cross diffusion from the air cathode to anode, which is inversely proportional to the electrode spacing [55]. The oxygen permeability through an eggshell membrane has been reported to be between 1.56×10^{-6} and 1.78×10^{-6} cm^3 O_2 STP sec^{-1} cm^{-2} $Torr^{-1}$ [56], and a similar rate of diffusion is expected in our system.

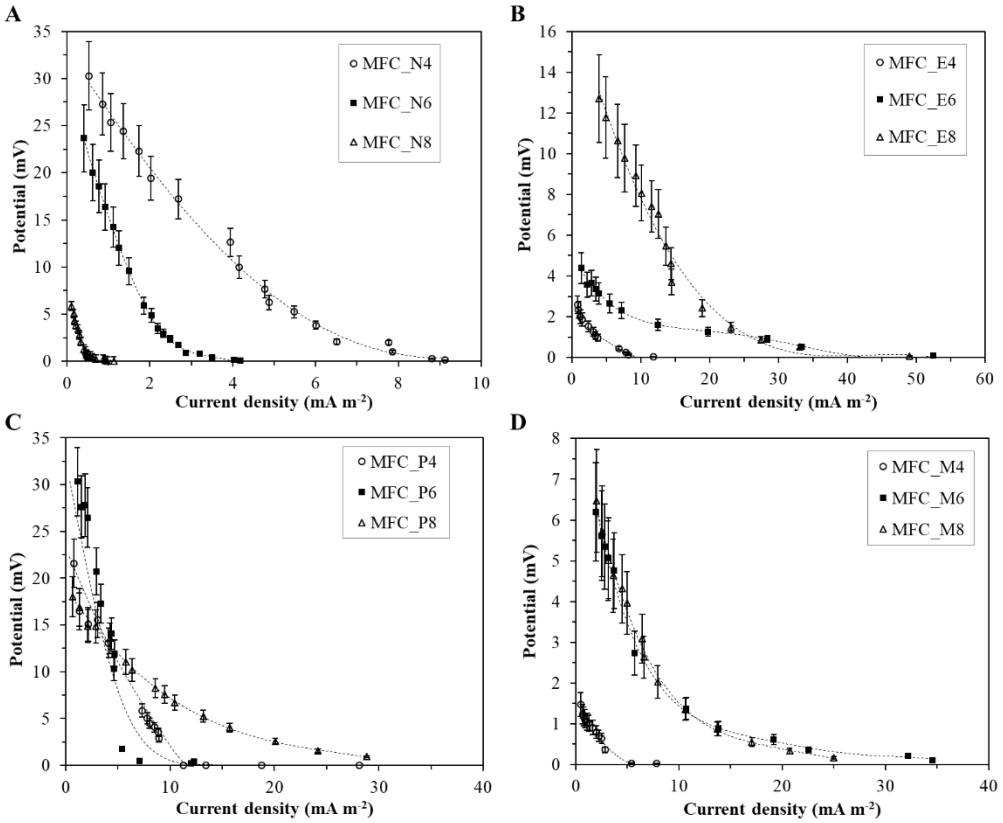

Figure 5.1. Polarisation curves for the MFCs after 2 weeks of enrichment for: [**A**] MFC_N; [**B**] MFC_E; [**C**] MFC_P; [**D**] MFC_M. Current density refers to the anode surface area, 0.32 cm^2. Data is the average of 2 devices with up to 19.5% error.

These values are approximately 3 to 5 orders of orders of magnitude higher than the case of PDMS [57] and Nafion [58]. On the other hand, when the electrode spacing was increased from 4 to 8 mm, the power density of MFC_N decreased significantly from 12.4 to 0.11 mW m^{-3}, while the power density of MFC_P was reduced by 33%. It should be noted that the error for the power densities was relatively high, up to 19.5%, and thus further work should be conducted to validate these findings. The better power performance of MFC_N and MFC_P for a short electrode spacing is likely to be due to the improvement of external mass transfer processes [48]. This is in agreement with previous studies that demonstrate increases in the maximum power output and coulombic efficiency when reducing the electrode spacing in single chamber MFCs [59–61]. The power densities and OCVs of the devices in this study are much lower than other micro-size MFCs reported in the literature (0.5-32.1 W m^{-3} and 300-600 mV respectively) [59]. A strict comparison with these devices is, however, not possible because they either refer to a two chamber configuration with FeCN as the catholyte or to gold electrodes [50,59,60], characteristics that would

enhance the power performance, at the expense of the cost. On the other hand, it should be noted that for sensing applications, the focus is not on enhancing the power output generated by the MFC, but rather on investigating and optimising its response to specific changes in the environment (e.g. in this study the concentration of labile organic content in water). Nonetheless, a poor power output may limit the sensitivity of MFC sensors [62].

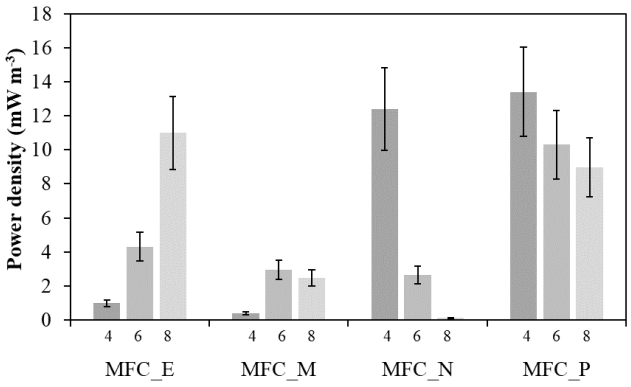

Figure 5.2. Maximum power densities obtained for each membrane material used and relative electrode spacing. The power density refers to the MFC chamber volume, (electrode spacing 4 mm = 128 µL, electrode spacing 6 mm = 192 µL, electrode spacing 8 mm = 256 µL). Electrode spacing for each device (in mm) is denoted by the corresponding number on the x-axis. Data is the average of 2 devices with up to 19.5% error.

5.4.2 Detecting labile organic carbon content in wastewater

To test the response to labile organic carbon content in water, the MFCs devices were fed with AW with a COD that varied within the range 9.8 – 19600 ppm, obtained by changing the concentration of potassium acetate in the feeding solution. The resulting amperometric response is shown in Figure 5.3. For the majority of the devices, the sensor's dynamic range was within the COD values of 9.8 – 4900 ppm, as shown in Figure S5.5. However, further tests are needed to clarify this due to large errors in the results. Data for MFC_M8 is not shown since the poor stability of the devices, caused by recurrent leaks at the air cathode, led to inconsistent performance. Changes in current may also be attributed to changes in the conductivity of the feed solution. To determine the effect of conductivity on the current generation, a control without a biofilm on the anode in the MFC should be conducted.

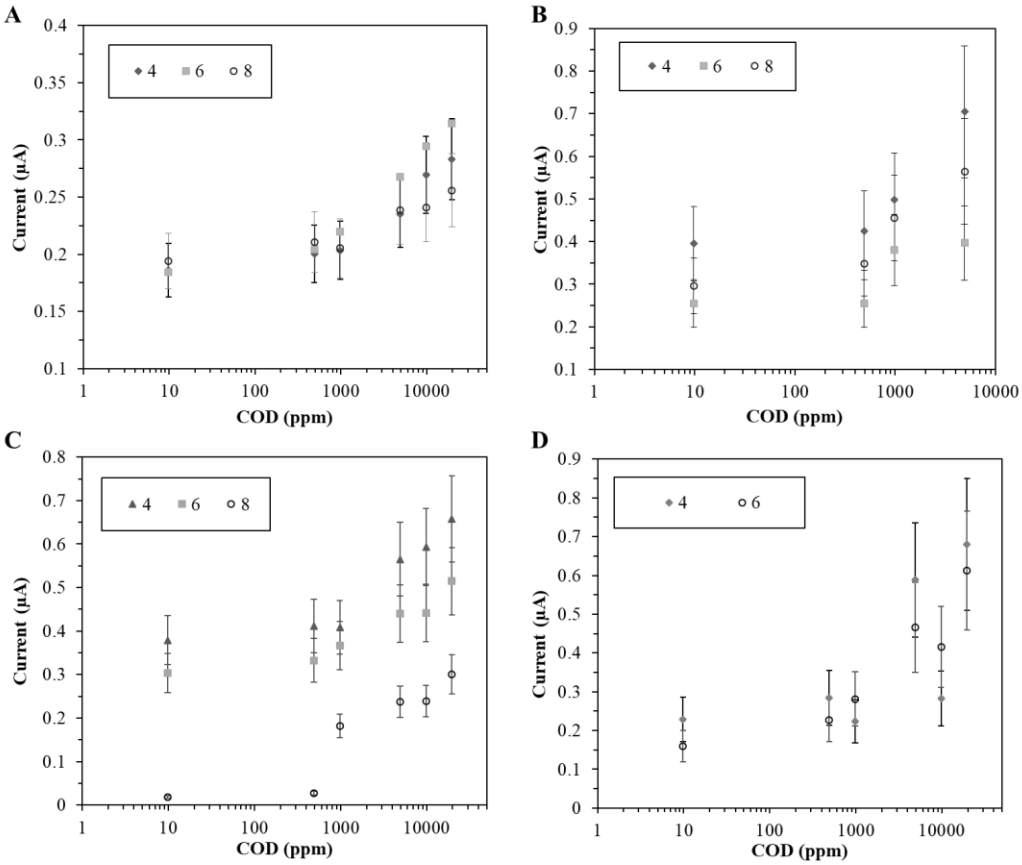

Figure 5.3. Amperometric response of the MFC sensors to increasing values of COD in the feeding solution. Semi-log plot. [**A**] MFC_N, [**B**] MFC_E, [**C**] MFC_P, **[D]** MFC_M. Numbers within each figure denote the electrode spacing of each device (mm). Error bars refer to two replicates.

The sensitivities to COD of the MFC sensors are reported in Figure 5.4. MFC_E gave the best sensitivity (0.018 ± 0.003 µA mM^{-1} cm^{-2}), followed by MFC_P (0.011 ± 0.002 µA mM^{-1} cm^{-2}), MFC_N (0.007 ± 0.003 µA mM^{-1} cm^{-2}), and MFC_M (0.005 ± 0.002 µA mM^{-1} cm^{-2}). This result demonstrates promise in the use of inexpensive membranes, such as the eggshell membrane, that, although not associated to high power output, can still lead to a sensitive biosensor. The greater sensitivity of MFC_E and MFC_P may be due to their reduced internal resistances when compared to MFC_N. This is in agreement with previous studies that demonstrated enhanced sensitivity for lower internal resistance [63]. Nonetheless, although characterised by the lowest internal resistance, the MFC_M devices showed the lowest sensitivity, probably because of the great instability in the power performance that characterised them, or due to their likely lower coulombic efficiency- where less substrate is converted to electricity and thus the current response curve has a lower slope. Note that, particularly for the MFC_N and MFC_E devices, the current responses to changes

in COD did not scale with the electrode spacings, due to variations in their performance over time.

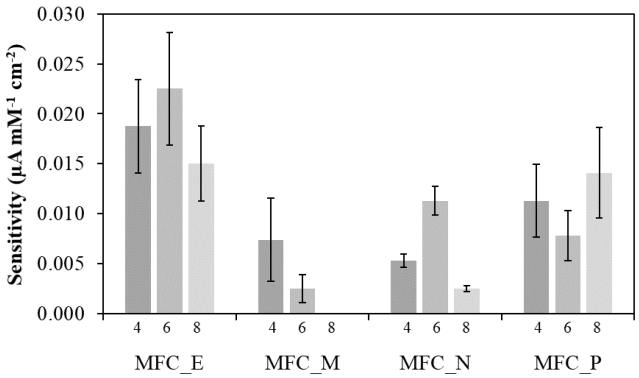

Figure 5.4: Summary of the sensitivities towards BOD for each MFC device. The values refer to an anode surface area of 0.32 cm^{-2}. Electrode spacing for each device (in mm) is denoted by the corresponding number on the x-axis. Error bars refer to two replicates.

For all the devices tested, the response time, was on average 50 ± 9 min, which is comparable to other MFCs of similar design [11,13]. If we define the detection time as the time taken for an initial change in the current after a step change in the COD, MFC_N and MFC_P devices showed the fastest response (4.6 ± 0.5 and 3.3 ± 0.5 min), compared to the MFC_E (5.6 ± 0.5) and MFC_M devices (8 ± 2 min). Surprisingly, although the electrode spacing had an influence on the power performance, it had no significant effect on sensitivity, dynamic range and response times of the MFC sensors.

Table 5.1 compares the performance of different types of MFC based BOD sensors from the literature with the devices reported in this study. As observed, the MFCs in this study are characterised by a much wider detection range for BOD (at least one order of magnitude) than other MFC sensors reported in the literature. This may be a result of miniaturisation and the consequent high electrode surface-area-to-volume ratio that lead to effective mass transfer, and therefore to minor differences in the substrate concentration between the bulk solution and the biofilm at the anode [46]. A like for like comparison is not possible here however, because other studies do not report COD values, and also use different substrates to represent BOD.

Figure 5.5 shows SEM images of the membranes (side exposed to the anodic chamber) after 12 weeks of operation. For comparison, Figure S5.6 shows the respective SEM images of control membranes that have not been used in an MFC, but have been treated

with the same assay for cell fixation. In the case of the eggshell membrane and the membrane-less device, full coverage of the membrane with a thick biofilm was observed. Although with a reduced coverage, PDMS also presented a biofilm.

Table 5.1. A summary of MFC based BOD biosensors

Configuration	**Membrane material**	**Linearity range (mg L^{-1})**	**Response time**	**Reference**
Two chamber	Nafion	20 - 200	1 h	[4]
Single chamber	Nafion	50 - 1000	0.6 - 2 h	[11]
Single chamber	SPEEK membrane	50-1100	80 min	[38]
Single chamber	Microporous filter paper	32-1280	20 h	[15]
Single chamber	Eggshell	9.8 – 4900	57 ± 6 min	This study
Single chamber	PDMS	9.8 – 4900	37 ± 2 min	This study
Single chamber	Membrane-less	9.8 – 4900	54 ± 10 min	This study
Single chamber	Nafion	9.8 - 4900	48 ± 1 min	This study

In the case of Nafion, only sporadic cells were observed. The morphology of the bacteria within the biofilm changed according to the membrane used, thus suggesting the presence of different organisms in each case. In particular, in both the case of the eggshell membrane and the PDMS, the bacteria have prevalently a rod shape, while in the membrane-less device the bacteria were mostly round in shape. Considering that both the eggshell membrane and the PDMS allow the transfer of oxygen [56,64,65], it is expected that in these cases the biofilm is composed of aerobes, which act as a living membrane preventing or minimising the introduction of oxygen in the anodic cell. This aerobic biofilm may contribute to the enhanced response of the MFC_E and MFC_P devices to changes in the feeding composition, which results in greater sensitivities when compared to MFC_N. This mechanism has been previously suggested for a membrane-less device [55]. A deeper investigation on the type of bacteria, by techniques such as next generation sequencing, would help to confirm this hypothesis. The presence of methane producing archea in the system, which would compete with the electroactive biofilm, can also be detected by identifying methane production in the cell. Finally, further electrochemical analyses of the biocathode (e.g. *via* cyclic voltammetry and electrochemical impedance spectroscopy) could help to clarify the limiting factors to the sensor sensitivity.

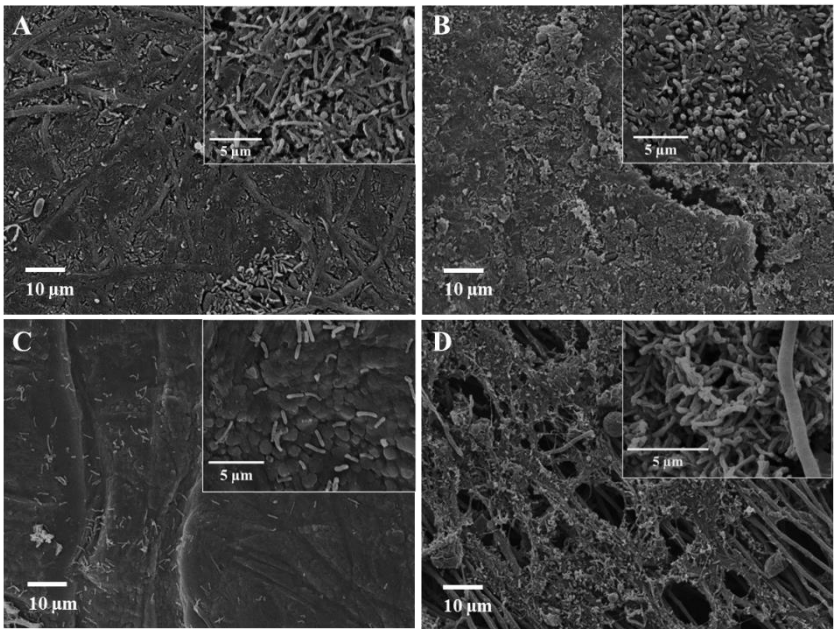

Figure 5.5. SEM images of the membranes/cathode facing the anode chamber after 12 weeks of operation. [**A**] MFC_E; [**B**] MFC_M; [**C**] MFC_N; [**D**] MFC_P.

Assuming a cost of 0.73 £ cm^{-2} for Nafion [66] and a cost of 0.10 £ g^{-1} for PDMS [67], leading to a 0.05 £ cm^{-2} cost for PDMS cast onto carbon cloth [68], then using PDMS results in a 93% reduction in the cost of manufacturing related to the membrane material. When using the eggshell membrane, which can be considered as a food waste, this reduction can be considered to be 100%. An effective and facile manufacturing route for eggshell membrane production, however, needs to be developed. As such, this work demonstrates an effective route for significant reductions in cost of MFC biosensors, whilst still maintaining appreciable power performance and demonstrating effective BOD sensing capability. This drastic reduction in the manufacturing costs make MFCs an important alternative to traditional analytical methods for water quality monitoring, that is also accessible to the poorest areas in the world.

5.5 Conclusions

In conclusion, in this study we demonstrated for the first time the use of two low cost membrane materials, of either a natural or a synthetic nature, in miniature MFC devices. We have also investigated the relevance that the electrode spacing had on

performance according to the membrane material used. Compared to other MFCs reported in the literature, the resulting MFCs could measure BOD within a range of concentrations that is at least an order of magnitude higher than the case of previously reported MFC sensors (9.8 – 4900 ppm), although further tests are needed to confirm this due to large errors present in the results. The use of the eggshell membrane led to the lowest internal resistances and the highest sensitivity towards labile organic carbon content in AW. When the PDMS membrane was tested, the maximum power density was similar to a Nafion-based MFC. The electrode spacing affected the power performance but not the sensing capabilities of the devices. In particular, for the case of the eggshell membrane and the membrane-less design, the larger the electrode spacing the higher the power output, due to a reduction in oxygen cross diffusion. On the other hand, when a synthetic membrane was used (i.e. PDMS and Nafion) large electrode spacing was associated to poor power output, with an increase in ohmic resistances within the MFC.

5.6 Associated content

Author Contributions

Formulation of ideas, design of methodology conducted by JC and MDL. Experiments conducted by JC, IB, FV, AO. Manuscript preparation by JC. Supervision from MDL and PJC.

Conflicts of Interest

The authors declare no conflict of interest.

Acknowledgements

The authors thank: Wessex Water for providing anaerobic sludge; The Engineering and Physical Science Research Council (EPSRC) and the Doctoral Training Centre for Sustainable Chemical Technologies for funding (EP/G03768X/1). Ursula Potter and Diana Lednitzky for their help with SEM imaging. Nicola Ansell for fruitful discussions.

Abbreviations

AW: Artificial wastewater,

BOD: Biological oxygen demand,

COD: chemical oxygen demand,

DO: Dissolved oxygen,

HMDS: Hexamethyldisilazane,

MFC: Microbial fuel cell,

MFC_E: Microbial fuel cell with eggshell membrane,

MFC_M: Membrane-less microbial fuel cell,

MFC_N: Microbial fuel cell with Nafion membrane,

MFC_PDMS: Microbial fuel cell with PDMS membrane,

OCV: Open circuit voltage,

PDMS: Polydimethylsiloxane,

SEM: Scanning electron microscope,

SPEEK: Sulfonated poly-ether ether ketone,

SPSEBS: sulfonated polystyrene-ethylene-butylene-polystyrene.

Nomenclature

Roman symbols

A: anode surface area,

ΔC: change in COD value,

ΔI: unit change in current output,

V_A: Anode chamber volume.

5.7 Supporting information

Table S5.1. Summary of biosensors used for BOD measurement. For comparison the standard BOD_5 test is also shown.

Type of biosensor	Biode-gradation marker	Transducer	Response time	Detection range mg L^{-1} O2	Limitations	Ref.
Standard electrode, BOD_5 test	Dissolved O_2	Iodometric dosage or electrochemical probe	5 d	0 – 6 without dilution	Long period of analysis, narrow range of measurement, variability and offline	[3]
Modified standard method for BOD_5 test	Dissolved O_2	Optical probe/Spectro-photometer/ Manometer	5 d	0 – 6 without dilution	Long period of analysis, narrow range of measurement, measurement variability	[3]
Redox mediator	Redox - mediator	Amperometer,	3 – 20 min	15 - 260	Low accuracy of equivalent BOD5 assessment	[69]
		Luminometer,	5 min	5.5 - 220		[70]
Bio-lumin-escent bacteria	Bioluminescence nt activity	Luminometer	120 min	12-200	Strain specific = limited range of biodegradable chemicals, Predicted BOD5	[71]
		Luminometer	25 min	1– 16		[72]
Immo-bolised bacteria	Dissolved O_2	Electrochemical probe	6 – 8 min	0.5 - 30	Diffusion of oxygen, chemicals in polymer matrix/ membrane, use of single strains	[73]
		Electrochemical probe	8 – 20 min	9.3 - 422		[74]
		Electrochemical probe	30 min	20 – 100,000		Ra-BOD® AppliTek
		Electrochemical probe	3 – 15 min	5 – 100,000		Biox-1010 Endress + Hauser

Table S5.2. Steady state current output of the MFCs after 2 weeks of enrichment, data is an average of 2 devices

MFC	Steady state current (µA)
MFC_N4	1.25 ± 0.24
MFC_N6	0.90 ± 0.18
MFC_N8	0.26 ± 0.05
MFC_E4	1.77 ± 0. 34
MFC_E6	1.87 ± 0. 36
MFC_E8	1.35 ± 0.26
MFC_P4	0.57 ± 0.11
MFC_P6	0.39 ± 0.08
MFC_P8	0.42 ± 0.08
MFC_M4	0.48 ± 0.09
MFC_M6	0.34 ± 0.07
MFC_M8	0.71 ± 0.14

Table S5.3. Summary of the performance of the MFCs used in this study.

MFC	OCV (mV)	Current density^{+} (mA m^{-2})	Power output (nW)	Power density^{+} (mW m^{-3})	Internal resistance (kΩ)
MFC_E4	6.4 ± 1.2	3.1 ± 0.6	0.13 ± 0.03	0.98 ± 0.2	5.8 ± 1.1
MFC_E6	11.6 ± 2.2	28.4 ± 5.5	0.83 ± 0.16	4.31 ± 0.8	1.2 ± 0.2
MFC_E8	20.3 ± 4.0	12.6 ± 2.6	2.83 ± 0.55	11.0 ± 2.1	1.7 ± 0.3
MFC_P4	26.2 ± 5.1	4.1 ± 0.8	1.71 ± 0.33	13.4 ± 2.6	6.4 ± 1.2
MFC_P6	34.6 ± 6.7	4.4 ± 0.9	1.97 ± 0.38	10.3 ±2.0	6.0 ± 1.2
MFC_P8	20.3 ± 4.0	9.5 ± 1.9	2.3 ± 0.44	8.97 ± 1.7	7.3 ± 1.4
MFC_M4	2.2 ± 0.4	2.5 ± 0.5	0.05 ± 0.01	0.40 ± 0.1	2.1 ± 0.4
MFC_M6	9.5 ± 1.9	3.7 ± 0.7	0.57 ± 0.11	2.94 ± 0.6	1.7 ± 0.3
MFC_M8	14.2 ± 2.7	6.4 ± 1.2	0.63 ± 0.12	2.47 ± 0.5	3.1 ± 0.6
MFC_N4	36.8 ± 7.1	3.9 ± 0.8	1.59 ± 0.31	12.4 ± 2.4	23.3 ± 4.5
MFC_N6	44.3 ± 8.6	1.1 ± 0.2	0.51 ± 0.10	2.65 ± 0.5	20.5 ± 4.0
MFC_N8	17.8 ± 3.5	0.3 ± 0.1	0.03 ± 0.01	0.11 ± 0.02	30.6 ± 6.0

+ Current density refers to the anode cross-sectional surface area, 0.32 cm^2. Power density refers to the MFC chamber volume, (electrode spacing 4 mm = 128 µL, electrode spacing 6 mm = 192 µL, electrode spacing 8 mm = 256 µL). COD of feed was 19600 ppm fed at 0.36 mL min^{-1}. Data is the average of 2 devices.

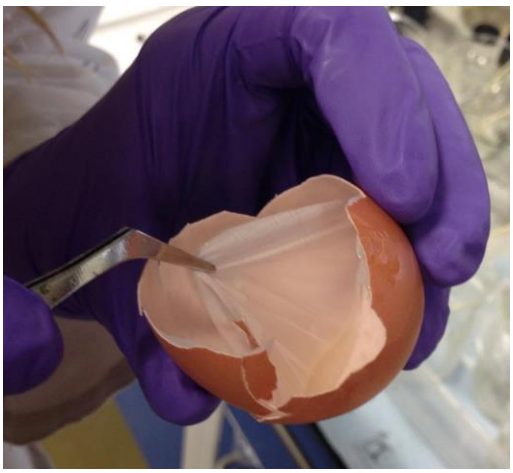

Figure S5.1. Extraction of eggshell membrane from a fresh egg

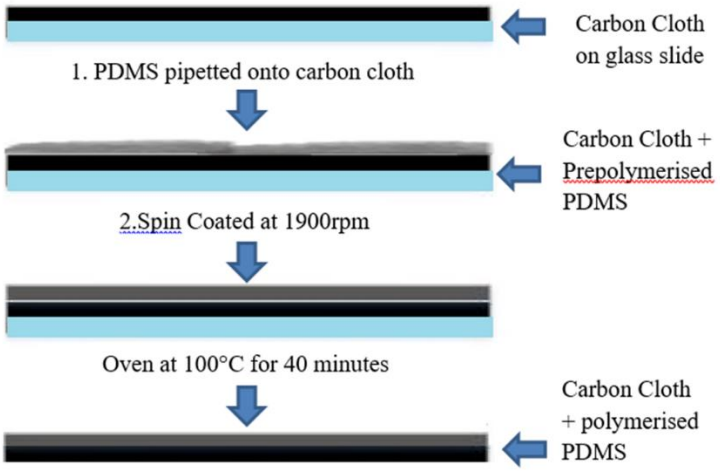

Figure S5.2. Preparation of PDMS membrane onto carbon cloth

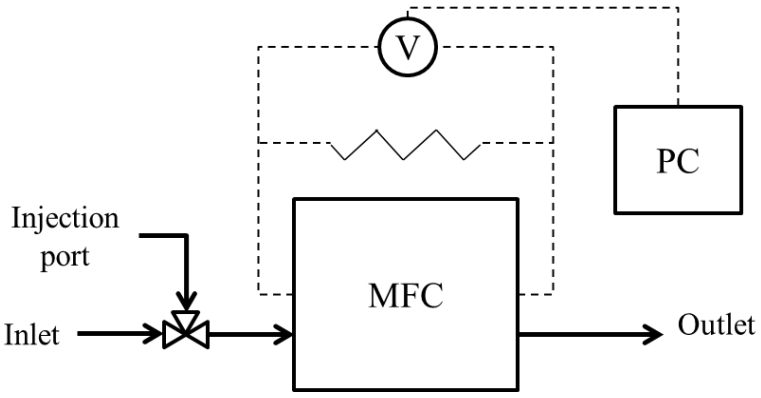

Figure S5.3. Experimental set up for the MFC biosensors testing.

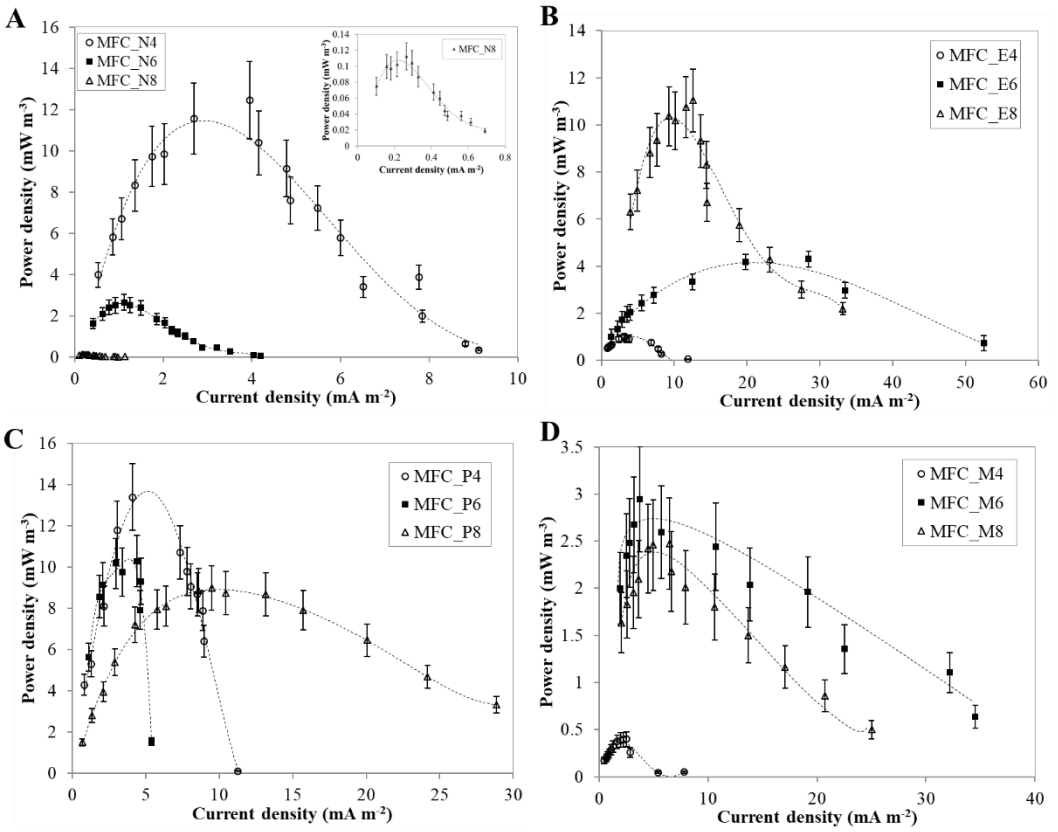

Figure S5.4. Power curves for the MFCs after 2 week of enrichment. [**A**]: MFC_N devices, with MFC_N8 expanded for clarity. [**B**]: MFC_E devices. [**C**]: MFC_P devices. [**D**]: Power MFC_M devices. Current density refers to the anode surface area, 0.32 cm^2. Power density refers to the MFC chamber volume, (electrode spacing 4 mm = 128 µL, electrode spacing 6 mm = 192 µL, electrode spacing 8 mm = 256 µL). Data is the average of 2 devices with up 19.5% error.

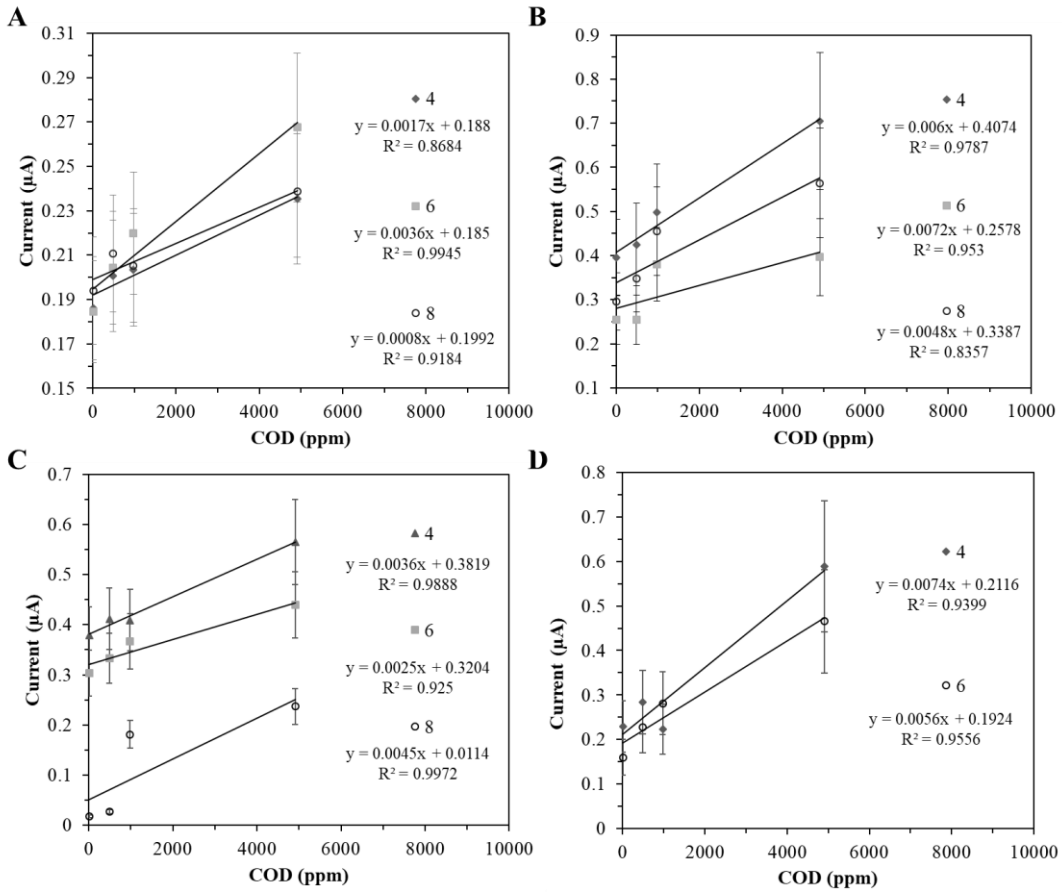

Figure S5.5. Linear range of the amperometric response of the MFC sensors to increasing values of COD in the feeding solution. [**A**]**:** MFC_N, [**B**] MFC_E, [**C**] MFC_P, [**D**] MFC_M. Numbers within each figure denote the electrode spacing of each device (mm). Error bars refer to two replicates.

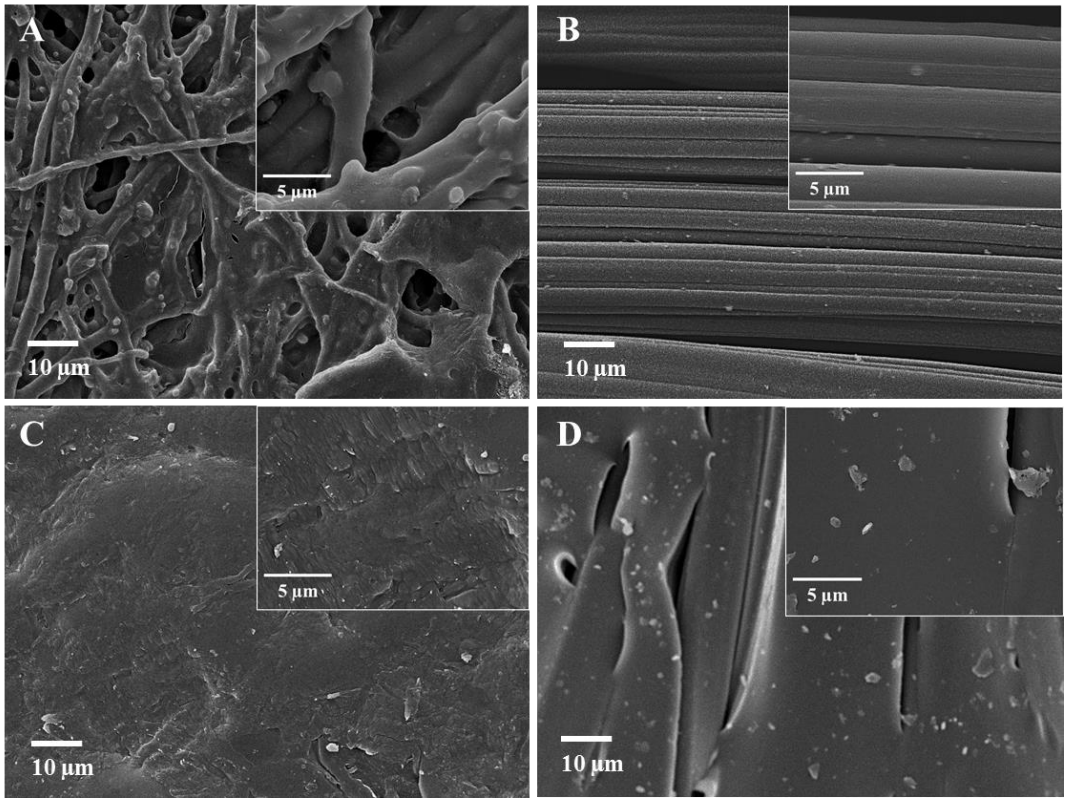

Figure S5.6. SEM images of unused membranes, treated with the same assay for cell fixation. [**A**] MFC_E; [**B**] cathode facing the anode chamber in the membrane-less device MFC_M; [**C**] MFC_N; [**D**] MFC_P.

Preparation of bacteria for SEM

Prepare fixative:

1. 2.5% GDA in buffer or culture medium.
2. Fix bacteria for 1-2 hours at room temperature or overnight at 4ºC
3. Rinse in buffer over 15min.
4. Postfix in aqueous 1% Osmium Tetroxide for 1hour in fume hood at room temp.
5. Wash in distilled water twice over 10min.
6. Dehydrate in Acetone in glass vials:
   50, 70, 90, 100% x3 changes each over 15 min.
7. 1:1 Acetone: HMDS for 15 min.
   100% HMDS x3 – 30 min
8. Pipette off as much HMDS as possible – leave partially covered in fume hood for HMDS to evaporate over 1-2 hours.
9. Mount samples for SEM

5.8 References

[1] A. Eaton, D.L.S. Clesceri, A.E. Greenberg, Standard Methods for the Examination of Water and Wastewater, 19th ed., American Public Health Association:Washington, 1995.

[2] IUPAC, Compendium of Chemical Terminology, 2nd ed. (the "Gold Book"), 2nd editio, Blackwell Scientific Publications, Oxford, 1997. doi:doi:10.1351/goldbook.

[3] S. Jouanneau, L. Recoules, M.J. Durand, A. Boukabache, V. Picot, Y. Primault, A. Lakel, M. Sengelin, B. Barillon, G. Thouand, Methods for assessing biochemical oxygen demand (BOD): A review, Water Res. 49 (2014) 62–82. doi:10.1016/j.watres.2013.10.066.

[4] I.S. Chang, J.K. Jang, G.C. Gil, M. Kim, H.J. Kim, B.W. Cho, B.H. Kim, Continuous determination of biochemical oxygen demand using microbial fuel cell type biosensor, Biosens. Bioelectron. 19 (2004) 607–613. doi:10.1016/S0956-5663(03)00272-0.

[5] M. Kim, S.M. Youn, S.H. Shin, J.G. Jang, S.H. Han, M.S. Hyun, G.M. Gadd, H.J. Kim, Practical field application of a novel BOD monitoring system, J. Environ. Monit. 5 (2003) 640–643. doi:10.1039/b304583h.

[6] B.H. Kim, I.S. Chang, G.C. Gil, H.S. Park, H.J. Kim, Novel BOD (biological oxygen demand) sensor using mediator-less microbial fuel cell, Biotechnol. Lett. 25 (2003) 541–545. doi:10.1023/A:1022891231369.

[7] G.-C. Gil, I.-S. Chang, B.H. Kim, M. Kim, J.-K. Jang, H.S. Park, H.J. Kim, Operational parameters affecting the performannce of a mediator-less microbial fuel cell, Biosens. Bioelectron. 18 (2003) 327–334. doi:10.1016/S0956-5663(02)00110-0.

[8] N. Pasco, K. Baronian, C. Jeffries, J. Webber, J. Hay, MICREDOX®—development of a ferricyanide-mediated rapid biochemical oxygen demand method using an immobilised Proteus vulgaris biocomponent, Biosens. Bioelectron. 20 (2004) 524–532. doi:10.1016/j.bios.2004.02.016.

[9] Y. Fan, H. Hu, H. Liu, Enhanced Coulombic efficiency and power density of air-cathode microbial fuel cells with an improved cell configuration, J. Power Sources. 171 (2007) 348–354. doi:10.1016/j.jpowsour.2007.06.220.

[10] B.E. Logan, Essential Data and Techniques for Conducting Microbial Fuel Cell and other Types of Bioelectrochemical System Experiments, ChemSusChem. 5 (2012) 988–994. doi:10.1002/cssc.201100604.

[11] M. Di Lorenzo, T.P. Curtis, I.M. Head, K. Scott, A single-chamber microbial fuel cell as a biosensor for wastewaters., Water Res. 43 (2009) 3145–3154. doi:10.1016/j.watres.2009.01.005.

[12] G.-X. Yang, Y.-M. Sun, X.-Y. Kong, F. Zhen, Y. Li, L.-H. Li, T.-Z. Lei, Z.-H. Yuan, G.-Y. Chen, Factors affecting the performance of a single-chamber microbial fuel cell-type biological oxygen demand sensor., Water Sci. Technol. 68 (2013) 1914–1919. doi:10.2166/wst.2013.415.

[13] B. Min, B.E. Logan, Continuous Electricity Generation from Domestic Wastewater and Organic Substrates in a Flat Plate Microbial Fuel Cell, Environ. Sci. Technol. 38 (2004) 5809–5814. doi:10.1021/es0491026.

[14] M. Di Lorenzo, A.R. Thomson, K. Schneider, P.J. Cameron, I. Ieropoulos, A small-scale air-cathode microbial fuel cell for on-line monitoring of water quality., Biosens. Bioelectron. 62 (2014) 182–188. doi:10.1016/j.bios.2014.06.050.

[15] O. Modin, B.-M. Wilén, A novel bioelectrochemical BOD sensor operating with voltage input, Water Res. 46 (2012) 6113–6120. doi:10.1016/j.watres.2012.08.042.

[16] Y. Zhang, I. Angelidaki, Submersible microbial fuel cell sensor for monitoring microbial activity and BOD in groundwater: focusing on impact of anodic biofilm on sensor applicability., Biotechnol. Bioeng. 108 (2011) 2339–2347. doi:10.1002/bit.23204.

[17] L. Peixoto, B. Min, G. Martins, A.G. Brito, P. Kroff, P. Parpot, I. Angelidaki, R. Nogueira, In situ microbial fuel cell-based biosensor for organic carbon, Bioelectrochemistry. 81 (2011) 99–103. doi:10.1016/j.bioelechem.2011.02.002.

[18] S.M. Daud, B.H. Kim, M. Ghasemi, W.R.W. Daud, Separators used in microbial electrochemical technologies: Current status and future prospects, Bioresour. Technol. 195 (2015) 170–179. doi:10.1016/j.biortech.2015.06.105.

[19] T. Huggins, H. Wang, J. Kearns, P. Jenkins, Z.J. Ren, Biochar as a sustainable electrode material for electricity production in microbial fuel cells, Bioresour. Technol. 157 (2014) 114–119. doi:10.1016/j.biortech.2014.01.058.

[20] Y. Yuan, T. Yuan, D. Wang, J. Tang, S. Zhou, Sewage sludge biochar as an efficient catalyst for oxygen reduction reaction in an microbial fuel cell, Bioresour. Technol. 144 (2013) 115–120. doi:10.1016/j.biortech.2013.06.075.

[21] H. Yuan, L. Deng, Y. Qi, N. Kobayashi, J. Tang, Nonactivated and Activated Biochar Derived from Bananas as Alternative Cathode Catalyst in Microbial Fuel Cells, Sci. World J. 2014 (2014) 1–8. doi:10.1155/2014/832850.

[22] M. Ghasemi, W.R.W. Daud, A.F. Ismail, Y. Jafari, M. Ismail, A. Mayahi, J. Othman, Simultaneous wastewater treatment and electricity generation by microbial fuel cell: Performance comparison and cost investigation of using Nafion 117 and SPEEK as separators, Desalination. 325 (2013) 1–6. doi:10.1016/j.desal.2013.06.013.

[23] S. Ayyaru, P. Letchoumanane, S. Dharmalingam, A.R. Stanislaus, Performance of sulfonated polystyreneeethyleneebutyleneepolystyrene membrane in microbial fuel cell for bioelectricity production, J. Power Sources. 217 (2012) 204–208. doi:10.1016/j.jpowsour.2012.05.053.

[24] J.R. Kim, S. Cheng, S.-E. Oh, B.E. Logan, Power Generation Using Different Cation, Anion, and Ultrafiltration Membranes in Microbial Fuel Cells, Environ. Sci. Technol. 41 (2007) 1004–1009. doi:10.1021/es062202m.

[25] I. Ieropoulos, J. Greenman, C. Melhuish, Improved energy output levels from small-scale Microbial Fuel Cells., Bioelectrochemistry. 78 (2010) 44–50. doi:10.1016/j.bioelechem.2009.05.009.

[26] Y. Zuo, S. Cheng, B.E. Logan, Ion Exchange Membrane Cathodes for Scalable Microbial Fuel Cells, 42 (2008). 6967-6972. doi: 10.1021/es801055r

[27] B. Min, S. Cheng, B.E. Logan, Electricity generation using membrane and salt bridge microbial fuel cells., Water Res. 39 (2005) 1675–1686. doi:10.1016/j.watres.2005.02.002.

[28] X. Zhang, S. Cheng, X. Wang, X. Huang, B.E. Logan, Separator Characteristics for Increasing Performance of Microbial Fuel Cells, 43 (2009). 8456-8461. doi: 10.1021/es901631p

[29] X. Zhang, S. Cheng, X. Huang, B.E. Logan, The use of nylon and glass fiber filter separators with different pore sizes in air-cathode single-chamber microbial fuel cells, Energy Environ. Sci. 3 (2010) 659–664. doi:10.1039/b927151a.

[30] S. Choi, J.R. Kim, J. Cha, Y. Kim, G.C. Premier, C. Kim, Enhanced power production of a membrane electrode assembly microbial fuel cell (MFC) using a cost effective poly [2,5-benzimidazole] (ABPBI) impregnated non-woven fabric filter, Bioresour. Technol. 128 (2013) 14–21. doi:10.1016/j.biortech.2012.10.013.

[31] M. Behera, M.M. Ghangrekar, Electricity generation in low cost microbial fuel cell made up of earthenware of different thickness, Water Sci. Technol. 64 (2011) 2468. doi:10.2166/wst.2011.822.

[32] J. Winfield, J. Greenman, D. Huson, I. Ieropoulos, Comparing terracotta and earthenware for multiple functionalities in microbial fuel cells, Bioprocess Biosyst. Eng. 36 (2013) 1913–1921. doi:10.1007/s00449-013-0967-6.

[33] J. Winfield, L.D. Chambers, J. Rossiter, I. Ieropoulos, Comparing the short and long term stability of biodegradable, ceramic and cation exchange membranes in microbial fuel cells, Bioresour. Technol. 148 (2013) 480–486. doi:10.1016/j.biortech.2013.08.163.

[34] J. Winfield, L.D. Chambers, A. Stinchcombe, J. Rossiter, I. Ieropoulos, The power of glove: Soft microbial fuel cell for low-power electronics, J. Power Sources. 249 (2014) 327–332. doi:10.1016/j.jpowsour.2013.10.096.

[35] J. Winfield, I. Ieropoulos, J. Rossiter, J. Greenman, D. Patton, Biodegradation and proton exchange using natural rubber in microbial fuel cells., Biodegradation. 24 (2013) 733–739. doi:10.1007/s10532-013-9621-x.

[36] C. Santoro, Y. Lei, B. Li, P. Cristiani, Power generation from wastewater using single chamber microbial fuel cells (MFCs) with platinum-free cathodes and pre-colonized anodes, Biochem. Eng. J. 62 (2012) 8–16. doi:10.1016/j.bej.2011.12.006.

[37] P. Cristiani, M.L. Carvalho, E. Guerrini, M. Daghio, C. Santoro, B. Li, Cathodic and anodic biofilms in Single Chamber Microbial Fuel Cells., Bioelectrochemistry. 92 (2013) 6–13. doi:10.1016/j.bioelechem.2013.01.005.

[38] S. Ayyaru, S. Dharmalingam, Enhanced response of microbial fuel cell using sulfonated poly ether ether ketone membrane as a biochemical oxygen demand sensor, Anal. Chim. Acta. 818 (2014) 15–22. doi:10.1016/j.aca.2014.01.059.

[39] Z. Xu, B. Liu, Q. Dong, Y. Lei, Y. Li, J. Ren, J. McCutcheon, B. Li, Flat microliter membrane-based microbial fuel cell as “on-line sticker sensor” for self-supported in situ monitoring of wastewater shocks, Bioresour. Technol. 197 (2015) 244–251. doi:10.1016/j.biortech.2015.08.081.

[40] I. Ieropoulos, J. Greenman, C. Melhuish, Miniature microbial fuel cells and stacks for urine utilisation, Int. J. Hydrogen Energy. 38 (2013) 492–496. doi:10.1016/j.ijhydene.2012.09.062.

[41] Y. Jiang, P. Liang, P. Liu, X. Yan, Y. Bian, X. Huang, A cathode-shared microbial fuel cell sensor array for water alert system, Int. J. Hydrogen Energy. 42 (2016). 4342-4348. doi:10.1016/j.ijhydene.2016.12.050.

[42] D. Dong, J. Yao, Y. Wu, X. Zhang, G. Xu, C.-Z. Li, H. Wang, A 3D fibrous cathode with high interconnectivity for solid oxide fuel cells, 13 (2011). 1038-1041. doi:10.1016/j.elecom.2011.06.025.

[43] J. Winfield, L.D. Chambers, J. Rossiter, A. Stinchcombe, X.A. Walter, J. Greenman, I. Ieropoulos, Fade to Green: A Biodegradable Stack of Microbial Fuel Cells, ChemSusChem. 8 (2015) 2705–2712. doi:10.1002/cssc.201500431.

[44] F. Zhang, T. Saito, S. Cheng, M.A. Hickner, B.E. Logan, Microbial Fuel Cell Cathodes With Poly(dimethylsiloxane) Diffusion Layers Constructed around Stainless Steel Mesh Current Collectors, 44 (2010). 1490-1495. doi: 10.1021/es903009d

[45] J. Chouler, G.A. Padgett, P.J. Cameron, K. Preuss, M.-M. Titirici, I. Ieropoulos, M. Di Lorenzo, Towards effective small scale microbial fuel cells for energy generation from urine, Electrochim. Acta. 192 (2016) 89–98. doi:10.1016/j.electacta.2016.01.112.

[46] A. Elmekawy, H.M. Hegab, X. Dominguez-Benetton, D. Pant, Internal resistance of microfluidic microbial fuel cell: challenges and potential opportunities., Bioresour. Technol. 142 (2013) 672–682. doi:10.1016/j.biortech.2013.05.061.

[47] Y.-P. Chen, Y. Zhao, K.-Q. Qiu, J. Chu, R. Lu, M. Sun, X.-W. Liu, G.-P. Sheng, H.-Q. Yu, J. Chen, W.-J. Li, G. Liu, Y.-C. Tian, Y. Xiong, An innovative miniature microbial fuel cell fabricated using photolithography., Biosens. Bioelectron. 26 (2011) 2841–2846. doi:10.1016/j.bios.2010.11.016.

[48] F. Qian, D.E. Morse, Miniaturizing microbial fuel cells., Trends Biotechnol. 29 (2011) 62–69. doi:10.1016/j.tibtech.2010.10.003.

[49] J. You, J. Greenman, C. Melhuish, I. Ieropoulos, Small-scale microbial fuel cells utilising uric salts, Sustain. Energy Technol. Assessments. 6 (2014) 60–63. doi:10.1016/j.seta.2014.01.005.

[50] S. Choi, H.-S. Lee, Y. Yang, P. Parameswaran, C.I. Torres, B.E. Rittmann, J. Chae, A μL-scale micromachined microbial fuel cell having high power density., Lab Chip. 11 (2011) 1110–1117. doi:10.1039/c0lc00494d.

[51] F. Qian, M. Baum, Q. Gu, D.E. Morse, A 1.5 μL microbial fuel cell for on-chip bioelectricity generation., Lab Chip. 9 (2009) 3076–3081. doi:10.1039/b910586g.

[52] H. Liu, B.E. Logan, Electricity generation using an air-cathode single chamber microbial fuel cell in the presence and absence of a proton exchange membrane., Environ. Sci. Technol. 38 (2004) 4040–4046. http://www.ncbi.nlm.nih.gov/pubmed/15298217.

[53] A.M. Castilla, S. Van Dongen, A. Herrel, A. Francesch, J. Martínez de Aragón, J. Malone, J. José Negro, Increase in membrane thickness during development compensates for eggshell thinning due to calcium uptake by the embryo in falcons, Naturwissenschaften. 97 (2010) 143–151. doi:10.1007/s00114-009-0620-z.

[54] W.Y. Zhang, G.S. Ferguson, S. Tatic-Lucic, Elastomer-supported cold welding for room temperature wafer-level bonding, in: 17th IEEE Int. Conf. Micro Electro Mech. Syst. IEEE, 2004.: pp. 741–744. doi:10.1109/MEMS.2004.1290691.

[55] E. Guerrini, M. Grattieri, S.P. Trasatti, M. Bestetti, P. Cristiani, Performance explorations of single chamber microbial fuel cells by using various microelectrodes applied to biocathodes, Int. J. Hydrogen Energy. 39 (2014) 21837–21846. doi:10.1016/j.ijhydene.2014.06.132.

[56] S.R. Kayar, G.K. Snyder, G.F. Birchard, C.P. Black, Oxygen permeability of the shell and membranes of chicken eggs during development, Respir. Physiol. 46 (1981) 209–221. doi:10.1016/0034-5687(81)90122-5.

[57] A. Lamberti, S.L. Marasso, M. Cocuzza, PDMS membranes with tunable gas permeability for microfluidic applications, RSC Adv. 4 (2014) 61415–61419. doi:10.1039/C4RA12934B.

[58] Y. Hirata, Y. Miura, T. Nakagawa, Oxygen permeability and the state of water in Nafion membranes with alkali metal and amino sugar counterions, J. Memb. Sci. 163 (1999) 357–366. doi:10.1016/S0376-7388(99)00185-4.

[59] S. Cheng, H. Liu, B.E. Logan, Increased power generation in a continuous flow MFC with advective flow through the porous anode and reduced electrode spacing., Environ. Sci. Technol. 40 (2006) 2426–2432. doi:10.1021/es051652w.

[60] M.M. Ghangrekar, V.B. Shinde, Performance of membrane-less microbial fuel cell treating wastewater and effect of electrode distance and area on electricity production, Bioresour. Technol. 98 (2007) 2879–2885. doi:10.1016/j.biortech.2006.09.050.

[61] C.-Y. Lee, Y.-N. Huang, The effects of electrode spacing on the performance of microbial fuel cells under different substrate concentrations, 68 (2013). 2028-2034. doi:10.2166/wst.2013.446.

[62] Y. Jiang, P. Liang, C. Zhang, Y. Bian, X. Yang, X. Huang, P.R. Girguis, Enhancing the response of microbial fuel cell based toxicity sensors to Cu(II) with the applying of flow-through electrodes and controlled anode potentials., Bioresour. Technol. 190 (2015) 367–372. doi:10.1016/j.biortech.2015.04.127.

[63] N.E. Stein, H.V. Hamelers, C.N. Buisman, The effect of different control mechanisms on the sensitivity and recovery time of a microbial fuel cell based biosensor, Sensors Actuators B Chem. 171–172 (2012) 816–821. doi:10.1016/j.snb.2012.05.076.

[64] A.H.J. Visschedijk, Effects of Barometric Pressure and Abnormal Gas Mixtures on Gaseous Exchange by the Effects of Barometric Pressure and Abnormal Gas Mixtures on Gaseous Exchange by the Avian Embryo, Am. Zool. 20 (1980) 469–476. http://www.jstor.org/stable/3882409 (accessed October 5, 2016).

[65] M.E. Cox, B. Dunn, Oxygen diffusion in poly(dimethyl siloxane) using fluorescence quenching. I. Measurement technique and analysis, J. Polym. Sci. Part A Polym. Chem. 24 (1986) 621–636. doi:10.1002/pola.1986.080240405.

[66] Sigma Aldrich, (2016). https://www.sigmaaldrich.com/ (accessed October 11, 2016).

[67] Ellsworth Adhesives Ltd, (2016). http://www.ellsworthadhesives.co.uk/ (accessed October 11, 2016).

[68] Fuel Cell Earth, (2016). https://www.fuelcellearth.com/ (accessed October 11, 2016).

[69] N. Yoshida, J. Hoashi, T. Morita, S.J. Mcniven, H. Nakamura, I. Karube, Improvement of a mediator-type biochemical oxygen demand sensor for on-site measurement, J. Biotechnol. 88 (2001) 269–275. doi:10.1016/S0168-1656(01)00282-6

[70] H. Nakamura, Y. Abe, R. Koizumi, K. Suzuki, Y. Mogi, T. Hirayama, I. Karube, A chemiluminescence biochemical oxygen demand measuring method, 602 (2007). 94-100. doi:10.1016/j.aca.2007.08.050

[71] T. Sakaguchi, K. Kitagawa, T. Ando, Y. Murakami, Y. Morita, A. Yamamura, K. Yokoyama, E. Tamiya, A rapid BOD sensing system using luminescent recombinants of Escherichia coli, 19 (2003). 115-121. doi:10.1016/S0956-5663(03)00170-2

[72] T. Sakaguchi, Y. Morioka, M. Yamasaki, J. Iwanaga, K. Beppu, H. Maeda, Y. Morita, E. Tamiya, Rapid and onsite BOD sensing system using luminous bacterial cells-immobilized chip, Biosens. Bioelectron. 22 (2007) 1345–1350. doi:10.1016/j.bios.2006.06.008

[73] C. Liu, H. Zhao, L. Zhong, C. Liu, J. Jia, X. Xu, L. Liu, S. Dong, A biofilm reactor-based approach for rapid on-line determination of biodegradable organic pollutants, Biosens. Bioelectron. 34 (2012) 77–82. doi:10.1016/j.bios.2012.01.020

[74] V. Arlyapov, S. Kamanin, O. Ponamoreva, A. Reshetilov, Biosensor analyzer for BOD index express control on the basis of the yeast microorganisms Candida maltosa, Candida blankii, and Debaryomyces hansenii, Enzyme Microb. Technol. 50 (2012) 215–220. doi:10.1016/j.enzmictec.2012.01.002

6 Influence of operational factors on the performance of a miniature microbial fuel cell as a toxicity sensor

The capability of the miniature MFC biosensor to detect toxic compounds in water is investigated in this chapter. The current responses to the toxicants formaldehyde and atrazine are determined. To guide research towards real water monitoring applications, the effect of operational parameters on MFC performance is investigated (labile organic load, temperature, pH, ionic strength). This work has been prepared as a publication and submission is pending, with details on the following page. Amendments have been made to account for stylistic consistency in this thesis.

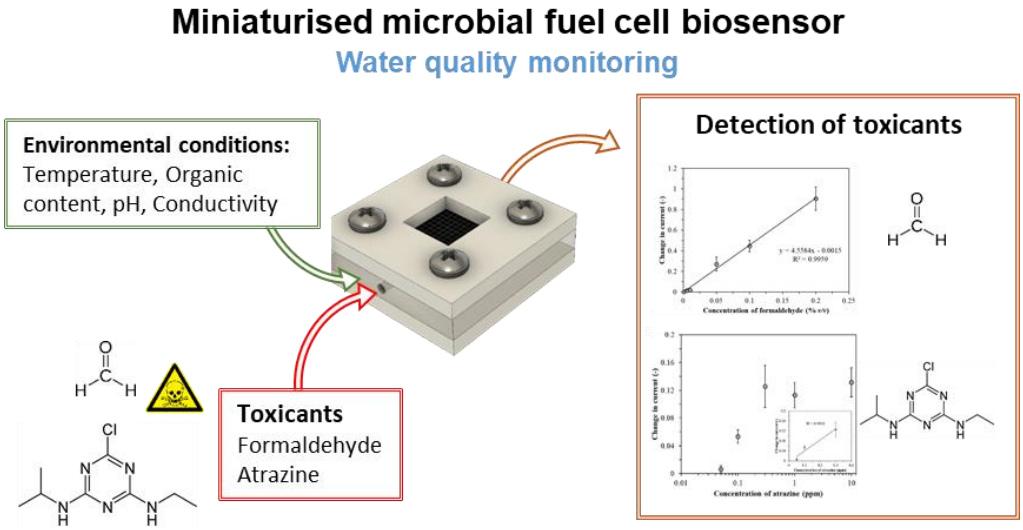

Statement of authorship

This declaration concerns the article entitled:	Influence of operational factors on the performance of a miniature microbial fuel cell as a toxicity sensor
Publication status:	Draft publication, pending submission.
Publication details:	N/A
Authorship contributions:	JC and MDL conceived the experiment. Design, implementation and analysis of experiments performed by JC. Manuscript prepared by JC and MDL. Project supervised by MDL.
Statement from candidate:	This paper reports on original research I conducted during the period of my Higher Degree by Research candidature.

Signed: Date:

Influence of operational factors on the performance of a miniature microbial fuel cell as a toxicity sensor

Jon Chouler [a,b], Mirella Di Lorenzo [a]

[a] University of Bath, Department of Chemical Engineering, Bath, BA2 7AY, UK

[b] Centre for Sustainable Chemical Technologies, University of Bath, Bath BA2 7AY, UK

6.1 Abstract

To protect the public and the environment, the release of any contaminants into water systems that may arise from industrial, agricultural and domestic activities must be monitored and controlled. This need demands for accurate and inexpensive detection systems that can be operated onsite by non-experts. The microbial fuel cell (MFC) technology has shown great potential for real time and onsite testing of water sources. With the intent of defining operational conditions for practical applications, in this study we investigate the effect of environmental factors, such as changes in temperature, pH and ionic strength, on the performance of a single chamber (128 μL) miniature MFC sensor. It resulted that the pH of the water influent had the greatest effect on performance, with a 0.531 ± 0.064 μA cm^{-2} current variation per unit change of pH. On the other hand, within the range tested, temperature and ionic strength had only a minor impact, with current changes of 0.010 ± 0.001 μA $°C^{-1}$ cm^{-2} and of 0.027 ± 0.003 μA mS^{-1} cm cm^{-2} respectively. Under the optimal environmental conditions identified, the sensor ability to detect formaldehyde and atrazine was tested. The sensitivity to formaldehyde was $1.43 \times 10^{-3} \pm 0.18 \times 10^{-3}$ ppm^{-1} cm^{-2}, with a detection range of 10 – 2000 ppm, while the sensitivity to atrazine was 1.39 ± 0.26 ppm^{-1} cm^{-2}, with a detection range of 0.05 – 0.3 ppm.

6.2 Introduction

Water is arguably the most important resource on this planet. It lies at the crux of sustainable development, and is essential for poverty alleviation, public health, food and energy security, and ecosystem quality [1]. Yet much of the world's population are faced with serious freshwater challenges. For instance, 663 million people are currently without access to secure drinking water sources, 2.4 billion lack access to adequate sanitation [2], and almost half the world population will live in areas of high water stress by 2030 [3]. Moreover, water sources may be contaminated by a multitude of compounds (such as organics, heavy metals, and pesticides) [4]. As such, the UN has defined the provision of clean water and adequate sanitation for all as one of their 17 Sustainable Development Goals [5]. Effective water management is critical to achieve this goal, and heavily relies on the deployment of low cost, real time and onsite monitoring systems for water quality [3].

Microbial fuel cells (MFC) have promising potential for effective water quality monitoring [6]. In an MFC, electrogenic microorganisms are utilised to degrade organic matter and generate electricity [7]. When the electrogenic biofilm, usually located at the anode of the MFC, are subjected to a bioactive compound, a change in the current generated is observed [8,9]. As such, MFCs can be used for the quantitative and qualitative assessment of water quality [10]. MFCs have gained much interest for biosensing owing to their rapid response times [11], robust long term operation [12], self-sustaining ability [13], low cost [14], simplicity of operation (with no need for an external transducer to process the signal response) [15], and their ability to respond to a wide range of toxic compounds [16,17].

Currently, MFC biosensors have been developed as toxicity sensors, using model compounds such as heavy metals, Pb^{2+} and Hg^{2+} [10,13,18], Ni [19], Cr^{6+} [20,21], Cd^{2+} [11,13], Cu^{2+} [8,15,22], as well as formaldehyde [16,23,24], and detecting the biochemical oxygen demand (BOD) [12,25,26] in water. So far, there are only two reported cases focused on trace organic compounds, these being diazinon (an organophosphate insecticide) [10] and bentazon (an herbicide) [19]. These studies have been limited to the investigation of one or two concentrations of the given compound and thus a deeper understanding of the dose-current response relationship of such compounds is needed. Moreover, many MFC biosensing studies rely on the use of macro-scale two chamber systems [8,10,15,19], which exhibit additional

operating costs due to the control of the catholyte, and increased capital cost of design [27]. Therefore, the use of single chamber devices, coupled with the concept of device miniaturisation [28] is particularly attractive. Such devices can pave the way towards simplified, fast response, cost-effective biosensing devices [14] with improved analysis times, reliability and sensitivity due to enhanced mass transfer processes within the cell [11,16].

A limitation of the use of MFCs for detection of toxic compounds is that the biosensor response may also be affected by changes in natural conditions such as temperature, pH, salinity and, if used for wastewater monitoring, BOD [23,26]. Such factors may affect the MFC performance [21], and weaken the response of the MFC towards toxicants [29]. The impact of simultaneous changes in components may also lead to potential false warnings [16]. The effects of such factors must therefore, be understood, so that they can eventually be properly controlled when operating an MFC as a sensor. Some work has been conducted to this end. For instance, it was found a low temperature can slow down the current response (by almost 50% between 30 and 20°C) of a sediment based MFC for monitoring of faecal contamination in groundwater [30]. Additionally, a high pH and low temperature were shown to significantly affect the treatment efficiency (by up to 55%), and thus the sensing capability of Cr^{6+} in a two chamber MFC biosensor. Finally organic substrate (glucose) and catholyte FeCN concentrations, as well as external load, were optimised for power performance in a two chamber MFC biosensor in batch operation for specific Cu^{2+} detection [13]. The study of environmental effects on miniature single chamber MFC biosensors, which operate continuously and thus are extremely suitable for online and onsite water quality monitoring [9], has yet to be rigorously conducted however, and is a critical step in enabling this technology for real water quality monitoring applications. Moreover, a strategy to fully understand the combined effect of environmental factors and multiple contaminants in water on MFC biosensors is needed [31].

In this context, this work presents the use of a miniature single chamber MFC based biosensor for water quality monitoring purposes. Initially the effect of environmental conditions (temperature, pH and ionic strength) on the performance of the MFC biosensor is investigated. Next, the miniature MFC is tested as a sensor for the detection of toxic compounds in water. Formaldehyde is firstly used as a model toxicant, to allow simple comparison to other studies related to MFC biosensors.

Afterwards, the response of the miniature single chamber MFC to atrazine (2-chloro-4-ethylamino-6-isopropylamino-1,3,4-triazine) toxicity is investigated.

6.3 Experimental

6.3.1 Materials

All reagents used were of analytical grade and purchased from Sigma-Aldrich and Alfa Aesar. All solutions used were prepared with reverse osmosis purified water. Artificial Wastewater (AW) was used as the feedstock containing (per litre of deionized water): 0.27 g $(NH_4)_2SO_4$, 0.06 g $MgSO_4.7H_2O$, 0.006 g $MnSO_4.H_2O$, 0.13 g $NaHCO_3$, 0.003 g $FeCl_3.6H_2O$, 0.004 $MgCl_2$, 3.1 $NaH_2PO_4.H_2O$ and 10.9 Na_2HPO_4. As a carbon source for the bacteria, potassium acetate was added to the AW at 100 mM unless otherwise specified. The medium was autoclaved prior to use.

6.3.2 Microbial fuel cells

The single chamber miniature MFC was manufactured as previously described [32]. The MFC has total anodic chamber volume of 128 µL (rectangular chamber: length = 8 mm, width = 4 mm, height = 4mm). The exposed surface area of the anode and cathode (made untreated carbon cloth, type-B, E-Tek, USA) were 0.32 cm^2 each, and the cathode was open to air.

6.3.3 Operation of the MFCs

All MFCs were fed with AW and their voltage monitored as previously described [32], with experimental rig shown in Figure S6.1. The operating temperature was controlled by placing the MFCs inside an incubator (Herp Nursery II Incubator, Lucky Reptile, Germany). Enrichment of the electrochemically active bacteria at the anode was performed over a period of seven days. MFCs were fed under continuous recirculating

conditions with AW containing 1% *v/v* mixed culture of bacteria (anaerobic sludge provided by Wessex Water, wastewater treatment works in Avonmouth, UK), which was replaced daily. Initially, MFCs were first operated under open circuit conditions for up to 2 h and then connected to an external load of 1 kΩ. After enrichment, the MFCs were continuously fed with AW containing no bacteria. Polarisation experiments and analysis were performed as previously described [32]. After polarisation, the MFCs were operated at the external resistance that gave the optimal power performance.

6.3.4 Testing the MFCs as biosensors

To perturb the operating conditions of the inlet solution (i.e. changes in labile organic carbon content, pH, ionic strength and introduction of a toxicant), a three-way valve prior to the MFC was used, as shown in Figure S6.1. All tests were carried out in triplicate. When the MFCs were tested as sensors for the labile organic carbon content in water, the concentration of potassium acetate in AW was varied between 0.1 – 200 mM. For all other tests the concentration of potassium acetate was maintained at 100 mM (with a base conductivity of 9.7 mS cm^{-1}). To determine the impact of temperature on the MFC, the temperature of AW was set to a range of values between 10 – 40°C by the use of the incubator and a water/ice bath for the feed tank. To investigate the effect of pH, the MFCs were fed with AW at pH values between 6.3 and 12.5 which was adjusted using small amounts of HCl and NaOH (so as to not affect conductivity fo the AW, which was negligable compared to the high acetate concentration). To determine the effect of ionic strength, NaCl was added to the AW feed at concentrations between 0 and 1.8 M (corresponding to conductivities between 9.7 – 111.9 mS cm^{-1}). These concentrations were set to mimic freshwater (0 M), brackish water (0.05 – 0.3 M), seawater (0.6 M) and hyper-saline lakes (1.8 M) [33]. Conductivity of each solution was determined using a conductivity probe (CON 110 Series, Oakton, US). Solutions were fed to the MFCs until a steady state was established, which was defined as the point where the change in potential over time, $^{\delta mV}/_{\delta t} \leq 0.02$ mV min^{-1}.

Subsequently, the MFCs were tested as a tool for detecting toxicants, in particular formaldehyde (between 10 and 2000 ppm) and atrazine (0.05 – 10 ppm) were

individually tested as model toxicants. The tests involved feeding the MFCs with AW containing 100 mM of potassium acetate and formaldehyde or atrazine, as specified, for a total of 10 and 30 min respectively. The longer exposure time for atrazine was chosen to better understand the toxicant effect on the anodic biofilm of the MFC. After being exposed to the target compound, the MFCs were fed with fresh AW containing 100 mM potassium acetate and no toxicant. To avoid irreversible damage to the anodic biofilm, only one test was performed per day per fuel cell.

6.3.5 Calculations

To determine the sensitivity of the MFC towards a specific disturbance applied to the system, Equation 6.1 was used.

$$sensitivity = \frac{\Delta I}{\Delta d \times A} \qquad \text{Equation 6.1}$$

Where ΔI (μA) is the unit change in the current output, Δd is the unit change in the disturbance (acetate concentration mM, formaldehyde ppm, atrazine ppm) and A = 0.32 cm^2 is the anodic macro surface area.

For toxicant tests, the current variability over time was offset by normalising the current at time t, I_t, by the baseline current prior to the disturbance event, I_B, to determine the normalised current, I_N, Equation 6.2.

$$I_N = \frac{I_t}{I_B} \qquad \text{Equation 6.2}$$

The sensitivity of the normalised current response from the MFC was then referred against the anode projected surface area to give the toxicant sensitivity, and calculated by use of Equation 6.3:

$$toxicant\ sensitivity = \frac{\Delta I_N}{\Delta d \times A} \qquad \text{Equation 6.3}$$

Where ΔI_N (-) is the unit change in the normalised current output. The ratios $^{\Delta I}/_{\Delta d}$ and $^{\Delta I_N}/_{\Delta d}$ were obtained from the linear slope of the respective current response *versus* disturbance magnitude curve. When analysing a disturbance current *versus* time response curve: the delay time, t_d, was defined as the time between the introduction of a disturbance and the first response from the MFC; the response time, t_{res}, was the time taken to reach 95% of the new steady state current; the recovery time, t_{rec}, was the time for the current to reach 95% of its steady state value after a toxic event (i.e. from when fresh AW is introduced to the MFC). The initial rate of the current response, $r_{initial}$, was defined by the initial slope of the current *versus* time curve immediately after a toxicant event.

6.4 Results and discussion

6.4.1 Effect of temperature, pH and ionic strength

To be used as sensor for toxicants detection, MFCs must generate a stable current baseline [34]. Any factor that may affect this baseline must be understood and eventually controlled or taken into account when processing the sensor readings. In this way, current changes unrelated to the presence of a bioactive compound could be filtered out and the risk of false alarms prevented. Temperature and pH, are known to have an effect on bacterial metabolism [35,36], while the ionic strength of the water sample influences the internal resistance in MFCs [37]. As such, these three parameters, defined by the environmental conditions in which the system is operated, can influence the electrochemical performance of the anodic biofilm and the MFC sensor outputs. With the aim of understanding how such parameters affect the performance of our miniature MFC device, temperature, pH and ionic strength of the feed solution were altered as detailed in the Experimental section.

Firstly, the MFCs were enriched for one week with anaerobic sludge to build-up an electroactive biofilm onto the anode surface. Afterwards, a polarisation experiment was performed, Figure 6.1. The OCV for the MFC was 87.8 $\pm$ 5.4 mV. The MFC exhibited a high internal resistance of 18 ± 1.1 kΩ, which is comparable to the values

of other miniature MFCs in the literature [32,38,39]. The maximum power density of the device was 0.359 ± 0.022 mW m^{-2} at a current density of 19.4 ± 1.2 mA m^{-2}, when operating at an external load of 30 kΩ. This external resistance was used for all subsequent tests.

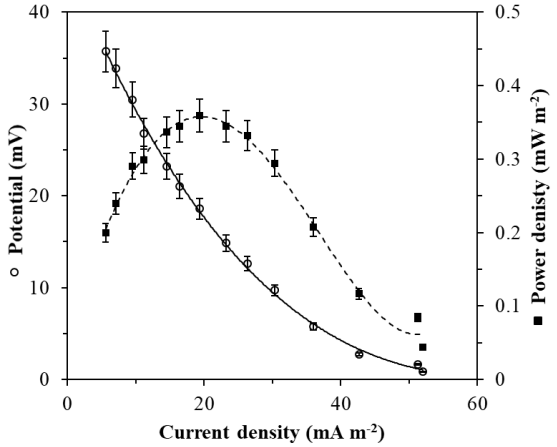

Figure 6.1. Power and polarisation curves for the MFC biosensor after one week of enrichment. Current density refers to the anode surface area, 0.32 cm^2. Power density refers to the MFC chamber volume, 128 µL. Data is the average of 3 devices with up to 6.2% error.

When the temperature was changed, a linear output current response was observed, within the range 15 – 30°C, with a gradient of 0.010 ± 0.001 µA $°C^{-1}$ cm^{-2} (R^2 = 0.93), Figure 6.2A and Figure S6.2. Within the range 15 – 35°C, however, the total current variation was 8%, with a peak performance at 30°C. Outside this range, the current output decays, probably because of inhibitory effects of temperature on the bacterial metabolism and, consequently, on electron generation [35]. After each temperature change, the system required 47.3 ± 12.6 min to reach a steady current output.

A much more marked dependence on pH was observed, Figure 6.2B and Figure S6.2. This result is not surprising considering the importance of pH in biochemical reactions [40]. A much longer time was required to reach a steady output current upon pH changes in the feeding solution than for the case of the temperature (83.8 ± 15.0 min). This slower response could be explained by considering the complex responses that the MFC have towards pH. Where, for instance, oxygen reduction reactions at the cathode produces an alkaline environment; and bacterial metabolism at the anode generally produce weak acidic compounds [36]. These responses may conflict or

complement pH changes to the electrolyte, thus elongating the overall time required for the MFC to equilibrate to a pH change. A linear relationship between current and pH was observed within the range of 7.5 – 10.9, with a gradient (per unit change of pH) of 0.531 ± 0.064 μA cm^{-2} (R^2 = 0.98). Poor current outputs corresponded to low pH values. This behaviour is in agreement with previous studies and has been addressed to a reduction in microbial activity at low pH [40–43]. It is supposed that although anodic bacterial activities may be inhibited to an extent, a higher pH may favour cathodic reactions and thus improve the performance of MFCs [40]. Alkaline conditions might also benefit biofilm formation in MFCs, which may lead to reduced charge transfer resistances and increased exchange current density at the anode [43]. In light of this result, the MFC should be operated at alkaline pH values to enhance power production.

The MFC current output increased up to an electrolyte conductivity of 36 mS cm^{-1}, Figure 6.2C and Figure S6.2. The time required to reach a steady state current was much slower than the case of the other two parameters tested, being 127.4 ± 63.1 min. This may be explained by the gradual effects that ionic strength has on the biofilm at the anode, including changes to the physiology and growth of the microbial consortia, which would not exhibit themselves as immediate changes to the current output of the MFC [44]. Between electrolyte conductivity values of 9.7 – 18.0 mS cm^{-1} a linear correlation was observed, with a gradient of 0.027 ± 0.003 μA mS^{-1} cm cm^{-2}. The increase in current generated with the ionic strength is associated to reduced ohmic resistances within the cell [44,45]. Moreover, high ionic strengths are preferred by anode associated bacteria, such as *Geobacteraceae*, which has been found to grow preferentially in 0.1 M NaCl [33]. The current decrease observed for NaCl concentrations higher than 0.3 M (corresponding to conductivities above 60 mS cm^{-1}) may be attributed to the inability of exoelectrogens to survive at high salt concentrations, with consequent electricity generation reduction [33,44]. However, the addition of NaCl to AW (containing 100 mM) acetate, may also dilute the substrate in the feed, and therefore reduce the power performance of the MFC.

Table S6.1 summarises the results obtained. As observed, within the range of values investigated, of utmost importance is to control the pH. Additionally the temperature and conductivity of the feed solution to the MFC should be monitored and maintained constant when possible.

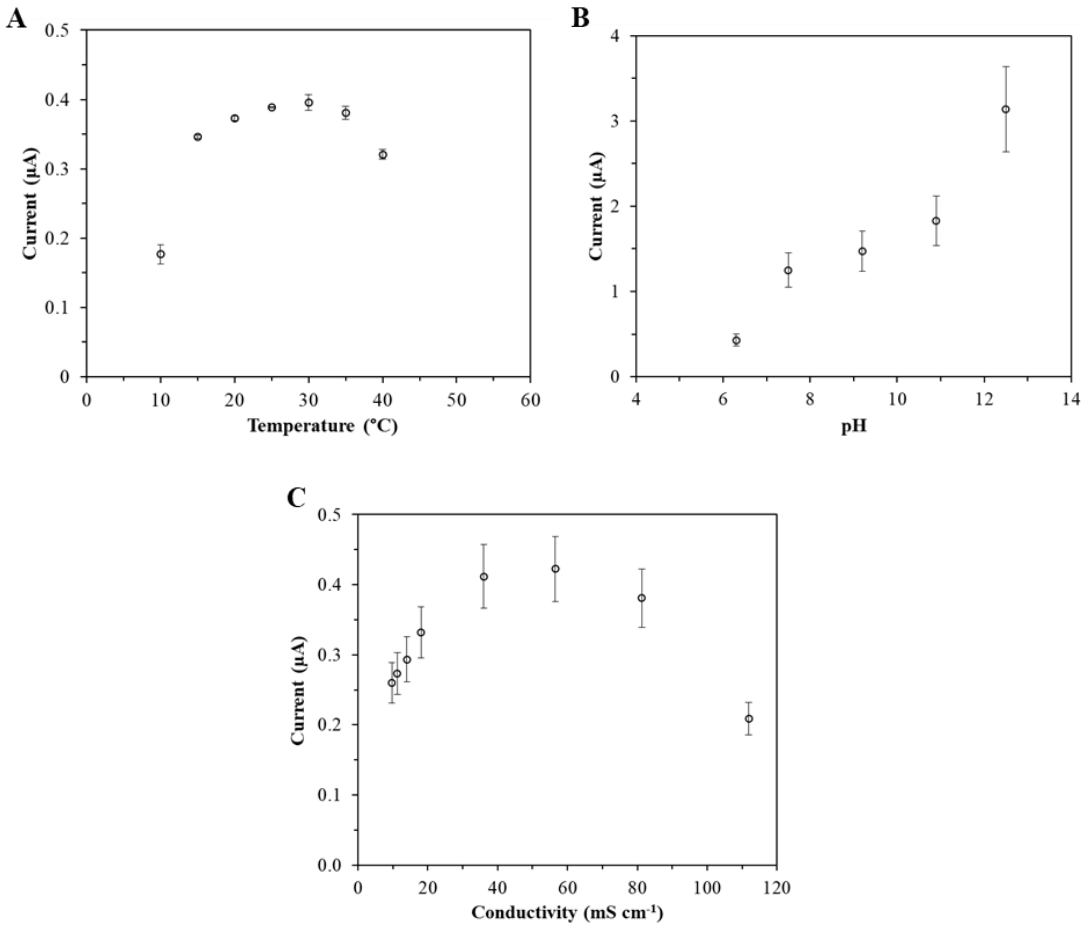

Figure 6.2. [**A**] Average steady state current from MFC biosensors as a function of temperature. Data is an average of 3 MFCs with up to 6% error. [**B**] Average steady state current from MFC biosensors as a function of pH. Data is an average of 3 MFCs with up to 12% error. [**C**] Average steady state current from MFC biosensors as a function of conductivity. Data is an average of 3 MFCs with up to 11% error.

While informative for progressing the practical use of MFCs for water quality monitoring, understanding the individual effect of operational variables on the current generated by the MFC is unfortunately not enough [46]. Real water systems contain a mixture of toxicants and organic compounds, and may also exhibit simultaneous changes over time. The complex and co-operative effect of such factors on the current generation of the MFC need be known to safely and reliably interpret signals from the MFC sensor, and enable it as an effective technology for the onsite detection of toxic compounds in water.

6.4.2 Testing the use of the miniature MFC as a sensor

For all the subsequent tests, the MFCs were operated under a control temperature of 20°C with a pH of 7.5. No NaCl was added (giving the AW a conductivity of 9.7 mS cm^{-1}), since the continued addition (especially at concentrations of 0.1 M and above) of NaCl has been found to alter the species present in the anodic biofilm and ultimately diminish the MFC's power performance [33].

The MFCs were fed with AW with varying COD values, obtained by changing the concentration of potassium acetate between 0.1 – 200 mM. The relative amperometric response is reported in Figure 6.3. A linear response between current output and acetate concentration was observed within the range 0.1 – 10 mM (corresponding to COD values of 10 – 1000 ppm acetate), with a sensitivity of 0.030 ± 0.003 μA mM^{-1} cm^{-2}. The lower detection limit was 0.1 mM (10 ppm). The MFC showed a wider detection range than other labile organic content sensors reported in the literature (with detection ranges typically between 3-500 ppm of BOD [47–52]). In this study, the wider COD range of detection may be a result of the system miniaturisation. Miniature MFCs are characterised by a higher electrode surface-area-to-volume ratio, with consequent enhancements of the mass transfer processes between the concentration of organic substrate in the bulk solution and at the surface of the electrode [28]. The average response time of the MFCs to a change in acetate concentration was 56.8 ± 8.6 min, Table S6.1, which is on the same order of magnitude to similar MFCs used as BOD sensors [48,51]. Above acetate concentrations of 100 mM, no further current enhancements were detected. As such, this concentration was considered to be saturating, in line with substrate saturation behaviour of microbial community growth kinetics [53]. To ensure saturated substrate conditions for further testing of toxicants, the concentration of acetate was maintained at 100 mM.

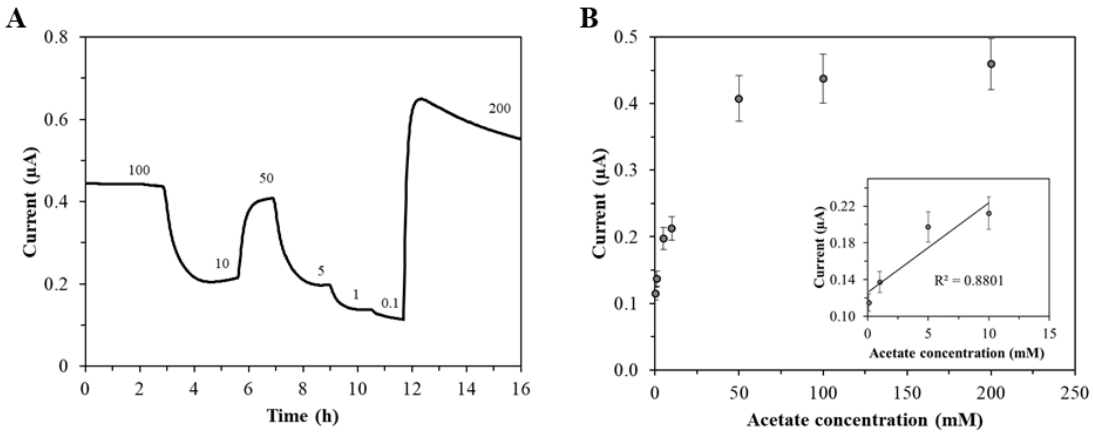

Figure 6.3. MFC response to AW containing varying potassium acetate concentrations indicated (in mM) with numbers in the figure. [**A**] Current output change with time. [**B**] Average steady state current from MFC biosensors as a function of potassium acetate concentration. Data is an average of 3 MFCs with 8.4% error.

The MFC was subsequently tested as a sensor for bioactive compounds in AW. Initially, formaldehyde was used as a model toxicant. Formaldehyde is a commonly used disinfectant and biocide [24], which has been widely tested as a model toxicant for MFC based sensors. Figure 6.4 shows the effect of injecting formaldehyde for a period of 10 min into the MFC biosensor on the output current, with results summarised in Table S6.2. For concentrations greater than 10 ppm, a drop in the current is observed, proportional to the concentration added, with a sensitivity of $1.43 \times 10^{-3} \pm 0.18 \times 10^{-3}$ ppm^{-1} cm^{-2}. No discernible effects were observed for formaldehyde concentrations below 10 ppm and hence data are not reported.

The MFC biosensor showed an almost instant response to the presence of formaldehyde, with a delay time, t_d, of 4.7 ± 1.8 min. For all concentrations below 2000 ppm, the current generated by the MFC returned to its original baseline current value, with an average recovery time, t_{rec}, of 67.3 ± 42.0 min. For these concentrations, it is assumed that the presence of formaldehyde only causes temporary changes to the electroactive bacteria at the anode [11]. Although, at low concentrations, some bacteria can also utilise formaldehyde. On the other hand, when a concentration of 2000 ppm was used, the baseline current was not restored. It is therefore assumed that such levels of formaldehyde caused permanent damage to the anodic biofilm. The recovery time, t_{rec}, of the current response increased as the concentration of formaldehyde increased, with a time of 28 min for 10 ppm and 117 min for 2000 ppm, Table S6.2, where these

times are significantly less than those for other formaldehyde MFC biosensors, Table 6.1. Moreover, the initial rate of current response, $r_{initial}$, upon injection of formaldehyde, showed a positive linear response to the concentration of formaldehyde, Table S6.2. Indeed, the analysis of initial rates could prove useful for rapid determination of the presence of a toxic compound in water and an indication of its concentration, which supports the possibility to use the MFC as a rapid shock-sensor for water analysis [20,54].

It results that the MFC developed in this study demonstrates similar detection ranges reported in other studies, Table 6.1 [16,23,24,31]. Promisingly, the MFC biosensor in this study showed an improved t_{res} to most other studies (which exhibit t_{res} between 125 – 200 min [16,23]). The rapid t_{res} is suspected to be due to the miniaturisation of the device, which improves mass transfer between the bulk fluid and the biofilm at the anode. This in effect reduces external mass transfer processes in the device [55], thereby improving detection of toxicants within the MFC [56].

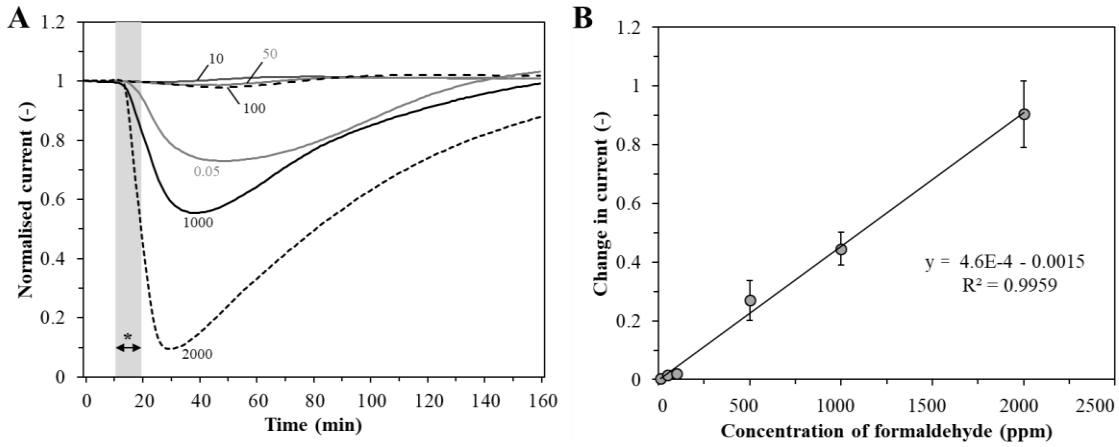

Figure 6.4. MFC biosensor response to formaldehyde. [**A**] Current output *versus* time. Formaldehyde in AW was injected into the MFCs for 10 min; subsequently the MFCs were fed with AW with no formaldehyde. The number adjacent to each line indicate the concentration of formaldehyde (ppm). [**B**] Change in current after formaldehyde injection *versus* formaldehyde concentration. For all data response is an average of 3 MFCs with up to a 12.5% error.

Table 6.1. Summary of other MFC based biosensors for formaldehyde detection

Microbe assayed	Config-uration	Anode chamber volume	Formaldehyde concentration monitored (ppm)	Response time, t_{res}	Recovery time, t_{rec}	Delay time, t_d	Ref.
Microalgae wastewater consortium	Single chamber	128 µL	10 - 2000	24.4 ± 7.7 min	46 ± 7.8 min	4.7 ± 1.8 min	This study
Shewanella oneidensis MR-1	Single chamber	140 µL	10 - 1000	200 min	~ 175 min	N/A	[23]
Geobacter sulfurre-ducens	Two chamber	144 µL	1000	~ 3 min	N/A	N/A	[24]
Shewanella oneidensis MR-1	Single chamber	120 mL	100 - 1000	> 9.7 h	N/A	N/A	[31]
Wild-type *Pseudo-monas aeruginosa* PAO1	Single chamber dual-channel system	90 µL	30 – 3500	< 125 min	~ 330 min	N/A	[16]

The MFC biosensors were then used to detect the toxicity of atrazine in AW. Atrazine is a member of the chlorinated *s*-triazine group of herbicides very toxic to aquatic life, and is listed as a priority substance for action under the Water Framework Directive [57]. Figure 6.5 shows the effect of injecting atrazine into the MFC biosensor for a period of 30 min. The results are also summarised in Table S6.2. The response to atrazine was characterised by an initial drop in the output current, followed by a slow recovery towards the baseline. For concentrations between 0.05 and 0.3 ppm, the initial current drop was proportional to the concentration added, with a sensitivity of 1.39 ± 0.26 ppm^{-1} cm^{-2}. Further increases in atrazine concentration did not cause marked changes in the output current. The lower detection limit for atrazine was 0.05 ppm. The average t_{rec} of the sensor was 28.6 ± 8.6 min, where greater t_{rec} were experienced on atrazine concentrations above 0.3 ppm (up to 44 min). The average t_{res} towards atrazine was 9.2 ± 3.6 min. This is the first time that the possibility of using MFCs to detect the toxicity of atrazine in water is demonstrated. Whole cell biosensors for the detection of atrazine reported include mainly optical methods, utilising either microalgae [58] or bioluminescent bacteria [59,60]. These systems demonstrate excellent detection limits, ranging from 1×10^{-5} ppm – 1 ppm [60], 4 – 8 ppm [59] and 0.25 – 10 ppm [58] The MFC sensor here reported, however, has the advantages of:

faster response times (detection times of atrazine microbial sensors previously reported range widely between 120 min [59] and 180 – 300 min [60]); use of mixed anaerobic consortia rather than pure species, which simplifies practical applications; and low cost and simple design as no external transducer is required.

Several studies have shown atrazine biodegradation by anaerobic wastewater consortia [61], as well as by pure species, such as *Pseudomonas* [62], *Rhodococcus* [63], and *Nicordioides* [64]. The biodegradation occurs by either N-dealkylation of atrazine into deisopropylatrazine and deethylatrazine or dechlorination into hydroxyatrazine [63]. This process is, however, very slow. For example, only 45% degradation has been reported after five days residence time in an anaerobic wastewater reactor [61]. Some studies have also shown the possibility to use MFCs for atrazine biodegradation. In a soil based MFC an 80% atrazine removal was achieved after 7 days [65]. In a batch MFC system, an 85% decrease in atrazine concentration was observed after 24 hours. Nearly 83% of this reduction, however, was addressed to atrazine sorption onto the biofilm or electrode surface [66]. More work, however, is needed to support and better understand the fate of atrazine at the biofilm in the MFC.

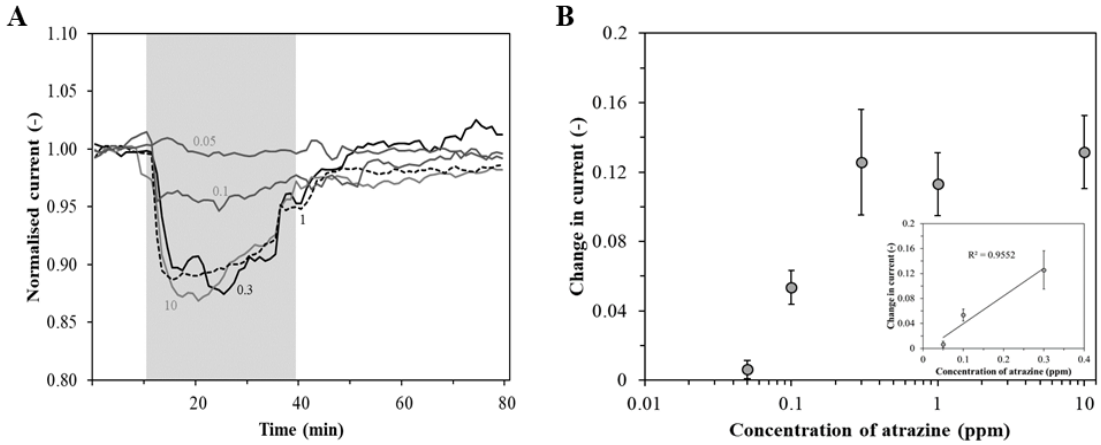

Figure 6.5. MFC biosensor response to atrazine. [**A**] Current output *versus* time. Atrazine in AW was injected into the MFCs for 30 min; subsequently the MFCs were fed with AW with no atrazine. Number adjacent to each line indicate the concentration of atrazine (ppm). [**B**] Change in current after atrazine injection *versus* atrazine concentration. For all data response is an average of 3 MFCs with up to 24% error.

6.5 Conclusions

MFCs present an attractive avenue towards the detection of bioactive contaminants in water systems. To this end, this work focuses on the development of a miniature single chamber MFC biosensor for real time water quality monitoring. Firstly, the effect of operational conditions, such as temperature, pH and ionic strength of the water sample on the sensor baseline current was investigated. Within the range of values tested, the pH was found to have the most significant effect on current production. Once optimal operational conditions were fixed, the sensing capability of the MFC device was tested. Formaldehyde was firstly used as a model toxicant and atrazine used as a case study. The MFC biosensor demonstrated a fast response to atrazine, with a sensitivity of 1.39 ± 0.26 ppm^{-1} cm^{-2} and a lower detection limit of 0.05 ppm. The ability of the MFC biosensor to detect atrazine toxicity, along with fast recovery of the baseline current after exposure, shows promise for the use of this technology for cost-effective online and real time detection of such chemicals.

6.6 Associated content

Author Contributions

JC and MDL conceived the experiment. Design, implementation and analysis of experiments performed by JC. Manuscript prepared by JC and MDL. Project supervised by MDL.

Conflicts of Interest

The authors declare no conflict of interest.

Acknowledgements

The authors would like to thank: Wessex Water for providing anaerobic sludge; The Engineering and Physical Science Research Council (EPSRC) and the Doctoral Training Centre for Sustainable Chemical Technologies for funding (EP/G03768X/1).

Abbreviations

AW: Artificial wastewater,

BOD: Biological oxygen demand,

COD: Chemical oxygen demand,

DOE: Design of experiment,

MFC: Microbial fuel cell,

OCV: Open circuit voltage.

Nomenclature

Roman symbols

A: Anode macro surface area,

Δd: Unit change in a disturbance,

I: Current,

ΔI: Unit change in current output,

I_B: Baseline current,

I_N: Normalised current,

ΔI_N: Unit change in normalised current output,

I_t: Current at time t,

P: Power,

R: Resistance,

$r_{initial}$: Initial rate of the current response,

t: Time,

t_d: Delay time,

t_{rec}: Recovery time,

t_{res}: Response time,

V: Voltage.

6.7 Supporting information

Table S6.1. Summary of the sensing performance of the MFC towards labile organic content and environmental parameters. Sensitivity is normalised by the anodic surface area (0.32 cm^2).

Parameter	**Delay time (min)**	**Response time (min)**
Acetate concentration (mM)		
0.1	6	56
1	8	48
5	5	69
10	5	62
50	6	44
200	4	62
Average	5.7 ± 1.2	56.8 ± 8.6
Temperature (°C)		
10	11	72
15	2	34
20	-	-
25	4	41
30	3	53
35	4	38
40	4	46
Average	4.7 ± 2.9	47.3 ± 12.6
pH		
6.3	6	81
7.5	7	107
9.2	9	70
10.9	5	94
12.5	4	67
Average	6.2 ± 1.7	83.8 ± 15
Ionic strength (mS cm^{-1})		
11.2	4	62
14	3	94
18	7	78
36	5	112
56.5	8	128
81.3	13	152
111.9	6	266
Average	6.6 ± 3.1	127.4 ± 63.1

Table S6.2. Summary of the sensing performance of the MFC towards formaldehyde and atrazine. Sensitivity is normalised by the anodic surface area (0.32 cm^2).

Concentration of toxicant	Change in normalised current, ΔI_N (-)	Initial rate of current response (μA min^{-1})	Response time (min)	Recovery time (min)	Delay time (min)
Formaldehyde (ppm)					
10	0.003	-0.0005	18	28	6
50	0.015	-0.0008	23	35	7
100	0.021	-0.0008	38	15	6
500	0.270	-0.0174	36	100	4
1000	0.446	-0.0373	28	109	2
2000	0.905	-0.1144	20	117	3
Average			27.2 ± 7.6	67.3 ± 42.0	4.7 ± 1.8
Atrazine (ppm)					
0.05	0.006	-0.0007	13	24	8
0.1	0.053	-0.0014	13	18	4
0.3	0.126	-0.0138	10	28	4
1	0.113	-0.0093	5	29	4
10	0.131	-0.0141	5	44	4
Average			9.2 ± 3.6	28.6 ± 8.6	4.8 ± 1.6

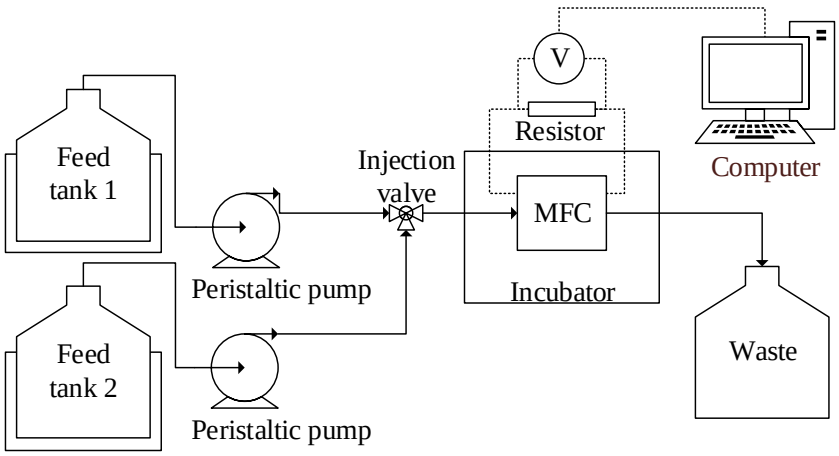

Figure S6.1. Experimental set up for testing the MFC biosensors. Disturbances (e.g. change in temperature, pH, ionic strength, labile organic content or a toxic compound) are introduced *via* a 3 way valve prior to the MFC using an alternative feed tank (1 & 2). Feed tank temperature is controlled by a water bath.

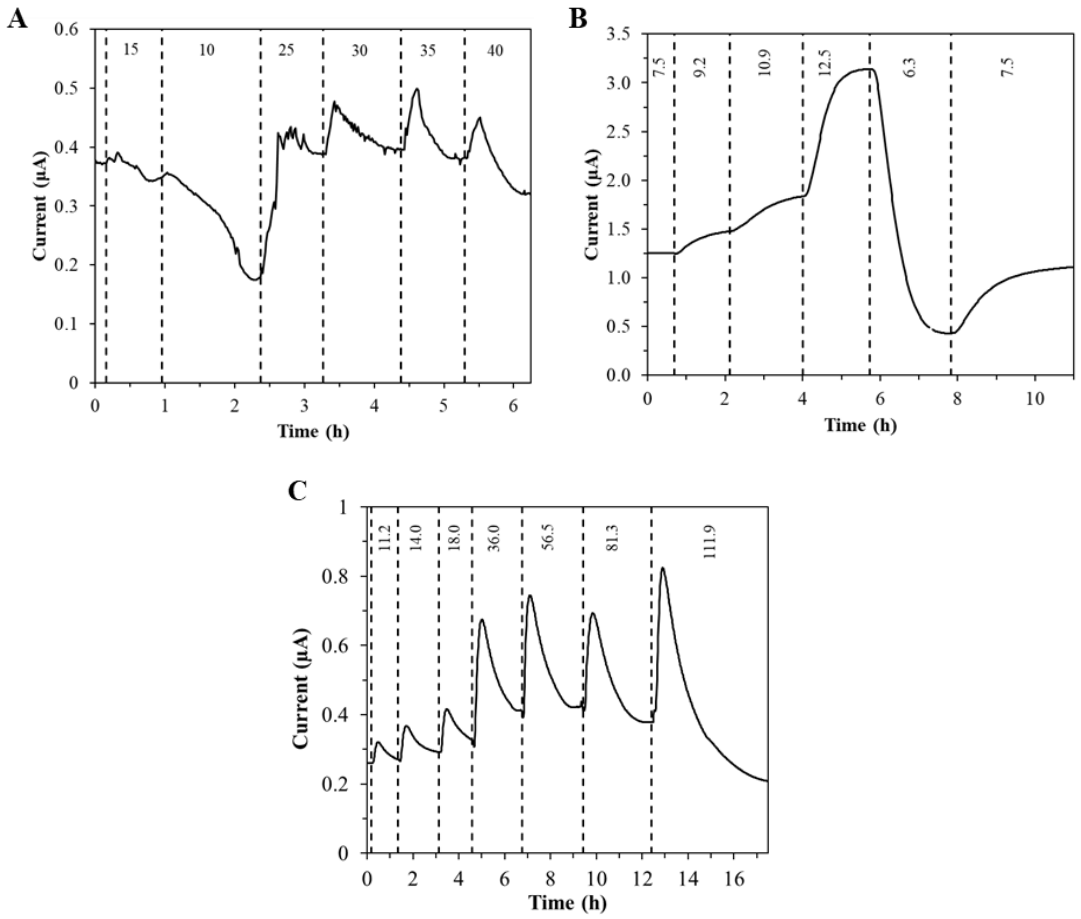

Figure S6.2. MFC current response with respect to time for AW with variations in environmental factors (as indicated with numbers in the figure of °C and mS cm^{-1} for temperature and conductivity respectively). [**A**] Temperature, data is an average of 3 MFCs with up to 6% error; [**B**] pH, data is an average of 3 MFCs with up to 12% error; [**C**] conductivity. Data is an average of 3 MFCs with up to 11% error.

6.8 References

[1] WWAP (United Nations World Water Assessment Programme), The United Nations World Water Development Report 2015: Water for a Sustainable World, Paris, 2015. doi:978-92-3-100071-3.

[2] World Health Organisation (WHO)., Clean Water and Sanitation: Why it matters, 2017. http://www.un.org/sustainabledevelopment/wp-content/uploads/2016/08/6_Why-it-Matters_Sanitation_2p.pdf (accessed September 21, 2017).

[3] International Hydrological Programme, IHP-VIII Water security: Responses to global challenges 2014-2021, 2016. http://unesdoc.unesco.org/images/0022/002251/225103e.pdf (accessed September 21, 2017).

[4] G.M. Carr, J.P. Neary, Water Quality for Ecosystem and Human Health, 2008. http://www.unep.org/PDF/Clearing_the_Waters.pdf (accessed January 20, 2015).

[5] United Nations, Sustainable development goals - United Nations, (2017). http://www.un.org/sustainabledevelopment/sustainable-development-goals/ (accessed September 7, 2017).

[6] H. Yang, M. Zhou, M. Liu, W. Yang, T. Gu, Microbial fuel cells for biosensor applications, Biotechnol. Lett. 37 (2015) 2357–2364. doi:10.1007/s10529-015-1929-7.

[7] B.E. Logan, Microbial Fuel Cells, Wiley, 2008.

[8] Y. Jiang, P. Liang, C. Zhang, Y. Bian, X. Yang, X. Huang, P.R. Girguis, Enhancing the response of microbial fuel cell based toxicity sensors to Cu(II) with the applying of flow-through electrodes and controlled anode potentials., Bioresour. Technol. 190 (2015) 367–372. doi:10.1016/j.biortech.2015.04.127.

[9] J. Chouler, M. Di Lorenzo, Water Quality Monitoring in Developing Countries; Can Microbial Fuel Cells be the Answer?, Biosensors. 5 (2015) 450–470. doi:10.3390/bios5030450.

[10] M. Kim, M.S. Hyun, G.M. Gaddb, H.J. Kim, A novel biomonitoring system using microbial fuel cells, J. Environ. Monit. 9 (2007) 1323–1328. doi:10.1039/b713114c.

[11] M. Di Lorenzo, A.R. Thomson, K. Schneider, P.J. Cameron, I. Ieropoulos, A small-scale air-cathode microbial fuel cell for on-line monitoring of water quality., Biosens. Bioelectron. 62 (2014) 182–188. doi:10.1016/j.bios.2014.06.050.

[12] M. Kim, S.M. Youn, S.H. Shin, J.G. Jang, S.H. Han, M.S. Hyun, G.M. Gadd, H.J. Kim, Practical field application of a novel BOD monitoring system, J. Environ. Monit. 5 (2003) 640–643. doi:10.1039/b304583h.

[13] D. Yu, L. Bai, J. Zhai, Y. Wang, S. Dong, Toxicity detection in water containing heavy metal ions with a self-powered microbial fuel cell-based biosensor, Talanta. 168 (2017) 210–216. doi:10.1016/j.talanta.2017.03.048.

[14] J. Chouler, I. Bentley, F. Vaz, A. O'Fee, P.J. Cameron, M. Di Lorenzo, Exploring the use of cost-effective membrane materials for Microbial Fuel Cell based sensors, Electrochim. Acta. 231 (2017) 319–326. doi:10.1016/j.electacta.2017.01.195.

[15] Y. Jiang, P. Liang, P. Liu, B. Miao, Y. Bian, H. Zhang, X. Huang, Enhancement of the sensitivity of a microbial fuel cell sensor by transient-state operation, Environ. Sci. Water Res. Technol. 3 (2017) 472–479. doi:10.1039/C6EW00346J.

[16] W. Yang, X. Wei, S. Choi, A Dual-Channel, Interference-Free, Bacteria-Based Biosensor for Highly Sensitive Water Quality Monitoring, IEEE Sens. J. 16 (2016) 8672–8677. doi:10.1109/JSEN.2016.2570423.

[17] X.C. Abrevaya, N.J. Sacco, M.C. Bonetto, A. Hilding-Ohlsson, E. Cortón, Analytical applications of microbial fuel cells. Part II: Toxicity, microbial activity and quantification, single analyte detection and other uses., Biosens. Bioelectron. 63 (2015) 591–601. doi:10.1016/j.bios.2014.04.053.

[18] S. Patil, F. Harnisch, U. Schröder, Toxicity response of electroactive microbial biofilms--a decisive feature for potential biosensor and power source applications., Chemphyschem. 11 (2010) 2834–2837. doi:10.1002/cphc.201000218.

[19] N.E. Stein, H.V.M. Hamelers, G. van Straten, K.J. Keesman, Effect of toxic components on microbial fuel cell-polarization curves and estimation of the type of toxic inhibition., Biosensors. 2 (2012) 255–268. doi:10.3390/bios2030255.

[20] B. Liu, Y. Lei, B. Li, A batch-mode cube microbial fuel cell based "shock" biosensor for wastewater quality monitoring., Biosens. Bioelectron. 62 (2014) 308–314. doi:10.1016/j.bios.2014.06.051.

[21] G.-H. Wang, C.-Y. Cheng, M.-H. Liu, T.-Y. Chen, M.-C. Hsieh, Y.-C. Chung, Utility of Ochrobactrum anthropi YC152 in a Microbial Fuel Cell as an Early Warning Device for Hexavalent Chromium Determination, Sensors. 16 (2016) 1272. doi:10.3390/s16081272.

[22] Y. Shen, M. Wang, I.S. Chang, H.Y. Ng, Effect of shear rate on the response of microbial fuel cell toxicity sensor to Cu(II)., Bioresour. Technol. 136 (2013) 707–710. doi:10.1016/j.biortech.2013.02.069.

[23] W. Yang, X. Wei, A. Fraiwan, C.G. Coogan, H. Lee, S. Choi, Fast and sensitive water quality assessment: A μL-scale microbial fuel cell-based biosensor integrated with an air-bubble trap and electrochemical sensing functionality, Sensors Actuators B Chem. 226 (2016) 191–195. doi:10.1016/j.snb.2015.12.002.

[24] D. Dávila, J.P. Esquivel, N. Sabaté, J. Mas, Silicon-based microfabricated microbial fuel cell toxicity sensor., Biosens. Bioelectron. 26 (2011) 2426–2430. doi:10.1016/j.bios.2010.10.025.

[25] M. Di Lorenzo, T.P. Curtis, I.M. Head, K. Scott, A single-chamber microbial fuel cell as a biosensor for wastewaters., Water Res. 43 (2009) 3145–3154. doi:10.1016/j.watres.2009.01.005.

[26] L. Peixoto, B. Min, G. Martins, A.G. Brito, P. Kroff, P. Parpot, I. Angelidaki, R. Nogueira, In situ microbial fuel cell-based biosensor for organic carbon, Bioelectrochemistry. 81 (2011) 99–103. doi:10.1016/j.bioelechem.2011.02.002.

[27] A. Elmekawy, H.M. Hegab, X. Dominguez-Benetton, D. Pant, Internal resistance of microfluidic microbial fuel cell: challenges and potential opportunities., Bioresour. Technol. 142 (2013) 672–682. doi:10.1016/j.biortech.2013.05.061.

[28] F. Qian, D.E. Morse, Miniaturizing microbial fuel cells., Trends Biotechnol. 29 (2011) 62–69. doi:10.1016/j.tibtech.2010.10.003.

[29] Y. Jiang, P. Liang, P. Liu, Y. Bian, B. Miao, X. Sun, H. Zhang, X. Huang, Enhancing Signal Output and Avoiding BOD/Toxicity Combined Shock Interference by Operating a Microbial Fuel Cell Sensor with an Optimized Background Concentration of Organic Matter, Int. J. Mol. Sci. 17 (2016) 1392. doi:10.3390/ijms17091392.

[30] S.B. Velasquez-Orta, D. Werner, J.C. Varia, S. Mgana, Microbial fuel cells for inexpensive continuous in-situ monitoring of groundwater quality, Water Res. 117 (2017) 9–17. doi:10.1016/j.watres.2017.03.040.

[31] X. Wang, N. Gao, Q. Zhou, Concentration responses of toxicity sensor with Shewanella oneidensis MR-1 growing in bioelectrochemical systems., Biosens. Bioelectron. 43 (2013) 264–267. doi:10.1016/j.bios.2012.12.029.

[32] J. Chouler, G.A. Padgett, P.J. Cameron, K. Preuss, M.-M. Titirici, I. Ieropoulos, M. Di Lorenzo, Towards effective small scale microbial fuel cells for energy generation from urine, Electrochim. Acta. 192 (2016) 89–98. doi:10.1016/j.electacta.2016.01.112.

[33] M. Miyahara, A. Kouzuma, K. Watanabe, Effects of NaCl concentration on anode microbes in microbial fuel cells., AMB Express. 5 (2015) 1–9. doi:10.1186/s13568-015-0123-6.

[34] N.E. Stein, H.V.M. Hamelers, C.N.J. Buisman, Stabilizing the baseline current of a microbial fuel cell-based biosensor through overpotential control under non-toxic conditions., Bioelectrochemistry. 78 (2010) 87–91. doi:10.1016/j.bioelechem.2009.09.009.

[35] L.H. Li, Y.M. Sun, Z.H. Yuan, X.Y. Kong, Y. Li, Effect of temperature change on power generation of microbial fuel cell, Environ. Technol. 34 (2013) 1929–1934. doi:10.1080/09593330.2013.828101.

[36] Z. He, Y. Huang, A.K. Manohar, F. Mansfeld, Effect of electrolyte pH on the rate of the anodic and cathodic reactions in an air-cathode microbial fuel cell, Bioelectrochemistry. 74 (2008) 78–82. doi:10.1016/j.bioelechem.2008.07.007.

[37] Y. Fan, E. Sharbrough, H. Liu, Quantification of the Internal Resistance Distribution of Microbial Fuel Cells, Environ. Sci. Technol. 42 (2008) 8101–8107. doi:10.1021/es801229j.

[38] S. Choi, H.-S. Lee, Y. Yang, P. Parameswaran, C.I. Torres, B.E. Rittmann, J. Chae, A μL-scale micromachined microbial fuel cell having high power density., Lab Chip. 11 (2011) 1110–1117. doi:10.1039/c0lc00494d.

[39] F. Qian, M. Baum, Q. Gu, D.E. Morse, A 1.5 μL microbial fuel cell for on-chip bioelectricity generation., Lab Chip. 9 (2009) 3076–3081. doi:10.1039/b910586g.

[40] G.-X. Yang, Y.-M. Sun, X.-Y. Kong, F. Zhen, Y. Li, L.-H. Li, T.-Z. Lei, Z.-H. Yuan, G.-Y. Chen, Factors affecting the performance of a single-chamber microbial fuel cell-type biological oxygen demand sensor., Water Sci. Technol. 68 (2013) 1914–1919. doi:10.2166/wst.2013.415.

[41] G.-C. Gil, I.-S. Chang, B.H. Kim, M. Kim, J.-K. Jang, H.S. Park, H.J. Kim, Operational parameters affecting the performannce of a mediator-less microbial fuel cell, Biosens. Bioelectron. 18 (2003) 327–334. doi:10.1016/S0956-5663(02)00110-0.

[42] E. Martin, O. Savadogo, S.R. Guiot, B. Tartakovsky, The influence of operational conditions on the performance of a microbial fuel cell seeded with mesophilic anaerobic sludge, Biochem. Eng. J. 51 (2010) 132–139. doi:10.1016/j.bej.2010.06.006.

[43] Y. Yuan, B. Zhao, S. Zhou, S. Zhong, L. Zhuang, Electrocatalytic activity of anodic biofilm responses to pH changes in microbial fuel cells, Bioresour. Technol. 102 (2011) 6887–6891. doi:10.1016/j.biortech.2011.04.008.

[44] Y. Gu, H. Feng, X. Ying, K. Chen, J. Cheng, H. Huang, S. Zhen, D. Shen, Effects of electrolyte conductivity on power generation in bio-electrochemical systems, Ionics (Kiel). 23 (2017) 2069–2075. doi:10.1007/s11581-017-2047-4.

[45] J.-Y. Nam, H.-W. Kim, K.-H. Lim, H.-S. Shin, B.E. Logan, Variation of power generation at different buffer types and conductivities in single chamber microbial fuel cells, Biosens. Bioelectron. 25 (2010) 1155–1159. doi:10.1016/j.bios.2009.10.005.

[46] S. Madani, R. Gheshlaghi, M.A. Mahdavi, M. Sobhani, A. Elkamel, Optimization of the performance of a double-chamber microbial fuel cell through factorial design of experiments and response surface methodology, Fuel. 150 (2015) 434–440. doi:10.1016/j.fuel.2015.02.039.

[47] B.H. Kim, I.S. Chang, G.C. Gil, H.S. Park, H.J. Kim, Novel BOD (biological oxygen demand) sensor using mediator-less microbial fuel cell, Biotechnol. Lett. 25 (2003) 541–545. doi:10.1023/A:1022891231369.

[48] M. Di Lorenzo, K. Scott, T.P. Curtis, K.P. Katuri, I.M. Head, Continuous Feed Microbial Fuel Cell Using An Air Cathode and A Disc Anode Stack for Wastewater Treatment, Energy & Fuels. 23 (2009) 5707–5716. doi:10.1021/ef9005934.

[49] I. Karube, T. Matsunaga, S. Mitsuda, S. Suzuki, Microbial electrode BOD sensors., Biotechnol. Bioeng. 19 (1977) 1535–1547. doi:10.1002/bit.260191010.

[50] H. Moon, I.S. Chang, K.H. Kang, J.K. Jang, B.H. Kim, Improving the dynamic response of a mediator-less microbial fuel cell as a biochemical oxygen demand (BOD) sensor., Biotechnol. Lett. 26 (2004) 1717–1721. doi:10.1007/s10529-004-3743-5.

[51] B. Min, B.E. Logan, Continuous Electricity Generation from Domestic Wastewater and Organic Substrates in a Flat Plate Microbial Fuel Cell, Environ. Sci. Technol. 38 (2004) 5809–5814. doi:10.1021/es0491026.

[52] Y. Zhang, I. Angelidaki, Submersible microbial fuel cell sensor for monitoring microbial activity and BOD in groundwater: focusing on impact of anodic biofilm on sensor applicability., Biotechnol. Bioeng. 108 (2011) 2339–2347. doi:10.1002/bit.23204.

[53] P. Ledezma, J. Greenman, I. Ieropoulos, Maximising electricity production by controlling the biofilm specific growth rate in microbial fuel cells., Bioresour. Technol. 118 (2012) 615–618. doi:10.1016/j.biortech.2012.05.054.

[54] Z. Xu, Y. Liu, I. Williams, Y. Li, F. Qian, H. Zhang, D. Cai, L. Wang, B. Li, Disposable self-support paper-based multi-anode microbial fuel cell (PMMFC) integrated with power management system (PMS) as the real time "shock" biosensor for wastewater, Biosens. Bioelectron. 85 (2016) 232–239. doi:10.1016/j.bios.2016.05.018.

[55] P.M. Doran, Bioprocess Engineering Principles, Academic Press, 2008.

[56] S. Choi, Microscale microbial fuel cells: Advances and challenges, Biosens. Bioelectron. 69 (2015) 8–25. doi:10.1016/j.bios.2015.02.021.

[57] EU Parliament, Directives: water policy, Off. J. Eur. Union. (2008) 84–97.

[58] C. Védrine, J.-C. Leclerc, C. Durrieu, C. Tran-Minh, Optical whole-cell biosensor using Chlorella vulgaris designed for monitoring herbicides, Biosens. Bioelectron. 18 (2003) 457–463. doi:10.1016/S0956-5663(02)00157-4.

[59] G. Strachan, S. Preston, H. Maciel, A.J.R. Porter, G.I. Paton, Use of bacterial biosensors to interpret the toxicity and mixture toxicity of herbicides in freshwater, Water Res. 35 (2001) 3490–3495. doi:10.1016/S0043-1354(01)00065-3.

[60] K. Jia, E. Eltzov, T. Toury, R.S. Marks, R.S. Ionescu, A lower limit of detection for atrazine was obtained using bioluminescent reporter bacteria via a lower incubation temperature, Ecotoxicol. Environ. Saf. 84 (2012) 221–226. doi:10.1016/J.ECOENV.2012.07.009.

[61] P.K. Ghosh, L. Philip, Atrazine degradation in anaerobic environment by a mixed microbial consortium, Water Res. 38 (2004) 2277–2284. doi:10.1016/j.watres.2003.10.059.

[62] R.M. Behki, S.U. Khan, Degradation of Atrazine by Pseudomonas: N-Dealkylation and Dehalogenation of Atrazine and Its Metabolites, J. Agric. Food Chem. 34 (1986) 746–749. doi:10.1021/jf00070a039.

[63] P.D. Kolekar, S.S. Phugare, J.P. Jadhav, Biodegradation of atrazine by Rhodococcus sp. BCH2 to N-isopropylammelide with subsequent assessment of toxicity of biodegraded metabolites, Environ. Sci. Pollut. Res. 21 (2014) 2334–2345. doi:10.1007/s11356-013-2151-6.

[64] E. Topp, W.M. Mulbry, H. Zhu, S.M. Nour, D. Cuppels, Characterization of S-triazine herbicide metabolism by a Nocardioides sp. isolated from agricultural soils., Appl. Environ. Microbiol. 66 (2000) 3134–3141. doi:10.1128/AEM.66.8.3134-3141.2000.

[65] A. Domínguez-Garay, K. Boltes, A. Esteve-Núñez, Cleaning-up atrazine-polluted soil by using Microbial Electroremediating Cells, Chemosphere. 161 (2016) 365–371. doi:10.1016/j.chemosphere.2016.07.023.

[66] C.M. Werner, C. Hoppe-Jones, P.E. Saikaly, B.E. Logan, G.L. Amy, Attenuation of trace organic compounds (TOrCs) in bioelectrochemical systems, Water Res. 73 (2015) 56–67. doi:10.1016/j.watres.2015.01.013.

[67] Weiyang Yang, Xuejian Wei, Seokheun Choi, A two-channel bacteria-based biosensor for water quality monitoring, in: IEEE SENSORS, IEEE, 2015. doi:10.1109/ICSENS.2015.7370674.

[68] Q. Jia, L. Wei, H. Han, J. Shen, Factors that influence the performance of two-chamber microbial fuel cell, Int. J. Hydrogen Energy. 39 (2014) 13687–13693. doi:10.1016/j.ijhydene.2014.04.023.

7 A screen-printed paper microbial fuel cell biosensor for detection of toxic compounds in water

Here, a screen-printed, biodegradable and portable paper-based MFC is developed. Its structural properties are tuned to render is suitable for water quality monitoring applications and then the devices ability to detect formaldehyde in wastewater is assessed. The effect of stacking the paper-based MFCs on current baseline and sensor sensitivity is investigated. This work has been submitted for publication as detailed on the following page. Amendments have been made to account for stylistic consistency in this thesis.

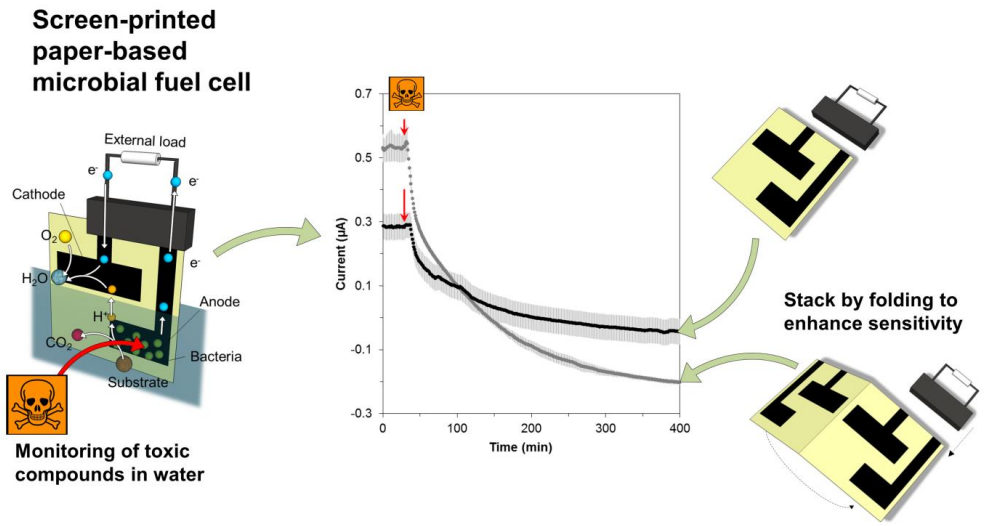

Statement of authorship

This declaration concerns the article entitled:	A screen-printed paper microbial fuel cell biosensor for detection of toxic compounds in water
Publication status:	Submitted for publication
Publication details:	Submitted to Biosensors and Bioelectronics, Elsevier.
Authorship contributions:	MDL, JLS and JC conceived the experiment. Design, implementation and analysis of the experiments were performed by: ACI for the device fabrication and manufacture; JC for the microbial fuel cell analysis and SR for the cyclic voltammetry. Manuscript prepared by JC, MDL and JLS. Supervision from MDL and JLS.
Statement from candidate:	This paper reports on original research I conducted during the period of my Higher Degree by Research candidature.

Signed: Date:

Published as: Chouler, J, Cruz-Izquierdo, A, Rengaraj, S, Scott, J & Di Lorenzo, M 2018, 'A screen-printed paper microbial fuel cell biosensor for detection of toxic compounds in water', Biosensors and Bioelectronics, vol. 102, pp. 49-56. https://doi.org/10.1016/j.bios.2017.11.018

A screen-printed paper microbial fuel cell biosensor for detection of toxic compounds in water

Jon Chouler [a,b], Álvaro Cruz-Izquierdo [c], Saravanan Rengaraj [a], Janet L. Scott [c], Mirella Di Lorenzo [a]

[a] Department of Chemical Engineering, University of Bath, Bath BA2 7AY, UK

[b] EPSRC Centre for Doctoral Training in Sustainable Chemical Technologies, University of Bath, Bath BA2 7AY, UK

[c] Department of Chemistry, University of Bath, Bath BA2 7AY, UK

7.1 Abstract

Access to safe drinking water is a human right, crucial to combat inequalities, reduce poverty and allow sustainable development. In many areas of the world, however, this right is not guaranteed, in part because of the lack of easily deployable diagnostic tools. Low cost and simple methods to test water supplies onsite can protect vulnerable communities from the impact of contaminants in drinking water. Ideally such devices would also be easy to dispose of so as to leave no trace, or have a detrimental effect on the environment. To this aim, we here report the first paper microbial fuel cell (pMFC) fabricated by screen-printing biodegradable carbon based electrodes onto a single sheet of paper, and demonstrate its use as a shock sensor for bioactive compounds (e.g. formaldehyde) in water. We also show a simple route to enhance the sensor performance by folding back-to-back two pMFCs electrically connected in parallel. This promising proof of concept work can lead to a revolutionizing way of testing water at point of use, which is not only green, easy to operate and rapid, but is also affordable to all.

7.2 Introduction

The provision of clean water is essential to allow economic growth and environmental sustainability [1]. Nonetheless, in many poor areas of the world, access to safe water is still a luxury [2]. In countries that lack suitable infrastructure, the assessment of water quality is a challenge [3]. Along with effective sanitation and wastewater treatment programs, it is extremely important to establish methods for water quality analysis that do not require expensive laboratory equipment and/or skilled personnel yet provide rapid response and have onsite functionality [4].

In recent years, microbial fuel cell (MFC) technology has demonstrated promising potential as a tool for water quality monitoring [5]. MFCs are devices that directly convert the chemical energy contained in organic matter into electricity *via* the metabolic processes of microorganisms [6,7]. On the anode surface of these devices, a biofilm develops, which contains electroactive bacteria capable of extracellularly transferring the electrons they generate from the oxidation of organic compounds to the electrode. Therefore, the current generated by MFCs can be directly related to the metabolic activity of these anodic bacteria [8]. Any disturbances to their metabolic pathways, caused by environmental changes, such as organic load, or the sudden presence of a bioactive and toxic compound, are translated into a change in the electricity generated [9,10]. This is the principle behind the use of MFCs as a tool to detect the presence of toxicants in water [11].The major advantage of MFC based sensors for water quality monitoring over other devices suggested in the literature is their simplicity. In MFCs, the anodic biofilm functions as the recognition component [5]. Its response to the presence of a toxicant causes a change in the rate of flow of electrons to the anode (the transducer), thus generating a measurable change in the output current. As such, there is no need for expensive external equipment that acts as a transducer, as is required in many other types of sensors proposed [12,13].

Despite their promise, practical implementation of MFCs as sensors is still restricted by the use of expensive manufacturing materials [14] and device designs that are not suitable for portable applications, due to the need for pumps and tubing during operation [15]. All these aspects reflect in an increase in both capital and operating costs. There is therefore a great need for innovative and cost-effective MFC designs.

Recently, paper electronics, which refer to the use of paper as a functional part of the electronic components of a device, are attracting increasing attention [16]. The use of paper can lead to the development of innovative, light and recyclable electronics, with the added benefits of cost-effectiveness, facile operation, easy disposal after use, ready portability and widespread availability [17]. Paper has been explored for the fabrication of MFCs to generate energy from urine [14] and tryptic soy broth [15,18], or to power single-use diagnostic devices [19]. The state of the art in the field of paper-based MFCs is summarized in Table S7.1. In most of these studies, additional expensive materials are required, such as Nafion, used as a proton exchange membrane [15,20] and chemicals, such as ferricyanide, used as an electron acceptor at the cathode [15,19–22]. These paper-based MFCs are constructed from multiple elements and materials [18,23], which may lead to manufacturing complexity. They also appear to be restricted by short operational times (typically 20 – 200 min) [19–21]. Finally, some studies refer to the use of pure cultures such as *Shewanella oneidensis* MR-1 [24,25]. further adds to the complexity of the system and is not compatible with practical in field applications [21]. All these aspects highlight the need for cheap, easy to use and robust paper MFC devices.

In this context, we report here the first single component paper MFC, with the aim of developing a functional, yet simple, light and cost-effective single-use sensing device. The device is fabricated by screen-printing carbon based electrodes onto a single sheet of paper. It is membrane-less, as the paper substrate itself acts as the separator between the two electrodes. Moreover, there is no need for sample pumping, since capillary forces in the paper create autonomous microfluidics that can be manipulated by changing the paper structure, thus tuning the performance of the device. In this work, we cross-linked the cellulose fibres within the paper-based MFC, with glyoxal (a common cross-linking agent [26]), in order to increase robustness and operational lifetime of the device. The resulting MFC device has an extremely simple and easy to fabricate design, and, most of all, it is prepared from fully biodegradable components.

We then investigate the electrochemical performance of the paper MFC and test its capability as a sensor for toxicants in water. In particular, to allow ready comparison with previous work, formaldehyde was used as a model bioactive compound, since it is a toxicant widely used for testing MFC based sensors. Finally, we report on increased baseline current and enhancement of the sensor sensitivity by the simple

design modification of folding two paper MFCs back-to-back, electrically connected in parallel.

7.3 Experimental

7.3.1 Device fabrication

Single component paper-based MFCs (pMFC) were fabricated by screen-printing a conductive ink onto a single sheet of paper (Fabriano 5 HP). The conductive ink consisted of 20 mg α-cellulose (C8002, Sigma Aldrich) dissolved in 1 g of organic electrolyte solution, which consisted of 1-ethyl-3-methylimidazolium (EMIMAc, Sigma Aldrich) and dimethyl sulfoxide (DMSO, Sigma Aldrich) (92:8% *w/w* ratio). Conductive components, 40 mg carbon nanofibers (PR-24-XT-HHT, Pyrograf Products Inc., USA) and 40 mg graphite powder (< 20 µm, 282863, Sigma Aldrich) were dispersed in this solution. Initially, half of the conductive materials were dispersed into the solvent mixture with a probe sonicator (microtip probe 6.3 mm ID, Fisher Scientific) for 30 s (5 s ON/OFF cycle), then half of the cellulose was added and the paste was stirred overnight using a magnetic stirrer, after which, the remaining powder mass was added to the paste and thoroughly dispersed using a pestle and mortar. Three layers of the conductive ink were screen-printed (43-80 µm mesh) onto the paper to form the electrodes, Figure 7.1. Each layer was printed, the entire sheet submerged in methanol for 20 min to phase invert the cellulose binder and displace the EMIMAc/DMSO solvent, and the sheet air dried. The pMFC devices were then washed and soaked in water overnight. To cross-link the cellulose fibres in the pMFC, the devices were submerged for 3 h in aqueous solutions of glyoxal of varying concentrations, 0 – 24% *w/v* at room temperature (20 ± 3°C), removed and heated at 140°C for 1 h in an oven to effect reaction. This resulted in degrees of cross-linking corresponding to 0 – 94.8 mg g_{paper}^{-1}, as confirmed by HPLC analysis, Table S7.2. The conductivity of the resulting electrodes was 48.9 ± 1.9 Ω sq^{-1}.

To prepare electrodes with chitosan coatings, the anode was immersed in a 0.1% *w/v* chitosan (Sigma Aldrich) dissolved in 2% *v/v* acetate solution, prior to glyoxal cross-linking. The chitosan solution functioned as both the anti-solvent and source of chitosan. The electrodes were then washed three times for 30 min in water to remove

any residual solvents. The conductivity of the resulting electrodes was 45.6 ± 2.7 Ω sq^{-1}.

7.3.2 Device material characterisation

All characterisation of the paper samples was performed in triplicate. The conductivity of the electrodes was determined by the four-terminal probe method running a cyclic voltammagram between 0.01 and -0.01 V with a 5 mV s^{-1} scan rate using an Ivium Compactstat 104 (B08084, Ivium Technologies, NL) on the electrode surface. The tensile strength of the pMFCs was measured on an Instron 3369 (Instron, UK), using 1 × 10 cm pre-wetted paper strips (thoroughly wetted by soaking in deionised water overnight). The degree of cross-linking of the cellulose fibres was determined by measurement of glycolic acid post treatment, as previously described [27]: cross-linked paper samples (0.4 g accurately weighed) were treated with 5 mL of 4 M NaOH at 100°C for 25 min; the extract diluted by a factor of 10 and filtered through a 0.2 µm nylon filter before HPLC analysis was performed (Shimatzu Class-VP HPLC with an Aminex HPX-87H column thermostated at 50°C 15 min isocratic elution with 10 mM H_2SO_4 at a flow rate of 0.6 mL min^{-1}; UV-vis. detection at 210 nm). A calibration curve of peak area *versus* glycolic acid concentration was constructed, Figure S7.1, and the glycolic acid concentration was determined, Equation 7.1:

$$Glyoxal\ concentration\ (mg\ {g_{paper}}^{-1}) = \frac{PA - b}{a \times DF \times WOF_{ini}} \times 0.7632 \qquad \text{Equation 7.1}$$

Where *PA* is the peak area, *a* and *b* are the gradient and intercept of the line of best fit in the calibration, and *DF* the dilution factor which takes into account the volume of the hydrolytic reaction (mL), WOF_{ini} is the initial weight of the Fabriano paper (g), and M_R(glyoxal)/M_R(glycolic acid) = 0.7632 [27].

7.3.3 Biofilm analysis

A Jeol JSM-6480LV scanning electron microscope (SEM) was used to characterise the morphology of the fixed [28] biofilm onto the electrode surface after enrichment and operation. All samples were coated with Au prior to imaging.

To assess the relative growth of the biofilm, crystal violet staining was performed [29]: after 24 h exposure of the anode to artificial wastewater and anaerobic sludge 0.5 × 0.7 cm electrode samples were excised and placed in 24 well plates. Samples were washed twice with 100 mM phosphate buffer saline (PBS) to remove non-attached bacteria and dried for 1 h at 50°C. Crystal violet solution (1 mL 0.1% *v/v*) was added and the samples developed at room temperature for 30 min, the stain removed and the samples washed 3 times with 100 mM PBS. To dissolve the dye, 1 mL pure ethanol was added per sample and, following a 10-fold dilution in water, the absorbance measured at 590 nm.

7.3.4 Operation of the paper-based MFCs

Artificial wastewater (AW) containing (per litre of deionized water): 0.27 g $(NH_4)SO_4$, 0.06 g $MgSO_4.7H_2O$, 6 mg $MnSO_4.H_2O$, 0.13 g $NaHCO_3$, 3 mg $FeCL_3.6H_2O$, 4 mg $MgCl_2$, 3.1 g $NaH_2PO_4.H_2O$, 10.9 g Na_2HPO_4 and 10 mM potassium acetate (COD = 950 ± 32 mg/L) was used as the carbon source for the bacteria. The medium was autoclaved and purged with nitrogen before being fed to the pMFCs. A printed circuit board (PCB) edge connector (TE Connectivity, UK) was used to connect the MFC anode and cathode to a voltmeter (ADC-24 Pico data logger, Pico technology, UK) and voltage, *V*, was continuously monitored under closed circuit conditions by applying an external load, R_{ext}, of 1 kΩ to polarise the cell. The resultant current (*I*) was calculated using Ohm's law ($I = V/R$) and the power, *P*, calculated as $P = VI$. To achieve enrichment of electrochemically active bacteria at the anode, the pMFCs were submerged in a sealed 100 mL vessel containing 10% *v/v* anaerobic sludge (provided by Wessex Water from a wastewater treatment plant in Avonmouth, UK), which was magnetically stirred, Figure S7.2. The pH of the solution was 7.5 ± 0.1 and the conductivity 7.14 ± 0.15 mS cm^{-1}. Ten percent of the solution was replaced daily with freshly prepared AW. Once a stable current was observed, the pMFCs were fed with

AW containing 10 mM potassium acetate, but no anaerobic sludge. To increase the output current whilst occupying the same operational space, two pMFCs were folded back-to-back and connected to a single PCB edge connector, Figure 7.1D. The resulting device was named fpMFC. All studies were performed in duplicate.

7.3.5 Electrochemical analysis

After enrichment, electrochemical analysis of the fuel cells was performed using an Autolab PGSTAT128N (Metrohm, UK), with the cells left at open circuit for up to 2 h beforehand to allow a steady state open circuit potential to develop. All electrochemical tests were performed with the anode as the working electrode and the cathode as the counter electrode. Polarisation curves were recorded in two electrode mode using a scan rate of 5 mV s^{-1}. Electrochemical impedance spectroscopy (EIS) was conducted over a frequency range of 50 kHz down to 0.1 Hz, using 10 steps per decade, with a sinusoidal perturbation of 10 mV amplitude, and an integration time set to 0.125 s, 3 cycles, using the anode as the working electrode, the cathode as counter electrode and an Ag/AgCl reference electrode. To determine the efficacy of proton diffusion within the pMFC, cyclic voltammetry, in two electrode mode at a scan rate of 5 mV s^{-1} and a potential window of -0.7 V to 0.7 V, was used. Only the anode of the pMFC was submerged in a solution of 5 mM ferricyanide in 50 mM phosphate buffer and 100 mM NaCl solution.

7.3.6 Toxicant analysis

A toxic event was mimicked by exposing the MFCs to a solution of 1000 ppm formaldehyde, by adding 1 mL concentrated formaldehyde solution (10% in AW) into the 100 mL incubation vessel. The current decay after exposure is defined as the initial rate of change of the current with respect to time, dI/dt, taken by the initial slope of the current response curve within the first 10 min of toxicant exposure. The delay time is defined as the time between the introduction of a toxicant and the first response from the MFC and the response time is defined as the time taken to reach 95% of the new steady state current after a toxic event.

7.4 Results and discussion

7.4.1 Device fabrication

Single component, air breathing, paper-based MFCs (pMFCs) were fabricated by screen-printing, using fully biodegradable materials. Figure 7.1A shows a schematic of the device, while its actual size is shown in Figure 7.1B.

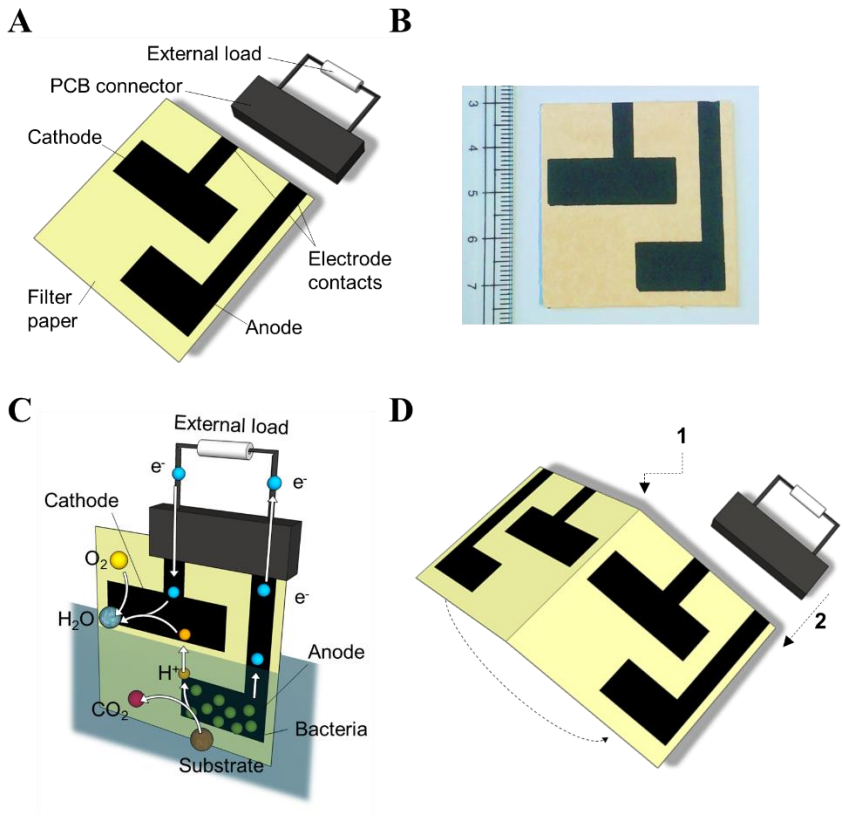

Figure 7.1. [**A**] Schematic of the pMFC and electrical connection; [**B**] Photograph of the actual pMFC, showing size; [**C**] Principle of operation of the pMFC; and [**D**] Assembly of the fpMFC by folding two pMFCs back-to-back (**1),** with parallel electrical connection (**2**).

Firstly, the device fabrication was optimized. In particular, to increase the paper tensile strength, improve its robustness and enhance the operational lifetime of the device, the cellulose fibres in the paper and the cellulose in the ink binder of the pMFC were cross-linked by reaction with glyoxal (a common cross-linking agent [26]). Various degrees of cross-linking were evaluated and the greatest improvement in the tensile strength of

the pMFC was achieved with 32 mg g_{paper}^{-1} of glyoxal, Figure S7.3, yielding a greater than threefold improvement *versus* non-treated paper, from 0.38 ± 0.33 MPa to 1.28 ± 0.09 MPa, Table S7.2. Increased levels of cross-linking had no further beneficial effects on the tensile strength of the paper. Thus, this degree of cross-linking was considered optimal to yield reproducibly cross-linked materials, and was used for all the subsequent tests.

The electrochemical performance, in terms of electron transfer capability, of the screen-printed device, before and after the cross-linking step, was investigated by cyclic voltammetry (CV) in a 5 mM ferricyanide solution used as a redox system, Figure S7.4. The non-cross-linked device exhibited a very low current with no evidence of oxidation or reduction peaks over the potential range -0.7 V to 0.7 V. On the other hand, the cross-linked device showed oxidation and reduction peaks at 0.34 V and -0.5 V respectively within the same potential range. As evidenced from the scanning electron microscopy (SEM) images of the electrodes, Figure 7.2, the cross-linking treatment affects the porous structure of the electrode. In particular, by cross-linking the cellulose binder, a more open structure in the dried ink is maintained, and shrinkage and collapse is reduced. It is hypothesized that this open structure facilitates diffusion through the electrodes, as well as between the two electrodes, since the paper porosity is similarly enhanced. Indeed, it has been previously demonstrated that the increase in pore size of an electrode separating layer leads to greater power generation in MFCs by lowering its internal resistance [30]. Moreover, glyoxal cross-linking may also introduce carbon containing crosslinks that may facilitate the electroactive reactions [53].

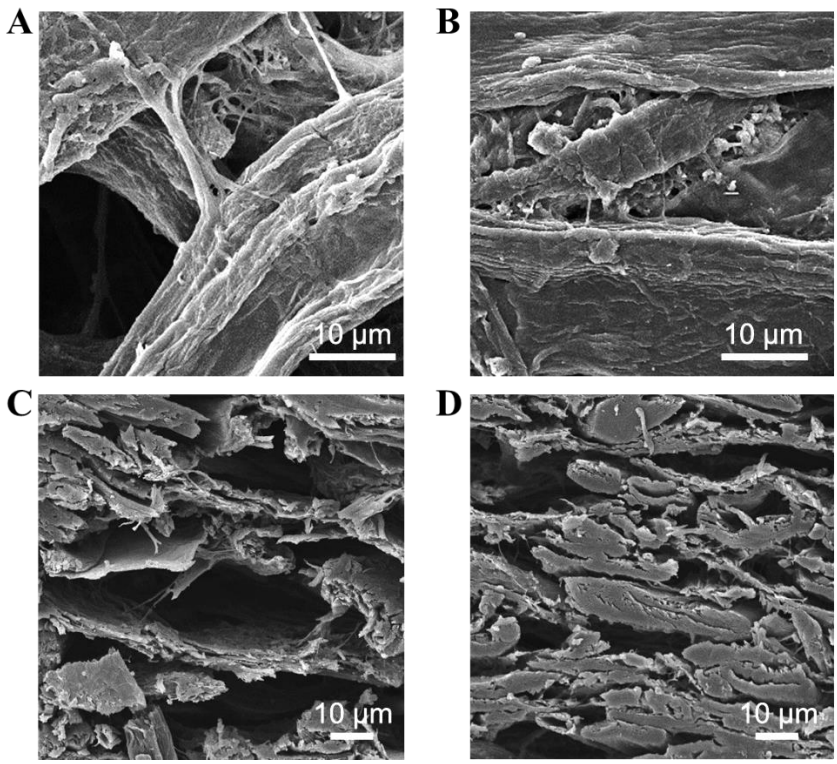

Figure 7.2. SEM images of: [**A**] paper surface after cross-linking, [**B**] non-cross-linked paper, [**C**] electrode cross section after cross-linking, [**D**] non-cross-linked electrode cross section.

7.4.2 Microbial fuel cell operation

The screen-printed device was subsequently tested as a microbial fuel cell. To this purpose, the electrodes were connected to a 1 kΩ resistor to polarize the cell, and the output voltage was continuously monitored. The electrode, acting as the anode, was submerged in a beaker containing artificial wastewater, with 10% *v/v* anaerobic sludge and 10 mM potassium acetate as a carbon source, Figure S7.2, while the cathode was exposed to air. Figure 7.1C shows the working principle of the pMFC. The organisms in the anodic biofilm catalyse the oxidation of acetate (the fuel) generating electrons (e^-) and protons (H^+). The electrons are transferred to the anode and move across the external circuit, while the solvated protons diffuse through the paper to the cathode. Here, the reaction is completed with the reduction of oxygen into water. No external membrane is required and the paper itself acts as a separator.

The current generated by the pMFC over time was monitored over a period of 8 days, Figure 7.3. After 4 days of operation, a steady state current density of 0.18 ± 0.04 µA cm^{-2} was achieved.

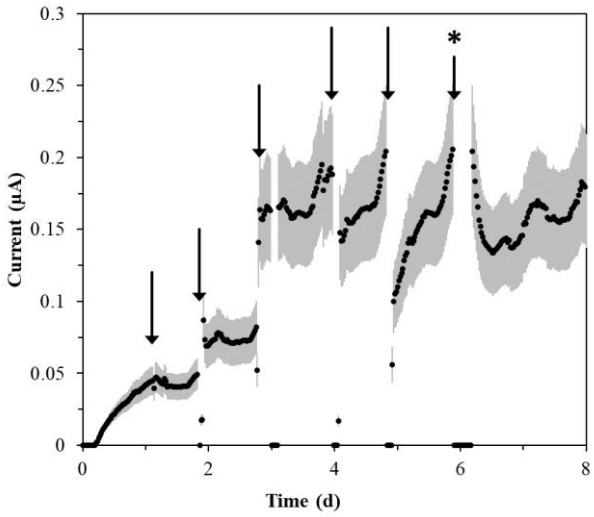

Figure 7.3. Enrichment of pMFC. Arrows indicate replacement of 10% of the feed with fresh AW containing 10 mM potassium acetate and no anaerobic sludge. At almost 6 days (indicated with a *) electrochemical analysis (linear sweep voltammetry and electrochemical impedance spectroscopy) was performed. The decrease in current noted after each addition of nutrient medium (indicated by arrows) was due to minor disruptions of the pMFC feed solution during medium replacement. Error bars (referring to experiments conducted in duplicate) are indicated by grey shaded region.

To investigate the effect of stacking the pMFCs, two pMFCs were folded back-to-back (device hereafter named fpMFC) and enriched as described above for the single pMFC. After 6 days of operation, the electrochemical performance of both the pMFC and the fpMFC was investigated by linear sweep voltammetry (LSV) and electrochemical impedance spectroscopy (EIS). Analysis of the power curves (Figure 7.4A), polarisation curves (Figure 7.4B) and impedance curves (Figure 7.4C) thus obtained, suggest significantly enhanced performance for the fpMFC *versus* the single cell pMFC, Table S7.3.

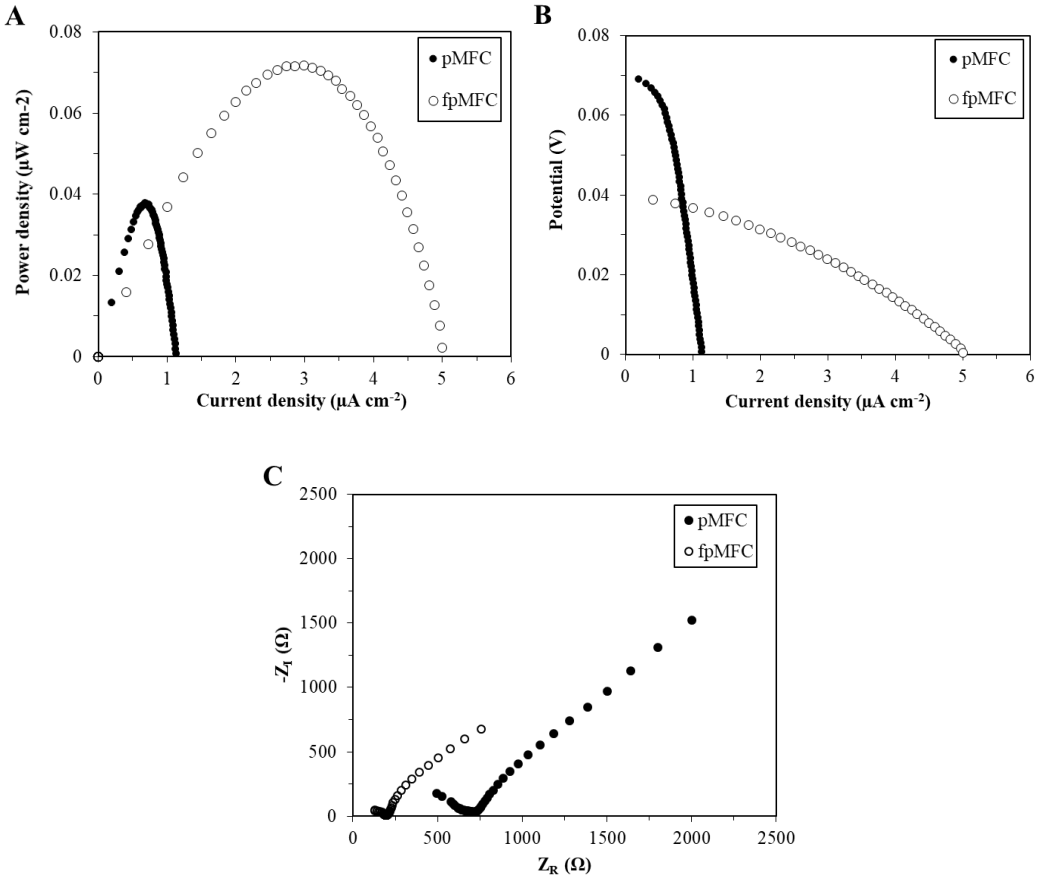

Figure 7.4. [**A**] Power and [**B**] polarisation curves for the pMFC and fpMFC. Power and current densities refer to the geometric anodic electrode area: 2 cm^2. [**C**] Comparison of electrochemical impedance spectroscopy curves for the pMFC and fpMFC.

The open circuit voltages (OCV) measured for pMFC and fpMFC were 68 ± 13 mV and 39 ± 8 mV respectively. These OCV values are much lower than for other MFC devices, which are typically in the range of 0.7 - 1.0 V [31]. These values are also an order of magnitude lower than other MFCs with paper-based electrodes (ranging from 302 – 550 mV), which variously use screen-printed carbon electrodes on paper operated in a two chamber configuration [19], have a combination of a carbon veil anode with a conductive ink cathode [14], or utilize a separator such as Nafion [15] or parchment paper [18]. Thus, it appears likely that the absence of a membrane in the pMFC is responsible for the lower OCVs obtained in this study, due to oxygen diffusion to the anode. This drawback is, however, counteracted by the advantage of screen-printing the whole device (or multiple devices) onto a single piece of paper using a single ink formulation (and thus single screen), which hugely simplifies its manufacture and reduces cost, facilitating mass production. The slightly lower OCV of the fpMFC when compared to the pMFC (a difference of 29 mV) may be due to

some loss in voltage *via* voltage reversal when electrically stacking MFC units, which has been widely reported [31–33]. Analysis of the polarisation curves, suggests that mass transfer limitations dominate over other losses in the cell (Figure 7.4B), in agreement with the performance of other paper-based MFCs reported [14,34].

To probe the effects of cross-linking more closely, images of the microbial biofilm developed on the electrode surface after enrichment (after 10 days of operation) were examined. The open structure generated by cross-linking provides greater surface area for the biofilm allowing the bacteria to colonize the pores of the electrode, Figure S7.5.

It was hypothesized that enhancing formation of a biofilm on the anode surface, would lead to improved power performance of the device. Chitosan, has been reported to allow immobilisation of whole cells onto surfaces [35] and has been employed to enhance biofilm attachment onto electrode surfaces [36–38]. To assess the efficacy of this strategy in these pMFCs, devices were prepared with anodes coated with a layer of chitosan (cpMFC) and bacterial colonisation after 24 h of incubation, compared with that of non-treated anodes. SEM images of the samples (Figure 7.5) show a visibly greater biofilm attachment for the case of the cpMFC. Moreover, crystal violet staining confirmed that the relative growth of the biofilm was over 5 times greater when using a chitosan layer on the anode (1.6% *versus* 8.7% relative growth, Figure S7.6). Control data, however, is also needed here. Despite the promise for increasing the biofilm attachment at the electrode, the electron transfer ability of the cpMFC device was poor, as confirmed by CV analysis, Figure S7.7. This behaviour was attributed to the presence of amine groups in chitosan that may hinder the diffusion of protons between the two electrodes, thus hindering the electrochemical performance of the device [36].

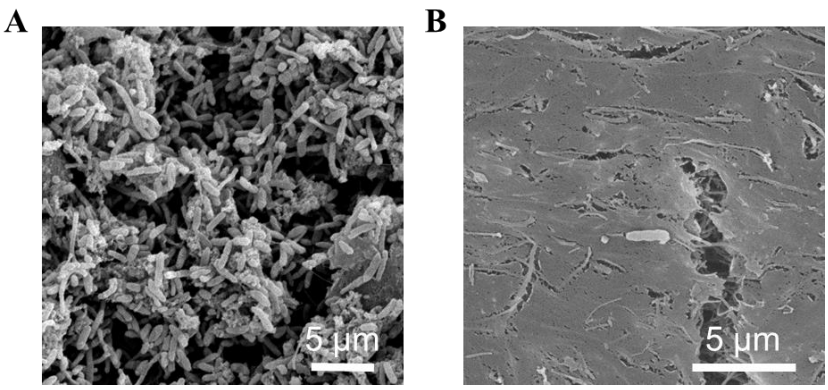

Figure 7.5. SEM images of the anode surface after 24 h inoculation in AW, containing 10% *v/v* anaerobic sludge for: [**A**] cpMFC; [**B**] pMFC. In both cases the anodes were connected to the cathode through a 1 kΩ external resistor and the cell voltage was monitored.

Stacking two devices together (fpMFC) led to a maximum power density of 0.07 ± 0.01 µW cm^{-2}, over 1.7 times the value obtained with a single cell. Moreover, the current density generated at the maximum power output of the fpMFC was 3.0 ± 0.6 µA cm^{-2}, over 4 times greater than that of the pMFC. The enhanced performance of the fpMFC might be a consequence of the lower internal resistance: 2.2 ± 0.4 kΩ for the fpMFC *versus* 5.7 ± 0.8 kΩ for pMFC, Figure 7.4C. It has been previously shown that, when electrically connecting MFC units in parallel, the internal resistance of the overall system decreases, since the system tends towards the lowest common denominator [39]. High internal resistances are usually observed in small scale MFCs [40,41]. Nonetheless, the internal resistances of both pMFC and fpMFC are almost one order of magnitude lower than similar air cathode paper-based MFC devices [18,42], which may be due to the lack of a membrane in the design.

7.4.3 Biosensing capability: detection of formaldehyde

The response of both the pMFC and fpMFC to the presence of 1000 ppm formaldehyde added to AW as a shock dose was subsequently investigated, Figure 7.6. In both cases, exposure to the toxic compound caused a marked drop in the current output. In particular, the rates of current decay within the first 10 min of exposure had absolute values of 0.011 µA min^{-1} and 0.021 µA min^{-1} for the pMFC and fpMFC, Table S7.4. The greater response of the fpMFC reflects its enhanced sensitivity [11]. After 4 h of

exposure, the steady state currents were -0.03 µA and -0.15 µA, representing an absolute total current drop of 0.3 µA and 0.6 µA for pMFC and fpMFC respectively. The current outputs reached negative values after 175 min and 115 min (for pMFC and fpMFC respectively) of exposure, thus indicating that the biofilm was severely affected by continuous exposure to the toxicant, in agreement with other studies [24,25,43]. The nature of the response of these devices to formaldehyde suggests that the pMFC and fpMFC would suit shock sensor applications for water quality monitoring [44]. The total response times (defined as the time taken to reach 95% of the steady state current after the toxic event) were 165 min (pMFC) and 200 min (fpMFC), which is much faster than other MFC biosensors subjected to the same shock (0.1% formaldehyde): > 200 min for a 140 µL single chambered MFC [24] and > 9.7 h for a 120 mL single chambered MFC, Table S7.5 [25].

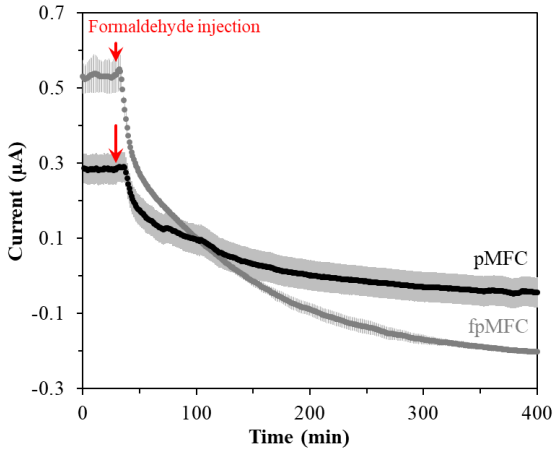

Figure 7.6. Amperometric response of the pMFC and fpMFC to an injection of 1000 ppm formaldehyde. The grey shaded region refers to the error between duplicate measurements.

Thus, our work shows that, not only is the output current enhanced by simply folding two pMFCs back-to-back, but that the sensing performance of the overall system also improves. This result suggests a simple route to further optimize the biosensor, which does not compromise the simplicity of the device or complicate its manufacture.

The pMFC demonstrated appreciable reproducibility particularly in terms of electroactive response to the presence of formaldehyde. Nonetheless, the output current is lower than other MFCs reported in the literature. A way to increase the current signal could be by improving the oxygen reduction reactions (ORR) at the

cathode. This is often done with platinum [45], however, recently more sustainable and cost-effective biomass derived ORR catalysts have been suggested [46]. Finally biofilm development could be enhanced by poising the potential of the anode to encourage electroactive biofilm development during enrichment, or through use of other material treatments to enhance the biofilm attachment at the anode (e.g. addition of polypyrole or polyaniline) [47].

7.5 Conclusions

In this work we report the first single component paper-based MFC with an extremely simple design and demonstrate the proof of concept of its use as a biosensor for toxicants in water.

Taking biodegradability, resource efficiency and cost as key design parameters, a screen-printed MFC was designed, which was built wholly of carbon based materials, with no metals in the disposable part of the device (the MFC itself). The natural biopolymer, cellulose, constitutes the bulk of the material: the paper upon which the device is constructed. Cellulose is also the ideal binder for the metal free conductive ink that constitutes the electrodes and allows proton transport by diffusion, thus obviating the need for a synthetic polymer membrane. The single component nature of the device ensures that a single chemical cross-linking step, using an agent that adds only the elements C, H and O, may be used to enhance the robustness of the MFC and maintain the porous nature of both paper and electrodes. Post use, should the MFC be discarded, it will biodegrade, leaving no trace, including no metal residues. The ease of power output scale-up of the device was demonstrated by folding two paper MFCs back-to-back and electrically connecting them in parallel, thus paving the way for stacking opportunities to enhance performance.

Finally, the potential of the devices as rapid onsite shock sensors for water quality assessment, particularly for detection of bioactive compounds in water, was demonstrated. Indeed, effective water quality monitoring is currently limited by either expensive, time consuming and offsite analytical methods that need to be performed in the laboratory, or by field test kits that have a limited reliability and high cost [5]. The implementation of our paper-based MFC biosensor for water quality monitoring can provide a solution to detecting toxic compounds in water that is easy to operate by

submersion into the sample to be analysed, simple to manufacture and is extremely cheap. Taking into account the materials specified in the experimental section, the estimated cost of the pMFC device is £0.43. This value could be significantly reduced by upscaled manufacturing and all processes, including printing, phase inversion (solvent bath), and cross-linking are amenable to roll to roll manufacture. Moreover, with careful design, there is scope for the MFC to be easily deployable in remote locations with data acquisition, analysis and even potentiostatic control possible using a mobile device (e.g. mobile phone) [48,49].

In real scenarios, the performance of the pMFC might be susceptible to environmental conditions, such as temperature, pH and conductivity [50], which should be simultaneously monitored and integrated in the sensor response. This principle has been recently demonstrated in the field of MFC based toxicant biosensors by calibrating the MFC output signal to a reference MFC in simultaneous operation [51]. Practical applications would also require pre-enrichment of the anodes of the pMFCs with electroactive bacteria. Indeed such a technique has previously been demonstrated to provide a functional working voltage with paper-based MFCs within just 35 min [14].

The distributed water quality monitoring that this device could enable would be of particular value in developing countries, where water and resources are extremely limited, and the need for water monitoring devices, that are cheap, simple to manufacture, and easy to dispose of, is clear. As such, our single-use device, which offers portability, facile use, and biodegradability, has the potential to improve the way water quality is monitored. It can provide those in remote and poor areas a way to quickly, simply and cost-effectively analyse water supplies that are critical to their health, livelihood security and wellbeing.

7.6 Associated content

Author Contributions

MDL, JLS and JC conceived the experiment. Design, implementation and analysis of the experiments were performed by: ACI for the device fabrication and manufacture;

JC for the microbial fuel cell analysis and SR for the cyclic voltammetry. Manuscript prepared by JC, MDL and JLS. Supervision from MDL and JLS.

Conflicts of Interest

The authors declare no conflict of interest.

Acknowledgements

The authors would like to thank: Zuhayr Rymansaib and Pejman Iravani from the Department of Mechanical Engineering, University of Bath, for assistance and help on the design of the pMFC; Carlos César Bof Bufon, from the Brazilian Nanotechnology National Laboratory (LNNano) in Campinas for fruitful discussions; Wessex Water for providing anaerobic sludge; Elizabeth Bevon from the EPSRC Centre for Doctoral Training in Sustainable Chemical Technologies, University of Bath, for assistance with CV experiments. We thank Sally Gaden, Bath City College, for advice on screen-printing. Funding from the Engineering and Physical Sciences Research Council (EPSRC) and the EPSRC Centre for Doctoral Training in Sustainable Chemical Technologies (EP/P510907/1; EP/G03768X/1; EPSRC EP/L016354/1) is acknowledged.

Abbreviations

AW: Artificial wastewater,

cpMFC: Chitosan coated paper microbial fuel cell,

CV: Cyclic voltammetry,

DMSO: Dimethyl sulfoxide

EIS: Electrochemical impedance spectroscopy,

EMIMAc: 1-Ethyl-3-methylimidazolium,

fpMFC: Folded paper microbial fuel cell,

HPLC: High performance liquid chromatography,

LSV: Linear sweep voltammetry,

MFC: Microbial fuel cell,

OCV: Open circuit voltage,

ORR: Oxygen reduction reaction,

PBS: Phosphate buffer solution,

PCB: Printed circuit board,

PDMS: Polydimethylsiloxane,

pMFC: Paper microbial fuel cell,

SEM: Scanning electron microscope.

Nomenclature

Roman symbols

a: *G*radient of glycolic acid/peak area calibration curve,

b: Intercept of glycolic acid/peak area calibration curve,

DF: Dilution factor,

I: Current

M_R: Molecular weight,

P: Power,

PA: Peak area,

R: Resistance,

R_{ext}: External load

t: Time,

V: Voltage,

WOF_{ini}: Initial weight of paper sample.

Table S7.1. Summary of paper-based microbial fuel cells described in the scientific literature (*power and current reported as absolute or density values as per reference)

Config.	Biocatalyst	Use of paper	Electrode materials	Membrane material	Analyte	Catholyte	Max. power*	Max. current*	Reported operation time	Ref.
Two chamber	Wild type *Shewanella oneidensis*	Whatman #1 filter paper reservoirs and membrane base	Anode: carbon cloth Cathode: carbon cloth	Sodium polystyrene sulfonate impregnated	L-broth medium	50 mM FeCN in 100 mM phosphate buffer solution	5.5 $\mu W\ cm^{-2}$	74 µA	40 min	[21]
Two chamber	*Shewanella oneidensis*-MR1	Wax printed chromate-graphy paper reservoirs	Anode: carbon cloth Cathode: carbon cloth	Nafion	3% tryptic soy broth	FeCN	25 $W\ m^{-3}$	52.25 µA	5 d	[15]
Two chamber stack	*Shewanella oneidensis*-MR1	Whatman #1 filter paper reservoirs and electrode support	Anode: screen-printed carbon on paper Cathode: screen-printed carbon on paper	Parchment paper	L-broth medium	50 mM FeCN in 100 mM phosphate buffer solution	1.27 $\mu W\ cm^{-2}$	5 µA	20 min	[19]
Single chamber	Urine from pre-enriched MFCs and wastewater	Photocopier paper structure and cathode support	Anode: carbon veil Cathode: conductive synthetic latex on paper	Photocopier paper	Human urine	Air	50 µW	N/A	61 d	[14]
Two chamber stack	*Shewanella oneidensis*-MR1	Whatman #1 filter paper chambers reservoirs	Anode: carbon cloth Cathode: carbon cloth	Nafion 117	L-broth medium	50 mM FeCN in 100 mM phosphate buffer solution	28 $\mu W\ cm^{-2}$	211 $\mu A\ cm^{-2}$	~ 200 min	[20]
Two chamber	*Shewanella oneidensis*-MR1	Whatman #1 filter paper reservoirs	Anode: carbon cloth Cathode: carbon cloth	Parchment paper	L-broth medium	50 mM FeCN in 100 mM phosphate buffer solution	10 $\mu W\ cm^{-2}$	50 $\mu A\ cm^{-2}$	18 h	[22]

Table S7.1. (continued) Summary of paper-based microbial fuel cells described in the scientific literature

(*power and current reported as absolute or density values as per reference)

Config.	Biocatalyst	Use of paper	Electrode materials	Membrane material	Analyte	Catholyte	Max. power*	Max. current*	Reported operation time	Ref.
Two chamber stack	*Pseudomonas aeruginosa*	Whatman #1 filter paper reservoirs and electrode support	Anode: Ag/Cr/Cu on paper Cathode: carbon cloth	Parchment paper	L-broth medium	50 mM FeCN in 100 mM phosphate buffer solution	~90 µW cm^{-2}	200-250 µA	20 min	[23]
Single chamber stack	*Shewanella oneidensis*-MR1	Whatman #1 filter paper reservoirs and electrode support	Anode: screen-printed carbon on paper Cathode: activated carbon on nickel on paper	Whatman #410 filter paper	L-broth medium	Air	9.3×10^{-4} µW cm^{-2}	~ 0.2 µA	60 min	[42]
Single chamber stack	*Shewanella oneidensis*-MR1 and wastewater consortium	Whatman #1 filter paper reservoirs and electrode support	Anode: carbon cloth Cathode: activated carbon on nickel on paper	Whatman #410 filter paper	L-broth medium	Air	13.6 µW	50 µA	20 min	[34]
Single chamber	*Shewanella oneidensis*-MR1	Whatman cellulose chromatography paper reservoirs and electrode support	Anode: 8B graphite pencil on paper Cathode: 8B graphite pencil on paper	Parchment paper	Tryptic soy broth	Air	0.568 µW cm^{-2}	7.5 µA	100 min	[18]
Single chamber	Wastewater consortium	Filter paper electrode support	Anode: carbon ink on paper Cathode: 0.5 mg cm^{-2} Pt on carbon cloth	None	Wastewater	Air	0.32 mW	0.12 mA cm^{-2}	1 month	[52]

Table S7.2. Degree of cross-linking of paper by use of glyoxal and corresponding tensile strength of the paper samples.

Glyoxal offered (% *w/v*)	Glyoxal reacted (mg g_{paper}^{-1})	Tensile strength (MPa)
0	0.00	0.38 ± 0.33
3	16.4 ± 0.3	1.41 ± 0.28
6	32.2 ± 0.3	1.28 ± 0.09
12	50.0 ± 2.2	0.97 ± 0.27
24	94.8 ± 3.5	0.95 ± 0.23

Table S7.3. Summary of performance of the pMFC and fpMFC. Power and current densities refer to an anodic electrode area of 2 cm^2.

Configuration	OCV (mV)	Power output (nW)	Power density (µW cm^{-2})	Internal resistance (kΩ)	Current density (µA cm^{-2})
pMFC	69 ± 13	75 ± 14	0.04 ± 0.01	5.7 ± 0.8	0.7 ± 0.1
fpMFC	39 ± 8	143 ± 26	0.07 ± 0.01	2.6 ± 0.4	3.0 ± 0.6

Table S7.4. Summary of the sensing capability of the pMFC and fpMFC towards a 1000 ppm injection of formaldehyde.

Configuration	Delay time (min)	Response time (min)	Initial response rate (µA min^{-1})	Baseline current (µA)	Total current change (µA)
pMFC	8 ± 1	165 ± 8	-0.011 ± 0.003	0.28 ± 0.04	0.31 ± 0.04
fpMFC	5 ± 1	200 ± 11	-0.021 ± 0.002	0.53 ± 0.04	0.68 ± 0.04

Table S7.5. Summary of other MFC based biosensors for formaldehyde detection

Microbe assayed	Configuration	Anode chamber volume	Formaldehyde concentration monitored (ppm)	Response time	Reference
Consortium (anaerobic sludge)	Single chamber paper-based MFC	100 mL	1000	200 min (fpMFC) 165 min (pMFC)	This study
Shewanella oneidensis MR-1	Single chamber 3 electrode system	140 µL	10 – 1000	> 200 min	[24]
Geobacter sulfurreducens	Two chamber	144 µL	1000	~ 3 min	[43]
Shewanella oneidensis MR-1	Single chamber 3 electrode system	120 mL	100 - 1000	> 9.7 h	[25]
Wild-type *Pseudomonas aeruginosa PAO1*	Single chamber, dual-channel system	90 µL	30 - 3500	< 125 min	[51]

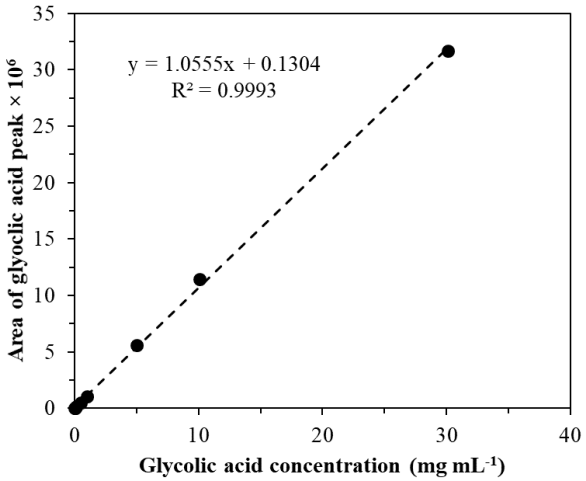

Figure S7.1. Calibration curve for HPLC peak area against glycolic acid concentration

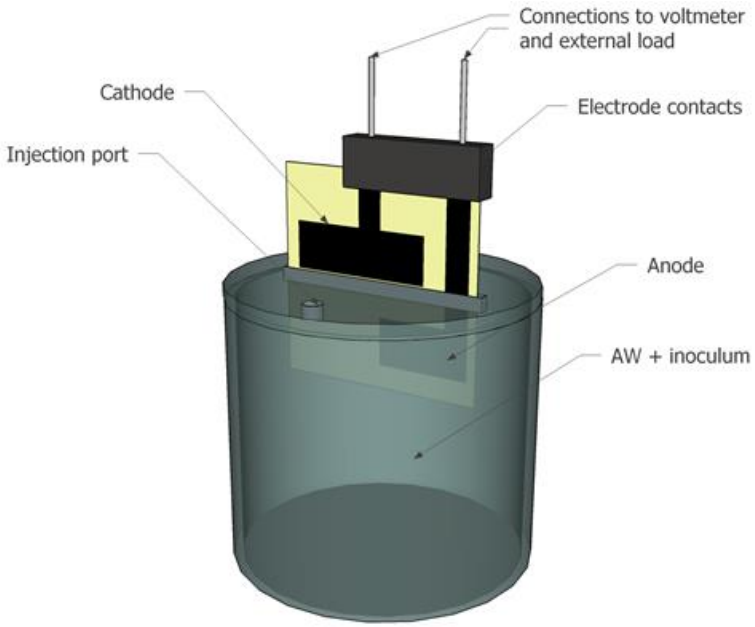

Figure S7.2. Schematic of the operation mode of the pMFC and fpMFC

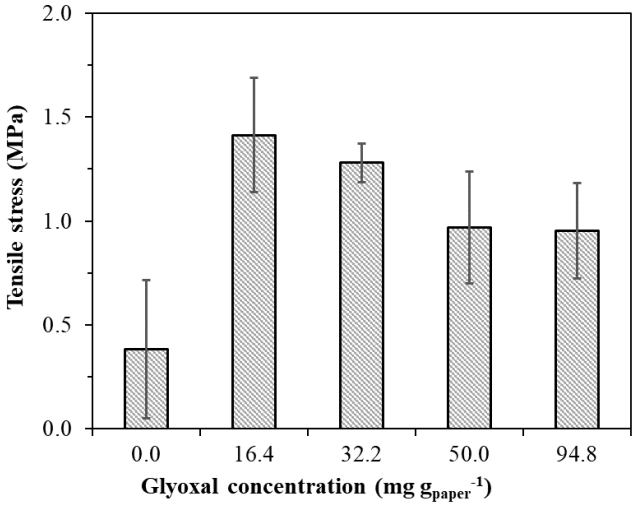

Figure S7.3. Effect of the degree of cross-linking on the tensile strength of the wetted paper. The concentrations of glyoxal in the final treated paper were achieved by exposure of paper to 0, 3, 6, 12, and 24 *w/v*% aqueous solutions of glyoxal.

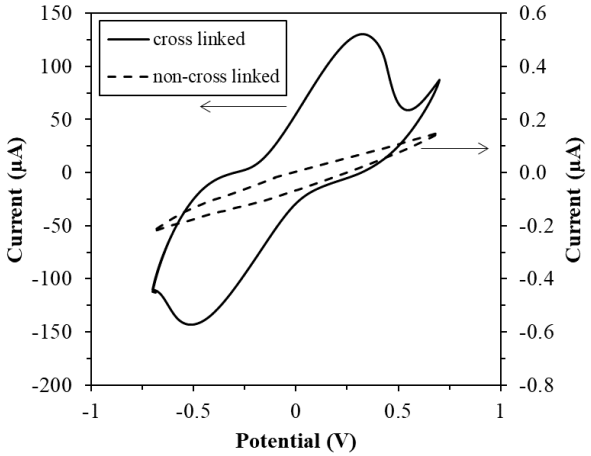

Figure S7.4. Cyclic voltammetry tests of the pMFC before and after cross-linking, performed with the anode immersed in 5 mM ferricyanide solution and the cathode exposed to air. The anode was operated as the working electrode and the cathode as the counter electrode. Five cycles were performed at a scan rate of 5 mV s^{-1}.

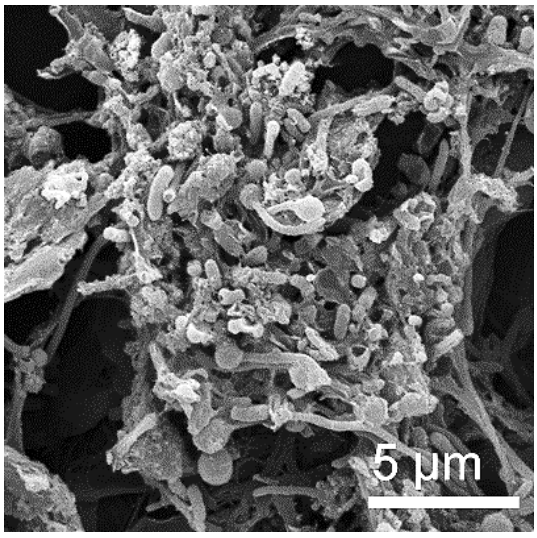

Figure S7.5. SEM image of the biofilm on the anode of the pMFC after 10 days of operation.

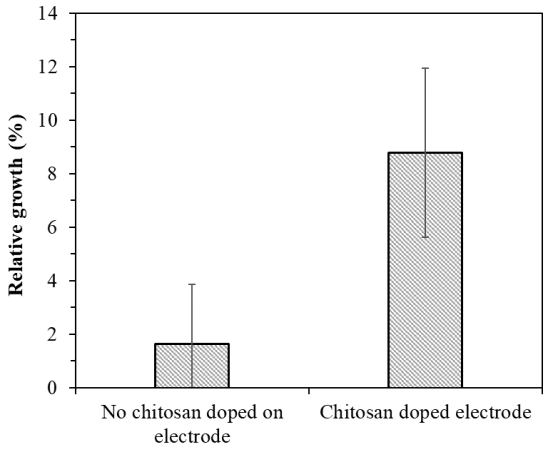

Figure S7.6. Relative growth of the biofilm on the anode of a pMFC when doped with and without chitosan.

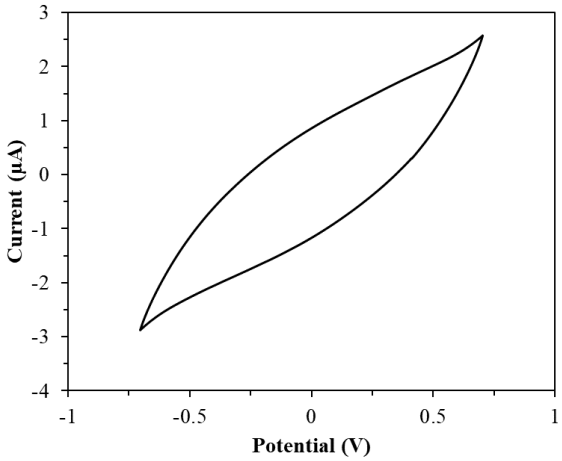

Figure S7.7. Cyclic voltammetry tests of the cpMFC after cross linking, performed with the anode immersed in 5 mM ferricyanide solution and the cathode exposed to air. The anode was operated as the working electrode and the cathode as the counter electrode. Scan rate: 5 mV s^{-1}.

7.8 References

[1] WWAP (United Nations World Water Assessment Programme), The United Nations World Water Development Report 2015: Water for a Sustainable World, Paris, 2015. doi:978-92-3-100071-3.

[2] E.D. Ongley, Water Quality Programs In Developing Countries, Water Int. 26 (2001) 14–23. doi:10.1080/02508060108686883.

[3] K. Sarpong Adu-manu, C. Tapparello, W. Heinzelman, F. Apietu Katsriku, J. Abdulai, Water Quality Monitoring Using Wireless Sensor Networks: Current Trends and Future Research Directions, ACM Trans. Sens. Networks. 13 (2017) 1–41. doi:10.1145/3005719.

[4] M. Palaniappan, P.H. Gleick, L. Allen, M.J. Cohen, J. Christian-Smith, C. Smith, Clearing the Waters: A focus on water quality solutions, Oakland, CA, USA, 2010. http://www.unep.org/PDF/Clearing_the_Waters.pdf (accessed January 20, 2015).

[5] J. Chouler, M. Di Lorenzo, Water Quality Monitoring in Developing Countries; Can Microbial Fuel Cells be the Answer?, Biosensors. 5 (2015) 450–470. doi:10.3390/bios5030450.

[6] M.C. Potter, Electrical Effects Accompanying the Decomposition of Organic Compounds, Proc. R. Soc. B Biol. Sci. 84 (1911) 260–276. doi:10.1098/rspb.1911.0073.

[7] R.M. Allen, H.P. Bennetto, Microbial fuel-cells, Appl. Biochem. Biotechnol. 39 (1993) 27–40. doi:10.1007/BF02918975.

[8] M. Di Lorenzo, A.R. Thomson, K. Schneider, P.J. Cameron, I. Ieropoulos, A small-scale air-cathode microbial fuel cell for on-line monitoring of water quality., Biosens. Bioelectron. 62 (2014) 182–188. doi:10.1016/j.bios.2014.06.050.

[9] N.E. Stein, H.V.M. Hamelers, C.N.J. Buisman, Stabilizing the baseline current of a microbial fuel cell-based biosensor through overpotential control under non-toxic conditions., Bioelectrochemistry. 78 (2010) 87–91. doi:10.1016/j.bioelechem.2009.09.009.

[10] M. Di Lorenzo, T.P. Curtis, I.M. Head, K. Scott, A single-chamber microbial fuel cell as a biosensor for wastewaters., Water Res. 43 (2009) 3145–3154. doi:10.1016/j.watres.2009.01.005.

[11] Y. Jiang, P. Liang, C. Zhang, Y. Bian, X. Yang, X. Huang, P.R. Girguis, Enhancing the response of microbial fuel cell based toxicity sensors to Cu(II) with the applying of flow-through electrodes and controlled anode potentials., Bioresour. Technol. 190 (2015) 367–372. doi:10.1016/j.biortech.2015.04.127.

[12] E. Vaiopoulou, P. Melidis, E. Kampragou, A. Aivasidis, On-line load monitoring of wastewaters with a respirographic microbial sensor, Biosens. Bioelectron. 21 (2005) 365–371. doi:10.1016/j.bios.2004.10.022.

[13] A. Mulchandani, I. Kaneva, W. Chen, Biosensor for Direct Determination of Organophosphate Nerve Agents Using Recombinant Escherichia coli with Surface-Expressed Organophosphorus Hydrolase. 2. Fiber-Optic Microbial Biosensor, Anal. Chem. 70 (1998) 5042–5046. doi:10.1021/AC980643L.

[14] J. Winfield, L.D. Chambers, J. Rossiter, J. Greenman, I. Ieropoulos, Urine-activated origami microbial fuel cells to signal proof of life, J. Mater. Chem. A. 3 (2015) 7058–7065. doi:10.1039/C5TA00687B.

[15] N. Hashemi, J.M. Lackore, F. Sharifi, P.J. Goodrich, M.L. Winchell, N. Hashemi, A paper-based microbial fuel cell operating under continuous flow condition, Technology. 4 (2016) 98–103. doi:10.1142/S2339547816400124.

[16] W. Zhao, A. van den Berg, Lab on paper, Lab Chip. 8 (2008) 1988–1991. doi:10.1039/b814043j.

[17] A.K. Yetisen, M.S. Akram, C.R. Lowe, Paper-based microfluidic point-of-care diagnostic devices, Lab Chip. 13 (2013) 2210–2251. doi:10.1039/c3lc50169h.

[18] S.H. Lee, J.Y. Ban, C.-H. Oh, H.-K. Park, S. Choi, A solvent-free microbial-activated air cathode battery paper platform made with pencil-traced graphite electrodes, Sci. Rep. 6 (2016) 28588-28596. doi:10.1038/srep28588.

[19] A. Fraiwan, S. Choi, A stackable, two-chambered, paper-based microbial fuel cell, Biosens. Bioelectron. 83 (2016) 27–32. doi:10.1016/j.bios.2016.04.025.

[20] A. Fraiwan, H. Lee, S. Choi, A Multianode Paper-Based Microbial Fuel Cell: A Potential Power Source for Disposable Biosensors, IEEE Sens. J. 14 (2014) 3385–3390. doi:10.1109/JSEN.2014.2332075.

[21] A. Fraiwan, S. Mukherjee, S. Sundermier, H.-S. Lee, S. Choi, A paper-based microbial fuel cell: instant battery for disposable diagnostic devices., Biosens. Bioelectron. 49 (2013) 410–414. doi:10.1016/j.bios.2013.06.001.

[22] A. Fraiwan, S. Choi, Bacteria-powered battery on paper, Phys. Chem. Chem. Phys. 16 (2014) 26288–26293. doi:10.1039/C4CP04804K.

[23] G. Choi, D.J. Hassett, S. Choi, A paper-based microbial fuel cell array for rapid and high-throughput screening of electricity-producing bacteria, Analyst. 140 (2015) 4277–4283. doi:10.1039/C5AN00492F.

[24] W. Yang, X. Wei, A. Fraiwan, C.G. Coogan, H. Lee, S. Choi, Fast and sensitive water quality assessment: A μL-scale microbial fuel cell-based biosensor integrated with an air-bubble trap and electrochemical sensing functionality, Sensors Actuators B Chem. 226 (2016) 191–195. doi:10.1016/j.snb.2015.12.002.

[25] X. Wang, N. Gao, Q. Zhou, Concentration responses of toxicity sensor with Shewanella oneidensis MR-1 growing in bioelectrochemical systems., Biosens. Bioelectron. 43 (2013) 264–267. doi:10.1016/j.bios.2012.12.029.

[26] G.G. Xu, C.Q. Yang, Y. Deng, Applications of bifunctional aldehydes to improve paper wet strength, J. Appl. Polym. Sci. 83 (2002) 2539–2547. doi:10.1002/app.10195.

[27] C. Schramm, B. Rinderer, Determination of cotton-bound glyoxal via an internal Cannizzaro reaction by means of high-performance liquid chromatography, Anal. Chem. 72 (2000) 5829–5833. doi:10.1021/ac000704r.

[28] J. Chouler, I. Bentley, F. Vaz, A. O'Fee, P.J. Cameron, M. Di Lorenzo, Exploring the use of cost-effective membrane materials for Microbial Fuel Cell based sensors, Electrochim. Acta. 231 (2017) 319–326. doi:10.1016/j.electacta.2017.01.195.

[29] J. Merritt, D.E. Kadouri, G.A. O'Toole, Growing and Analyzing Static Biofilms, Curr. Protoc. Microbiol. 00:B-1B:1B (2005) 1–29. doi:10.1002/9780471729259.mc01b01s00.

[30] X. Zhang, S. Cheng, X. Huang, B.E. Logan, The use of nylon and glass fiber filter separators with different pore sizes in air-cathode single-chamber microbial fuel cells, Energy Environ. Sci. 3 (2010) 659–664. doi:10.1039/b927151a.

[31] I. Ieropoulos, J. Greenman, C. Melhuish, Improved energy output levels from small-scale Microbial Fuel Cells., Bioelectrochemistry. 78 (2010) 44–50. doi:10.1016/j.bioelechem.2009.05.009.

[32] S.-E. Oh, B.E. Logan, Voltage reversal during microbial fuel cell stack operation, J. Power Sources. 167 (2007) 11–17. doi:10.1016/j.jpowsour.2007.02.016.

[33] P. Ledezma, J. Greenman, I. Ieropoulos, MFC-cascade stacks maximise COD reduction and avoid voltage reversal under adverse conditions., Bioresour. Technol. 134 (2013) 158–165. doi:10.1016/j.biortech.2013.01.119.

[34] A. Fraiwan, L. Kwan, S. Choi, A disposable power source in resource-limited environments: A paper-based biobattery generating electricity from wastewater, Biosens. Bioelectron. 85 (2016) 190–197. doi:10.1016/j.bios.2016.05.022.

[35] M. Rinaudo, Chitin and chitosan: Properties and applications, Prog. Polym. Sci. 31 (2006) 603–632. doi:10.1016/j.progpolymsci.2006.06.001.

[36] E. Antolini, Composite materials for polymer electrolyte membrane microbial fuel cells, Biosens. Bioelectron. 69 (2015) 54–70. doi:10.1016/j.bios.2015.02.013.

[37] S.R. Higgins, D. Foerster, A. Cheung, C. Lau, O. Bretschger, S.D. Minteer, K. Nealson, P. Atanassov, M.J. Cooney, Fabrication of macroporous chitosan scaffolds doped with carbon nanotubes and their characterization in microbial fuel cell operation, Enzyme Microb. Technol. 48 (2011) 458–465. doi:10.1016/j.enzmictec.2011.02.006.

[38] C. Lau, M.J. Cooney, P. Atanassov, Conductive macroporous composite chitosan-carbon nanotube scaffolds, Langmuir. 24 (2008) 7004–7010. doi:10.1021/la8005597.

[39] G. Papaharalabos, J. Greenman, C. Melhuish, I. Ieropoulos, A novel small scale Microbial Fuel Cell design for increased electricity generation and waste water treatment, Int. J. Hydrogen Energy. 40 (2015) 4263–4268. doi:10.1016/j.ijhydene.2015.01.117.

[40] S. Choi, H.-S. Lee, Y. Yang, P. Parameswaran, C.I. Torres, B.E. Rittmann, J. Chae, A μL-scale micromachined microbial fuel cell having high power density., Lab Chip. 11 (2011) 1110–1117. doi:10.1039/c0lc00494d.

[41] F. Qian, M. Baum, Q. Gu, D.E. Morse, A 1.5 μL microbial fuel cell for on-chip bioelectricity generation., Lab Chip. 9 (2009) 3076–3081. doi:10.1039/b910586g.

[42] H. Lee, S. Choi, An origami paper-based bacteria-powered battery, Nano Energy. 15 (2015) 549–557. doi:10.1016/j.nanoen.2015.05.019.

[43] D. Dávila, J.P. Esquivel, N. Sabaté, J. Mas, Silicon-based microfabricated microbial fuel cell toxicity sensor., Biosens. Bioelectron. 26 (2011) 2426–2430. doi:10.1016/j.bios.2010.10.025.

[44] B. Liu, Y. Lei, B. Li, A batch-mode cube microbial fuel cell based “shock” biosensor for wastewater quality monitoring., Biosens. Bioelectron. 62 (2014) 308–314. doi:10.1016/j.bios.2014.06.051.

[45] E. Martin, B. Tartakovsky, O. Savadogo, Cathode materials evaluation in microbial fuel cells: A comparison of carbon, Mn2O3, Fe2O3 and platinum materials, Electrochim. Acta. 58 (2011) 58–66. doi:10.1016/j.electacta.2011.08.078.

[46] J. Chouler, G.A. Padgett, P.J. Cameron, K. Preuss, M.-M. Titirici, I. Ieropoulos, M. Di Lorenzo, Towards effective small scale microbial fuel cells for energy generation from urine, Electrochim. Acta. 192 (2016) 89–98. doi:10.1016/j.electacta.2016.01.112.

[47] Y. Zou, J. Pisciotta, R.B. Billmyre, I. V. Baskakov, Photosynthetic microbial fuel cells with positive light response, Biotechnol. Bioeng. 104 (2009) 939–946. doi:10.1002/bit.22466.

[48] F.-T. Lin, Y.-C. Kuo, J.-C. Hsieh, H.-Y. Tsai, Y.-T. Liao, H.-C. Lee, A Self-Powering Wireless Environment Monitoring System Using Soil Energy, IEEE Sens. J. 15 (2015) 3751–3758. doi:10.1109/JSEN.2015.2398845.

[49] J.L. Delaney, E.H. Doeven, A.J. Harsant, C.F. Hogan, Use of a mobile phone for potentiostatic control with low cost paper-based microfluidic sensors, Anal. Chim. Acta2. 803 (2013) 123–127. doi:10.1016/j.aca.2013.06.005.

[50] L. Peixoto, B. Min, G. Martins, A.G. Brito, P. Kroff, P. Parpot, I. Angelidaki, R. Nogueira, In situ microbial fuel cell-based biosensor for organic carbon, Bioelectrochemistry. 81 (2011) 99–103. doi:10.1016/j.bioelechem.2011.02.002.

[51] W. Yang, X. Wei, S. Choi, A Dual-Channel, Interference-Free, Bacteria-Based Biosensor for Highly Sensitive Water Quality Monitoring, IEEE Sens. J. 16 (2016) 8672–8677. doi:10.1109/JSEN.2016.2570423.

[52] Z. Xu, Y. Liu, I. Williams, Y. Li, F. Qian, H. Zhang, D. Cai, L. Wang, B. Li, Disposable self-support paper-based multi-anode microbial fuel cell (PMMFC) integrated with power management system (PMS) as the real time “shock” biosensor for wastewater, Biosens. Bioelectron. 85 (2016) 232–239. doi:10.1016/j.bios.2016.05.018

[53] Q. Yang, F. Dou, B. Liang, Q. Shen, Studies of cross-linking reaction on chitosan fiber with glyoxal. Carbohydrate Polymers, 59(2) (2005) 205-210. Doi:10.1016/j.carbpol.2004.09.013

8 A miniature photosynthetic microbial fuel cell biosensor for the detection of bioactive compounds in water

This chapter reports the development of a light dependent photosynthetic MFC biosensor. Its power generation properties are investigated, and its biosensing ability is analysed by assessing its amperometric response to a model toxicant, formaldehyde. This work has been prepared as a publication and submission is pending, with details on the following page. Amendments have been made to account for stylistic consistency in this thesis.

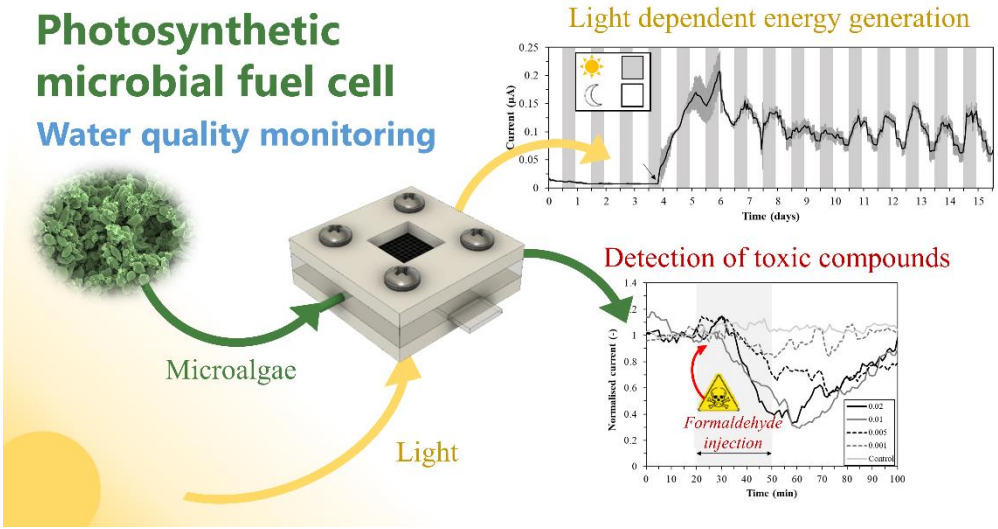

Statement of authorship

This declaration concerns the article entitled:	A miniature photosynthetic microbial fuel cell biosensor for the detection of bioactive compounds in water
Publication status:	Draft publication, pending submission.
Publication details:	N/A
Authorship contributions:	MDL, PJC and JC conceived the experiment. Design, implementation and analysis of experiments performed by JC, MM, WM. Manuscript prepared by JC and MDL. Project supervised by MDL and PJC.
Statement from candidate:	This paper reports on original research I conducted during the period of my Higher Degree by Research candidature.

Signed: Date:

Published as Chouler, J, Monti, M, Morgan, W, Cameron, P & Di Lorenzo, M 2019, 'A photosynthetic toxicity biosensor for water', Electrochimica Acta. https://doi.org/10.1016/j.electacta.2019.04.061

A miniature photosynthetic microbial fuel cell biosensor for the detection of bioactive compounds in water

Jon Chouler [a,b], Matthew Monti [a], William Morgan [a], Petra J. Cameron [c], Mirella Di Lorenzo [a]

[a] Department of Chemical Engineering, University of Bath, Bath, BA2 7AY, UK

[b] EPSRC Centre for Doctoral Training in Sustainable Chemical Technologies, University of Bath, Bath, BA2 7AY, UK

[c] Department of Chemistry, University of Bath, Bath, BA2 7AY, UK

8.1 Abstract

Effective detection of contaminants in water is at the basis of safe water provision to communities. Traditional analytical methods are, however, expensive, time consuming and cannot be easily adapted to emerging pollutants (e.g. herbicides, pharmaceuticals and their metabolites). Microalgae have been shown to be an ideal sensing probe for bioactive compounds, with great sensitivity and limit of detections at very low concentration levels (in the nM range). In this study, we explore for the first time the use of microalgae in microbial fuel cells as a means to generate a portable and cost-effective sensor for onsite monitoring of pollutants in water. In particular, we report an innovative miniature single chamber photosynthetic MFC (photoMFC) and demonstrate its ability to detect a bioactive contaminant in water, such as formaldehyde. The photoMFC, inoculated with a mixed microalgae culture from a wastewater treatment algal pond, generated a peak power and current density of 0.18 mW m^{-2} and 7.2 mA m^{-2} respectively, when exposed to light. A current response to formaldehyde proportional to its concentration was produced in less than one hour, with a sensitivity of $6.92 \times 10^{-3} \pm 1.67 \times 10^{-3}$ ppm^{-1} cm^{-2}. In conclusion, this work provides the first proof of concept for the use of photoMFCs as a water sensor, with the great benefit of simple operation (with light as the sole energy source) and rapid onsite biosensing capability.

8.2 Introduction

The pollution of freshwater systems by chemical contaminants, such as heavy metals, pesticides, herbicides and pharmaceuticals, poses a significant threat to aquatic life and humans that depend on these water systems [1]. To complement effective wastewater treatment and sanitation programs, real time water quality monitoring techniques, capable of rapid onsite detection of pollutants released into waterways, are needed to prevent or minimize damage to the environment [2]. Ideally, such techniques would reduce or eliminate the need for expensive, offsite, complex and time consuming laboratory techniques [3]. In recent years, microbial fuel cell (MFC) technology has demonstrated great promise in water quality monitoring [3]. MFCs are devices that directly convert the chemical energy contained in organic matter into electricity *via* the metabolic processes of microorganisms [4,5]. The current generated by the electroactive bacteria at the anode, can be directly related to their metabolic activity [6]. Any disturbance to this activity, such as the sudden presence of a bioactive compound, will thus cause a change in the current generated, which can be detected [7-9]. MFC sensors have the advantage of simplicity; the anodic biofilm functions as the recognition element, thus removing the need for external equipment to act as a transducer [3].

In recent years, there has been much interest in a branch of the MFC technology where the bioelectrochemical system (BES) is fuelled by light [10], with the clear benefits associated, considering the vast and almost limitless amount of energy available from solar radiation [11].

In these systems, photosynthetic organisms are used for current generation [12], and their operation and design vary widely. A recent review by McCormick *et al.*[10] has identified three categories: 1) Photosynthetic MFCs which use chemoautotrophic microbes to generate electricity under anaerobic conditions in a light dependent manner [13]; 2) Complex photosynthetic MFCs (complex photoMFCs), which utilise light dependent BESs containing living heterotrophic and autotrophic species [14] and; 3) Biophotovoltaic systems (BPVs), where living oxygenic photosynthetic microbes are used to generate current through the photolysis of water and supply it to the electrode without the aid of heterotrophic species [15]. The operation of complex photoMFCs and BPVs is demonstrated in Figure 8.1.

It should be noted that complex photoMFCs and BPVs have distinct advantages over photosynthetic MFCs which use chemoautotrophic microbes. They do not require mediators for electroactive operation [16], offer facile set-up by use of microbial consortia [14], and provide enhanced energy production [10].

Light dependent cathode microbe interactions have also been explored for energy harvesting [17], but for the sake of this study, we will focus only on anode specific configurations, where the phototrophic biological components are localised to and interact with the anode.

In the case of anode specific complex photoMFCs and BPVs, the process of electron transfer from phototrophic organisms to the anode is not fully understood [18]. Many studies to date have used mixed cultures of phototrophic organisms [16,19,20], which may also include electrochemically active bacteria [12]. On one hand, it is often assumed that in a mixed culture, the bacteria (or possibly cyanobacteria) are responsible for electron transfer to the anode. During the process, the phototrophic organisms reduce carbon dioxide and generate organic matter that is oxidised by the electrochemically active bacteria, Figure 8.1A [12]. Alternatively, it has also been proposed that, during photosynthesis, carbon dioxide is reduced and water is oxidised to generate oxygen, electrons and protons [15,18]. Electrons are collected at the anode, while the protons diffuse to the cathode, where they react with oxygen to form water, Figure 8.1B.

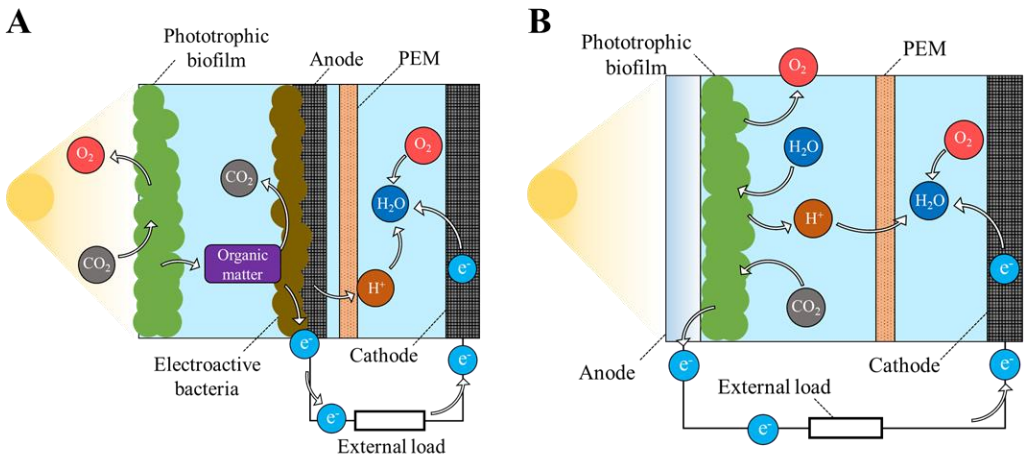

Figure 8.1. Schematic of the operation of light dependent bioelectrochemical systems: [**A**] complex photosynthetic microbial fuel cells; [**B**] biophotovoltaic systems.

Most research to date on complex photoMFCs and BPVs has focused on their power generation capability. The striking aspects of these technologies are their ability to harvest solar energy to directly generate electricity [21], and the ease and potential longevity of operation as there is no need for continuous provision of organic carbon for energy [22]. Complex photoMFC and BPVs will need, however, to compete with other renewable energy resources, such as wind and conventional solar power, in terms of energy efficiency, cost and environmental benefits [12]. As such, substantial power performance improvements are needed to make this technology commercially competitive [23].

On the other hand, a niche application, which could prove to be more practical, would be the use of these systems as biosensors for water quality monitoring. Indeed, photosynthetic cultures are commonly used for aquatic toxicological testing, due to their sensitivity towards hazardous chemicals and their rapid response times [24]. As well as for bioassays, microalgae have also been employed in a range of biosensors in the past decade, utilising amperometric, conductometric and optical methods [25].

In this context, we here report an innovative single chamber air cathode photosynthetic MFC and explore its use as a biosensor for the detection of toxic compounds in water. To the author's knowledge, this is the first time a miniature single chamber photosynthetic microbial fuel cell has been tested as a biosensor for toxicants in water. The electrochemical performance of the resulting device and its response to formaldehyde, used as a model toxicant, were investigated to provide a proof of concept of the potential of this technology for water quality monitoring.

8.3 Experimental

8.3.1 Materials

All chemicals used were of analytical grade and were purchased from Sigma-Aldrich or Alfa Aesar. All solutions were prepared with reverse osmosis purified water. Artificial wastewater (AW) was prepared with the following constituents: $(NH_4)_2SO_4$, 270 mg L^{-1}; $MgSO_4.7H_2O$, 60 mg L^{-1}; $MnSO_4.H_2O$, 6 mg L^{-1}; $NaHCO_3$, 130 mg L^{-1}; $FeCl_3.6H_2O$, 3 mg L^{-1}; $MgCl_2$, 4 mg L^{-1} and distilled water. AW was autoclaved prior to use.

8.3.2 Photosynthetic MFC construction

The single chamber, air cathode photosynthetic microbial fuel cell (photoMFC) was constructed following the geometry of a previous design [26], Figure 8.2A, with a total anodic chamber volume of 128 µL. Polydimethylsiloxane (PDMS) was casted around a PA 2200 nylon mould to form a rectangular flow chamber, which was sandwiched between two acrylic plates, Figure 8.2A. The top acrylic plate had an opening as large as the channel top cross sectional area to accommodate an air breathing cathode design. For the cathode, carbon cloth (untreated carbon cloth, type-B, E-Tek, USA) was hot pressed to a Nafion 117 membrane (Sigma Aldrich) [27], and stainless steel gauze (Type 304, Alfa Aesar) was used as a current collector in conjunction with titanium wire (Advent research materials, Oxford, UK) to connect the cathode to the electrical circuit. A planar fluorine-doped tin oxide (FTO) coated glass electrode (13 Ω sq^{-1}, Sigma Aldrich) was used as the anode, it has previously been shown that this material allows the sufficient development of photosynthetic biofilms [28]. Silver-loaded conductive paint (Chemtronics, CW2400, RS components) was used to form a contact with the electrical circuit and the FTO glass surface. The anode was placed underneath the PDMS channel. All devices and experiments were conducted in triplicate.

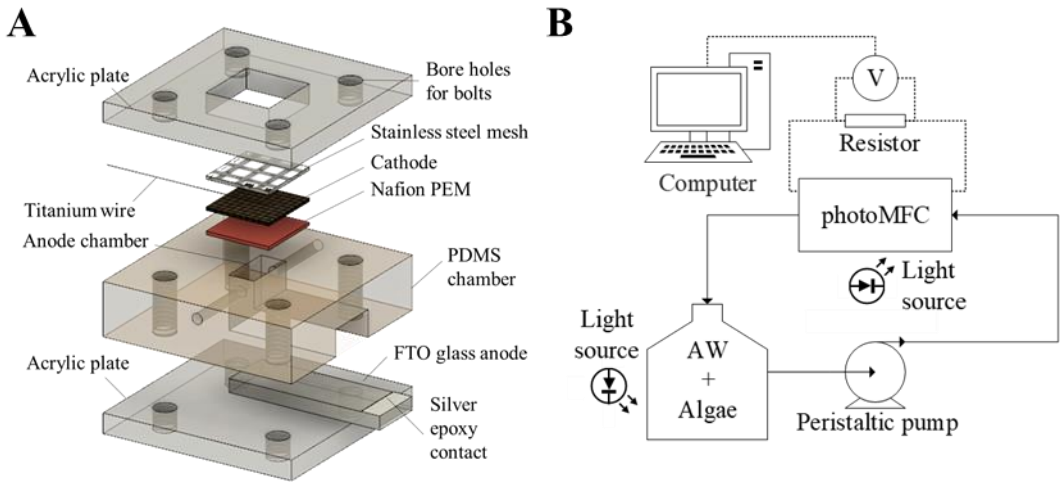

Figure 8.2. [**A**] Schematic of the photoMFC construction (to scale); [**B**] schematic of the experimental set up for operation of the photoMFC.

8.3.3 Operation of the photosynthetic MFC

A mixed culture of microalgae, consisting of a culture derived from a pilot high-rate algal pond (HRAP) wastewater treatment facility (Beckington STW, Wessex Water, UK), which predominantly contains the microalgae strain AV12 (*Scenedesmus obliquus*), combined with microalgae strain AV2 (*Chlorella luteoviridis),* was used to inoculate the photoMFCs.

The choice for a mixed culture was made on the basis of previous results that show enhanced power performance of photosynthetic MFCs enriched with mixed cultures [12,19]. The culture was cultivated in AW at room temperature under aerobic conditions (but no air bubbling) until the cell density reached 500 mg L^{-1} (dry weight). To initiate biofilm growth, the green microalgae consortium in AW was injected into the photoMFC and allowed to settle and attach to the anode under static conditions. Two hours was allowed for an open circuit potential to develop, and then the photoMFC was connected to a 1 kΩ resistor to drive the development of an electroactive biofilm. The potential generated from the photoMFCs was recorded, and the output current calculated, as previously described [27]. The photoMFCs were enriched under static conditions for almost four days, then operated in recirculation mode with an AW feed solution (pH 7.5 ± 0.1 and conductivity 6.15 ± 0.24 mS), with a cell mass controlled between 400 - 500 mg L^{-1} (by systematic dilution with AW), at a volumetric flow rate of 0.12 mL min^{-1} by using a multichannel peristaltic pump (ISM933C, Ismatec, Germany), Figure 8.2B. The cultures were kept in 1 L containers with constant magnetic stirring. A diffuse white light source was provided by a fluorescent light box (Lightbox, UK) placed 20 mm underneath the photoMFCs, providing a luminous intensity of 3 W m^{-2} (through the glass electrode) at a colour temperature of 7000 K. A light box was also placed next to the feedstock solution, Figure 8.2B. The photoMFCs were operated under 12 h dark/light cycles to mimic natural sunlight. Temperatures remained approximately constant (20 ± 2°C) throughout the experiment, and the photoMFCs were stored inside a light impermeable container to eliminate the effect of ambient light on the photoMFC operation.

8.3.4 Electrochemical methods

Electrochemical analysis was performed using an Autolab PGSTAT128N (Metrohm, UK), with devices left under open circuit potential for up to 2 h beforehand to allow a steady state open circuit potential to develop. Polarisation tests were conducted in two-electrode mode, with the anode as the working electrode and the cathode as the counter electrode, and were undertaken *via* linear sweep voltammetry (LSV) at a scan rate of 5 mV s^{-1}. Power, P, was calculated as the product of voltage, V, and current, I, using Joule's law: $P = V \times I$. Resistance, R, was determined using Ohm's law: $R = V / I$. Power density and current density were calculated by dividing the current by the total projected surface area of the anode, (A = 0.32 cm^2). The internal resistance (R_{int}) of the MFC was calculated from the linear fit of the ohmic region of the polarisation cell potential curve ($R_{int} = \Delta V/\Delta I$).

Electrochemical impedance spectroscopy (EIS) was conducted at open circuit voltage over a frequency range of 1 MHz down to 0.1 Hz, using 10 steps per decade, with a sinusoidal perturbation of 10 mV amplitude, and an integration time set to 0.125 seconds, 3 cycles. EIS was conducted in three-electrode mode by using the anode as the working electrode, the cathode as the counter electrode, and a Ag/AgCl reference electrode. Complex plane plot data was fit to a two-time constant equivalent circuit model, using ZView (Scribner Associates Inc.), as outlined in Figure S8.1. Following the electrochemical analysis, and for the rest of the study, photoMFCs were operated under their optimal resistance for power performance, as determined from polarisation tests.

8.3.5 Toxicant analysis

To determine the capability of the photoMFC to detect toxic compounds in water formaldehyde was injected into the photoMFCs. Formaldehyde was chosen as a model bioactive compound to facilitate comparison with previous works, since it is a compound typically tested for MFC based biosensors [29–31]. To mimic a toxic event, formaldehyde dissolved in AW (concentrations 10, 50, 100 and 200 ppm) was injected into the photoMFC for 30 min by using a three-way valve prior to the device [26]. Before the injection of formaldehyde, the photoMFC was fed with AW containing no

photosynthetic culture for at least 2 h until a steady baseline current was established. In line with the toxicant dosing, a control toxic event was performed by feeding the photoMFC with AW containing no formaldehyde. After toxicant analysis, the photoMFC was flushed with AW for at least one hour before being replaced to the original culture in AW feedstock. To avoid irreversible damage to the biofilm at the anode, only one test was performed per day. The amperometric response of the photoMFCs was characterised as described in Figure 8.3. To offset the variability in baseline current over time and allow comparability between subsequent toxicant tests, the current at time t, I_t, was normalised against the baseline current, I_B, to yield a normalised current, I_N, as per Equation 8.1:

$$I_N = \frac{I_t}{I_B} \qquad \text{Equation 8.1}$$

Subsequently, the sensitivity of the photoMFC was determined by normalising to the anodic macro surface area as per Equation 8.2:

$$sensitivity = \frac{\Delta I_N}{\Delta C_f \times A} \qquad \text{Equation 8.2}$$

Where C_f is the concentration of formaldehyde dosed into the photoMFC.

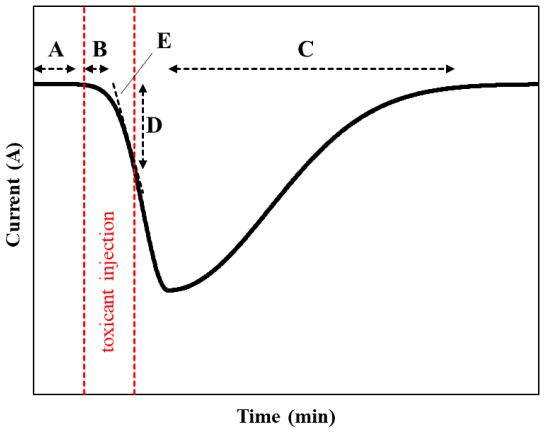

Figure 8.3. Characterisation of a typical amperometric toxicant response curve from the photoMFC device. [**A**]: *The baseline current*- the average steady state current before the toxic injection; [**B**]: *Delay time*- the time between the toxic injection and an initial response; [**C**]: *Total recovery time*- the time taken for the current to recover to 95% of the baseline current; [**D**]: *Toxic current drop*- the current drop experienced during the toxic event; [**E**]: *Initial rate*- the slope of the current response curve when experiencing a toxic injection.

8.3.6 Residence time distribution analysis

To ascertain the flow properties within the photoMFC when formaldehyde was introduced, a step tracer experiment was conducted to determine the mean residence time of molecules within the photoMFC. Ergo, the amount of time expected for formaldehyde to be fully present within the photoMFC anodic chamber at the expected concentration and the amount of time required to flush the photoMFC with AW after a toxic injection may be understood. To conduct the step tracer experiment, fluorescein at a concentration of 0.1 mg mL^{-1} was dissolved in acetone and used as a tracer solution. Initially, the pMFC (prior to operation with microalgae) was filled with tracer solution and at time $t = 0$, a solution of pure acetone was introduced into the system at a flow rate of 0.12 mL min^{-1}. The absorbance of the outlet at 452 nm was measured with respect to time at a frequency of 50 Hz using a UV-vis flow cell and spectrometer (Avalight-DH-S-BAL light source, AvaSpec-2048L spectrometer, Avantes, Netherlands). The mean residence time and variance was determined by numerical integration using Simpson's method [32].

8.3.7 Scanning electron microscopy

A Jeol JSM-6480LV scanning electron microscope (SEM) was used to characterise the morphology of the biofilm on the anode surface after enrichment and operation. Fixation of the biofilm was performed using a modification of a previously described method [26] as detailed in the supporting information. All samples were coated with Au prior to imaging.

8.4 Results and discussion

8.4.1 Enrichment of the photosynthetic MFC

The photoMFCs were enriched under static conditions for four days, and then fed under flow (at 0.12 mL min^{-1}) with AW containing photosynthetic culture within the concentration range of 400-500 mg L^{-1}. During all operation, the photoMFCs were subjected to an artificial night/day cycle (12 h each). The enrichment of the photoMFCs is shown in Figure 8.4. A sharp increase in the current is observed with the application of flow to the system, indicating that the provision of sufficient nutrients to the system is essential for electrogenesis. After only two days of operation under flow, a day-night current generation trend was observed. In particular, the current output was larger when the anode was exposed to light, with an initial current increase rate (at the moment the photoMFC was exposed to light) of 16 ± 4 nA h^{-1}. This trend is in agreement with other photosynthetic MFCs reported, inoculated either with microalgae taken from a freshwater pond [16] or *Chlorella vulgaris* [22]. Indeed, the step-up in the output current when switching from dark to light suggests that photolysis of water by photosystem II is the source of electrons [15,18]. Another possibility is that electrons are generated from the activity of heterotrophic bacteria in the biofilm that oxidise organic compounds released by the microalgae during photosynthesis.

If this were the predominant phenomenon, however, the output power would be higher during the night-time. The reason for this is that photosynthetic microalgae would accumulate organic substrate (in the form of starch) during the day-time, and then ferment and excrete these as organic substrates compatible for heterotrophic bacteria

metabolism during the night-time [33-35]. Note that, although this may not be the predominant phenomenon, the synergistic efforts of photosynthetic and heterotrophic microorganisms may still be present in this system.

After nine days of enrichment the photoMFC reached an average steady state day-time and night-time current of 0.095 ± 0.012 μA and 0.075 ± 0.013 μA respectively. This performance represents a day-time to night-time current ratio of 1.3:1, which is similar to previously reported photosynthetic MFC systems [20,36].

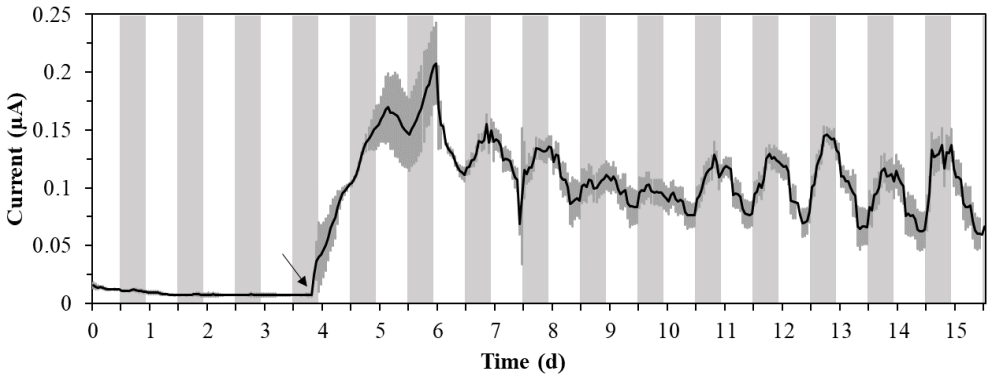

Figure 8.4. Enrichment of the electrochemically active microbial culture within the miniature photoMFC. Artificial wastewater containing between 400-500 mg L^{-1} of mixed microalgae culture was fed to the anode chamber. For 4 days the culture feed was static, after 4 days the AW and microalgae culture was put under flow at 0.12 mL min^{-1}, as indicated by the arrow in the graph. Shaded regions show periods of time when the photosynthetic MFCs were illuminated at a light flux of 3 W m^{-2} (12 h night/day cycles). Error bars refer to triplicate experiments.

The photoMFCs demonstrated a stable operation for 20 days, at which point the current generated began to decay both during the day-time and night-time, Figure 8.5A. A first order current decay was observed with rate constants of -0.075 day^{-1} for the day-time average current, and -0.097 day^{-1} for the night-time current, Figure 8.5B. A decrease in the electricity generation by photosynthetic MFCs has indeed been previously observed. In particular, a depreciation in the power generated by photosynthetic MFCs has been observed after: 12 days and 19 days using *Chlorella vulgaris* and *Synechocystis sp.* [22]; 6 days using *Chlorella emersoni* [18]; and 8 days when using a photosynthetic pond culture [20] and a natural hot spring community [19]. This decrease in power performance over time may be attributed to potential oxygen

accumulation in the anodic biofilm which reduces heterotroph electroactive contribution [16,22, 37].

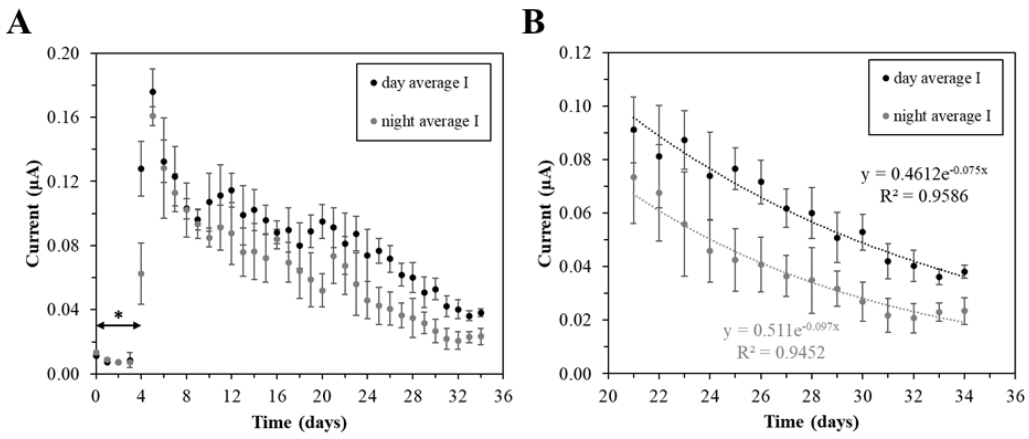

Figure 8.5. Average day time and night time currents of the photosynthetic MFCs: [**A**] over their one month operation period, * indicates period of static enrichment; [**B**] to the end of their lifetime from days 21 to 34. Data is an average of three devices.

8.4.2 Electrochemical characterisation

After two weeks of operation, the electrochemical performance of the photoMFCs was characterised by polarisation tests (Figure 8.6A) and electrochemical impedance spectroscopy (Figure 8.6B), with results summarised in Table S8.1. The open circuit voltage (OCV) for the photoMFC was 45.1 ± 4.9 mV, which is lower than other photosynthetic MFCs, characterised by OCVs ranging from 125 – 500 mV [16,19,20,22,23]. This low value of OCV is probably due to the high internal resistance of the system, 76.1 ± 9 kΩ (as determined from the ohmic region of the polarisation curve, Figure 8.6A), which indeed has been reported also for other miniature MFCs [38-40]. The presence of ohmic resistances on the polarisation curve suggests that the electrical resistances of the electrodes, membrane and electrolyte contribute to the internal resistance. Contrary to what is expected in such a miniature device, mass transfer limitations are also apparent [41]. In this specific case, however, the presence of mass transfer limitations in the photoMFC may be related to biofilm related phenomena, such as the penetration of light and production of electrons in a potentially dense photosynthetic biofilm [15]. A maximum power density of 0.18 ± 0.01 mW m^{-}

^{2} (with corresponding current density of 7.2 ± 0.6 mA m^{-2}) was generated by the photoMFC. This value is similar (albeit slightly lower) than other single chamber photosynthetic MFCs in the literature, whose power outputs range from 0.0248 – 10.3 mW m^{-2} [16,20,22,23]. Note however, that a direct comparison between these systems and our work is difficult, due to differences in electrode materials (tin-oxide on polyethylene terephthalate [23], or carbon based anodes with coatings [20]), the presence of oxygen reduction reaction catalysts at the cathode (namely platinum [16,20,22,23]), variability in light source intensity, and photosynthetic culture used (including cyanobacteria [16,22], and fresh water consortia [20]). Nonetheless, our photoMFC shows an increase in power by two orders of magnitude when compared to similar systems of larger scale (180 – 500 mL), which use similar electrode materials (untreated carbon based cathode and FTO glass anode), characterised by power densities within the range 1.0 – 3.6 µW m^{-2} [18,42]. The better power performance of the photoMFC, despite the high internal resistances and mass transfer limitations, may be attributed to the beneficial effects of miniaturisation on power performance [39]. A reason behind the limited power generation could be that the dissolved oxygen generated during photosynthesis may act as a terminal electron acceptor, thus reducing the electrogenic activity of the system [23,42]. The optimum external resistance, as defined by polarisation tests, to apply to the photoMFC was 110 kΩ, and for all subsequent tests, the photoMFCs were connected to this electrical load.

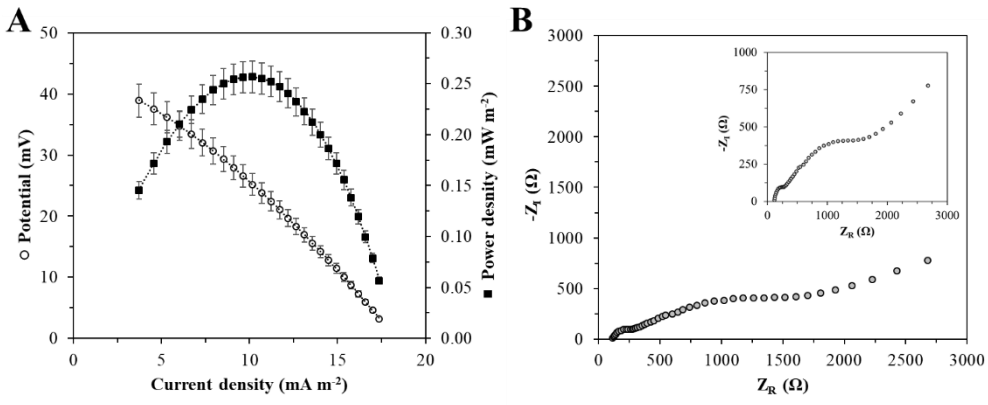

Figure 8.6. [**A**] Polarisation and power curve for the photoMFC. Power and current density refer to anodic geometric surface area, 0.32 cm^{2}. Data is the average of three devices. [**B**] Complex plane (Nyquist) plot for the photoMFC, with the asymmetric plot overlaid.

EIS analysis (Figure 8.6B) revealed an ohmic resistance (R_Ω) of 81 ± 5 Ω, and a total charge transfer resistance (R_{ct}) of 1273 ± 36 Ω, determined by fitting the data to a two time constant model equivalent circuit model, Figure S8.1. The two time constants present indicate that there are two physical processes limiting the performance of the system. The high value of R_Ω derives from the relatively low ionic strength of the AW medium. Compared to other EIS analyses of photosynthetic MFC [16,20], this work demonstrates a higher R_{ct}, which may indicate a limited electron transfer between the biofilm and the electrode surface, which suggests other sinks for electrons or perhaps nonspecific low efficiency electron transfer systems from the biofilm cells to the electrode. A reduction in R_{ct} could be achieved with electrode designs that improve biofilm attachment- for instance by using biocompatible coatings to increase the rate of electron transfer at the electrode surface [43]; or by enhancing the surface area with 3D porous electrodes that would lead to larger electroactive surface area of the electrode and increase the rate of interfacial electron transfer at the anode surface [21,28,44].

8.4.3 Formaldehyde detection

After two weeks of operation, the photoMFCs were tested as sensors for the detection of formaldehyde, a biocide commonly tested in MFC biosensor studies [29-31,45]. A summary of MFC biosensors for formaldehyde detection recently reported in the literature is shown in Table S8.2. The toxic event was performed by feeding the photoMFC with formaldehyde in AW for 30 minutes, as outlined in the experimental section. To facilitate the comparison between toxicant events from day to day, and thereby eliminate the variability in current over time, the current generated from the photoMFC was normalised by using Equation 8.1. Figure 8.7A shows the effect of formaldehyde on the current generated by the photoMFCs. Upon addition of formaldehyde, a drop in the current was observed, which within the values 10 – 200 ppm, depended on its concentration, Figure 8.7B. Within this dynamic range the sensitivity (as defined by Equation 8.2) was $6.92 \times 10^{-3} \pm 1.67 \times 10^{-3}$ ppm^{-1} cm^{-2} (R^2 = 0.97).

The lower limit of detection was 10 ppm, which is similar to the lower detection limit demonstrated by other miniature (≤ 140 μL anodic chamber volume) MFC based

biosensors for formaldehyde [29,45]. Concentrations less than 10 ppm showed no perceptible current response.

The initial rate of current change upon formaldehyde injection, also showed a proportional response to the concentration, Figure S8.2. Monitoring and analysis of the initial slope of the current could provide a more rapid means to discern the presence of toxic compounds when detecting toxicants in water samples. This method of analysis may prove useful if using the sensor as a 'shock-based' biosensor [46]. After the 30 min dosing of formaldehyde, the current generated by the photoMFCs recovered to its baseline value after at least one hour. Consequently, it is assumed that the presence of formaldehyde only temporarily affected the metabolic and photosynthetic processes of the biofilm at the anode [6]. This time is faster than other ones reported for MFC sensors, where bacteria are used as the biosensing element (~3 h [29] and 5 h [45]).

For all toxic events, there was a delay time of 11 ± 1.8 min, which was not related to the concentration of toxicant added. The mean residence time, and therefore the amount of time for a full step response in concentration of formaldehyde inside the photoMFC, was 1.7 ± 0.1 min, as determined by a residence time distribution analysis, using a step tracer experiment with fluorescein, Figure S8.3. Taking this into account, there was a corrected delay time between the change in current output and the initial injection of toxicant of 9.3 ± 1.9 min. This delay in response could be explained by the presence of mass transfer limitations within the photoMFC as evidenced by the polarisation curve, Figure 8.6A. Mass transfer limitations would arise from resistance to the transport of formaldehyde from the bulk liquid phase through the stagnant boundary layer at biofilm surface (external mass transfer processes), and from the mass transport and consumption by reaction of formaldehyde through the biofilm (internal mass transfer processes) [47].

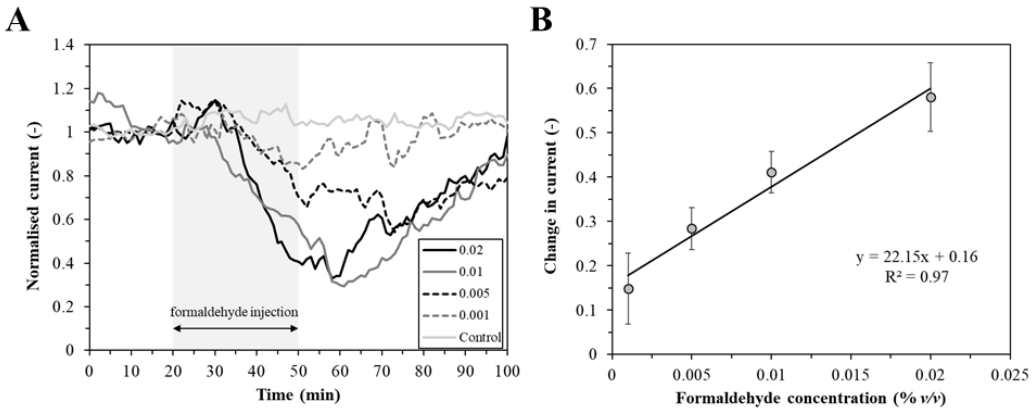

Figure 8.7. PhotoMFC amperometric response to formaldehyde. [**A**] Current output *versus* time when dosed with AW containing formaldehyde at 10 – 200 ppm. A 30 min long formaldehyde injection was applied to the system, followed by feeding with AW containing no formaldehyde. Legend refers to the specific formaldehyde concentration (ppm) applied. Data is the average of 3 devices with 14% accuracy. [**B**] Normalised change in current during the toxic event *versus* the formaldehyde concentration dosed. Error bars refer to triplicate experiments.

Anodes with biofilms subjected to formaldehyde injection were analysed by SEM, Figure 8.8A, along with a control consisting of anodes from photoMFC not exposed to the toxicant, Figure 8.8B. In all the biofilms analysed, the predominant microalgae species seems to be *Chlorella luteoviridis* (identified by wrinkled spherical shape and lack of flagella) [48] and *Scenedesmus obliquus* (with characteristic lunate shape, protruding spines from outer corners and surface reticulations) [49,50]. Moreover, a mixed culture containing both bacteria (with a mixture of round and predominantly rod shaped bacteria, < 1 µm in length) and microalgae (noticeable by their larger size, approximate spherical diameter < 5 µm) in the biofilm is observed. These images suggest that a symbiotic relationship between the bacteria and microalgae within the biofilm may exist, and, as such, electrogenesis *via* the photolysis of water by photosystem II [15,18], might be combined with electrons generation by heterotrophic bacteria that oxidise organic compounds produced by the microalgae during photosynthesis [34,35].

Biofilms exposed to formaldehyde, appeared to be characterised by a greater abundance of bacteria. This result may suggest that microalgae in the biofilm are more susceptible to the presence of formaldehyde than bacteria, which would cause their detachment from the anodic biofilm. However, more quantitative data is needed to

clarify this. Moreover, further analysis of the interactions between the bacteria and microalgae in mixed biofilms is needed for photosynthetic MFCs to ascertain the functions and roles of these microbes in these systems.

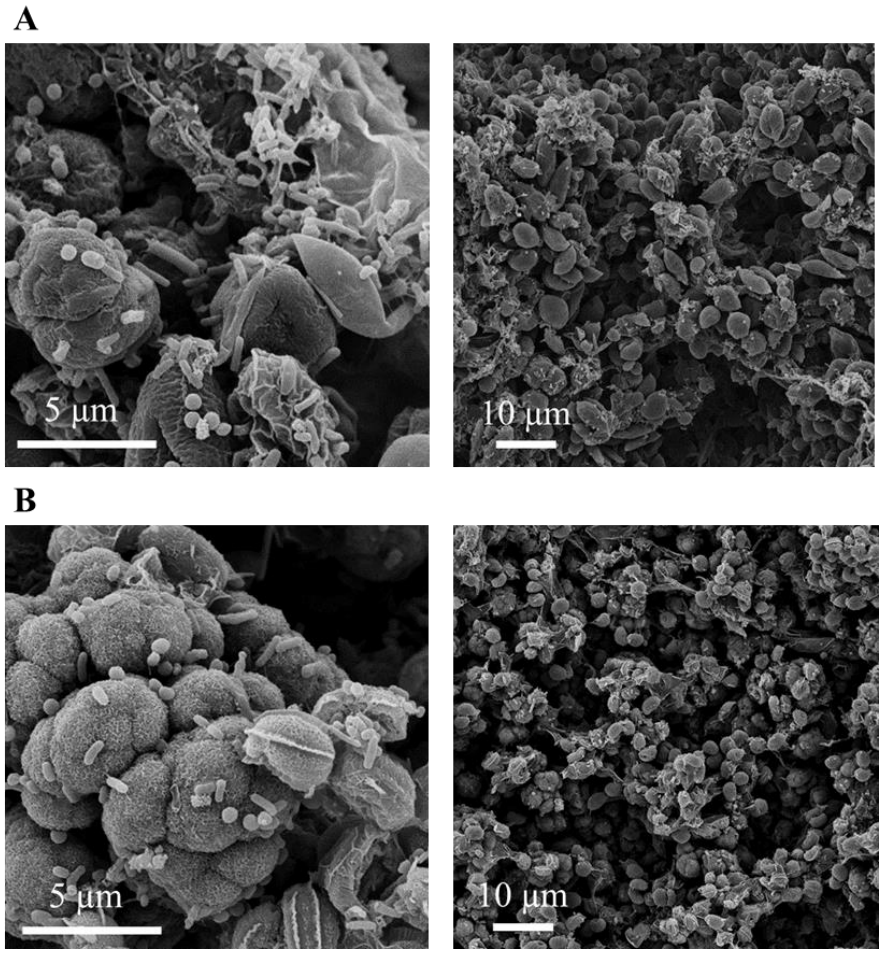

Figure 8.8. SEM images of the anodic biofilm within the photoMFC with: [**A**]: analysis subsequent to formaldehyde dosing; [**B**]: analysis of devices never subjected to formaldehyde.

8.5 Conclusions

To conclude, this study presents the first use of a photosynthetic microbial fuel cell for toxicant detection in water. A simple photoMFC was developed, characterised by a miniature single chamber air breathing configuration, enriched with a mixed culture of microalgae. The photoMFC was capable of generating a power density of 0.18 mW m^{-2}, with corresponding current density 7.2 mA m^{-2}. Owing to the increased surface

area to volume ratio of the miniaturised device, this current was significantly larger than values reported for other photosynthetic MFCs with similar electrode configurations [18,42]. The photoMFC demonstrated promising proof of concept capability of detecting formaldehyde between 10 – 200 ppm. Through the measurement of the electrogenic activity of microalgae in the photoMFC, detection of these contaminants could be rapid, cost-effective (given the relatively low cost and simple treatment of materials used in manufacture) and onsite (due to the devices small size and facile portability).

The use of photoMFCs for biosensing may also have distinct advantages over MFC sensors. Firstly, the operation of photoMFCs is much simplified, since the key input is light (an almost limitless resource), whereas MFCs must be fed continuously with organic carbon. This aspect complicates the operation of MFCs, as the level of organics in the feeding water must be saturating to allow reliable performance and avoid current variations caused by the concentration of carbon source in the system [6]. Moreover, considering the successful use of microalgae in aquatic toxicological testing [24], photoMFCs have the potential for enhanced sensitivity towards emerging contaminants, such as herbicides and pharmaceuticals, which pose a particular global environmental concern [51]. The stability in the long term of the photoMFC must, however, be enhanced. In this study, the photoMFC was probably limited by oxygen accumulation in the anodic chamber, which could be overcome by using co-cultures that include aerobic chemotrophs that consume oxygen for cellular respiration [52]. Moreover, the use of transparent three dimensional porous anode materials or anodic biocompatible coatings would increase the power performance by ameliorating the cell attachment and therefore the photoelectroactive biofilm development [28,16]. Finally, taking into account the SEM results, which suggested that the exposure to formaldehyde affected the microalgae more than the bacteria within the biofilm, the use of pure cultures of microalgae may enhance the sensitivity of the photoMFC towards toxicants.

8.6 Associated content

Author Contributions

MDL, PJC and JC conceived the experiment. Design, implementation and analysis of experiments performed by JC, MM, WM. Manuscript prepared by JC and MDL. Project supervised by MDL and PJC.

Conflicts of Interest

The authors declare no conflict of interest.

Acknowledgements

The authors would like to thank: Philippe Mozzanega and Dimitrios Kaloudis for assistance and provision of microalgae cultures. Andrew Hall and Ulrich Hintermair for use of equipment for residence time distribution analysis. Funding from the Engineering and Physical Sciences Research Council (EPSRC) and the EPSRC Centre for Doctoral Training in Sustainable Chemical Technologies (EP/G03768X/1) is acknowledged.

Abbreviations

AW: Artificial wastewater,

BES: Bioelectrochemical system,

BPV: Biophotovoltaic system,

CPE: Constant phase element,

EIS: Electrochemical impedance spectroscopy,

FTO: Fluorine-doped tin oxide,

HRAP: High rate algal pond,

LSV: Linear sweep voltammetry,

MFC: Microbial fuel cell,

OCV: Open circuit voltage,

PDMS: Polydimethylsiloxane,

PEM: Proton exchange membrane,

photoMFC: Photosynthetic microbial fuel cell,

SEM: Scanning electron microscope.

Nomenclature

Roman symbols

A: Anode macro surface area,

C_f: Concentration of formaldehyde,

I: Current,

I_B: Baseline current,

I_t: Current at time t,

I_N: Normalised current,

P: Power,

R: Resistance,

R_{ct}: Charge transfer resistance,

R_{int}: Internal resistance,

R_Ω: Ohmic resistance,

t: Time,

V: Voltage,

W_d is the diffusion-related resistance.

8.7 Supporting information

Table S8.1. Summary of the power performance of the photoMFC. Power and current density refer to anodic geometric surface area, 0.32 cm^2.

OCV (mV)	Maximum power (nW)	Power density (mW m^{-2})	Current density (mA m^{-2})	R_{int} (kΩ)	External resistance (kΩ)	$R_Ω$ (Ω)	R_{ct} (Ω)	C_{dl} (F)	CPE ($s^{α}$ $Ω^{-1}$)	α
45.1 ± 4.9	5.76 ± 0.49	0.18 ± 0.01	7.2 ± 0.6	76.1 ± 9	110 ± 9	81 ± 5	1273 ± 36	2.41 × 10^{-7} ± 3.03 × 10^{-8}	1.09 × 10^{-4} ± 8.52 × 10^{-6}	0.57 ± 0.03

Table S8.2. Summary of other MFC based biosensors for formaldehyde detection

Microbe assayed	Configuration	Anode chamber volume	Formaldehyde concentration monitored (ppm)	Response time	Recovery time	Ref.
Microalgae consortium	Single chamber photosynthetic MFC	128 µL	10 - 200	42 ± 7.5 min	62 ± 8 min	This study
Shewanella oneidensis MR-1	Single chamber 3 electrode system	140 µL	10 - 1000	> 200 min	~ 175 min	[29]
Geobacter sulfurreducens	Two chamber	144 µL	1000	~ 3 min	N/A	[31]
Shewanella oneidensis MR-1	Single chamber 3 electrode system	120 mL	100 - 1000	> 9.7 h	N/A	[30]
Wild-type Pseudomonas aeruginosa PAO1	Single chamber, dual-channel system	90 µL	30 - 3500	< 125 min	~ 330 min	[45]

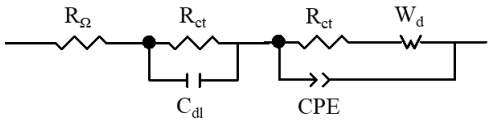

Figure S8.1. Equivalent circuit model used to model EIS data. Where R_Ω is the ohmic resistance, R_{ct} is the charge transfer resistance, W_d is the diffusion-related resistance (using a Warburg diffusion element), C_{dl} is the double layer capacitance, and CPE is a constant phase shift element. Constant phase shift elements have been used to account for the depressed nature of the semicircles, and to account for surface roughness and inhomogeneity at the electrode surface.

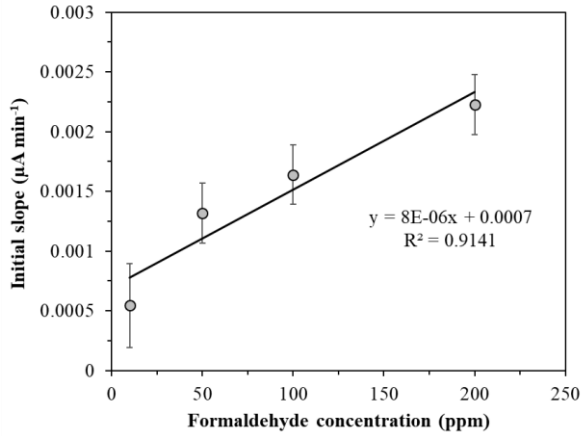

Figure S8.2. Initial slope of the current response towards the injection of formaldehyde at concentrations between 10 – 200 ppm. Error bars refer to triplicate experiments.

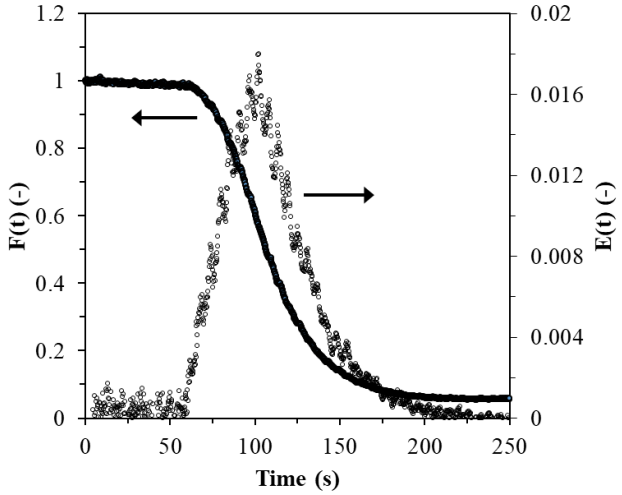

Figure S8.3. Step tracer experiment data for residence time distribution analysis of the photoMFC. F(t) represents the step response curve of the normalised concentration of tracer compound, fluorescein, and E(t) represents the residence time distribution function as previously described [32].

8.8 References

[1] WHO, Chemical mixtures in source water and drinking-water., Geneva, 2017. http://apps.who.int/iris/bitstream/10665/255543/1/9789241512374-eng.pdf?ua=1 (accessed July 24, 2017).

[2] C.J. Houtman, Emerging contaminants in surface waters and their relevance for the production of drinking water in Europe, J. Integr. Environ. Sci. 7 (2010) 271–295. doi:10.1080/1943815X.2010.511648.

[3] J. Chouler, M. Di Lorenzo, Water Quality Monitoring in Developing Countries; Can Microbial Fuel Cells be the Answer?, Biosensors. 5 (2015) 450–470. doi:10.3390/bios5030450.

[4] M.C. Potter, Electrical Effects Accompanying the Decomposition of Organic Compounds, Proc. R. Soc. B Biol. Sci. 84 (1911) 260–276. doi:10.1098/rspb.1911.0073.

[5] R.M. Allen, H.P. Bennetto, Microbial fuel-cells, Appl. Biochem. Biotechnol. 39 (1993) 27–40. doi:10.1007/BF02918975.

[6] M. Di Lorenzo, A.R. Thomson, K. Schneider, P.J. Cameron, I. Ieropoulos, A small-scale air-cathode microbial fuel cell for on-line monitoring of water quality., Biosens. Bioelectron. 62 (2014) 182–188. doi:10.1016/j.bios.2014.06.050.

[7] Y. Jiang, P. Liang, C. Zhang, Y. Bian, X. Yang, X. Huang, P.R. Girguis, Enhancing the response of microbial fuel cell based toxicity sensors to Cu(II) with the applying of flow-through electrodes and controlled anode potentials., Bioresour. Technol. 190 (2015) 367–372. doi:10.1016/j.biortech.2015.04.127.

[8] N.E. Stein, H.V.M. Hamelers, C.N.J. Buisman, Stabilizing the baseline current of a microbial fuel cell-based biosensor through overpotential control under non-toxic conditions., Bioelectrochemistry. 78 (2010) 87–91. doi:10.1016/j.bioelechem.2009.09.009.

[9] M. Di Lorenzo, T.P. Curtis, I.M. Head, K. Scott, A single-chamber microbial fuel cell as a biosensor for wastewaters., Water Res. 43 (2009) 3145–3154. doi:10.1016/j.watres.2009.01.005.

[10] A.J. McCormick, P. Bombelli, R.W. Bradley, R. Thorne, T. Wenzel, C.J. Howe, Biophotovoltaics: oxygenic photosynthetic organisms in the world of bioelectrochemical systems, Energy Environ. Sci. 8 (2015) 1092–1109. doi:10.1039/C4EE03875D.

[11] T.J. Donohue, R.J. Cogdell, Microorganisms and clean energy., Nat. Rev. Microbiol. 4 (2006) 800–801. doi:10.1038/nrmicro1534.

[12] D.P. Strik, R.A. Timmers, M. Helder, K.J. Steinbusch, H. V. Hamelers, C.J. Buisman, Microbial solar cells: applying photosynthetic and electrochemically active organisms, Trends Biotechnol. 29 (2011) 41–49. doi:10.1016/j.tibtech.2010.10.001.

[13] M. Rosenbaum, U. Schröder, F. Scholz, In Situ Electrooxidation of Photobiological Hydrogen in a Photobioelectrochemical Fuel Cell Based on Rhodobacter sphaeroides, Environ. Sci. Technol. 39 (2005) 6328–6333. doi:10.1021/ES0505447.

[14] M. Rosenbaum, Z. He, L.T. Angenent, Light energy to bioelectricity: photosynthetic microbial fuel cells, Curr. Opin. Biotechnol. 21 (2010) 259–264. doi:10.1016/j.copbio.2010.03.010.

[15] J.M. Pisciotta, Y. Zou, I. V. Baskakov, Role of the photosynthetic electron transfer chain in electrogenic activity of cyanobacteria, Appl. Microbiol. Biotechnol. 91 (2011) 377–385. doi:10.1007/s00253-011-3239-x.

[16] Y. Zou, J. Pisciotta, R.B. Billmyre, I. V. Baskakov, Photosynthetic microbial fuel cells with positive light response, Biotechnol. Bioeng. 104 (2009) 939–946. doi:10.1002/bit.22466.

[17] M. Rosenbaum, F. Aulenta, M. Villano, L.T. Angenent, Cathodes as electron donors for microbial metabolism: Which extracellular electron transfer mechanisms are involved?, Bioresour. Technol. 102 (2011) 324–333. doi:10.1016/j.biortech.2010.07.008.

[18] K. Schneider, R.J. Thorne, P.J. Cameron, An investigation of anode and cathode materials in photomicrobial fuel cells, Philos. Trans. R. Soc. London A Math. Phys. Eng. Sci. 374 (2016) 1–22. http://rsta.royalsocietypublishing.org.ezproxy1.bath.ac.uk/content/374/2061/20150080 (accessed July 17, 2017).

[19] K. Nishio, K. Hashimoto, K. Watanabe, Light/electricity conversion by a self-organized photosynthetic biofilm in a single-chamber reactor, Appl. Microbiol. Biotechnol. 86 (2010) 957–964. doi:10.1007/s00253-009-2400-2.

[20] Y. Zou, J. Pisciotta, I. V. Baskakov, Nanostructured polypyrrole-coated anode for sun-powered microbial fuel cells, Bioelectrochemistry. 79 (2010) 50–56. doi:10.1016/j.bioelechem.2009.11.001.

[21] A. Elmekawy, H.M. Hegab, K. Vanbroekhoven, D. Pant, Techno-productive potential of photosynthetic microbial fuel cells through different configurations, Renew. Sustain. Energy Rev. 39 (2014) 617–627. doi:10.1016/j.rser.2014.07.116.

[22] A.J. McCormick, P. Bombelli, A.M. Scott, A.J. Philips, A.G. Smith, A.C. Fisher, C.J. Howe, Photosynthetic biofilms in pure culture harness solar energy in a mediatorless bio-photovoltaic cell (BPV) system, Energy Environ. Sci. 4 (2011) 4699–4709. doi:10.1039/c1ee01965a.

[23] A.E. Inglesby, K. Yunus, A.C. Fisher, U. Schröder, J. Keller, S. Freguia, P. Aelterman, W. Verstraete, K. Rabaey, J.P. Johnson, V.M. Rotello, M.T. Tuominen, D.R. Lovley, In situ fluorescence and electrochemical monitoring of a photosynthetic

microbial fuel cell, Phys. Chem. Chem. Phys. 15 (2013) 6903–6911. doi:10.1039/c3cp51076j.

[24] C.J. Choi, J.A. Berges, E.B. Young, Rapid effects of diverse toxic water pollutants on chlorophyll a fluorescence: Variable responses among freshwater microalgae, Water Res. 46 (2012) 2615–2626. doi:10.1016/j.watres.2012.02.027.

[25] R. Brayner, A. Couté, J. Livage, C. Perrette, C. Sicard, Micro-algal biosensors, Anal. Bioanal. Chem. 401 (2011) 581–597. doi:10.1007/s00216-011-5107-z.

[26] J. Chouler, I. Bentley, F. Vaz, A. O'Fee, P.J. Cameron, M. Di Lorenzo, Exploring the use of cost-effective membrane materials for Microbial Fuel Cell based sensors, Electrochim. Acta. 231 (2017) 319–326. doi:10.1016/j.electacta.2017.01.195.

[27] J. Chouler, G.A. Padgett, P.J. Cameron, K. Preuss, M.-M. Titirici, I. Ieropoulos, M. Di Lorenzo, Towards effective small scale microbial fuel cells for energy generation from urine, Electrochim. Acta. 192 (2016) 89–98. doi:10.1016/j.electacta.2016.01.112.

[28] R. Thorne, H. Hu, K. Schneider, P. Bombelli, A. Fisher, L.M. Peter, A. Dent, P.J. Cameron, Porous ceramic anode materials for photo-microbial fuel cells, J. Mater. Chem. 21 (2011) 18055–18060. doi:10.1039/c1jm13058g.

[29] W. Yang, X. Wei, A. Fraiwan, C.G. Coogan, H. Lee, S. Choi, Fast and sensitive water quality assessment: A μL-scale microbial fuel cell-based biosensor integrated with an air-bubble trap and electrochemical sensing functionality, Sensors Actuators B Chem. 226 (2016) 191–195. doi:10.1016/j.snb.2015.12.002.

[30] X. Wang, N. Gao, Q. Zhou, Concentration responses of toxicity sensor with Shewanella oneidensis MR-1 growing in bioelectrochemical systems., Biosens. Bioelectron. 43 (2013) 264–267. doi:10.1016/j.bios.2012.12.029.

[31] D. Dávila, J.P. Esquivel, N. Sabaté, J. Mas, Silicon-based microfabricated microbial fuel cell toxicity sensor., Biosens. Bioelectron. 26 (2011) 2426–2430. doi:10.1016/j.bios.2010.10.025.

[32] H.S. Fogler, Elements of Chemical Reaction Engineering, 4th ed., Pearson International, 2009.

[33] K. Nishio, K. Hashimoto, K. Watanabe, Light/electricity conversion by defined cocultures of Chlamydomonas and Geobacter, J. Biosci. Bioeng. 115 (2013) 412–417. doi:10.1016/j.jbiosc.2012.10.015.

[34] Z. He, J. Kan, F. Mansfeld, L.T. Angenent, K.H. Nealson, Self-Sustained Phototrophic Microbial Fuel Cells Based on the Synergistic Cooperation between Photosynthetic Microorganisms and Heterotrophic Bacteria, Environ. Sci. Technol. 43 (2009) 1648–1654. doi:10.1021/es803084a.

[35] L. Darus, P. Ledezma, J. Keller, S. Freguia, Oxygen Suppresses Light-Driven Anodic Current Generation by a Mixed Phototrophic Culture, Environ. Sci. Technol. 48 (2014) 14000–14006. doi:10.1021/es5024702.

[36] P. Bombelli, T. Müller, T.W. Herling, C.J. Howe, T.P.J. Knowles, A High Power-Density, Mediator-Free, Microfluidic Biophotovoltaic Device for Cyanobacterial Cells, Adv. Energy Mater. 5 (2015) 1401299–1401305. doi:10.1002/aenm.201401299.

[37] C.-C. Lin, C.-H. Wei, C.-I. Chen, C.-J. Shieh, Y.-C. Liu, Characteristics of the photosynthesis microbial fuel cell with a Spirulina platensis biofilm, Bioresour. Technol. 135 (2013) 640–643. doi:10.1016/j.biortech.2012.09.138.

[38] Y.-P. Chen, Y. Zhao, K.-Q. Qiu, J. Chu, R. Lu, M. Sun, X.-W. Liu, G.-P. Sheng, H.-Q. Yu, J. Chen, W.-J. Li, G. Liu, Y.-C. Tian, Y. Xiong, An innovative miniature microbial fuel cell fabricated using photolithography., Biosens. Bioelectron. 26 (2011) 2841–2846. doi:10.1016/j.bios.2010.11.016.

[39] F. Qian, D.E. Morse, Miniaturizing microbial fuel cells., Trends Biotechnol. 29 (2011) 62–69. doi:10.1016/j.tibtech.2010.10.003.

[40] J. You, J. Greenman, C. Melhuish, I. Ieropoulos, Small-scale microbial fuel cells utilising uric salts, Sustain. Energy Technol. Assessments. 6 (2014) 60–63. doi:10.1016/j.seta.2014.01.005.

[41] A. Elmekawy, H.M. Hegab, X. Dominguez-Benetton, D. Pant, Internal resistance of microfluidic microbial fuel cell: challenges and potential opportunities., Bioresour. Technol. 142 (2013) 672–682. doi:10.1016/j.biortech.2013.05.061.

[42] G. Venkata Subhash, R. Chandra, S. Venkata Mohan, Microalgae mediated bio-electrocatalytic fuel cell facilitates bioelectricity generation through oxygenic

photomixotrophic mechanism, Bioresour. Technol. 136 (2013) 644–653. doi:10.1016/j.biortech.2013.02.035.

[43] G.G. Kumar, V.G.S. Sarathi, K.S. Nahm, Recent advances and challenges in the anode architecture and their modifications for the applications of microbial fuel cells., Biosens. Bioelectron. 43 (2013) 461–475. doi:10.1016/j.bios.2012.12.048.

[44] K. Guo, A. Prévoteau, S.A. Patil, K. Rabaey, Engineering electrodes for microbial electrocatalysis, Curr. Opin. Biotechnol. 33 (2015) 149–156. doi:10.1016/j.copbio.2015.02.014.

[45] W. Yang, X. Wei, S. Choi, A Dual-Channel, Interference-Free, Bacteria-Based Biosensor for Highly Sensitive Water Quality Monitoring, IEEE Sens. J. 16 (2016) 8672–8677. doi:10.1109/JSEN.2016.2570423.

[46] B. Liu, Y. Lei, B. Li, A batch-mode cube microbial fuel cell based “shock” biosensor for wastewater quality monitoring., Biosens. Bioelectron. 62 (2014) 308–314. doi:10.1016/j.bios.2014.06.051.

[47] P.M. Doran, Bioprocess Engineering Principles, Academic Press, 2008.

[48] G. Gärtner, B. Uzunov, E. Ingolic, W. Kofler, G. Gacheva, P. Pilarski, L. Zagorchev, M. Odjakova, M. Stoyneva, Microscopic investigations (LM, TEM and SEM) and identification of Chlorella isolate R-06/2 from extreme habitat in Bulgaria with a strong biological activity and resistance to environmental stress factors, Biotechnol. Biotechnol. Equip. 29 (2015) 536–540. doi:10.1080/13102818.2015.1013283.

[49] K.V. Ajayan, M. Selvaraju, P. Unnikannan, P. Sruthi, Phycoremediation of Tannery Wastewater Using Microalgae Scenedesmus Species, Int. J. Phytoremediation. 17 (2015) 907–916. doi:10.1080/15226514.2014.989313.

[50] Science Photo Library Ltd., Science Photo Library, (2017). http://www.sciencephoto.com/.

[51] WHO, Guidelines for Drinking-water Quality, 2011. doi:10.1016/S1462-0758(00)00006-6.

[52] H. Kayano, I. Karube, T. Matsunaga, S. Suzuki, O. Nakayama, A photochemical fuel cell system using Anabaena N-7363, Eur. J. Appl. Microbiol. Biotechnol. 12 (1981) 1–5. doi:10.1007/BF00508110.

9 Conclusions and future work

The aim of this PhD project was to develop cost-effective, sustainable MFCs for straightforward and rapid monitoring of water quality. The work presented in this thesis demonstrates important steps towards this goal. The development of a miniature MFC that utilised cost-effective membranes and oxygen reduction reaction catalysts at the cathode, and its ability to detect the toxicity of formaldehyde and atrazine, and organic load was demonstrated. Moreover, a novel paper-based MFC biosensor and microalgae based miniature photosynthetic MFC were developed, both capable of detecting toxicants (in this case formaldehyde as a model toxicant) in wastewater, thus paving avenues towards extremely low cost and sensitive biosensors for water quality monitoring. In this chapter, a comparison between the MFC biosensors developed in this work is given. Then, a perspective on addressing barriers to implementing the MFC technology is provided.

9.1 Comparison: MFCs as biosensors

9.1.1 Detection of labile organic load

In this thesis, the development of MFCs as biosensors for organic load and to detect the toxicity of formaldehyde and atrazine was pursued. Single chamber, miniature MFCs using different membrane materials were developed to detect COD content (using acetate) in artificial wastewater. A summary of their performance, along with the device developed in Chapter 6 (named MFC_L), is provided in Table 9.1.

Table 9.1. Summary of MFC biosensors developed in this thesis for detecting organic load

Device	Chapter	Membrane	Detection range (mg L^{-1}, acetate)	Response time (min)	Sensitivity (μA mM^{-1} cm^{-2})
MFC_E	5	Eggshell tissue	10 – 4900	57 ± 6	0.018 ± 0.003
MFC_P	5	PDMS	10 – 4900	37 ± 2	0.011 ± 0.002
MFC_N	5	Nafion	10 – 4900	48 ± 1	0.007 ± 0.003
MFC_M	5	None	10 – 4900	54 ± 10	0.005 ± 0.002
MFC_L	6	Nafino	10 - 1000	56 ± 8	0.030 ± 0.003

A linear response between current output and acetate concentration was observed within the range 0.1 – 10 mM (corresponding to COD values of 10 – 1000 ppm acetate). Indeed, the linear detection response achieved by the devices in Chapter 5 was larger at 10 – 4900 ppm acetate, however due to large errors further work is needed to confirm this. When compared to other MFC based biosensors in the literature, Table 5.1, the devices in this thesis present similar detection ranges (ranging from 10 – 1280 ppm) and response times. Although a direct comparison is not possible, given that other studies use different substrates. However, this work, through the development of MFC devices using cost effective membrane materials, provides an avenue towards more cost-effective MFC biosensors, which will aid their commercial application. A maximum sensitivity of 0.030 ± 0.003 μA mM^{-1} cm^{-2} was achieved by the MFC_L device. The reason behind its greater sensitivity when compared to the devices in Chapter 5 is unknown, but suspected to be due to a different bacterial mixture used that derived from a sewage sludge taken at a different date. Further work is needed to determine the cause behind this difference.

When compared to other BOD biosensors in the literature, Table S5.1, the MFC biosensors in this thesis demonstrate similar response times (with BOD biosensors having response times of 3 – 120 minutes), which supports their use as rapid online monitoring BOD sensors. However, the MFC biosensors in this work suffer from poor operational stability and have only been studied using one substrate (acetate). The benefit of the MFC biosensors *versus* other biosensors in the literature is that they do not depend on single microbial strains, and hence have the potential to detect a wider range of biodegradable compounds in water.

Given the instability, and at times, large errors of measurement demonstrated by the MFC biosensors in this thesis, there is much to be done to progress the technology to online BOD monitoring (for example at a wastewater treatment works). However, the

current BOD_5 standard method for determining BOD of wastewater is a time consuming and offsite method, which also accepts a large margin of error (up to 15%). In this respect, MFC biosensors could be a promising replacement for the BOD_5 method, since they could be used online and onsite. For commercial application however, their reliability and accuracy must be improved. Moreover, the fact that wastewater has a very low conductivity (100 - 2000 µS cm^{-1}) also limits their functionality with real wastewater.

9.1.2 Formaldehyde

MFC biosensors were also developed to detect the toxicity of formaldehyde in artificial wastewater. A summary of the different devices that were developed for detecting the toxicity of formaldehyde in AW are provided in Table 9.2.

Table 9.2. Summary of MFC biosensors developed in this thesis for formaldehyde toxicity detection.

Device	Chapter /Reference	Detection range (mg L^{-1}, acetate)	Response time (min)	Recovery time (min)	Sensitivity (× 10^{-3} ppm^{-1} cm^{-2})
MFC_L	6	10 – 2000	27.2 ± 7.6	67.3 ± 42.0	1.43 ± 0.18
pMFC	7	1000	165 ± 8	N/A	N/A
fpMFC	7	1000	200 ± 11	N/A	N/A
photoMFC	8	10 – 200	42 ± 7.5	62 ± 8 min	6.92 ± 1.67

In general, the MFC biosensors were capable of detecting the toxicity of formaldehyde in water with improved response times when compared to other MFC based biosensors for formaldehyde reported in the literature (between 125 and 200 min), as shown earlier in Table S8.2. This may be attributed to to the miniaturisation of the device, which improves mass transfer between the bulk fluid and the biofilm at the anode. This in effect reduces external mass transfer processes in the device, thereby improving detection of toxicants within the MFC.

Comparing between the MFC_L and photoMFC, similar response and recovery times were observed. The lower detection limit of both devices was 10 ppm, which is similar to other MFC based biosensors reported, Table S8.2. The MFC_L device, that did not

use microalgae at the anode biofilm, demonstrated a wider detection range of up to 2000 ppm of formaldehyde. However, further toxicity tests with higher concentrations of formadehyde on the photoMFC ought to be conducted. Promisingly, the use of a mixed microalgae and bacteria culture at the anode, as in the photoMFC device, allowed improved sensitivity towards formaldehyde toxicity, at over 3 times the sensitivity of MFC_L. This may be due to the use of microalgae at the anode, which have been shown to be effective in aquatic toxicological testing, due to their sensitivity towards hazardous chemicals and their rapid response times. The work in this thesis provides a proof of concept for the use of microalgae as an effective biosensing element in MFCs, although more work is needed to determine the specific contribution of microalgae in these systems (especially since the photoMFC in this work utilised a mixed bacteria and microlage biofiolm).

The paper based MFC in this thesis, pMFC and fpMFC, showed promise towards the development of cheap and portable MFC based biosensors, with similar response times towards a 1000 ppm injection of formaldehyde when compared to the other MFCs in this work, and MFC biosensors in the literature. In order to compare this device to the MFC_L and photoMFC, a wider range of formaldehyde concentrations need to be investigated with the pMFC biosensor.

The World Health Organisation standard for formaldehyde detection is to use high-performance liquid chromatography, which has the ability to detect formaldehyde down to 6 ppb [1]. In this respect, the MFC biosensors reported in this work offer an attractive alternative that is potentially online and rapid. However, formaldehyde concentrations in water sources may range between 20 ppb up to 600 ppm [2]. Therefore, the detection limits of the MFC biosensors need to be vastly improved, especially to provide effective detection to the maximum allowable limit of formaldehyde, 2.6 ppm [1].

9.1.3 Challenges ahead

There is much work to be done to progress the use of MFC biosensors outside of the laboratory and towards in field and commercial applications. The most significant issue that must be addressed is the use of the MFC biosensing technology for analysis of real water samples, whose complexity generates a variety of issues around reliability

and selectivity for water quality monitoring. The most suitable method of applying the MFC technology in field must also be determined. Moreover, the further development of novel MFC systems with enhanced reliability and stability must be pursued. The following information gives recommendations for the progression of the MFC technology for water quality monitoring.

9.2 Monitoring real water quality

The miniature MFC developed in Chapter 4, 5 and 6 demonstrated the use of cost-effective materials (e.g. eggshell membrane, biomass derived catalysts) in a device that was potentially suited towards monitoring of labile organic content in wastewater (between 10 – 1000 ppm), as well as the rapid detection of toxic compounds (formaldehyde and atrazine) at ppm levels.

For implementation of MFC biosensors for real water quality monitoring, it is recommended to conduct a factorial design of experiment (DOE) study. This is in order to confidently identify if the MFC biosensor is capable of detecting specific toxic compounds in spite of natural variations (e.g. organic load, temperature, pH), or the presence of other toxicants, that may occur in a real water sample, therefore identifying if the technology is apt for the desired application. It will also give an insight to the effects of co-contamination and combinatory effects of toxicants in water sources.

Factorial (DOE) has shown to be a powerful statistical method that allows the effect of several parameters and their interactions on a system response to be determined with minimised experimental effort whilst not compromising accuracy of the results [3]. Recently, factorial DOE has been used to assess MFC performance [3,4]. However, these studies have been limited to the analysis of up to three parameters (conductivity, temperature and external resistance [4], or pH and buffer concentration [3]), whereas in reality the factors that may change in water systems, and thus affect the performance and sensing capability of an MFC, far exceeds this. Examples are given in Figure 9.1.

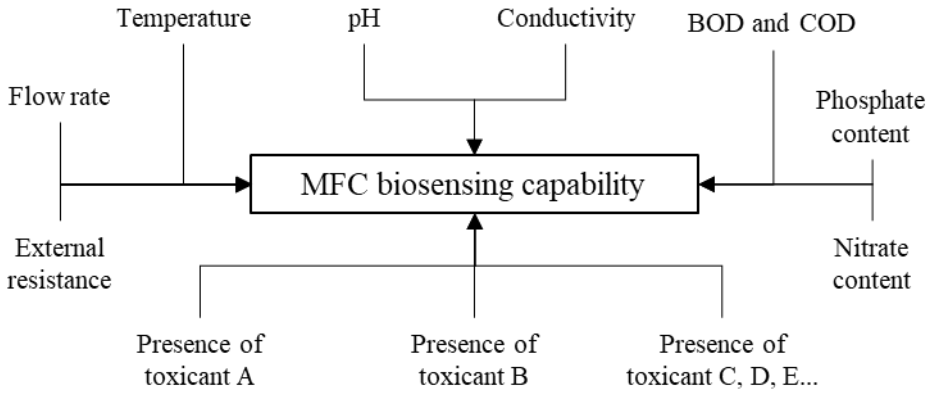

Figure 9.1. Example factors in water systems that may affect the biosensing capability of an MFC for water quality monitoring

The number of factors which may affect the performance and sensing capability of an MFC are vast, and to assess their effect when using factorial DOE may take a large amount of experimental effort. For instance, if one had 10 parameters in the water system to assess (this could be environmental factors and/or a combination of toxicants), Table 9.3 shows the number of experimental runs required to assess the system at different resolution levels, assuming the standard two levels of analysis for each parameter (one high and one low value). A full factorial DOE would require 1024 runs, however a resolution 5 fractional factorial DOE would require only 128 experiments. In this way, one obtains enough data to interpret both individual and interactive effects on the system outputs (in this case current output of the MFC). A fractional factorial DOE with lower resolution (3, 4) would indeed require less runs, but would give less information on the interactive effects of parameters, which is not recommended for complex water systems.

Table 9.3. Number of experimental runs required to fulfil factorial DOE methods

Analysis method for 10 parameters	Number of runs
Full factorial DOE	1024
Fractional Factorial DOE (resolution 5)	128
Fractional Factorial DOE (resolution 4)	32
Fractional Factorial DOE (resolution 3)	16

For analysis of the experimental data, it is recommended to use response surface methodology, as previous reported [3]. Moreover, central composite design may be

used to capture the nonlinear behaviour of the output response to parameters, which can be fit to a Taylor expansion quadratic model, Equation 9.1:

$$y = b_0 + \sum_{i=1}^{k} b_i x_i + \sum_{i=1}^{k} b_{ii} {x_i}^2 + \sum_{i=1}^{k} \sum_{i<j}^{k} b_{ij} x_i x_j + e \qquad \text{Equation 9.1}$$

Where y is the response, x_i and x_j are experimental factors, e is the experimental error, b_0 is the estimate of the response when all factors are set to their midpoint value, b_i is a direct measure of linear dependence of factor i, b_{ij} is a measure of the interaction between factors i and j, and b_{ii} is a quadratic term for factor i used to describe non-linearity in the model, and k is the number of factors in the system.

The subsequent analysis of the output data can be assessed on software, such as Design-Expert (StatEase), or MODDE (UMetrics), and typically should include a multi-linear regression model including analysis of variables such as model fit (R^2), future prediction precision (Q^2), model validity and reproducibility, coefficient plots (to give the magnitude of effect of a parameter or interaction on the output response) and normal probability plot of residuals (which allows one to detect outliers and assess the normality of residuals).

Indeed the work load to conduct such a study is large (with at least 128 experiments needed for 10 variables), but the information such a study can provide will be invaluable for progressing the frontiers of this technology. The next step will be to conduct field trials at desired water sampling locations (be it wastewater effluents, riverine and natural aquatic environments, or industrial/municipal effluents), which should ideally operate inline with the process and function in real time, Figure 9.2.

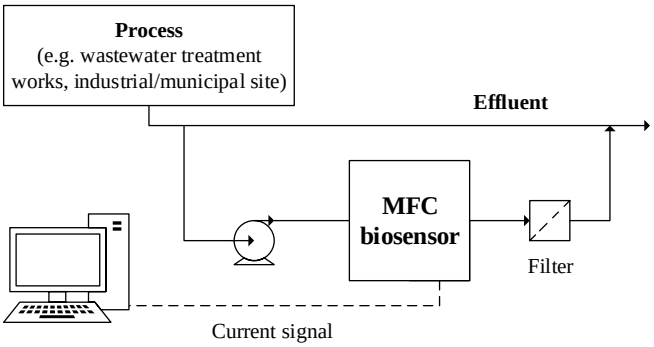

Figure 9.2. Concept for MFC biosensing in field. The MFC may be installed at the effluent of the process, and used to monitor its quality in real time. Filtration of the MFC outlet may be required to prevent microbial contamination of the effluent.

When conducting field trials, various control mechanisms could be considered that have the potential to enhance the sensitivity and the reliability of the water quality measurements. Current methods typically depend on a fixed external load attached to the MFC to control the current generated from the device, but other techniques should be considered. For instance, potentiostatic control of the MFC has been shown to enhance the sensitivity of the MFC response to Cu^{2+} [5], which should be investigated further in real water samples. It may be argued that potentiostatic control may be expensive and unsuited to in field and remote monitoring, but recent years has seen the development of very cost-effective and easy to manufacture potentiostats (< $600) [6], and even the use of a mobile phone that can be used for potentiostatic control [7], which are well suited to in field applications. Alternatively, the MFC response could be compared to a reference in order to negate changes in environmental conditions. One may be able to reference the MFC response to online data for parameters such as pH, temperature and conductivity, and subsequently analyse the MFC signal whilst accounting for known changes in these parameters. Although this approach could become costly for applications where such equipment is not available, it could be well suited to wastewater treatment analysis where such parameters are commonly monitored already. Finally, novel methods of controlling and analysing the MFC signal should be investigated. For example, maximum power point tracking (MPPT) technology could be used to enhance the current signal of the MFC [8], thereby enhancing its sensing capacity too. Any changes in the power produced or control effort (i.e. the resistance applied to the MFC *via* the potentiometer in MPPT systems) could be associated with the presence of toxic compounds or change in organic load

for instance. In a similar fashion, controlling the voltage of the MFC using a gain scheduling strategy [9] could provide a means to keep the signal of the MFC constant and maintain operation for long periods of time. Similar to MPPT control, any changes in the voltage measured or the effort required in the control strategy (once again in this case voltage is kept constant by potentiometric control) may be affiliated to the presence of bioactive compounds.

In the circumstance that it is found that MFC biosensors cannot be used for the detection of specific compounds within complex mixtures, it may be that MFC biosensors are more suited towards generic shock sensing of water sources. In this instance, an MFC would operate inline with the water source, and its current would be expected to operate within a given current range based on the natural variation of the feed (e.g. natural fluctuations in temperature, pH, and organic load). However, if the water source should then experience a shock event such as a high organic loading or the presence of toxic compound, then the current generated from the MFC would move outside the expected range. This signal change would then act as an alarm for further necessary analysis of the water, Figure 9.3. Such a technique would have great value as an early alarm system for wastewater or industrial effluent and aid towards the effective and timely control of pollution events. It should be noted however, that with inline operation the bacteria within the MFC may adapt resistance to, and therefore exhibit reduced sensitivity towards, given toxic compounds. In such a case, the MFC biosensor may still provide useful for online shock sensing when exposed to an entirely new toxic event or extreme change in conditions.

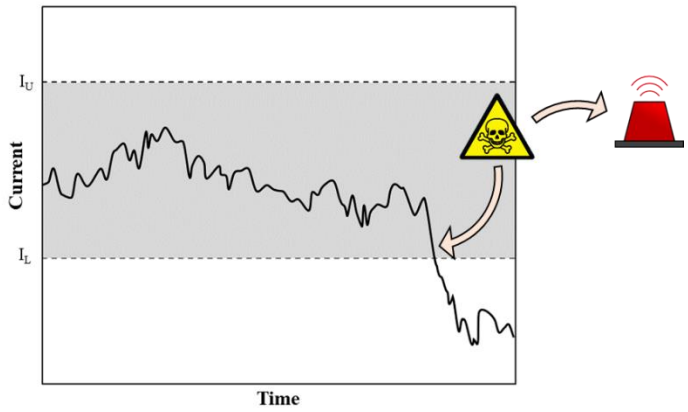

Figure 9.3. MFCs as shock biosensors. During normal operation the MFC produces a current between an upper and lower current limit, I_U and I_L respectively, which will account for natural variation of the influent. A toxic event causes the current to fall outside the safety range, and an alarm is given for further testing and/or a call for containment of the toxic event.

9.3 Novel designs

The development of a paper-based MFC biosensor was demonstrated in Chapter 7, which provided a proof of concept for such a device to detect toxic compounds in water, by detecting 1000 ppm formaldehyde in water. The device was not only cheap to produce (£0.43 per unit), but owing to its mode of operation (simple submersion of a portable device in a water sample), represents a highly effective method of biosensing by obviating the need for sample pumping which is required for many other flow based MFC devices. The ability to detect toxicity shows promise to detect other compounds of interest in water, and since the sensor can be used once then safely disposed of (due to its biodegradability), the detection of contaminants in remote regions and in developing countries would be a significant application of this technology. However, to achieve this further work is needed. First of all, the ability to detect other compounds reliably should be determined (once again following a factorial DOE approach if studying a large number of variables), but also the methods in order to use the device in the field should be determined. In particular, methods to pre-enrich the anode of the MFC with an electroactive biofilm and then suspend the culture for later use should be sought. This way, paper-based MFCs can be prepared off site, stored, and then deployed for rapid, onsite and cheap water quality monitoring

assessments, all before being safely disposed of by biodegradation. Indeed, the storage of electroactive biofilms has been shown for power generating MFC devices [10], but should be investigated in this context to enable this technology.

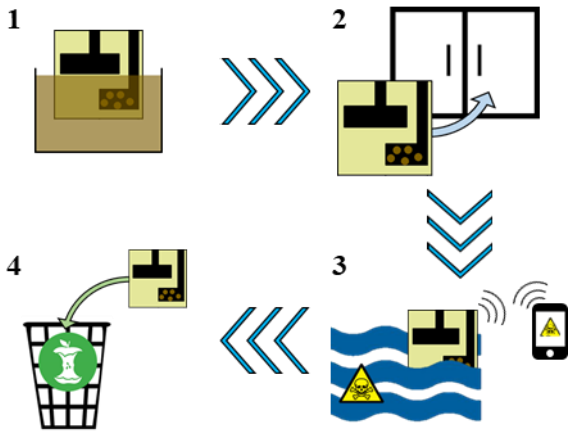

Figure 9.4. Concept for the use of paper-based MFC biosensors. **1**) Pre-enrichment of an electroactive biofilm on the MFC; **2**) Storage of the MFC; **3**) Deployment of the MFC in a water source for detecting toxicants and signal sent to user (for instance to a mobile phone); **4**) Safe disposal of device by biodegradation.

Other designs of MFC should also be investigated for biosensing applications, in particular ones that demonstrate improved reliability, and additionally remove the necessity for pumping and flow systems in order for the MFC to function. Such flow systems can increase the capital and operational cost of the MFC biosensor significantly, which may not be feasible for its commercial applications. Alternative designs should be sought. For example, sediment MFCs represent a class of MFC that can very easily be placed in the field with little maintenance costs, and have indeed been used to power remote sensors in the field [11]. Their potential for biosensing has yet to be investigated fully however, and the use of sediment MFC biosensors could prove useful in water quality monitoring of riverine environments, reed bed wastewater treatment systems, or industrial water effluents. Another interesting design that has low operational costs is the floating MFC, which have largely been investigated for their use in energy generation [12,13]. These configurations, as the name suggests, will float on the top of a water surface, thus making them very suitable for low cost and long term analysis of water sources such as reservoirs, rivers, or even

open wastewater treatment tanks. Development of these systems has just begun, but they could provide a very cost-effective and easy to operate method of monitoring water sources in real time.

9.4 Photosynthetic MFC biosensors

Chapter 8 demonstrated the development of a miniature photosynthetic MFC which utilised microalgae as the sensing element in the system, and as well as demonstrating sustainable operation (with light as the key input), demonstrated the promising capability to detect toxicants in water by detecting formaldehyde between 10 – 200 ppm. The use of microalgae in this work shows great promise towards the use of this technology for detecting emerging contaminants in water, including herbicides, pesticides and pharmaceuticals, to which microalgae may be far more sensitive towards when compared to bacteria. Further investigation for this technology to such compounds is needed, and if successful, the photosynthetic MFC could be a valuable tool for analysis of treated wastewater, which in coming years will be subject to more stringent water quality regulations. Certain aspects of the photosynthetic MFC should also be investigated in order to improve power performance and biosensing capability. More analysis to explain the relatively short lifetime of the device (nearly 1 month) should be conducted, which may include investigating the fluid dynamics within the cell to optimise the biofilm density for long term performance [14] and investigating other strains of microalgae that will exhibit long term electroactive ability. The design of the miniature MFC may be enhanced to increase the power generated by the device also, by further exploiting the concepts of cross sectional area, electrode spacing and chamber length of the anode chamber that were covered in Chapter 4 and 5. As well as for detection of bioactive compounds in water, the technology may also prove useful for process monitoring applications. For instance, a photosynthetic MFC biosensor could be installed inline with an algae based open raceway pond or photobioreactor (for treating wastewater for example). The current generated from the sensor could be used as a rapid indicator of microbial community health within the process and may even be capable of indicating process reliability and efficiency. Indeed this could go beyond the use of microalgae based MFCs, and bacteria based MFC biosensors could be installed with other processes (anaerobic digestion tanks, fermenters and other

bioreactors) and used as a rapid and simple way to indicate the process performance in real time.

9.5 References

[1] World Health Organisation (WHO), Formaldehyde in Drinking-water: Background document for development of WHO Guidelines for Drinking-water quality, 2005, WHO Geneva

[2] World Health Organisation (WHO), Formaldehyde: Concise Internation Chemical Assessment Document 40, 2002, WHO Geneva

[3] S. Madani, R. Gheshlaghi, M.A. Mahdavi, M. Sobhani, A. Elkamel, Optimization of the performance of a double-chamber microbial fuel cell through factorial design of experiments and response surface methodology, Fuel. 150 (2015) 434–440. doi:10.1016/j.fuel.2015.02.039.

[4] S.B. Velasquez-Orta, D. Werner, J.C. Varia, S. Mgana, Microbial fuel cells for inexpensive continuous in-situ monitoring of groundwater quality, Water Res. 117 (2017) 9–17. doi:10.1016/j.watres.2017.03.040.

[5] Y. Jiang, P. Liang, C. Zhang, Y. Bian, X. Yang, X. Huang, P.R. Girguis, Enhancing the response of microbial fuel cell based toxicity sensors to Cu(II) with the applying of flow-through electrodes and controlled anode potentials., Bioresour. Technol. 190 (2015) 367–372. doi:10.1016/j.biortech.2015.04.127.

[6] E.S. Friedman, M.A. Rosenbaum, A.W. Lee, D.A. Lipson, B.R. Land, L.T. Angenent, A cost-effective and field-ready potentiostat that poises subsurface electrodes to monitor bacterial respiration, Biosens. Bioelectron. 32 (2012) 309–313. doi:10.1016/j.bios.2011.12.013.

[7] J.L. Delaney, E.H. Doeven, A.J. Harsant, C.F. Hogan, Use of a mobile phone for potentiostatic control with low cost paper-based microfluidic sensors, Anal. Chim. Acta2. 803 (2013) 123–127. doi:10.1016/j.aca.2013.06.005.

[8] H.C. Boghani, J.R. Kim, R.M. Dinsdale, A.J. Guwy, G.C. Premier, Control of power sourced from a microbial fuel cell reduces its start-up time and increases

bioelectrochemical activity, Bioresour. Technol. 140 (2013) 277–285. doi:10.1016/j.biortech.2013.04.087.

[9] H.C. Boghani, I. Michie, R.M. Dinsdale, A.J. Guwy, G.C. Premier, Control of microbial fuel cell voltage using a gain scheduling control strategy, J. Power Sources. 322 (2016) 106–115. doi:10.1016/j.jpowsour.2016.05.017.

[10] J. Winfield, L.D. Chambers, J. Rossiter, J. Greenman, I. Ieropoulos, Urine-activated origami microbial fuel cells to signal proof of life, J. Mater. Chem. A. 3 (2015) 7058–7065. doi:10.1039/C5TA00687B.

[11] C. Donovan, A. Dewan, D. Heo, H. Beyenal, Batteryless, Wireless Sensor Powered by a Sediment Microbial Fuel Cell, Environ. Sci. Technol. 42 (2008) 8591–8596. doi:10.1021/es801763g.

[12] Y. Huang, Z. He, J. Kan, A.K. Manohar, K.H. Nealson, F. Mansfeld, Electricity generation from a floating microbial fuel cell., Bioresour. Technol. 114 (2012) 308–313. doi:10.1016/j.biortech.2012.02.142.

[13] E. Martinucci, F. Pizza, D. Perrino, A. Colombo, S.P.M. Trasatti, A. Lazzarini Barnabei, A. Liberale, P. Cristiani, Energy balance and microbial fuel cells experimentation at wastewater treatment plant Milano-Nosedo, Int. J. Hydrogen Energy. 40 (2015) 14683–14689. doi:10.1016/j.ijhydene.2015.08.100.

[14] Y. Shen, M. Wang, I.S. Chang, H.Y. Ng, Effect of shear rate on the response of microbial fuel cell toxicity sensor to Cu(II)., Bioresour. Technol. 136 (2013) 707–710. doi:10.1016/j.biortech.2013.02.069.